Abstract

Title of dissertation: ENGINEERING ENHANCED STRUCTURAL STABILITY TO THE STREPTOCOCCAL BACTERIOPHAGE ENDOLYSIN PLYC

Ryan Daniel Heselpoth, Doctor of Philosophy, 2014

Dissertation Directed by: Associate Professor Daniel C. Nelson
Institute for Bioscience and Biotechnology Research
and Department of Veterinary Medicine

Antibiotic misuse and overuse has prompted bacteria to rapidly develop resistance, thereby hindering the efficacy of these chemotherapeutics. Due to antibiotic resistant strains expeditiously disseminating, antimicrobial resistance has been labeled as one of the greatest threats to human health globally. An emerging alternative antimicrobial strategy involves using bacteriophage-derived enzymes, termed endolysins. Endolysins are peptidoglycan hydrolases that liberate lytic bacteriophage virions late in the infection cycle by cleaving critical covalent bonds in the bacterial cell wall. As a result, the high intracellular osmotic pressure induces cell lysis. Antimicrobial strategies have been devised involving the extrinsic application of recombinant endolysins to susceptible Gram-positive pathogens. The efficacy of these enzymes has been validated *in vitro* and *in vivo*, with no resistance observed to date. One such example is the streptococcal-specific endolysin PlyC. This endolysin is currently the most bacteriolytically-active and possesses the ability to lyse human and animal pathogens known to cause serious health complications. Unfortunately, like numerous other endolysins, PlyC is relatively unstable and accordingly has short shelf life expectancy.

With a long-term goal of using endolysins for industrial applications, furthering the development of a thermolabile translational antimicrobial with a short shelf life is ambitious. The main objective of this dissertation is to develop and validate bioengineering strategies for thermostabilizing bacteriolytic enzymes. Using PlyC as the model enzyme, we first used a rationale-based computational screening methodology to identify stabilizing mutations to a thermosusceptible region of the catalytic subunit, PlyCA. One mutation, T406R, caused a 2.27°C increase in thermodynamic stability and a 16 fold improvement in kinetic stability. Next, we developed a substantiated novel directed evolution protocol that involves randomly incorporating mutations into a bacteriolytic enzyme followed by a screening process that effectively identifies mutations that are stabilizing. Finally, applying multiple rounds of directed evolution to PlyC allowed for the identification of a thermostabilizing mutation, N211H, which increased the thermodynamic stability by 4.10°C and kinetic stability 18.8 fold. Combining the N211H and T406R mutations was additive in terms of thermal stability, with thermodynamic and kinetic stability enhancements of 7.46°C and 28.72 kcal/mol activation energy (E_A) of PlyCA unfolding, respectively.

ENGINEERING ENHANCED STRUCTURAL STABILITY TO THE STREPTOCOCCAL BACTERIOPHAGE ENDOLYSIN PLYC

By

Ryan Daniel Heselpoth

Dissertation submitted to the Faculty of the Graduate School of the
University of Maryland, College Park, in partial fulfillment
of the requirements for the degree of
Doctor of Philosophy
2014

Advisory Committee:
Associate Professor Daniel C. Nelson, Chair
Dr. John P. Marino
Professor Jonathan D. Dinman
Professor Philip N. Bryan
Associate Professor Utpal Pal

Acknowledgements

First and foremost, I would like to sincerely thank my supervisor, Dr. Daniel Nelson, for everything he has done for me over the past five years of my graduate career. His incredible guidance, wisdom, support, patience and generosity have been invaluable to me. The time spent in the Nelson lab has been nothing short of gratifying and my experiences, both personal and professional, will have an everlasting impact on me as I move forward in my scientific career, and for that I am eternally grateful.

Additionally, I would like to thank the following people for their contributions: The members of my doctoral advisory committee, including Dr. John. P. Marino, Professor Jonathan D. Dinman, Professor Philip N. Bryan, and Dr. Utpal Pal, for their support throughout my graduate education. Various scientists at the Institute for Bioscience and Biotechnology Research, including Dr. James T. Hoopes, Professor Zvi Kelman, Dr. Travis D. Gallagher, Dr. Amanda Altieri and Dr. Robert G. Brinson, for their appreciated instruction and advice relating to my numerous dissertation-related projects.

I would also like to thank the various lab members I have had the privilege to work with over the past several year, which collectively include Dr. Yang Shen, Dr. Michael S. Mitchell, Dr. Steve M. Swift, Patrick M. Bales, Sara B. Linden, Emilija Renke, Sarah May, Janet Yu and Mariel Escatte.

Table of Contents

Acknowledgements ... ii

Table of Contents ... iii

List of Tables ... vi

List of Figures ... viii

List of Abbreviations ... xi

Chapter I: Introduction and Literature Review ... 1
- Antibiotics and Resistance Development ... 1
  - Antibiotic Discovery and Resistance Timeline ... 1
  - Health and Economic Implications ... 12
- Alternative Antimicrobial Approaches ... 15
- Bacteriophage-Derived Peptidoglycan Hydrolases ... 22
  - Lysis From Without ... 26
  - Structure of Gram-positive and Gram-negative Endolysins ... 26
  - Bacteriolytic Mechanism of Endolysins ... 28
  - Antimicrobial Potential (Resistance, Toxicity, Immunogenicity, Synergy) ... 32
  - Engineering Endolysin Properties ... 38
  - Endolysin-Related Applications ... 44
    - Medicine ... 44
    - Food Safety ... 49
    - Agriculture ... 54
- PlyC, a Thermolabile Streptococcal Endolysin with Unique Characteristics ... 57
  - *In vitro* and *in vivo* Validation of Antimicrobial Efficacy ... 58
  - Molecular, Biochemical and Structural Characterization of PlyC ... 62
  - Transient Shelf Life of PlyC Caused by the Thermolability of PlyCA ... 71
- Protein Engineering Methodologies ... 74
  - Rationale-based Methods for Protein Thermostabilization ... 76
  - Random Methods for Protein Thermostabilization ... 82
- Purpose of Research ... 86

Chapter II: Increasing the Stability of the Bacteriophage Endolysin PlyC Using Rationale-Based FoldX Computational Modeling ... 89
- Abstract ... 90
- Introduction ... 91
- Materials and Methods ... 94
  - Computational Modeling of PlyC Mutants ... 94
  - Bacterial Strains and Culture Conditions ... 95
  - Cloning and Site-Directed Mutagenesis ... 95
  - Protein Expression and Purification ... 96
  - *In vitro* Endolysin Activity on *S. pyogenes* ... 96

Circular Dichroism Spectroscopy 97
Differential Scanning Calorimetry 98
Calculating the Activation Energy of PlyCA Unfolding 98
45°C Kinetic Stability Assay 99
Results 100
Prediction of Stabilizing Mutations to the PlyCA CHAP Domain 100
Protein Solubility, Purity and Secondary Structure Determination 103
Kinetic Analysis of Bacteriolytic Activity against *S. pyogenes* 110
Circular Dichroism Thermal Stability Analysis 110
Differential Scanning Calorimetry 113
45°C Kinetic Inactivation Analysis 115
Discussion 115
Acknowledgements 122

Chapter III: A New Screening Method for the Directed Evolution of Thermostable Bacteriolytic Enzymes 123
Abstract 124
Protocol 126
Determining Optimal Heating Conditions 126
Generating the Mutant Library 130
96-Well Microtiter Plate Preparation and Cell Growth Conditions 131
Replica Plating, Protein Expression Induction and Lysate Preparation 131
Soluble Lysate Heat Treatment 132
Representative Results 133
Discussion 137
Acknowledgements 144

Chapter IV: Directed Evolution of the Thermosusceptible Bacteriophage Endolysin PlyC 145
Abstract 146
Introduction 147
Materials and Methods 151
Bacterial Strains and Culture Conditions 151
Molecular Cloning of PlyC Structural and Directed Evolution Constructs 151
Protein Expression and Purification 154
Directed Evolution Genetic Diversification and Screening Methodology 154
Thermal Inactivation Experiments 155
Circular Dichroism Spectroscopy 155
Differential Scanning Calorimetry 156
Bacteriolytic Activity Quantitation against *S. pyogenes* 156
Constructing Arrhenius Plots for Calculating Activation Energy of PlyCA Unfolding 157
Results 158
Thermodynamic Analysis of the Structural Components of PlyC 158
Directed Evolution Screening Synopsis 161
Structural and Thermodynamic Stability of the Directed Evolution Lead

Candidate 168
Protonated H211 Employs a Charge-Mediated Stabilizing Mechanism 168
H211 Electrostatically Interacts with E113 and D150 of the GyH Domain.....178
Bacteriolytic Activity Comparison between Wild-Type PlyC and PlyC (PlyCA) N211H 185
Combining Beneficial Mutations from Different Engineering Approaches is Additively Thermostabilizing 187
Discussion.....191
Acknowledgements.....196

Chapter V: Discussion and Future Directions 197
Discussion.....197
Summary and Conclusions 213
Future Research 216
Computational Screening of the GyH and Helical Docking Domains of PlyCA 216
Further Structural Characterization and Thermostabilization Strategies using PlyC (PlyCA) N211H, T406R and N211H T406R 217
Applying Chimeragenesis to Other Gram-Positive Endolysins.....218

Appendix A: Sequence Information for Constructs used in Dissertation-Related Studies.....220

Appendix B: SDM Primers for PlyC Computational Screening Studies (Chapter II).....242

Appendix C: SDM Primers for PlyC Directed Evolution Studies (Chapter IV) 244

Appendix D: Unpublished Dissertation-Related Preliminary Data.....246

Appendix E: List of Submitted or Published Co-Authored Manuscripts 253

Bibliography 264

List of Tables

Chapter I

Table 1-1: Antibiotic Resistance Timeline 9

Table 1-2: Some of the major human phage therapy studies performed in Poland and the former Soviet Union 23

Chapter II

Table 2-1: List of the final 10 FoldX PlyC mutant candidates 104

Table 2-2: Far-UV CD protein secondary structure estimation using the CONTIN deconvolution method 108

Table 2-3: Bacteriolytic activity quantitation by means of *S. pyogenes* turbidity reduction assay 111

Table 2-4: Comparison of $T_{1/2}$ values derived from the CD melting experiments 112

Table 2-5: Calorimetric determination of PlyCA T_G and the corresponding ΔH_{VH} values 114

Table 2-6: Determination of the PlyCA E_A (kcal/mol) of unfolding from applying a kinetic model to the calorimetric data 116

Chapter III

Table 3-1: Candidate Pool Genomic Analysis 134

Chapter IV

Table 4-1: List of different PlyC constructs thermodynamically characterized by DSC 159

Table 4-2: DSC T_G comparative analysis of PlyCA and PlyCB thermal transitions exhibited by the PlyC structural components 162

Table 4-3: Kinetic stability comparison at 45°C between wild-type PlyC, PlyC 33D2 and the isolated point mutations collectively encoded by PlyC 33D2.....167

Table 4-4: Kinetic stability comparison at 45°C between the charge-specific N211 mutants.....172

Table 4-5: Thermal stability associated with the different N211 charge mutants of PlyCA as explicated by means of CD thermal denaturation experiments and DSC ...174

Table 4-6: Calorimetric and kinetic analysis of PlyC (PlyCA) N211H T406R 190

Chapter V

Table 5-1: List of thermophilic peptidoglycan hydrolase catalytic domain candidates ..210

List of Figures

Chapter I

Figure 1-1: DAP-type and Lys-type peptidoglycan structure.....29

Figure 1-2: Cleavage site specificity by the major classes of endolysins.....31

Figure 1-3: Thin-section electron micrograph of PlyC-treated group A streptococci treated.....60

Figure 1-4: PlyCB acts as the cell wall binding domain of PlyC 66

Figure 1-5: X-ray crystal structure of PlyC 67

Figure 1-6: Directed evolution methodology overview.....87

Chapter II

Figure 2-1: Log distribution of the predicted change in folding free energy for all 2945 possible PlyCA CHAP domain point mutants calculated with FoldX 3.0 101

Figure 2-2: Comparison between the $\Delta\Delta G_{FoldX}$ and $\Delta\Delta G_{Rosetta}$ values of the final 31 mutant candidates retained after manual curation 102

Figure 2-3: SDS-PAGE analysis of the FoldX PlyC mutants.....105

Figure 2-4: Secondary structure and thermal stability determination.....107

Figure 2-5: Kinetic stability of wild-type PlyC and PlyC (PlyCA) T406R at 45°C 117

Figure 2-6: Local structure around wild-type PlyCA T406 with the proposed conformation of the mutant T406R superimposed 120

Chapter III

Figure 3-1: 96-well microtiter plate templates for directed evolution assay 127

Figure 3-2: Residual activity kinetic analysis comparing WT PlyC and 29C3 136

Figure 3-3: Residual activity kinetic analysis comparing WT PlyC to 29C3 at 35°C and 40°C.....138

Figure 3-4: Residual activity kinetic analysis comparing WT PlyC to 29C3 at 45°C.....139

Figure 3-5: Directed evolution assay methodology.....140

Chapter IV

Figure 4-1: SDS-PAGE analysis of the PlyC structural constructs.....160

Figure 4-2: Flowchart of the PlyC directed evolution methodology.....163

Figure 4-3: SDS-PAGE analysis of PlyC 33D2 constructs and PlyC (PlyCA) N211 charge mutants.....165

Figure 4-4: Kinetic stability of the directed evolution round 3 lead candidate, PlyC 33D2, and the isolated PlyC 33D2 point mutations.....166

Figure 4-5: Biophysical thermal analysis of wild-type PlyC and PlyC (PlyCA) N211H.....169

Figure 4-6: Kinetic half-life calculation for charge-specific PlyC (PlyCA) N211 mutants.....171

Figure 4-7: CD and DSC thermal analysis of charge-specific PlyC (PlyCA) N211 mutants.....173

Figure 4-8: pH-dependent thermal stability of wild-type PlyC and PlyC (PlyCA) N211H.....176

Figure 4-9: Modeling H211 into the 3.3-Å crystal structure of PlyC.....179

Figure 4-10: SDS-PAGE analysis of the putative H211 electrostatic interaction mutants.....182

Figure 4-11: Structural stability determination for the acidic amino acid candidate mutants in a ± N211H background.....184

Figure 4-12: Bacteriolytic activity evaluation against *S.pyogenes in vitro* 186

Figure 4-13: Modeling H211 and R406 into the PlyCA subunit.....188

Figure 4-14: Thermodynamic and kinetic stability of PlyC (PlyCA) N211H T406R.....189

Chapter V

Figure 5-1: Kinetic stability of different *Listeria* endolysins 200

Figure 5-2: Thermodynamic and kinetic stability of *B. anthracis* endolysin PlyG.....201

Figure 5-3: Plate lysis assay example 208

Appendix D

Figure D-1: DSC analysis of the isolated EAD and CBD of PlyG.....247

Figure D-2: Kinetic inactivation of wild-type PlyC and PlyCΔΔPly511_N at 45°C 249

Figure D-3: Thermodynamic characterization of Ply511 EAD and PlyCΔΔPly511N....250

Figure D-4: Biophysical characterization of a thermostabilized streptococcal chimera endolysin 252

List of Abbreviations

In alphabetical order

A	Pre-exponential factor
AA	Amino acid
Amp^r	Ampicillin-resistant
AMPs	Antimicrobial peptides
α_D	Distorted alpha-helix
α_R	Regular alpha-helix
ARDB	Antibiotic Resistance Genes Database
ATP	Adenosine triphosphate
β_D	Distorted beta-strand
β_R	Regular beta-strand
BS^3	Bis (sulfosuccinimidyl) suberate
CBADH	*Clostridium beijerinckii* alcohol dehydrogenase
CBD	Cell wall binding domain
CBD-MS	Cell wall binding domain-based magnetic separation
CBHI	Cellobiohydrolase I
CD	Circular dichroism
CDC	Center for Disease Control and Prevention
CF	Cystic fibrosis
CFP	Cyan fluorescent protein
CFSAN	Center for Food Safety and Applied Nutrition
CFU	Colony forming unit
CHAP	Cysteine, histidine-dependent amidohydrolase/peptidase
Cm^r	Chloramphenicol-resistant
C_p	Excess heat capacity
CRE	Carbapenem-resistant Enterobacteriaceae
CSF	Cerebrospinal fluid
DNA	Deoxyribonucleic acid
DSC	Differential scanning calorimetry
dsDNA	Double-stranded deoxyribonucleic acid
DSF	Differential scanning fluorimetry
DsRed	Discosoma sp. red fluorescent protein
EAD	Enzymatically active domain
EDTA	Ethylenediaminetetraacetic acid
EMS	Ethyl methane sulfonate
ENU	Ethylnitrosourea
E_A	Activation energy
epPCR	Error-prone polymerase chain reaction
EPS	Exopolymeric substance
FDA	United States Food and Drug Administration
G	Gibb's free energy

GAS	Group A streptococcus
GBS	Group B streptococcus
GCS	Group C streptococcus
GDS	Group D streptococcus
GES	Group E streptococcus
GFP	Green fluorescent protein
GFS	Group F streptococcus
GGS	Group G streptococcus
GLS	Group L streptococcus
GlcNAc	N-acetylglucosamine
GNS	Group N streptococcus
GyH	Glycosol hydrolase
HAI	Hospital-acquired infection
HGT	Horizontal gene transfer
hSHAPE	2' hydroxyl acylation analyzed by primer extension
H_{VH}	van't Hoff enthalpy
IDSA	Infectious Disease Society of America
IMAC	Immobilized metal affinity chromatography
ip.	Intraperitoneal
IUBMB	International Union of Biochemistry and Molecular Biology
k	Rate constant
LB	Luria-Beterani
LS	Light scattering
MBEC	Minimum biofilm elimination concentration
mBTL	Meta-bromo-thiolactone
mDAP	Meso-diaminopimelic acid
MDR	Multidrug resistance
MIC	Minimum inhibitory concentration
MNNG	Methylnitronitrosoguanidine
MRE	Mean residue ellipticity
MRSA	Methicillin-resistant *Staphylococcus aureus*
MSSA	Methicillin-susceptible *Staphylococcus aureus*
MurNAc	N-acteylmuramic acid
NCBI	National Center for Biotechnology Information
NIST	National Institute of Standards and Technology
NRMSD	Normalized root mean square deviation
NSAIDs	Non-steroidal anti-inflammatory drugs
nt	Nucleotide
OD	Optical density
OE-PCR	Overlap-extension polymerase chain reaction
PBS	Phosphate buffered saline
PCR	Polymerase chain reaction
PDR	Pandrug-resistant
PEG	Polyethylene glycol
Phos	Phosphate
PIA	Polysaccharide intercellular adhesin

PTDs	Protein transduction domains
Q	Heat evolved at a given temperature
QIDP	Qualified Infectious Disease Product
QS	Quorum sensing
QSI	Quorum sensor inhibitor
Q_t	Total heat of a thermodynamic process
R	Universal gas constant
r genes	Resistance genes
RI	Refractive index
RNA	Ribonucleic acid
rRNA	Ribosomal ribonucleic acid
SDM	Site-directed mutagenesis
SDS	Sodium dodecyl sulfate
SDS-PAGE	Sodium dodecyl sulfate polyacrylamide gel electrophoresis
SEC	Size-exclusion chromatography
T	Temperature
$T_{1/2}$	Circular dichroism melt equilibrium temperature
$t_{1/2}$	Half-life
TB	*Mycobacterium tuberculosis*
TBADH	*Thermoanaerobacter brockii* alcohol dehydrogenase
TCEP	Tris-(2-carboxyethyl)phosphine
T_G	Thermal transition temperature
T_m	Melting temperature
TNF	Tumor necrosis factor
TRAIL	Tumor necrosis factor-related apoptosis-inducing ligand
TyrRS	Tyrosyl-transfer ribonucleic acid synthetase
v	Differential scanning calorimetry scan rate
VISA	Vancomycin-intermediate *Staphylococcus aureus*
VGT	Vertical gene transfer
V_{max}	Maximum velocity
VRSA	Vancomycin-resistant *Staphylococcus aureus*
WHO	World Health Organization
WT	Wild-type
XDR	Extensively drug-resistant

Chapter I

Introduction and Literature Review

Antibiotics and Resistance Development

The discovery and consequent medicinal application of antibiotics has long been considered one of the most important findings in modern medicine. Since their introduction in the 1940s, the antimicrobial efficacy of antibiotics has translated to a significant reduction in human morbidity and mortality provoked by pathogenic bacteria (Andersson and Hughes, 2010). However, the intensive use of antibiotics (estimated in 2002 to be 100,000-200,000 tonnes per annum worldwide (Wise, 2002)) and subsequent misuse has dramatically increased the frequency of pathogen resistance formation in hospital and community environments. According to the Antibiotic Resistance Genes Database (ARDB), there is now an estimated 23,000 potential resistance genes (r genes) of nearly 400 different types predicted from available bacterial genome sequences (Liu and Pop, 2009). The loss in antimicrobial efficacy instituted by these resistance genes, coupled with the significant decrease in new antibiotic development due to market failure and regulatory disincentives, has provoked the Infectious Disease Society of America (IDSA) to label antimicrobial resistance as one of the greatest threats to human health on a global scale (Infectious Disease Society of America, 2011).

Antibiotic Discovery and Resistance Timeline

Antimicrobials are among the most successful chemotherapeutics in the history of medicine. These agents have been exploited over millennia to control and prevent many infectious diseases throughout history known to be leading causes of human morbidity

and mortality, thereby saving countless lives. Unfortunately, the modern antibiotic era has been met with rapid and wide-spread resistance formation by bacterial pathogens, thus stimulating a transition to a post-antibiotic era where medical advances to date are negated (Guay, 2008; Lew et al., 2008; Woodford and Livermore, 2009). As a result, there is clear definitive need for an alternative antimicrobial approach to common non-efficacious chemotherapeutics.

The use of antimicrobial agents long outdates the modern antibiotic era. Prior to identifying and investigating the causative agents of infectious disease in a laboratory setting, therapeutic progress relied solely on the unpredictability of chance and empirical observation. For this reason, the earliest examples of successful antimicrobials employed by mankind are natural products. For example, Chinese herbalists for millennia used qinghaosu (artemisinin), a potent modern day anti-malarial drug, from *Artemisia* plants as a remedy for many illnesses (Cui and Su, 2009). Quinine, an anti-malarial compound from the bark of the cinchona tree, and emetine, a compound collected from the ipecacuanha root used to treat amoebic dysentery, are two other ancient remedies that were initially introduced in the seventeenth century to Europe and South America (Finch et al., 2012). Other common herbs used include extract from the male fern *Dryopteris filix-mas*, which helps eradicate tapeworm infections, as well as santonin from the seed-heads of *Artemisia cina* and chenopodium oil of *Chenopodium ambrosioides*, both of which act against intestinal roundworms. In addition to herbal-derived remedies and contrary to the prevalent notion of initial antibiotic use being confined only to 20th century, histological studies of skeletal remains from an ancient Sudanese Nubian population showed traces of the antibiotic tetracycline dating back to 350-550 CE

(Armelagos, 1969; Bassett et al., 1980; Cook et al., 1989; Nelson et al., 2010). Moreover, since the sixteenth century, mercury had been used for its antibacterial properties to treat syphilis infections (Finch et al., 2012).

The foundation for modern twentieth century chemotherapy was constructed by the German scientist Paul Ehrlich during his quest to identify antiprotozoal agents to combat the newly discovered parasites of trypanosomiasis, the causative agent of African sleeping sickness, and malaria (Finch et al., 2012). Based on the observation that aniline and other synthetic dyes could specifically stain these parasites when isolated from the tissues of infected patients, Ehrlich rationalized that compounds could be developed that would "be able to exert their full action exclusively on the parasite harbored within the organism." It was this key concept that fueled Ehrlich in 1904 to begin a voluminous and systematic screening program to uncover safe arsenical derivatives against syphilis, a sexually transmitted disease caused by the spirochete *Treponema pallidium* that was endemic and almost incurable at the time. In collaboration with chemist Alfred Bertheim and bacteriologist Sahachiro Hata, Ehlrich was able to synthesize and screen hundreds of compounds against syphilis-infected rabbits. Five years later in 1909, the sixth arsenical compound in the 600^{th} series tested, hence termed compound 606, was experimentally shown to fully cure syphilis-infected rabbits and furthermore exhibited significant promise as a human therapeutic due the compound's efficacy and acceptable safety profile when treating patients infected with the venereal disease (Ehrlich and Hata, 1910). Despite the laborious injection process and side effects associated with compound 606, the drug, later known as arsphenamine (Salvarsan), and its improved, less toxic derivative neoarphenamine (Neosalvarsan), were effective at treating both syphilis and African

sleeping sickness in humans. As a result, this particular antimicrobial represented the most actively prescribed drug until being replaced by penicillin in the 1940s (Mahoney et al., 1943).

Although Ehrlich never fulfilled his personal goal of using dyes as a therapeutic agent, this conceptual antimicrobial approach paid dividends years later. Scientists at the German pharmaceutical company Bayer in 1924 were able to develop a drug named suramin (Germanin), which was a colorless derivative of trypan blue dye, to treat the parasitic diseases trypanosomiasis and onchocerciasis (Finch et al., 2012). Additionally, studying the effects of numerous modifications to Ehrlich's methylene blue dye prompted scientists at Bayer to introduce similar molecular alterations to quinine-like compounds. These systematic screens resulted in the development of the world's first synthetic antimalarial drug, plasmochin (pamaquine), and the acridine derivative, atebrin.

The continued interest in therapeutic dyes ultimately led to the discovery of the first broad-spectrum antibacterial agents, termed sulfa drugs or sulfonamides. In 1932, Gerhard Domagk, an experimental pathologist at Bayer, screened a large number of synthetic dyes for antimicrobial activity. One dye, sulfonamidochrysoidine (KI-730, Prontosil), which was synthesized by Bayer chemists Josef Klarer and Fritz Mietzsch, demonstrated antibacterial activity against a wide-range of bacterial species known to be causative agents for a number of infectious diseases (Domagk, 1935). It was later concluded by the Tréfouëls and their colleagues in France that the sulfanilamide chemical group of the dye was responsible for the antimicrobial efficacy of the compound. The use of subcutaneous sulfanilamide lowered the mortality rate of acute meningococcal meningitis from 70-90% in the pre-antibiotic era to approximately 10% (Schwentker et

al., 1984). As a chemical, sulfanilamide, which consists of a sulfonamide functional group attached to aniline, was readily used in the dye industry since 1908 and thus was not patentable by Bayer as an antimicrobial. The cheap cost of synthesizing this particular off-patent chemical group coupled with how simplistic the sulfanilamide moiety was to modify ultimately prompted other companies to immediately started mass producing the drug for commercial application (Aminov, 2010). Accordingly, with sulfanilamides representing the oldest class of antibiotics on market, they also represent one of the most broadly distributed cases of drug resistance by virtue of the sulfa drug resistance genes being encoded by class 1 integrons, which are mobile genetic elements that can be easily transmitted and integrated into the genome of the host bacterium.

The development of classical antibiotics was instigated by the discovery of the β-lactam antibiotic penicillin by Alexander Fleming in 1928. Although other scientists before Fleming have documented similar observations relating to the antimicrobial efficacy of *Penicillium*, it was his persistent belief in cultivating the active substance derived from the mold and utilizing it as a therapeutic agent that set him apart. Early attempts by Fleming to exploit penicillin were met with failure, mostly due to the inability to devise experimental approaches to successfully purify and concentrate the antimicrobial. Due to the work of Howard Florey and Ernest Chain from Oxford University, it was not until 1940 that a protocol describing the purification of penicillin in sufficient quantities for clinical testing was published (Chain et al., 2005). Their protocol led to the mass production and distribution of penicillin in 1943. Interestingly, the first reported hospital use of a drug that would be classified today as an antibiotic was documented nearly 30 years prior to the discovery of penicillin. Bacterial extracts of the

drug named pyocyanase, which is derived from *Pseudomonas aeruginosa* (formally known as *Bacillus pyocyaneus*), was prepared in 1899 by the German physicians Rudolph Emmerich and Oscar Löw (Emmerich and Löw, 1899). Both *P. aeruginosa* cells and pyocyanase extracts displayed antimicrobial activity against a wide-range of pathogenic bacterial species, prompting Emmerich and Löw to attempt to use the pyocyanase extract as a therapeutic. Unfortunately, pyocyanase treatment was shortly abandoned due to the inherent toxicity and poor efficacy of the extract.

Despite the drug's success as an antibacterial agent, penicillin was more effective against Gram-positive bacteria species than Gram-negative, thus inciting scientists to continue looking for alternative antibiotics. In 1943, the first aminoglycoside antibiotic, streptomycin, was discovered by Selman A. Waksman, a Ukrainian émigré, and Albert Schatz, who was Waksman's research student at the time, during a systematic screening of soil organisms, namely actinomycetes. The antibacterial spectrum of streptomycin perfectly complimented penicillin by inhibiting many Gram-negative bacteria, including *Mycobacterium tuberculosis* (TB).

Following the conclusion of the Second World War, the discovery of streptomycin provoked pharmaceutical companies to start investing in antibiotic drug discovery. An immense amount of soil samples from all over the world were screened for antibiotic-producing microorganisms and although thousands of newly discovered antibiotics failed preliminary toxicity tests, most of the major families of antibiotics had been discovered by the mid-1950s, including the peptide antibiotics (e.g. bacitracin (1945)), chloramphenicol (1947), the tetracycline antibiotics (e.g. chlortetracycline (1948)), the macrolide antibiotics (e.g. erythromycin (1952)), the cyclic peptide

antibiotics (e.g. cycloserine (1955)) and cephalosporin C (1955), which represents the second major group of β-lactam antibiotics. In addition to naturally occurring antibiotics, synthetic antibiotic compounds have been produced, including the tuberculosis remedy isoniazid (1952), as well as the first quinolone antibacterial agent nalidixic acid (1962). Overall, the golden era of antibiotic discovery existed between the 1950s and 1970s, with only the oxazolidinone antibiotic class being discovered since then.

There are five basic antibacterial mechanisms utilized by antibiotics that either disrupts essential bacterial cell metabolic processes or structures (Finch, 2010). The most common mechanism employed by antibiotics involves interfering with peptidoglycan biosynthesis through inhibiting cell wall cross-linking or precursors (e.g. penicillins, cephalosporins, glycopeptides, carbapenems, monobactams, aztreonam, bacitracin, cycloserine, fosfomycin, isoniazid, ethambutol). The second largest class of antibiotics is the translation inhibitors, which directly interact with the bacterial 30S (e.g. aminoglycosides, tetracyclines) or 50S (e.g. macrolides, chloramphenicol, clindamycin, linezolid, streptogramins) ribosomal subunits to suppress protein synthesis. Other antibiotic mechanisms include disruption of cell membrane permeability (e.g. polymyxin, ionophores), hindrance of DNA (e.g. quinolones, novobiocin, nitrofurans, metronidazole) and RNA (e.g. rifampin, isoniazid, bacitracin) synthesis, and antimetabolite activity that blocks enzyme-catalyzed reactions of the bacterial cell metabolism, such as mycolic acid synthesis inhibitors (e.g. isoniazid) and folic acid synthesis inhibitors (e.g. sulfonamides, dapsone, trimethoprim).

The efficacy of a therapeutic agent is ultimately compromised over time by the

potential of tolerance or resistance to the compound through Darwinian evolution (Davies and Davies, 2010). This observation is seen repeatedly with chemotherapeutic agents that target disease-causing bacteria, fungi, parasites and viruses. The complexity of these biochemical and physiological resistance mechanisms has impeded the formulation of effective approaches for the prevention and control of resistance formation.

Bacterial resistance to antimicrobials has gotten the most attention due to the rapid evolution and dissemination of these drug-resistant microorganisms, as well as their drastic effect on human morbidity and mortality. Since the discovery and mass production of the first class of antibiotics, there are many subsequent examples of expeditious antibiotic resistance development after the initial therapeutic introduction of the drug. In addition to the aforementioned resistance formation to sulfa drugs, which represents the first class of antibiotics, resistance was observed to penicillin prior to the extensive use of the antibiotic. In 1940, two years before the first reported therapeutic use of the antibiotic, two members of the penicillin discovery team, Edward Abraham and Ernst Chain, identified an enzyme from *Staphylococcus*, termed penicillinase, which could degrade penicillin and render the drug inactive (Abraham and Chain, 1940). Other examples of antibiotic resistance include resistance against streptomycin, tetracycline, erythromycin, methicillin, spectinomycin, gentamicin, vancomycin, imipenem, ceftazidime, levofloxacin, linezolid, daptomycin and ceftaroline (Table 1-1).

Additionally, bacterial pathogens associated with epidemics of human disease have evolved into multidrug-resistant (MDR) forms, particularly in hospital settings, and consequently have been labeled as “superbugs” due to the enhanced morbidity and

Table 1-1. Antibiotic Resistance Timeline. (Adapted from Centers for Disease Control and Prevention, 2013 and Unemo and Shafer, 2011)

Antibiotic	Introduced	Resistance Observed	Organism
Penicillin	1942	1940	*Staphylococcus*
		1958	*Gonococcus*
		1965	*Pneumococcus*
Streptomycin	1949	1958	*Gonococcus*
Tetracycline	1950	1959	*Shigella*
		1985	*Gonococcus*
Erythromycin	1953	1968	*Streptococcus*
		1977	*Gonococcus*
Methicillin	1960	1962	*Staphylococcus*
Spectinomycin	1961	1987	*Gonococcus*
Gentamicin	1967	1979	*Enterococcus*
Vancomycin	1972	1988	*Enterococcus*
		2002	*Staphylococcus*
Imipenem	1985	1998	Enterobacteriaceae
Ceftazidime	1985	1987	Enterobacteriaceae
		2001	*Gonococcus*
Levofloxacin	1996	1996	*Pneumococcus*
Linezolid	2000	2001	*Staphylococcus*
Daptomycin	2003	2005	*Staphylococcus*
Ceftaroline	2010	2011	*Staphylococcus*

mortality affiliated with these microorganisms. Some examples of nosocomial MDR pathogens include *Acinetobacter baumanni, Burkholderia cepacia, Campylobacter jejuni, Citrobacter freundii, Clostridium difficile, Enterobacter* spp., *Enterobacter faecium, Enterococcus faecalis, Escherichia coli, Haemophilus influenza, Klebsiella pneumoniae, N. gonorrhoeae, Proteus mirabilis, P. aeruginosa, Salmonella* spp., *Serratia* spp., *Staphylococcus aureus, Staphylococcus epidermidis, Stenotrophomonas maltophilia* and *Streptococcus pneumoniae* (Davies and Davies, 2010). Particular strains of MDR TB have been uncovered and labeled as extensively drug-resistant (XDR) microorganism, while MDR strains of *Acinetobacter, Pseudomonas* and Enterobacteriaceae have been characterized as pandrug-resistant (PDR). XDR TB display resistance against isoniazid and rifampin, fluoroquinolones and at least one of the three injectable second-line drugs (i.e. amikacin, kanamycin or capreomycin) (Dorman and Chaisson, 2007). PDR bacterial strains are specifically resistant to the seven antimicrobial agents cefepime, ceftazidime, imipenem, meropenem, piperacillin-tazobactam, ciprofloxacin and levofloxacin (Falagas and Karageorgopoulos, 2008). With the continual decrease in antibacterial efficacy, the lack in development of novel efficacious antibiotics has threatened a regression to the pre-antibiotic era.

Bacterial resistance to antibiotics may be an intrinsic trait of the microorganism that renders it naturally resistant, or the bacterium may acquire resistance by either inducing mutations to its own DNA or acquiring resistance genes from another source. Natural resistance refers to antibiotic resistance of bacteria species without any additional genetic alterations. Examples of inherent resistance mechanisms include the lack of an intracellular transport system for the antibiotic, presence of energy-dependent multidrug

efflux pumps, absence of the antibiotic target molecule or structure (e.g. mycoplasma is resistant to β-lactam antibiotics due to the absence of a cell wall structure) and physical barriers (e.g. restricted permeability of the outer membrane of Gram-negative bacteria) (Normark and Normark, 2002).

Acquired resistance can be accomplished through vertical or horizontal gene transfer. Vertical gene transfer (VGT) involves the direct transmission of resistance genes that are generated spontaneously in the presence of antibiotics to bacterial progeny during DNA replication (Lawrence, 2005). Horizontal gene transfer (HGT) consists of the lateral acquisition of plasmid-encoded antibiotic genes that originate from a bacterial or viral source. The three HGT methods are equivalent to the three techniques used by bacteria to generate genetic diversity, which include conjugation, transformation and transduction (Ochman et al., 2000). Conjugation, the main mechanism of HGT, promotes the transfer of genetic material through direct cell-to-cell contact between related or unrelated bacteria species. Conjugation can also result in the exchange of genetic material between different biological domains, such as bacteria and plants, and bacteria and yeast (Buchanan-Wollaston et al., 1987; Heinemann and Sprague, 1989). Transformation involves the uptake of naked DNA, mainly supplied from the death and lysis of another bacterium, through absorption due to the natural competency of the bacterial cell. Particular bacteria species, such as *N. gonorrhoeae* and *H. influenza*, display perpetual competence, whereas other bacteria species, such as *S. pneumoniae* and *Bacillus subtilis*, are only competent at a certain physiological stage in their life cycle (Dubnau, 1999). Finally, new genetic material can be inserted either as an isolated plasmid or integrated into the genome of the bacterium by bacterial viruses known as bacteriophage (phage).

Although phage are highly ubiquitous in the environment (Jiang and Paul, 1998; Schicklmaier and Schmieger, 1995), the spectrum of bacteria that can be transduced depends on the presence of a specific receptor molecule on the cell surface. As a result, genetic exchange promoted by transduction typically occurs between two related bacterial species.

Inherent and acquired resistance by bacteria exploits several conserved techniques to render antibiotics ineffective (Finch, 2010). The main mechanisms include:

- Expressing enzymes that target and inactive the antibiotic before or after the drug enters the bacterial cell
- Modifying the cell envelope to decrease permeability
- Expelling the antibiotic from the intracellular environment by transmembrane efflux pumps
- Altering the target to decrease antibiotic binding affinity
- Evading target recognition by the antibiotic through the acquisition of a novel metabolic pathway
- Protecting the target by producing a protein to prevent the antibiotic from reaching it

These various resistance processes do not exist in isolation and instead rely on the cooperation of two or more distinct mechanisms in order to confer any level of resistance.

Health and Economic Implications

The efficacy of antibiotics is readily deteriorating due to their overuse, with large

quantities of antibiotics being commonly used to promote the growth of food-producing animals, and misuse, with up to 50% of all antibiotics prescribed for people not being needed or optimally effective (Centers for Disease Control and Prevention, 2013; Wise, 2002). The World Health Organization (WHO) and CDC both recognize antibiotic-resistant microorganisms as one of the greatest threats to human health worldwide due to the prolonged illness, greater risk of death and higher economic costs associated with these infections. Their rapid emergence and dissemination has prompted world health leaders to describe antibiotic-resistant microorganisms as "nightmare bacteria" that "pose a catastrophic threat" to people in every country of the world. Combined with the rapid loss of antimicrobial efficacy, the dramatic reduction in antibiotic development over the past 30 years has stimulated the prevalence of antimicrobial resistance on a global scale.

According to the IDSA, nearly two million people in the United States develop hospital-acquired infections (HAIs), resulting in nearly 100,000 deaths annually. It is estimated that the vast majority of those deaths are caused by antibiotic-resistant pathogens. Methicillin-resistant *S. aureus* (MRSA) alone kills more people in the United States every year than emphysema, HIV/AIDS, Parkinson's disease and homicide combined (Klevens et al., 2007). The CDC estimates that of the 140,000 healthcare-associated Enterobacteriaceae infections in the United State annually, about 9,300 are caused by carbapenem-resistant Enterobacteriaceae (CRE). Up to half of all bloodstream infections caused by CRE result in death.

Along with the health complications associated with antimicrobial resistance, the non-specific disruption of the normal colonic microflora by broad spectrum antibiotics has been implicated as a causative agent for life-threatening *C. difficile* nosocomial

infection (Kelly et al., 1994). Dormant *C. difficile* spores are germinated upon antibiotic treatment, subsequently allowing the actively growing bacteria to readily colonize the colon epithelial tissue and flourish due to the decreased commensal microflora population. The consequential release of exotoxins by *C. difficile* causes diffuse colonic epithelial necrosis with pseudomembrane formation, causing colitis (Jobe et al., 1995). Currently, nearly 250,000 people in the United States each year require hospital care for *C. difficile* infections, culminating in at least 14,000 deaths. Along with CRE and drug-resistant *N. gonorrhoeae*, the pathogenicity of *C. difficile* has caused the CDC to label the microorganism as an urgent threat to human health.

Infections associated with antibiotic-resistant microorganisms continually add substantial and avoidable costs to an already overburdened United States healthcare system. Antibiotic-resistant infections directly cause prolonged and/or costlier treatments, extended hospital stays with additional hospital visits and healthcare use, and increased disability and death when compared to antibiotic-susceptible bacteria. The total domestic economic ramifications of antibiotic resistance are extensive, yielding an estimated $20 billion in excess direct healthcare costs in the United States as well as societal costs totaling $35 billion due to loss in productivity (Roberts et al., 2009).

The development of new antibiotics has been impeded by market failure and regulatory disincentives. Besides the reduction in therapeutic efficacy caused by resistance formation, the introduction of a new antibacterial agent, which is estimated to cost between $400-$800 million per approved drug (DiMasi et al., 2003), is not as profitable as other therapeutic classes of drugs because of the length of treatment (Spellberg et al., 2008). Antibiotics are transient therapies utilized for no more than two

weeks in order to cure infectious disease. Alternatively, the treatment of incurable chronic diseases, such as heart disease, cancer and diabetes, are typically required to be taken over the lifetime of the patient to suppress symptoms. Pharmaceutical and biotechnology companies are also deterred from developing new antibiotics because of the ambiguous regulatory guidelines. Drug companies have stated there are significant regulatory hurdles imposed by the United States Food and Drug Administration (FDA), which are attributable to the confusion concerning what studies and evidence the agency deems acceptable to demonstrate the safety and efficacy of a new drug (Blaser and Bartlett, 2006; Boucher, 2008). Furthermore, the FDA tightened the statistical standard that companies must achieve to show antimicrobial efficacy in clinical trials, thereby raising drug development costs because of increased clinical trial size and duration (Coates et al., 2002). However, the FDA has recently begun taking steps to incentivize new antimicrobial development to combat the epidemic of antibiotic-resistant infections. As part of the program established by the administration, any drug designated as a Qualified Infectious Disease Product (QIDP) gets a priority review and an expedited review process. If approved, the drug also then qualifies for an additional five years of marketing exclusivity.

Alternative Antimicrobial Approaches

As global health and economic complications tied to antibiotic resistance become more prevalent, there is an increasing need for developing alternative antimicrobial approaches. Successfully doing so will improve productivity and quality of life, ultimately allowing people to live longer, healthier lives. Some examples of alternative

antibacterial therapies currently being investigated include immunotherapy, quorum sensing inhibitors, antimicrobial peptides, iron chelators and phage therapy.

The practice of bacterial vaccine therapy to prevent or cure infectious disease was initiated in 1879 when French chemist and microbiologist Louis Pasteur created the first live attenuated bacterial vaccine against *Pasteurella multocida* (Pasteur, 1880). Since then, bacterial vaccines have proven to be effective against a variety of pathogens, including *Bacillus anthracis* (1880) (Tigertt, 1980), *Vibrio cholera* (1884) (Levine and Pierce, 1992), *Salmonella typhi* (1896) (Colebrook, 1954; Kolle and Hetsch, 1929; Pfeiffer and Kolle, 1896; Wright and Semple, 1897), *Yersinia pestis* (1897) (Haffkine, 1897; Lowy, 1996), *Bordetella pertussis* (1915) (Luttinger, 1915), *Corynebacterium diphtheriae* (1923) (Glenny and Hopkins, 1923), *Clostridium tetani* (1926) (Ramon and Zoeller, 1926, 1927), *Mycobacterium bovis* (1927) (Parish, 1965), *Neisseria meningitidis* (1970) (Gotschlich et al., 1969a; Gotschlich et al., 1969b), *S. pneumoniae* (1977) (Austrian et al., 1976) and *H. influenzae* (1985) (Centers for Disease Control and Prevention, 1985). Serum therapy, which involves the administration of immune serum (i.e. antiserum) from immunized animals or humans for the treatment and prevention of infectious disease, has also displayed antibacterial efficacy since its introduction in 1890 (Behring and Kitasako, 1890; Buchwald and Pirofski, 2003). For example, serum therapies were able to lower diphtheria mortality from 50-80% to 6-15% (Buchwald and Pirofski, 2003) and immunoneutralize the tetanus toxin (Grundbacher, 1992) and pyrogenic exotoxins that cause scarlet fever (Buchwald and Pirofski, 2003; Weisse, 2001). Besides the several drawbacks affiliated with serum therapy, such as the occurrence of serum sickness, the risk of disease transmission and lot-to-lot variations of

different serum preparations, the routine use of bacterial vaccines was diminished over the past 70 years due to the advent of antibiotic therapy (Casadevall, 1996).

Quorum sensing (QS) is defined as a cell-density-dependent regulatory mechanism based on the release of low molecular weight signal molecules that coordinate the gene expression in a given population of bacteria (Ng and Bassler, 2009). The formation and behavior within biofilms, protective microenvironments comprised of bacteria and exopolymeric substances (EPS), are regulated through bacterial QS chemical signals to stimulate virulence gene expression. At least 65% of pathogenic bacteria are linked to bacterial communities which proliferate by forming biofilms (Lewis, 2007), which is problematic considering bacteria are typically 1,000 times more resistant to antibiotics in these specialized structures than their planktonic counterparts (Koch and Hoiby, 2000; Olson et al., 2002). One strategy currently being explored involves using quorum sensor inhibitors (QSI) to prevent biofilm biosynthesis. For example, partial inhibition of the quorum-sensing receptors LasR and RhlR by the QSI meta-bromo-thiolactone (mBTL) adequately inhibits production of the pyocyanin toxin as well as biofilm formation in *P. aeruginosa* (O'Loughlin et al., 2013). Anti-biofilm agents, such as QSI, have therapeutic potential because of their ability to degrade biofilm structures and resensitize the planktonic bacteria to antimicrobials. Taking into account the major health complications caused by biofilm growth on prosthetic devices, an anti-biofilm QSI could serve as a valuable prophylactic to apply to ventilators, catheters, etc., where the nidus of infection can be formed (Tillotson and Theriault, 2013).

Antimicrobial peptides (AMPs) are a group of gene-encoded low molecular weight (10-50 amino acids) natural compounds produced in all organisms (Joerger,

2003). These typically cationic (general +2 to +9), amphipathic peptides display nonspecific antibacterial activity by instigating cell membrane micellization or depolarization (Lohner and Blondelle, 2005; Toke, 2005), inhibiting cell wall biosynthesis (Breukink and de Kruijff, 2006; Hasper et al., 2006) or degrading bacterial nucleic acids (Vankemmelbeke et al., 2005; Zarivach et al., 2002). Despite nearly two decades of identifying or bioengineering AMPs, there has been limited success in the clinic (Zhang and Falla, 2006). To date, there are four total cationic AMPs or proteins that have advanced to phase 3 clinical trials. These antimicrobials are specific for curing or preventing impetigo and diabetic foot ulcers (the frog magainin derivative MSI-78), oral mucosaitis (the pig protegrin derivative IB-367; Iseganan), sepsis (the human bactericidal permeability protein derivative $rBPI_{23}$; Neuprex) and catheter-associated infections (cattle indolicidin variant CP-226; Omiganan) (Hancock and Sahl, 2006). Of the four, only two peptides demonstrated efficacy.

Iron is essential for many cellular reactions in bacterial pathogens, including oxygen transport, energy production and the regulation of gene expression. It has also been shown that biofilm formation on abiotic surfaces is largely stimulated by iron, in part by regulating surface motility and maintaining the biofilm polysaccharide matrix (Banin et al., 2005; Berlutti et al., 2005; Patriquin et al., 2008; Singh, 2004; Singh et al., 2002). With this understanding, iron chelators have been researched and developed as antimicrobial agents to prevent and/or disrupt biofilm structures. For example, iron chelators have been effective for the prevention and inhibition of *P. aeruginosa* biofilms on both cystic fibrosis (CF) airway epithelial cells and abiotic surfaces. Lactoferrin, an iron-binding protein present in airway secretions, inhibited biofilm formation by blocking

P. aeruginosa adherence (Singh et al., 2002). Ethylenediaminetetraacetic acid (EDTA), a general metal chelator, disrupted *P. aeruginosa* biofilms growing on polycarbonate chips (Banin et al., 2006), catheters (Kite et al., 2004; Raad et al., 2003; Yakandawala et al., 2007) and stainless steel discs (Ayres et al., 1998). Using a cystic fibrosis co-culture model, combining tobramycin, the primary antibiotic used to treat CF lung infections, with either of the two FDA-approved iron chelators, deferoxamine or deferasirox, reduced the established *P. aeruginosa* biofilm mass by approximately 90% and decreased resensitized viable bacteria by 7-log units (Moreau-Marquis et al., 2009).

Phages, discovered independently by Frederick Twort and Felix d'Herelle respectively in 1915 and 1917, were first used therapeutically in 1919 by d'Herelle to successfully treat severe dysentery (Summers, 1999). Prior to viral infection, bacterial cells are involved in replicating their own DNA, as well as transcribing and translating its genetic information in order to perform biosynthesis, growth and cell division. After infection, the viral DNA takes over the molecular machinery of the host cell in order to synthesize the nucleic acids and proteins required for the production of new virions. The viral DNA replaces the host bacterium's DNA as the template for both replication and transcription to respectively generate more viral DNA and mRNA. The viral mRNAs are then translated by using the bacterial ribosomes, tRNAs and amino acids to produce the various viral proteins.

Bacterial infections caused by phage can either be lysogenic (temperate) or lytic (virulent). For the double-stranded DNA (dsDNA) phage lytic cycle, the host cell infection process consists of four primary steps. The first step involves an initial weak interaction between the phage and bacterium involving the tail fibers of the phage

recognizing and reversibly adhering to a specific epitope that is displayed on the surface of the target bacterium. Next, one or more components of the base plate of the phage irreversibly bind to bacterial cell surface. The sheath of the phage then contracts and allows the core to mechanically or enzymatically penetrate the bacterial envelope. Nucleic acid from the phage head passes through the core structure and into the periplasm of the bacterium. The irreversibly surface-bound phage remains on the outside of the bacterium as "ghost".

The subsequent steps of the lytic replication cycle involve synthesis of phage components, assembly, maturation and virion release. Early dsDNA lytic phage genes are transcribed and translated to produce a set of proteins primarily needed for phage DNA replication. Some examples of early proteins include a viral DNA-dependent DNA polymerase, a DNAse enzyme that targets and degrades host DNA, and peptidoglycan cell wall hydrolases (i.e. endolysins). Expression of late genes commences after a sufficient number of phage genomes have been replicated. These late phage genes mainly encode the structural proteins that make up the capsomeres and the various components of the tail assembly. The capsomeres assemble to form the capsid structure of the phage and are spontaneously packaged with a copy of the phage genome. The tail and accessory structures assemble and complex with the capsid to form the mature infective virion. The exact moment of host cell lysis is regulated by a small membrane protein called a holin, which, in combination with the endolysin, constitutes the lytic system of dsDNA lytic phage (Wang et al., 2000). Holins, which are expressed late in the lytic phage replication cycle, oligomerize on the inner membrane to generate pore-forming complexes that disrupt membrane potential and permeabilize the lipid bilayer to allow the cytosolic

endolysins access to the periplasmic peptidoglycan (Wang et al., 2003; Young, 1992). Peptidoglycan functions as the major structural unit of the bacterial cell, supporting an internal osmotic pressure of 20-50 atmospheres in the case of Gram-positive microorganisms (Arnoldi et al., 2000; Doyle and Marquis, 1994; Whatmore and Reed, 1990). The endolysin subsequently degrades the bacterial cell wall to incite hypotonic lysis and progeny virion liberation.

Several characteristics of lytic phage that makes them potentially attractive therapeutic agents include their antibacterial efficacy against pathogenic bacteria, safety due to their high specificity, low dosage requirements to achieve optimal therapeutic effects because of their self-replicating and self-limiting nature, and rapid engineering potential to combat newly emerging bacterial threats (Sulakvelidze et al., 2001). In addition to d'Herelle's laboratory in Paris, which later became the large French company L'Oréal, the United States began producing therapeutic phages for commercial use. In the 1940s, the Eli Lilly Company from Indianapolis produced seven phage human therapeutic products that targeted pathogenic microbes such as staphylococci, streptococci and *E. coli*. These preparations consisted of sterile broth from phage-lysed cultures of the targeted bacteria (e.g. Colo-lysate, Ento-lysate, Neiso-lysate and Staphylo-lysate) or the same preparations in a water-soluble jelly base (e.g. Colo-jel, Ento-jel and Staphylo-jel). They were used to treat an assortment of infections with varying degrees of success, including abscesses, suppurating wounds, vaginitis, acute and chronic infections of the upper respiratory tract, and mastoid infections (Sulakvelidze et al., 2001). Although issues with efficacy and the eventual discovery of antibiotics caused phage therapy to cease in most of the Western world, the therapeutic use of phages with or

without antibiotics continued in Eastern Europe and in the former Soviet Union. There are currently over a hundred phage therapy publications available in the Georgian, Russian and English literature, including Ph.D. theses and meeting presentations from the former Soviet Union, that report the successful exploitation of phage therapy for prophylaxis and treatment of bacterial infections in humans. Some of the major human phage therapy studies performed in Poland and the former Soviet Union that were published in peer-reviewed journals are depicted in Table 1-2.

Bacteriophage-Derived Peptidoglycan Hydrolases

A promising alternative antimicrobial approach to conventional antibiotics involves the use of bactericidal enzymes derived from lytic phage, termed endolysins. Endolysins are peptidoglycan cell wall hydrolases that act on the host bacterium cell wall late in the phage replication cycle. These enzymes hydrolyze critical covalent bonds essential for maintaining cell wall structural integrity. As a result, the intense intracellular turgor pressure ruptures the cell to cause hypotonic lysis and progeny virion release.

Due to the absence of an outer membrane, extrinsically applied recombinant endolysins have direct access to the bacterial cell wall to lyse susceptible Gram-positive pathogens, thereby highlighting its therapeutic potential. The efficacy of endolysins have been validated *in vitro* and/or *in vivo* against a variety of Gram-positive pathogens, including *Listeria monocytogenes* (Gaeng et al., 2000; Loessner et al., 2002), *S. pneumoniae* (Entenza et al., 2005; Jado et al., 2003; Loeffler et al., 2003; Loeffler et al., 2001; McCullers et al., 2007), *Streptococcus pyogenes* (Hoopes et al., 2009; Nelson et al., 2001), *Streptococcus agalactiae* (Cheng et al., 2005; Pritchard et al., 2004;

Table 1-2. Some of the major human phage therapy studies performed in Poland and the former Soviet Union. (Adapted from Sulakvelidze et al., 2001)

Reference(s)	Infection(s)	Etiologic agent(s)	Comments
(Babalova et al., 1968)	Bacterial dysentery	*Shigella*	*Shigella* phages were successfully used for prophylaxis of bacterial dysentery.
(Bogovazova et al., 1992)	Infections of skin and nasal mucosa	*K. ozaenae, K. rhinoscleromatis, K. pneumoniae*	Adapted phages were reported to be effective in treating *Klebsiella* infections in all of the 109 patients.
(Cislo et al., 1987)	Suppurative skin infections	*Pseudomonas, Staphylococcus, Klebsiella, Proteus, E.coli*	Thirty-one patients having chronically infected skin ulcers were treated orally and locally with phages. The success rate was 74%.
(Ioseliani et al., 1980)	Lung and pleural infections	*Staphylococcus, Streptococcus, E. coli, Proteus*	Phages were successfully used together with antibiotics to treat lung and pleural infections in 45 patients.
(Kochetkova et al., 1989)	Postoperative would infections in cancer patients	*Staphylococcus, Pseudomonas*	A total of 131 cancer patients having postsurgical would infections participated in the study. Of these, 65 patients received phages and the rest received antibiotics. Phage treatment was successful in 82% of the cases, and antibiotic treatment was successful in 61% of the cases.
(Kucharewicz-Krukowska and Slopek, 1987)	Various infections	*Staphylococcus, Klebsiella, E. coli, Pseudomonas, Proteus*	Immunogenicity of therapeutic phages was analyzed in 57 patients. The authors concluded that the phages' immunogenicity did no impede therapy.
(Kwarcinski et al., 1994)	Recurrent subphrenic abscess	*E. coli*	Recurrent subphrenic abscess (after stomach resection) caused by an antibiotic-resistant strain of *E. coli* was successfully treated with phages.
(Litvinova et al., 1978)	Intestinal dysbacteriosis	*E. coli, Proteus*	Phages were successfully used together with bifidobacteria to treat antibiotic-associated dysbacteriosis in 500 low-birth-weight infants.
(Meladze et al., 1982)	Lung and pleural infections	*Staphylococcus*	Phages were used to treat 223 patients having lung and pleural infections, and the results were compared to 117 cases where antibiotics were used. Full recovery was observed in 82% of the patients in the phage-treated group, as opposed to 64% of the patients in the antibiotic-treated group.
(Miliutina and Vorotyntseva, 1993)	Bacterial dysentery and salmonellosis	*Shigella, Salmonella*	The effectiveness of treating salmonellosis using phages and a combination of phages and antibiotics was examined. The combination of phages and antibiotics was reported to be effective in treating cases where antibiotics alone were ineffective.

(Perepanova et al., 1995)	Inflammatory urologic diseases	*Staphylococcus, E. coli, Proteus*	Adapted phages were used to treat acute and chronic urogenital inflammation in 46 patients. The efficacy of phage treatment was 92% (marked clinical improvements) and 84% (bacteriological clearance).
(Sakandelidze and Meipariani, 1974)	Peritonitis, osteomyelitis, lung abscesses, and postsurgical would infections	*Staphylococcus, Streptococcus, Proteus*	Phages administered subcutaneously or through surgical drains in 236 patients having antibiotic-resistant infections eliminated the infections in 92% of the patients.
(Sakandelidze, 1991)	Infectious allergoses (rhinitis, pharyngitis, dermatitis, and conjunctivitis)	*Staphylococcus, Streptococcus, E. coli, Proteus,* Enterococci, *Pseudomonas*	A total of 1,380 patients having infectious allergoses were treated with phages (360 patients), antibiotics (404 patients), or a combination of phages and antibiotics (576 patients). Clinical improvement was observed in 86, 48 and 83% of the cases, respectively.
(Slopek et al., 1984; Slopek et al., 1983a, b; Slopek et al., 1985a, b, c; Slopek et al., 1987)	Gastrointestinal tract, skin, head and neck infections	*Staphylococcus, Pseudomonas, E. coli, Klebsiella, Salmonella*	A total of 550 patients were treated with phages. The overall success rate of phage treatment was 92%.
(Stroj et al., 1999)	Cerebrospinal meningitis	*K. pneumoniae*	Orally administered phages were used successfully to treat meningitis in a newborn (after antibiotic therapy failed).
(Tolkacheva et al., 1981)	Bacterial dysentery	*E. coli, Proteus*	Phages were used together with bifidobacteria to treat bacterial dysentery in 59 immunosuppressed leukemia patients. The superiority of treatment with phage-bifidobacteria over antibiotics was reported.
(Weber-Dabrowska et al., 1987)	Suppurative infections	*Staphylococcus,* various Gram-negative bacteria	Orally administered phages were used to successfully treat 56 patients, and the phages were found to reach the patients' blood and urine.
(Zhukov-Verezhnikov et al., 1978)	Suppurative surgical infections	*Staphylococcus, Streptococcus, E. coli, Proteus*	The superiority of adapted phages (phages selected against bacterial strains isolated from individual patients) over commercial phage preparations was reported in treating 60 patients having Suppurative infections.

Pritchard et al., 2007), *Streptococcus uberis* (Celia et al., 2008), *Streptococcus suis* (Wang et al., 2009), *B. anthracis* (Porter et al., 2007; Schuch et al., 2002; Yoong et al., 2006), *S. aureus* (Donovan et al., 2006b; O'Flaherty et al., 2005; Obeso et al., 2008; Rashel et al., 2007; Sass and Bierbaum, 2007; Takac et al., 2005), *Clostridium perfringens* (Zimmer et al., 2002) and *E. faecalis* (Yoong et al., 2004). After only 13 years since their first documented use an antimicrobial in 2001 (Nelson et al., 2001), endolysins are now being pre-clinically developed and subjected to clinical trials as a human therapeutic. For example, the ContraFect endolysin CF-301 (Gilmer et al., 2013), which has specificity for all forms of *S. aureus*, including MRSA and vancomycin-intermediate (VISA) and -resistant (VRSA) isolates, as well as *S. pyogenes* and *S. agalactiae*, is currently in phase 1 clinical trials for treating staphylococcal bacteremia infections.

Endolysins are emerging antimicrobial option because of the several favorable traits associated with these enzymes, including:

- Well-established efficacy against drug-resistant microorganisms
- Broad application range (humans, animals, food, environment)
- Nonexistent resistance formation observed to date
- Low toxicity due to the high specificity of the enzyme
- Vast availability of endolysin candidates as a result of bacteriophage ubiquity
- Extensive bioengineering potential prompted by the modular architecture of the typical Gram-positive endolysin structure

Lysis From Without

Contrary to Gram-negative bacteria species, the absence of a protective outer membrane for Gram-positive bacteria makes their cell wall structures externally accessible to peptidoglycan-acting antimicrobial agents. While endolysins require a phage particle for DNA delivery as well as holins for substrate accessibility to achieve lysis from within the host bacterium, the extrinsic application of an endolysin to a Gram-positive organism would remove those two restrictions. Accordingly, endolysins have been expressed and purified as recombinant proteins, and then extraneously applied to susceptible Gram-positive pathogens to induce lysis upon direct contact with the cell wall.

Structure of Gram-positive and Gram-negative Endolysins

The protein structure of Gram-positive and Gram-negative endolysins varies due to differences in cell wall architecture between these major bacterial groups. Endolysins that target Gram-positive bacterial species are typically 25-40 kDa and employ a modular structure, with an N-terminal enzymatically active domain (EAD) linked to a C-terminal cell wall binding domain (CBD) (Borysowski et al., 2006; Fischetti, 2010; Loessner, 2005; Loessner et al., 1995; Lopez and Garcia, 2004). The EAD structure is evolutionarily conserved and responsible for the hydrolytic activity of the enzyme (i.e. cleaving particular covalent bonds within the bacterial peptidoglycan). The CBD structure is evolutionarily variable and accountable for guiding the endolysin to its substrate through the reversible binding of a highly specific cell wall associated epitope, typically a carbohydrate. Efficient cleavage requires that the CBD binds to its unique cell

wall ligand, thereby conferring species, strain or serotype endolysin specificity (Fischetti, 2010). For some endolysins, it has been shown that the CBD bound tightly to the cell wall debris after cell lysis in order to prevent the possibility of the enzyme diffusing to and killing other uninfected bacterial cells (Loessner et al., 2002). There is structural evidence that the N-terminal EAD and C-terminal CBD of Gram-positive endolysins interact with each other prior to the CBD binding to the bacterial cell wall to render the EAD inactive. Along these lines, when the CBD binds to its cell wall epitope, there is a structural alteration that activates the EAD. To illustrate this phenomena, the pneumococcal endolysin Cpl-1 was crystallized in free and choline-bound states (Hermoso et al., 2003). In the absence of choline, the tertiary structure of Cpl-1 was oriented into a hairpin conformation with the two domains directly interacting. Conversely, choline recognition by the CBD altered the structure of Cpl-1 to allow the EAD to be properly oriented for hydrolysis of the bacterial cell wall.

Gram-negative endolysins are generally 15-20 kDa and comprised of a single globular EAD. These endolysins lack a CBD because the moderately thin peptidoglycan (5-10 nm) of Gram-negative bacteria, which lies adjacent to the outer membrane, lacks surface proteins and carbohydrates (Stark et al., 2010). Two exceptions can be observed from endolysins encoded by the *P. aeruginosa* phages φKZ and EL (Briers et al., 2009; Briers et al., 2007). These endolysins, KZ144 and EL188, consists of an N-terminal CBD and a C-terminal EAD. The KZ144 endolysin binds to *P. aeruginosa* with high affinity and can additionally interact with the peptidoglycan from other Gram-negative bacteria.

Bacteriolytic Mechanism of Endolysins

Peptidoglycan hydrolases, including endolysins, autolysins and exolysins, cleave critical covalent bonds in the cell wall structure to induce lysis or cell wall remodeling. Peptidoglycan is essential for maintaining cell shape and counteracting the high intracellular osmotic pressure (Royet and Dziarski, 2007). Its structure consists of a linear polysaccharide backbone of alternating units of β-1,4-linked N-acetylglucosamine (GlcNAc) and N-acteylmuramic acid (MurNAc). The lactyl group of every MurNAc unit is substituted with stem peptides, typically consisting of four alternating L- and D-amino acids. For Gram-negative bacteria and Gram-positive bacilli, the four amino acids in order starting closest to MurNAc are L-alanine, D-iso-glutamic acid, meso-diaminopimelic acid (mDAP) and D-alanine (i.e. DAP-type peptidoglycan) (Fig. 1-1a). For Gram-positive bacteria, the stem peptide moiety is identical to that of Gram-negative bacteria with the exception of the third amino acid position, for which mDAP is replaced by L-lysine (i.e. Lys-type peptidoglycan) (Fig. 1-1b). Adjacent stem peptides are then cross-linked, either directly by an mDAP to D-alanine interpeptide bond (Gram-negative and Gram-positive bacilli) or through an interpeptide bridge of amino acids (Gram-positive). The composition of the interpeptide bridge varies. For example, the cell wall of *S. aureus* contains a pentaglycine interpeptide bridge, whereas the stem peptides in the cell wall of *S. pyogenes* are interconnected by a dialanine interpeptide bridge.

Depending on the particular bond that is cleaved within the cell wall structure, endolysins can be organized into at least five different groups: N-acetylmuramidases, lytic transglycosylases, N-acetyl-β-D-glucosaminidases, N-acetylmuramoyl-L-alanine amidases and endopeptidases (Borysowski et al., 2006). The first two lytic activities are

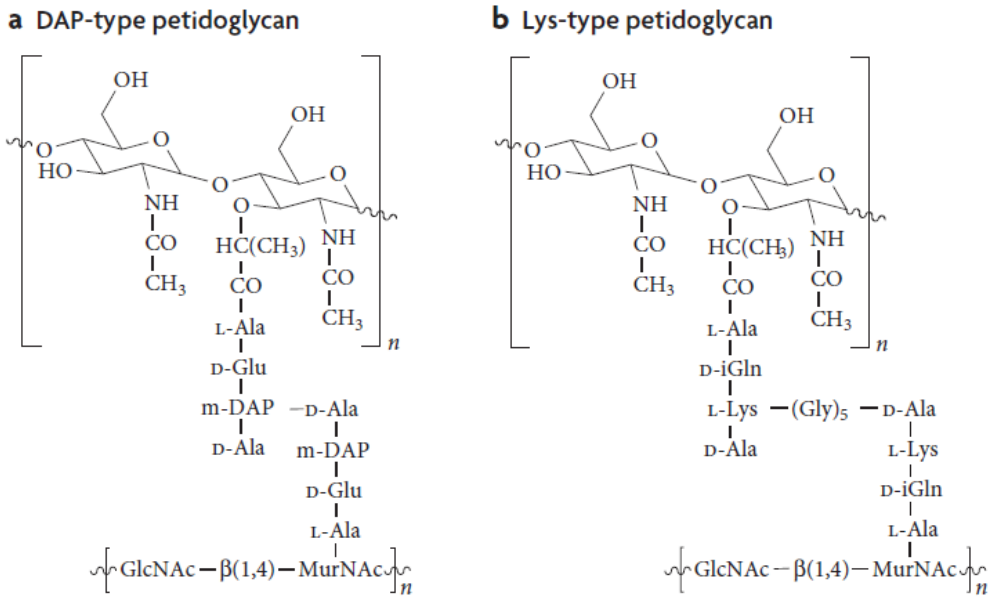

Figure 1-1. DAP-type and Lys-type peptidoglycan structure. Bacterial peptidoglycan can be classified into one of two types: (a) DAP-type or (b) Lys-type. DAP-type is specific to Gram-negative and Gram-positive bacilli species, whereas Lys-type is found in non-bacilli Gram-positive species. (Source: Royet and Dziarski, 2007)

that of N-acetylmuramidases (i.e. lysozymes) and lytic transglycosylases. They both cleave the N-acetylmuramoyl-β-1,4-N-acetylgluocosamine bond, which is one of the two alternating glycosidic bonds of the glycan moiety (Fig. 1-2, label 1). The other glycosidic bond in the glycan strand is cut by N-acetyl-β-D-glucosaminidases, which cleaves the linkage between N-acetylglucosaminyl-β-1,4-N-acetylmuramine (Fig. 1-2, label 2). N-acetylmuramoyl-L-alanine amidases, the most commonly observed lytic activity of endolysins, hydrolytically process the amide bond formed between MurNAc and L-alanine, which is the linkage responsible for conjoining the sugar and stem peptide moieties of peptidoglycan (Fig. 1-2, label 3). The last group of endolysins, endopeptidases, cleaves between two amino acids that constitute either the stem peptide (Fig. 1-2, label 4) or interpeptide bridge (Fig. 1-2, label 5).

According to the International Union of Biochemistry and Molecular Biology (IUBMB) enzyme nomenclature, glucosaminidases, muramidases, L-alanine-amidases and endopeptidases are classified as hydrolases. Additionally, glucosaminidases and muramidases are further termed glycosidases or glycosol hydrolases. Lytic transglycosylases are not hydrolases and instead use an intramolecular interaction to break the glycosidic bond between N-acetylmuramoyl-β-1,4-N-acetylgluocosamine by promoting the formation of a concomitant 1,6-anhydromuramoyl product (Holtje et al., 1975; Thunnissen et al., 1994). Due to the conservation in the EAD sequence and structure of endolysins, databases have grouped these domains into specific families. These subgroups relate to the hydrolytic mechanism for which the cleavage occurs rather than the specific bond cleaved. For example, cysteine, histidine-dependent amidohydrolase/peptidase (CHAP) domains are a commonly observed endolysin family

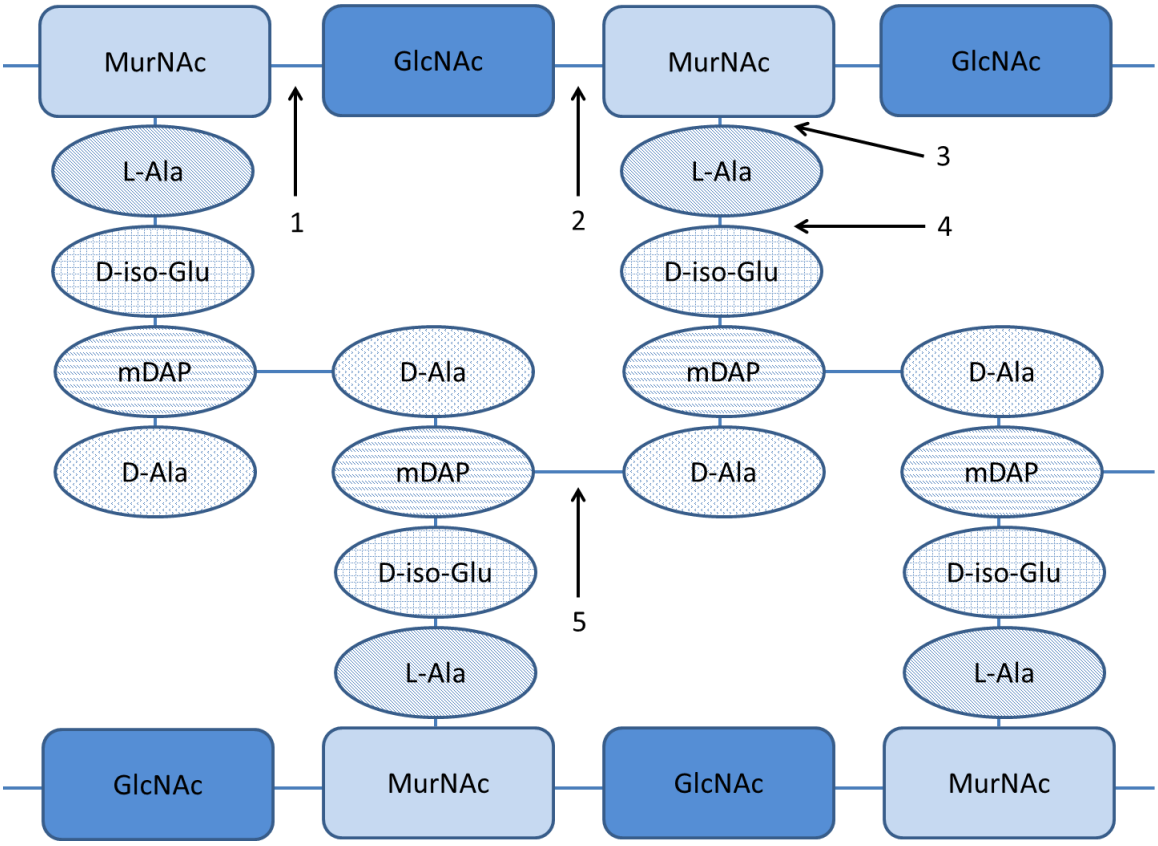

Figure 1-2. Cleavage site specificity by the major classes of endolysins. Depending on the particular covalent bond that is disrupted in the cell wall structure, endolysins can be organized into one of five groups: (1) N-acetylmuramidases (i.e. lysozymes) and lytic transglycosylases; (2) N-acetyl-β-D-glucosaminidases; (3) N-acetylmuramoyl-L-alanine amidases; (4) stem peptide endopeptidase; (5) interpeptide bridge endopeptidase.

that utilizes a cleavage mechanism where a cysteine is deprotonated by a nearby histidine to promote a nucleophilic attack by the cysteine on the scissile bond. Some CHAP domains have been reported to display amidase activity (Nelson et al., 2006a), whereas others have shown endopeptidase specificity, cleaving between the terminal D-alanine of the stem peptide and the adjacent amino acid of the interpeptide bridge (Becker et al., 2009; Pritchard et al., 2004).

Antimicrobial Potential (Resistance, Toxicity, Immunogenicity, Synergy)

One major concern with the application of an antibacterial agent is the eventual development of resistance by the bacterial microorganism targeted. With respect to the modern-day global health and economic implications of antibiotic resistance, there is an urgent need for novel antimicrobials that are immalleable to resistance evolution. The misuse and overuse of broad-range antibiotics has accelerated the development and dissemination of antibiotic-resistant genes among the bacterial community by placing selective pressure not only on the targeted pathogen, but also on nearby susceptible commensal bacteria (Nelson et al., 2012). In this regard, the high specificity of most endolysins is advantageous over classic broad-range antibiotics. Additionally, the coevolution of phage and their explicit bacterial host over millions of years has resulted in Gram-positive endolysins binding to and cleaving conserved cell wall targets that are required for bacterial viability and hence these targets are immutable due to bactericidal ramifications (Fischetti, 2008; Loessner, 2005). This is exemplified by the receptor epitopes targeted by pneumococcal and streptococcal endolysins. Pneumococcal endolysins bind to choline on the pneumococcal surface, which is essential for cell

viability (Garcia et al., 1983; Lopez and Garcia, 2004). Similarly, streptococcal endolysins have been shown to interact with polyrhamnose of *S. pyogenes*, which has been shown to be important for cell survival (Fischetti, 2003; Yamashita et al., 1999). By virtue of the cell wall of Gram-positive bacteria being the outermost structure, the extrinsic application of endolysins can avoid common resistance mechanisms exploited by bacteria, including neutralization or degradation by antimicrobial-specific intracellular proteins and enzymes, expulsion by efflux pumps and decreased membrane permeability.

Several endolysin resistance studies have been performed by the Fischetti laboratory using both native and engineered endolysins. The pneumococcal endolysin Pal was repeatedly added to actively growing *S. pneumoniae* either in low concentrations on agar plates or using increasing concentrations in liquid culture. In both scenarios, no resistant pneumococcal strains were encountered (Loeffler et al., 2001). In a related study, the *B. anthracis* endolysin PlyG was repeatedly added to *Bacillus* cells in the presence of the mutagenic chemical methane-sulphonic acid ethyl ester in an effort to expedite the evolution of resistant strains to the endolysin (Schuch et al., 2002). Similar to the Pal resistance studies, there were no PlyG-resistant strains of *Bacillus* recovered, whereas the same experimental method generated 1,000-10,000 fold increases in novobiocin and streptomycin resistance. Engineered endolysins efficacious towards antibiotic-resistant bacteria were also used in resistance studies. Increasing concentrations of the chimeric *S. aureus* endolysin ClyS was added to MRSA cells in parallel with the antibiotic mupirocin over a total of eight days (Pastagia et al., 2011). At the conclusion of the experiment, the minimum inhibitory concentration (MIC) for ClyS remained unchanged, while the MIC for mupirocin increased tenfold. It is important to note that,

although there have been no documented cases of endolysin resistance to date, resistance to other peptidoglycan cell wall hydrolases has been observed. For example, bacterial strains have become resistant to human lysozyme by various secondary cell wall modifications, such as O-acetylation and N-deacetylation of the peptidoglycan and D-alanylation of teichoic acids (Guariglia-Oropeza and Helmann, 2011; Vollmer, 2008). Likewise, certain *S. aureus* strains have developed resistance against the *Staphylococcus simulans* bacteriocin lysostaphin, which targets pentaglycine interpeptide bridge of *S. aureus* as a glycyl-glycine endopeptidase (DeHart et al., 1995; Grundling et al., 2006; Sugai et al., 1997). *S. aureus* accomplishes this by altering the length (e.g. downsizing from pentaglycine to a single glycine (Sugai et al., 1997)) or amino acid composition (e.g. incorporating serine residues (DeHart et al., 1995)) of its peptidoglycan interpeptide bridge.

The high degree of selectivity by an endolysin CBD is not only advantageous for impeding resistance development, but this property also reduces their inherent toxicity as an antimicrobial. Endolysins have the innate ability to search out and destroy pathogenic bacterial species while evading the desirable commensal microflora that are often harmed by antibiotics or chemical preservatives. Adverse to topical application, one safety concern with endolysin therapy involves the release of proinflammatory cellular components during the treatment of systemic infections. Due to the bacteriolytic mechanism exploited by these enzymes, the continuous systemic administration of endolysins in humans or animals would result in the release of proinflammatory bacterial cell components, such as teichoic acids, lipotechoic acids and peptidoglycan that could ultimately promote serious complications like septic shock and multiple organ failure

(Nau and Eiffert, 2002). There is *in vivo* evidence that suggests this concern could be alleviated by varying the endolysin concentration during treatment. While one murine sepsis study showed that the continuous intravenous application of the pneumococcal Cpl-1 endolysin enhanced the concentration of proinflammatory cytokines (Entenza et al., 2005), results from a similar study showed that using lower concentrations of Cpl-1 actually reduced cytokine concentrations relative to untreated infected mice (Witzenrath et al., 2009). To explain this observation, it was hypothesized that using higher concentrations of endolysin stimulates a more complete digestion of the bacterial cell wall, thereby generating higher levels of proinflammatory cell wall fragments that continuously circulate in the serum. In addition to altering endolysin concentration, the congruent use of anti-inflammatory agents, including steroids and non-steroidal anti-inflammatory drugs (NSAIDs), can help combat inflammation. Besides their high specificity, endolysins are biodegradable because of their proteinacious nature, which further limits the possibility of toxic side effects.

Seeing as endolysins are proteinacious and genetically encoded by phage, immunogenicity studies relating to the systemic and mucosal therapeutic application of these antimicrobials in animals and humans have been conducted *in vitro* and *in vivo*. When rabbit hyperimmune serum was raised against the Cpl-1 endolysin, it was found that the *in vitro* activity of Cpl-1 against pneumococcal cells was slightly decreased but never fully inactivated (Loeffler et al., 2003). In the same study, it was elucidated that mouse IgG antibodies were raised against Cpl-1 when several doses of the endolysin were administered intravenously. Endolysin efficacy was also investigated *in vivo* using immunized and naïve mice. Following Cpl-1 treatment of immunized and naïve mice

infected with *S. pneumoniae*, it was determined that there was no significant difference between the two groups regarding the reduction in pneumococcal cells by the enzyme, suggesting that the antibodies raised against Cpl-1 were unable to inhibit the enzyme *in vivo*. Similar results were obtained when using different endolysins and pathogens (*S. pyogenes*, *B. anthracis* and *S. aureus*). In each of these experiments, antibodies were successfully developed against these various endolysins (Fischetti, 2010) but the antibodies were incapable of neutralizing their bacteriolytic efficacy (Jado et al., 2003; Rashel et al., 2007). In an attempt to explain how endolysins are able to avoid antibody inactivation, it has been theorized that the reported high binding affinity (e.g. *L. monocytogenes* endolysins Ply118 and Ply500 have nanomolar binding affinities) (Loessner et al., 2002; Schmelcher et al., 2010) and rapid kinetics of endolysins are able to outcompete the immune system of the host.

Results from additional immunogenicity studies using the Cpl-1 endolysin in the treatment of systemic infections demonstrated that antimicrobial had a half-life of approximately 20 minutes, which is comparable to other foreign proteins like streptokinase, a thrombolytic enzyme used for treatment of acute myocardial infarction (Brucato and Pizzo, 1990; Loeffler et al., 2003). Beyond delivering endolysins repeatedly or by intravenous diffusion to achieve systemic concentrations during treatment, chemically modifying or bioengineering endolysins have proven to prolong half-life. PEGylation is a commonly used chemical modification for successfully slowing the systemic clearance rate of molecules by reducing antibody binding affinity (Kim et al., 2008; Ramon et al., 2005; Walsh et al., 2003). Unfortunately, it has been reported that the cysteine-specific PEGylation of Cpl-1 ultimately abolished lytic activity (Resch et al.,

2011a). However, PEGylating other peptidoglycan hydrolases, such as the bacteriocin lysostaphin, significantly improved the pharmacokinetics while rendering the enzyme still bacteriolytically active (Walsh et al., 2003). Bioengineering improved endolysin pharmacokinetic properties has proven to be more successful than introducing chemical modifications. For example, dimerization of Cpl-1 by engineering a C-terminal intermolecular disulfide bond increased activity and promoted a tenfold deceleration of plasma clearance (Resch et al., 2011b). Seeing as several endolysins have been implicated to undergo dimerization, an engineering strategy of constructing stable disulfide-based endolysin dimers may be successful at expanding systemic half-life.

In combination with other peptidoglycan hydrolases or antibiotics, endolysins have demonstrated synergistic therapeutic efficacy when analyzed *in vitro* and *in vivo*. Achieving synergism between two or more antimicrobials translates to lower dosage requirements and improved efficacy while reducing the chances of resistance formation by concurrently acting on multiple unique targets. Synergy between two endolysins has been observed when using enzymes with different peptidoglycan cut sites, as the simultaneous cleavage of two distinct bonds in the cell wall would conceivably have enhanced destabilizing effects (Schmelcher et al., 2012a). Improved lytic activity could also be due to the cleavage of a particular site by the first catalytic domain improving substrate accessibility for the catalytic domain of the second endolysin (Loeffler and Fischetti, 2003; Schmelcher et al., 2012b). An example of endolysin synergism was exemplified by the pneumococcal endolysins Cpl-1 and Pal. The combinational use of Cpl-1 (muramidase) and Pal (L-alanine amidase) provoked *in vitro* and *in vivo* synergistic efficacy (Jado et al., 2003; Loeffler and Fischetti, 2003). The bacteremic titer when the

two pneumococcal endolysins were used together in a murine sepsis challenge was reduced to a greater extent compared to when either endolysin was used alone. Synergistic effects were also observed *in vitro* when using the *S. aureus* endolysin LysK (L-alanine amidase/D-alanyl-glycine endopeptidase) with lysostaphin (glycyl-glycine endopeptidase) (Becker et al., 2008). Similarly, combining lysostaphin with either of the chimeric streptococcal/staphylococcal endolysins λSA2-E-Lyso-SH3b and λSA2-E-Lyso-SH3b resulted in synergistic ramifications *in vitro* and *in vivo* using a mouse model of bovine mastitis (Schmelcher et al., 2012b). Synergy has also been validated when combining endolysins with antibiotics. For example, anti-pneumococcal synergy was established when combining Cpl-1 with penicillin or gentamicin (Djurkovic et al., 2005). Synergistic efficacy was also seen either *in vitro* when the staphylococcal MV-L endolysin was added to either glycopeptide antibiotics vancomycin or teicoplanin to kill VISA (Rashel et al., 2007), or *in vivo* when the chimeric staphylococcal ClyS endolysin was combined with oxacillin to cure mice from MRSA-induced septicemia (Daniel et al., 2010).

Engineering Endolysin Properties

The coevolution of phage and bacteria over millions of years has resulted in the extensive optimization of endolysins that efficiently and rapidly induce bacterial lysis in an intracellular environment. Considering there was no evolutionary pressure to perfect these enzymes for exogenous application, there is engineering potential for endolysins to alter their functionality in and tolerance of complex extracellular environments, including food matrices, blood and the surface of mucous membranes (Schmelcher et al., 2012a).

Several endolysin engineering strategies have been utilized, including chimeragenesis (i.e. domain swapping), directed evolution and peptide/protein fusions.

The modular protein architecture of Gram-positive endolysins makes them ideal candidates for constructing chimeras with modified catalytic and binding properties. This engineering approach has been successfully exploited by nature itself, where several chimeric phage endolysins have been identified as a result of horizontal gene transfer (Hendrix, 2002), such as the *L. monocytogenes* endolysin PlyPSA (Zimmer et al., 2003) and the pneumococcal endolysin Pal (Sheehan et al., 1997). The structure of PlyPSA consists of a CBD that resembles that of other *Listeria* endolysins but consists of an evolutionary divergent EAD that is homologous to amidase domains from *Bacillus* and *Clostridium* phages. Crystal structures of endolysins as well as detailed bioinformatic analysis of their protein sequences have provided the necessary framework to devise and construct functional chimeras consisting of domains from different origins. The earliest studies involving domain shuffling of peptidoglycan hydrolases were conducted in the 1990s. Swapping domains between the pneumococcal autolysin LytA (amidase) and endolysin Cpl-1 (muramidase) culminated in chimeric enzymes with exchanged lytic activities and regulatory properties (Diaz et al., 1990). Furthermore, cell wall specificity was altered by interchanging the choline-dependent CBD from LytA with the choline-independent CBD from the pneumococcal Cpl-7 endolysin (Diaz et al., 1991). While the previous two examples proved exchanging modules between peptidoglycan hydrolases that target the same bacterial species can result in a functional chimeric enzyme with unique properties, it was still unknown if it was feasible to synthesize chimeras using two peptidoglycan hydrolases specific to bacteria from different genus classifications. This

was answered in 1993, when the EAD of the *Clostridium acetobutylicum* autolysin Lyc was fused to the choline-dependent CBD of Cpl-1. The resulting chimeric enzyme displayed lytic activity against choline-containing pneumococcal cell walls but was devoid of activity against *C. acetobutylicum* cell walls (Croux et al., 1993a). In an independent study, fusing the CBD of Lyc to the EAD of LytA improved activity against *C. acetobutylicum* 250-fold (Croux et al., 1993b). Constructing chimeras has also been shown to be useful for broadening specificity. For example, fusing the full-length or truncated *S. agalactiae* B30 endolysin to lysostaphin produced chimeric enzymes that displayed antibacterial efficacy towards both streptococcal and staphylococcal cells (Donovan et al., 2006a). In experiments where *Listeria* endolysin CBDs were labeled with GFP and consequently added to cells for bacterial diagnostic purposes, fusing the Ply500 CBD, which is specific for serovar 4, 5 and 6 *L. monocytogenes* strains, to the PlyP35 CBD, which targets the majority of serovar 1/2 and 3 strains, produced heterologous GFP constructs that had broad binding specificity for *Listeria* cells from all species and serovars (Schmelcher et al., 2011). It was also shown that combining two Ply500 CBDs together resulted in a 50-fold increase in affinity to the cell wall when compared to a construct consisting of a single Ply500 CBD.

Random mutagenesis and site-directed mutagenesis (SDM) studies have been performed with endolysins to enhance desirable properties. Directed evolution, which cultivates Darwinian evolution in a laboratory setting to engineer desirable macromolecular properties, was applied to the *S. agalactiae* endolysin PlyGBS, also known in the literature as B30, to improve its bacteriolytic activity (Cheng and Fischetti, 2007). Random mutations were introduced into PlyGBS by either *E. coli* mutator strains

or error-prone polymerase chain reaction (epPCR) and consequently screened for improved lytic potency using soft agar overlay assays. These assays consist of first replica plating the original transformation plate containing PlyGBS mutant colonies while simultaneously inducing protein expression, followed by exposing the plate to chloroform vapors to liberate the overexpressed endolysins and then finally overlaying the plate with soft agar containing *S. agalactiae* target cells. Activity was assessed based on the qualitative evaluation of lytic clearing zones. After multiple rounds of random mutagenesis and screening, the lead PlyGBS mutant candidate exhibited a 28-fold increase in bacteriolytic activity compared to wild-type. This evolved construct consisted of a frameshift mutation that resulted in the deletion of the C-terminal CBD, leaving only the N-terminal endopeptidase EAD as well as 13 out-of-frame amino acids at the C-terminus. Aside from improving the EAD activity, directed evolution can be used for increasing CBD binding affinity, augmenting thermal stability or modifying pH and salt dependence for activity.

Structure-guided SDM has also been effectively harnessed for modifying endolysin properties (Diez-Martinez et al., 2013; Low et al., 2011). Taking into consideration the cell wall surface of Gram-positive bacterial species is generally negative charged, a 2011 study showed the activity of an endolysin EAD correlated with its net (positive) charge in the absence of the CBD (Low et al., 2011). This conceptual understanding was then incorporated into endolysin bioengineering studies for increasing EAD activity and CBD-independence. For example, the endogenous XlyA EAD, which is an amidase derived from a *B. subtilis* prophage and consists of a net charge of Z = -3 at pH 7.5, demonstrated lytic activity in a CBD-dependent manner. By mutating five non-

cationic surface residues to lysines to shift the net charge from Z = -3 to Z = +3, the resulting XlyA EAD mutant lysed *B. subtilis* cells at a rate nearly identical to that of full-length XlyA. A reverse loss-of-function engineering approach was then conducted using the PlyBa04 EAD, which is a muramidase derived from the *B. anthracis* Ba04 phage and carries a net charge of Z = +1 at pH 7.5. The native PlyBa04 EAD was able to lyse *B. cereus* cells as efficiently as the full-length endolysin. However, when four neutral residues on the surface of the PlyBa04 EAD were mutated to aspartic acid to change the net charge from Z = +1 to Z = -3, the resulting PlyBa04 mutant showed little or no lytic activity towards *Bacillus*. The same negatively charged EAD mutant was made in the context of the full-length protein, and it was uncovered that a significant fraction of wild-type activity was preserved. Therefore, changing the net charge of the PlyBa04 EAD from positive to negative correspondingly transitioned the lytic activity of the module from a CBD-independent to a CBD-dependent state. An alternative study established a direct correlation between the net charge of the CBD of an endolysin and its bacteriolytic activity (Diez-Martinez et al., 2013). Introducing 15 amino acid substitutions to reverse the charge of the CBD belonging to the pneumococcal endolysin Cpl-7 from Z = -14.93 to Z = +3.0 at neutral pH significantly increased the activity of the endolysin against *S. pneumoniae* (including MDR strains), *S. pyogenes* and other pathogens.

The current therapeutic strategy involving the exogenous application of endolysins has been limited to Gram-positive pathogens due to the existence of the outer membrane structure of Gram-negative bacteria. To overcome this, engineering strategies are being explored in an attempt to allow endolysins to penetrate this protective barrier in Gram-negative pathogens in order to access the subsequent peptidoglycan layer. One

strategy involves fusing peptidoglycan hydrolases to various cationic, polycationic and other membrane-disrupting peptides. Human lysozyme was fused to cecropin, which is an antimicrobial peptide that forms pores in the outer membrane, and the resulting construct had considerable antimicrobial efficacy against several Gram-negative bacterial species (Lu et al., 2010). A subset of endolysins reportedly encompasses intrinsic charge and/or hydrophobic motifs that interact with the outer membrane to increase permeability. For example, the extrinsic application of the *Bacillus amyloliquefaciens* endolysin Lys1521 established antibacterial efficacy towards not only Gram-positive bacteria, but *E. coli* and *P. aeruginosa* as well (Morita et al., 2001a; Morita et al., 2001b; Orito et al., 2004). Likewise, in addition to Gram-positive species, the *Acinetobacter baumannii* endolysin LysAB2 displays activity against a variety of Gram-negative bacteria, including *A. baumannii*, *E. coli*, *Citrobacter freundii*, *Salmonella enterica* and *Enterobacter aerogenes* (Lai et al., 2011). While the use of an endolysin that possesses the ability to permeabilize or disrupt outer membrane structures of Gram-negative bacteria is desirable *in vitro*, their therapeutic use *in vivo* may be limited due to toxicity issues stemming from interactions with eukaryotic cell membranes.

Intracellular pathogens are problematic because they are able to evade the host immune system as well as antimicrobials that cannot penetrate the eukaryotic cell surface. To address this concern, peptidoglycan hydrolases are being fused to cationic or amphipathic peptides, termed protein transduction domains (PTDs) (i.e. cell-penetrating peptides, membrane-permeable peptides or Trojan horse peptides), that naturally interact with the eukaryotic membrane to promote internalization (Dietz, 2010; Dietz and Bahr, 2004; Splith and Neundorf, 2011). Engineering macromolecule translocation from the

extracellular to intracellular environment of eukaryotic cells has been successfully accomplished through PTD fusions. Therefore, fusing peptidoglycan hydrolases to PTDs could be an effective antimicrobial strategy for targeting and killing Gram-positive pathogens that invade, persist and replicate within eukaryotic cells, such as *S. aureus*, *L. monocytogenes*, *S. pyogenes* and *B. anthracis* (Borysowski and Gorski, 2010). Preliminary studies using lysostaphin or staphylococcal endolysins fused to PTDs have generated promising results (Schmelcher et al., 2012a). Both constructs were capable of reducing intracellular drug-sensitive or -resistant *S. aureus* cells in bovine mammary gland epithelial cells, murine osteoblasts and human brain microvasculature epithelial cells.

Endolysin-related Applications

Medicine

Although the molecular cloning, protein purification and subsequent biochemical characterization of endolysins has been a research concentration in laboratories for decades, the medicinal application of these enzymes was not formulated until 2001. It was this year in which the first *in vivo* endolysin study was performed by Fischetti's group to validate the therapeutic potential of these enzymes to prevent and treat bacterial infections (Nelson et al., 2001). Fischetti's group, which termed endolysins as "enzybiotics" in order to describe their antimicrobial potential, first pretreated mice with a single 250 U dose of the streptococcal PlyC endolysin in the oral cavity and then subsequently added 10^7 colony forming units (CFU) of live *S. pyogenes*. The pretreated

mice were protected from bacterial colonization (28.5% infected, n = 21) compared to the untreated control mice (70.5% infected, n = 17). In the same study, *S. pyogenes* was introduced to the oral cavity of nine mice and were found to be heavily colonized for four consecutive days by oral swabs. On day 4, the infected mice were then orally treated with 500 U of PlyC. Two hours post-endolysin treatment, the nasopharyngeal cavity of all nine mice was found to be sterilized.

Among the most studied endolysins *in vivo* are Pal and Cpl-1, both of which are derived from phage that infect *S. pneumoniae*. The *in vitro* application of Pal at 100 U/ml was able to induce a ~4-log decrease in viability after 30 seconds when applied to 15 different clinical strains of *S. pneumoniae,* including several strains that were penicillin-resistant (Loeffler et al., 2001). In an *in vivo* murine model for nasopharyngeal *S. pneumoniae* colonization, 18 mice were first colonized intranasally with 10^8 CFU of *S. pneumoniae*. 42 hours post-infection, half of the mice (n = 9) were then treated with 1400 U of Pal. This single dose of Pal was able to eliminate *S. pneumoniae* nasopharyngeal colonization within 5 hours. Another study involved using a murine bacteremia model, where 20 mice were intravenously infected with 3 x 10^8 CFU of *S. pneumoniae* (Loeffler et al., 2003). One hour later, 10 mice were intravenously treated with a single bolus containing 2,000 µg of Cpl-1. All endolysin-treated mice survived throughout the duration of the 48 hour experiment, whereas only 20% of the untreated mice survived, with a median survival time of 25.56 hours. Both Cpl-1 and Pal were also shown to protect mice from pneumococcal bacteremia induced by intraperitoneal (ip.) injection in a synergistic manner *in vivo* (Jado et al., 2003). While intraperitoneally administering 200 µg of either Cpl-1 or Pal one hour post-infection was found to be the required dose to

protect mice intraperitoneally infected with 5 x 10^7 CFU of *S. pneumoniae*, only 2.5 µg of each endolysin was required to achieve the same effect when both Cpl-1 and Pal were used simultaneously. More recent *in vivo* studies using Cpl-1 include: continuous 250 mg/kg endolysin infusion treatment of *S. pneumoniae*-induced endocarditis in rats, resulting in sterilizing 10^5 CFU/ml pneumococci in the blood after 30 minutes and a > 4-log CFU/g reduction in bacterial titers on heart valve vegetations (Entenza et al., 2005); prevention of otitis media secondary problems as a result of primary influenza infections through Cpl-1 stimulated pneumococcal decolonization (McCullers et al., 2007); treatment of pneumococcal meningitis in rats by either intracisternal (20 mg/kg) or ip. (200 mg/mkg) injection of Cpl-1 decreased pneumococcal titers in cerebrospinal fluid (CSF) by 3 or 2 logs, respectively (Grandgirard et al., 2008); and treatment of severe pneumonia in mice (Witzenrath et al., 2009). In the latter study, the survival rate of mice treated with Cpl-1 or amoxicillin 24 hours after infection was 100% and 86%, respectively. When treatment started after the onset of bacteremia at 48 hours post infection, Cpl-1 or amoxicillin treatment led to the respective mouse survival rates of 42% and 71%.

Another streptococcal species that has been subjected to *in vivo* endolysin treatment is *S. agalactiae* (Group B Streptococcus, GBS), the most common causative agent of neonatal sepsis and meningitis, using murine vaginal and oropharynx infection models (Cheng et al., 2005). Thirty mice were initially inoculated vaginally with 10^6 streptomycin-resistant GBS. Twenty-four hours later, the vaginal cavities were swabbed to determine the initial colonization rate of GBS. The mice were then treated with 10 U of the GBS endolysin PlyGBS (n = 15) or enzyme buffer only (n = 15) and the vaginal

cavities were swabbed at 2 and 4 hour time points post-treatment to determine bacterial titers. Mice treated with PlyGBS displayed a significant ~3-log decrease in GBS CFU at the 2 and 4 hour time points when compared to the buffer only controls. To determine if PlyGBS could be used for postpartum treatment in newborns, 38 mice were inoculated with 10^8 CFU of streptomycin-resistant GBS in the oropharynx. The next morning, mice were oropharyngeally swabbed in order to calculate baseline GBS colonization. Mice were then treated orally and nasally with 10 U of PlyGBS (n = 20) or enzyme buffer only (n = 18). GBS titers elucidated by oropharyngeal swabs at 2 and 24 hour time points showed the endolysin-treated mice had a significant reduction in GBS colonization at both time points compared to the bacterial levels in the buffer control group.

Besides the treatment of streptococcal infections, the therapeutic efficacy of endolysins has been validated against *B. anthracis*, an infectious agent commonly associated with biowarfare. PlyG, an endolysin from the *B. anthracis* γ phage, displayed the ability to kill both vegetative cells and germinating spores (Schuch et al., 2002). Mice ip. infected with 10^6 CFU of *Bacillus* cells died within 5 hours when treated with enzyme buffer only. Mice ip. treated with 50 U of PlyG 15 minutes post-infection led to 13 of the 19 mice (68.4%) surviving the duration of the 72 hour experiment and extended the life of the remaining mice several fold over the untreated controls. Furthermore, a 5 minute treatment with 10 U of PlyG was able to generate a 7,500-fold reduction in heat-activated *Bacillus* spores viability. Another *Bacillus* endolysin, PlyPH, was biochemically characterized to display lytic activity over a broad pH range of 4.0-10.5 and exhibited the ability to rescue mice from ip. challenge of *Bacillus* (Yoong et al., 2006). Mice (n = 26) were injected with 2.5 x 10^6 CFU of *Bacillus* cells into the peritoneal cavity and then

treated 10 minutes later with approximately 1,200 µg of PlyPH (n = 13) or enzyme buffer only (n = 13). At the conclusion of the 38 hour study, ~40% of the PlyPH-treated mice survived, whereas 100% of the buffer-treated mice were unable to be rescued.

There are several studies that report the ability to control *S. aureus* infections in animal models through the use of endolysin therapy. The MV-L endolysin, encoded by the *S. aureus* phage ΦMR11, displayed *in vitro* and *in vivo* bacteriolytic activity against multidrug-resistant *S. aureus* strains, including MRSA and VISA clinical isolates. In a murine ip. infection model, the peritoneal cavity of mice was injected with 5 x 10^9 CFU of MRSA cells, followed by treatment at 0, 30 or 60 minute time points post-infection with 500 U of MV-L or enzyme buffer only. Endolysin treatment at 0, 30 and 60 minutes post-infection resulted in respective mouse survival rates of 100%, 100% and 60% at the conclusion of the 60 day study. Conversely, 100% of the mice were killed within 24 hours post-infection when treated with enzyme buffer only at each time point. In another study, the chimeric staphylococcal endolysin ClyS was shown to be more effective than the standard topical antimicrobial mupirocin for treating murine epidermal infections caused by methicillin-susceptible *S. aureus* (MSSA) and MRSA (Pastagia et al., 2011). At 24 hours postcolonization with MSSA or MRSA, the infected epidermal tissue of mice was treated with either 10% (wt/wt) of ClyS in Aquaphor or 2% mupirocin. With respect to the untreated controls, ClyS treatment caused a 3-log reduction in bacterial colonization while mupirocin achieved a 2-log decrease.

In a mouse nasal decolonization model, a 2-log reduction in MRSA viability was observed 1 hour after nasal and oral treatment with 960 µg of ClyS (n = 20) when compared to buffer-treated mice (n = 20) (Daniel et al., 2010). Additionally, over the

course of a 10 day experiment, a single ip. injection of 1,000 µg of ClyS promoted the survival of 14 out of 16 mice (87.5%) that were subjected to a murine septicemia model for MRSA infection. As a basis of comparison, mice treated with enzyme buffer (n = 14) were dead from bacterial sepsis within 24 hours. Using the aforementioned murine septicemia model, therapeutic synergism was attained when using ClyS in combination with oxacillin. Mice were intraperitoneally injected with ~5 x 10^5 CFU of MRSA and then treated intraperitoneally 3 hours post-infection with 166 µg ClyS, 100 µg oxacillin or 166 µg Clys combined with 50 or 100 µg of oxacillin. At the conclusion of the 10-day study, mice treated with ClyS or oxacillin individually resulted in 30% (n = 20) and 35% (n = 23) survival rates, respectively. Contrarily, ClyS simultaneously applied with 50 or 100 µg of oxacillin significantly increased mouse survival to a respective 80% (n = 10) and 82% (n = 22). A successful 2-log decrease in *S. aureus* colonization was reported when applying the isolated CHAP domain ($CHAP_k$) of the staphylococcal endolysin LysK in a murine intranasal infection model (Fenton et al., 2010). *S. aureus* endolysins LysGH15 (50 µg per mouse, n = 3) and P-27/HP (250 µg per mouse, n = 15) were able to induce a respective ~7- and 2-log decrease in staphylococcal colonization in murine spleens and subsequently prevent bacteremia lethality (Gu et al., 2011a; Gu et al., 2011b; Gupta and Prasad, 2011).

Food Safety

Foodborne illness is a costly public health problem that is both prevalent and preventable. The CDC estimates 1 in 6 people (or 48 million people) domestically each year are infected by foodborne pathogens by consuming contaminated foods or

beverages, resulting in over 120,000 hospitalizations and 3,000 deaths. There have been over 250 different foodborne diseases elucidated, many of which the causative agent is a particular bacterial species. The Food and Drug Administration's Center for Food Safety and Applied Nutrition (CFSAN) has constructed a list of foodborne pathogenic microorganisms that cause human disease in the United States. Some examples of Gram-positive pathogens on this list include *L. monocytogenes, C. perfringens, Clostridium botulinum, B. cereus* and *S. aureus*. Significantly, lytic phages have been identified for each of the aforementioned bacterial pathogens and, in many cases, the endolysins they encode have been cloned, biochemically characterized to various extents and experimentally validated to be effective for both detecting and eradicating foodborne pathogens.

Considering many foodborne illnesses caused by Gram-positive pathogens develop rapidly and often require supportive care for treatment, preventing the initial infection is critical. Current bacterial diagnostic techniques, such as immunoassays and DNA-based methods, require up to 10^7 cells in order to accurately identify the causative bacterial pathogen. However, the infectious dose of many foodborne bacterial pathogens is often orders of magnitude less. Additionally, these methodologies often take several days to complete. To this end, the development of new rapid diagnostics with increased sensitivity is required for effectively lowering the number of foodborne illnesses.

Endolysin CBDs have high specificity and nanomolar equilibrium association constants for their particular cell wall receptor (Loessner et al., 2002) and remain functional without the presence of the N-terminal EAD. This mechanistic understanding outlines the potential of these domains to be utilized for biotechnological purposes as an

alternative diagnostic tool for foodborne bacterial pathogens. CBDs can be chemically crosslinked with an organic dye or genetically fused to a reporter protein (e.g. GFP, CFP, DsRed) for fluorescent detection by spectrophotometric or microscopic analysis. Furthermore, CBDs can be conjugated to magnetic nanoparticles for selective enrichment of target bacteria to a detectable level for diagnostics.

Listeriosis is an infection caused by the major foodborne pathogen *L. monocytogenes* that can cause meningitis, meningoencephalitis, septicemia and generalized infection of the fetus and abortion (Vazquez-Boland et al., 2001). Depending on the risk group studied, the fatality rate associated with listeriosis can be as high as 50% for newborns and 20% for the elderly (Bortolussi, 2008). The CDC estimates that approximately 1,600 illnesses and 260 deaths are due to listeriosis in the United States annually. *L. monocytogenes* present in contaminated food products is often difficult to detect due to the typically small *L. monocytogenes* cell populations coupled with the low sensitivity of current listerial diagnostics.

Presently, growing *Listeria* from contaminated food products in selective enrichment media is an absolute requirement in order to increase the number of total viable *Listeria* cells to detectable levels. The efficiency of the standard selective enrichment protocol is hindered by the total length of the 96 hour protocol. As an alternative detection methodology, paramagnetic beads coated with purified recombinant *Listeria*-specific endolysin CBDs were used for the detection of *Listeria* in food samples, a diagnostic approach known as CBD-based magnetic separation (CBD-MS). Detections rates for a variety of *Listeria* species and serovars (*L. monocytogenes*, *L. ivanovii* and *L. innocua*) in foods naturally and artificially exceeded 90% in heterogeneous microbial

communities (Kretzer et al., 2007). A total of 275 potentially naturally contaminated food samples were tested for *Listeria* contamination using either standard selective enrichment media or CBD-MS. In totality, *Listeria* was detected in 42 samples using standard selective enrichment media, compared to the 45 samples that were found to be *Listeria*-positive using CBD-MS. Besides the enhancement in sensitivity, the CBD-MS method is more rapid and only requires half the time (48 hours) compared to the standard selective enrichment media method. The CBD-MS method was also shown to be applicable to other bacterial species, such as *B. cereus* and *C. perfringens*. In addition, the CBD-MS separation method was combined with real-time quantitative PCR to yield a highly sensitive detection limit for *L. monocytogenes* in raw milk ranging from 10^2 to 10^3 CFU/ml (Walcher et al., 2010). Another endolysin-related methodology being utilized for the detection of bacteria involves fusing phage endolysin CBDs to various fluorescent markers. The fluorescent CBDs can then be used for the detection and differentiation of bacterial species and strains. For example, eight different *Listeria* CBDs, each of which had unique cell wall specificity, were fused to a collection of differently colored reporter proteins (Schmelcher et al., 2010). When added to a mixed population of *L. monocytogenes*, the fluorescent CBDs made it possible to rapidly detect and distinguish individual cells with serovar to strain specificity using fluorescence microscopy. This technique was further used in combination with CBD-MS for the recovery and identification of different *Listeria* serovars and strains from artificially contaminated milk or cheese. CBD-based detection methods have also been described for *B. anthracis* (Fujinami et al., 2007; Sainathrao et al., 2009). The latter study was able to employ a

bioengineered CBD derived from the PlyG endolysin that was coupled to fluorescent Qdot® nanocrystals for strain-specific detection of *B. anthracis*.

Supplementary to using isolated CBDs for bacterial diagnostics, the antimicrobial efficacy of full-length endolysins has been validated as a means to control a series of food-borne pathogens, including *S. aureus*, *S. agalactiae*, *S. uberis*, *L. monocytogenes*, *Clostridium butyricum* and *Erwinia amylovora*. Purified endolysins were shown to successfully control food-borne pathogens when utilized as biopreservatives for food products. For example, the *S. aureus* ΦH5 phage endolysin LysH5 rapidly reduced staphylococcal cell populations growing in pasteurized milk to undetectable levels after 4 hour incubation at 37°C (Obeso et al., 2008). A number of other endolysins, including the streptococcal endolysins B30 (Donovan et al., 2006a) and Ply700 (Celia et al., 2008), as well as the chimeric streptococcal-staphylococcal constructs λSA2E-Lyso-SH3b and λSA2E-LysK-SH3b (Schmelcher et al., 2012b), have been shown to display bacteriolytic activity in milk or milk products. With the ability to retain significant lytic activity after incubating at 90°C for 30 minutes, the kinetically stable *L. monocytogenes* endolysins Ply511, Ply118 and Ply500 could be applicable as a disinfectant for food products that undergo elevated heat treatment, such as pasteurized milk (Schmelcher et al., 2012c). These three *Listeria* endolysins were also effective for decreasing *L. monocytogenes* viability on iceberg lettuce by up to 2.4-log units after storage for 6 days. Another example of using phage endolysins to prevent the growth of food-borne pathogens involved pre-treating pear slices with *E. coli* lysates containing overexpressed *E. amylovora* phage ΦEa1h lysozyme. After inoculating the fruit with bacteria and

incubating the samples at 26°C for 5 days, lysate pre-treatment was able prevent *E. amylovora* colonization on the surface of the pear slices (Kim et al., 2004).

Endolysins can also be alternatively exploited by starter microorganisms, such as *Lactococccus lactis*, used for fermentation processes in order to prevent contamination and consequent economic loss for manufacturers. Contamination during fermentation can decrease food quality as well as possibly presenting future health risks if no further pasteurization occurs. Whereas broad spectrum antimicrobials cannot be used due to the nonspecific killing of the starter microorganisms, the high specificity of endolysins makes them ideal antimicrobial candidates for controlling contamination. One validated strategy involves genetically inserting endolysin genes into starter microorganisms, followed by the expression and secretion of the enzyme into the environment for the eventual eradication of unwanted bacteria. Genetically modifying fermentation bacteria for the expression and secretion of endolysins derived from both *Listeria* (Gaeng et al., 2000; Stentz et al., 2010; Turner et al., 2007) and *Clostridium* phages (Mayer et al., 2010), as well as the exolysin lysostaphin (Turner et al., 2007), has been reported, although the application of these microorganisms to food products has yet to be shown.

Agriculture

Several agricultural applications for phage endolysins have been explored. For instance, endolysin-producing transgenic plants were able to avoid phytopathogenic bacterial infections. Transgenic potatoes producing T4 lysozyme were resistant against *Erwinia carotovora*, a plant pathogen known to cause black leg and soft rot (de vries et al., 1999; Düring et al., 1993). Lysozyme, which continuously accumulates within the

transgenic plant tissue, is simultaneously released as a result of plant cell damage caused by *E. carotovora* pectinases. As a result, the intracellular lysozyme is liberated and has the ability to lyse the phytopathogens upon direct contact. Besides the implications affiliated with phytopathogen resistance, transgenic plants programmed to express endolysins can serve as bioreactors capable of large-scale production of translational antimicrobials in an inexpensive manner. To illustrate this point, the *S. pneumoniae* endolysins Cpl-1 and Pal (Oey et al., 2009b) and the *S. agalactiae* endolysin PlyGBS (Oey et al., 2009a) were integrated into the plastid genome of the tobacco plant *Nicotiana tabacum*. The total protein expression of Cpl-1 and Pal was respectively estimated to represent ~10% (i.e. 0.5 g protein per kg of fresh weight) and ~30% (i.e. 2 g protein per kg of fresh weight) of the total soluble protein levels of the plant, while expression of PlyGBS was calculated to reach more than 70% of the total plant soluble protein. These immense protein expression yields were rationalized to be caused by the highly stable intracellular environment provided by the chloroplasts, as indicated by the absence of endolysin turnover during plant development.

In the case of animal agriculture, endolysins have been investigated as a disinfectant, prophylactic and therapeutic antimicrobial agent as an alternative means for preventing or combating animal disease. Equine strangles is a highly contagious infection of the lymph nodes of horses caused by *Streptococcus equi*. This disease is characterized by the expeditious onset of fever followed by upper respiratory tract catarrh, causing nasal discharge and acute swelling with subsequent abscess formation in the throat area (Sweeney et al., 2005). If left untreated, infected horses can suffocate due to enlarged lymph nodes that obstruct the airway. Serious complications associated with equine

strangles occur in approximately 20% of infected horses, resulting in mortality rates as high as 8% on farms where the infection is endemic (Sweeney et al., 1987). The efficacy of the streptococcal endolysin PlyC was benchmarked as a narrow-spectrum disinfectant for eliminating *S. equi* on horse stable surfaces and equipment (Hoopes et al., 2009). PlyC was shown to be 1,000 more active per weight than Virkon-S, a common disinfecting agent, with 1 µg of endolysin possessing the ability to sterilize a 10^8 CFU/ml culture of *S. equi* in 30 minutes. Furthermore, PlyC was efficacious when applied as an aerosol to common stable and horse-related equipment contaminated with *S. equi* and capable of retaining lytic activity in conditions that mimic a horse stable, including the presence of nonionic detergents, hard water or organic materials.

Use of peptidoglycan hydrolases for prophylactic and therapeutic applications specific to animal disease have also been tested and validated. Bovine mastitis, a microbial intramammary infection that induces inflammation of the mammary gland in cattle, affects one third of all dairy cows (Sordillo and Streicher, 2002). This specific disease causes reduced milk production in addition to increased replacement costs, discarded milk, treatment costs, veterinary fees and labor costs. The National Mastitis Council estimates economic losses are approximately $200 per cow annually in the United States, equating to a total exceeding $2 billion. Treatment of bovine mastitis with classical antibiotics is frequently ineffective and thus alternative antimicrobial approaches are needed (Brouillette and Malouin, 2005). While an assortment of bacteria cause bovine mastitis (e.g. *P. aeruginosa*, *S. agalactiae*, *E. coli*, *Mycoplasma*, *K. pneumoniae*), staphylococci are the most prevalent pathogen associated with the disease and, as such, have been targeted in early studies using peptidoglycan hydrolases to

prevent or treat infection. Lysostaphin at a concentration of 10 µg/ml in milk was able to generate a 5 to 6 log reduction in *S. aureus* (Bramley and Foster, 1990). After a 10^8 CFU inoculation of *S. aureus*, infusion of the lactating murine mammary gland with 10 µg of enzyme stimulated a 2 to 3 log reduction in bacteria within 30 minutes. Pre-treating the murine mammary gland with 10 µg of lysostaphin either immediately before or 1 hour prior to staphylococcal challenge caused a 6 log decrease in *S. aureus* viability. In an independent study, *S. aureus* was introduced to the teat cistem of cattle and infections were established for a minimum of 3 weeks (Oldham and Daley, 1991). A bactericidal concentration of lysostaphin was maintained in the milk extracted from the mammary gland of infected cows for up to 36 to 48 hours following treatment with a single 100 mg teat infusion of enzyme. The cure rate of infected cows administered 100 mg of lysostaphin over three consecutive p.m. milkings was 20%, which is comparable to the 29% cure rate obtained using the antibiotic sodium cephapirin. Moreover, transgenic mice (Kerr et al., 2001) and cows (Wall et al., 2005) producing lysostaphin in the mammary glands were resistant to *S. aureus*-induced mastitis. Considering the application of a single antimicrobial may ultimately promote resistance formation, using chemotherapeutic agents in combination may prove to be a more efficient strategy. To this end, using lysostaphin together with the chimeric endolysin λSA2E-LysK-SH3b prompted the synergistic killing of *S. aureus* both *in vitro* and in a murine model of bovine mastitis (Schmelcher et al., 2012b).

PlyC, a Thermolabile Streptococcal Endolysin with Unique Characteristics

In terms of bacteriolytic activity and structural composition, the streptococcal-

specific endolysin PlyC is an evolutionary outlier when compared to all other characterized endolysins to date. PlyC, derived from the streptococcal C_1 phage (Nelson et al., 2003), was first described in 1957, when C_1 phage lysates were shown to possess the ability to cause rapid lysis of groups A (GAS) and C (GCS) streptococci (Krause, 1957). This observation prompted the eventual use of this phage enzyme as a tool for isolating peptidoglycan-associated proteins and extracting DNA from group A streptococci (Fischetti et al., 1985; Wheeler et al., 1980). Over the past 13 years, PlyC has been validated both *in vitro* and *in vivo* for its anti-streptococcal efficacy (Nelson et al., 2001). Unlike other monomeric Gram-positive endolysins, PlyC consists of a novel multimeric structure that deploys a catalytic mechanism several orders of magnitude more bacteriolytically active when compared to other endolysins (McGowan et al., 2012; Nelson et al., 2006a). Similar to other mesophilic phage-derived endolysins, PlyC displays poor thermal stability, thereby limiting the feasibility of developing the enzyme as an antimicrobial for industrial application due to short shelf life expectancy. Bioengineering strategies directed towards the catalytic subunit of PlyC can be utilized to increase the stability of the structure and consequently progress the shelf life of the translational antimicrobial.

In vitro and *in vivo* Validation of Antimicrobial Efficacy

The use of a phage endolysin as a therapeutic alternative to classical antibiotics was first documented in 2001, when PlyC was shown to both prevent and eradicate *S. pyogenes* infection in a murine sepsis model for oral and nasal mucosal infection (Nelson et al., 2001). In this study, the *in vitro* efficacy of PlyC was first investigated against

streptococcal and non-streptococcal bacterial species. Initially, the lytic activity of PlyC against the major human pathogen, group A streptococci (i.e. *S.* pyogenes), was assessed. The endolysin was diluted to three different concentrations and added to ~10^7 group A streptococci. An aliquot of each sample was removed, diluted and plated on agar plates at 5, 30 and 60 seconds and 5 and 10 minutes to calculate total viable cell counts. Exposing the streptococci to 1,000 U of PlyC completely killed all the cells in the first 5 seconds, whereas 100 U of the endolysin was capable of decreasing streptococcal viability by an order of 3 logs in 5 seconds, 4 logs in 1 minute and 5 logs in 10 minutes. Lysis of endolysin-treated group A streptococci could be visualized by thin-section electron microscopy (Fig. 1-3). The lytic activity displayed by PlyC towards group A streptococci is ~100-200 fold higher than any other presently characterized endolysin.

To elucidate the antimicrobial spectrum of PlyC, a total of 250 U of PlyC was added to a collection of streptococcal (GAS, GBS, GCS, group D streptococcus (GDS), group E streptococcus (GES), group F streptococcus (GFS), group G streptococcus (GGS), group L streptococcus (GLS), group N streptococcus (GNS), *Streptococcus crista*, *Streptococcus intermedius*, *Streptococcus gordonii*, *Streptococcus mitis*, *Streptococcus mutans*, *Streptococcus oralis*, *Streptococcus parasanguis*, *Streptococcus salivarius*) and non-streptococcal (*Bacillus pumulis*, *S. aureus*, *S. epidermidis*, *E. coli*, *Neisseria lactamicus*, *Porphyromonas gingivalis*, *P. aeruginosa*) bacteria and the enzyme kinetics were monitored for a total of 8 hours. PlyC exhibited lytic activity against all GAS strains tested, including the serological grouping strain, an M protein-negative strain, 8 unique M protein types and an A variant strain. The enzyme also showed reduced activity against GCS, GES and *S. gordonii*. Using a murine model, the ability of

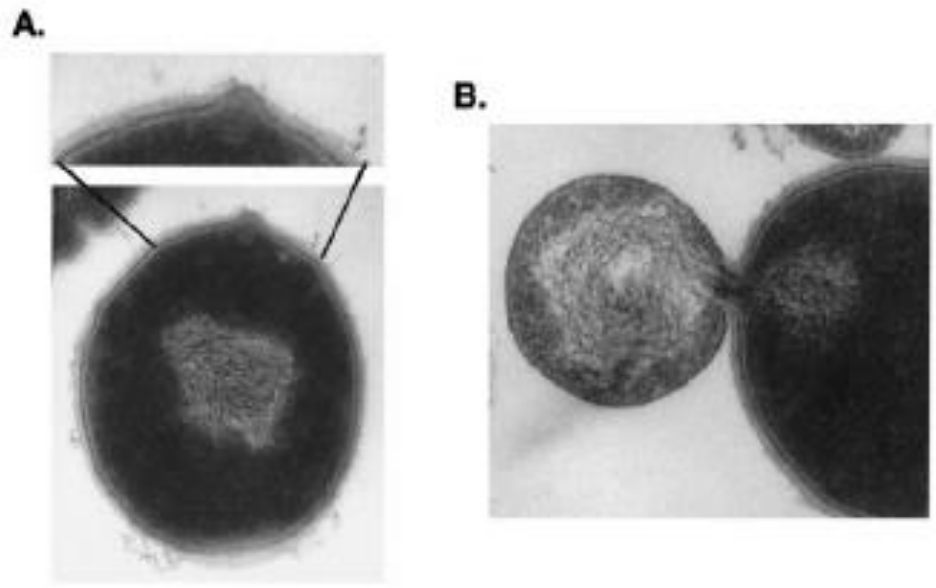

Figure 1-3. Thin-section electron micrograph of PlyC-treated group A streptococci treated. Group A streptococci were treated with the endolysin PlyC for 15 seconds and then visualized for lysis by thin-section electron microscopy (50,000x). (a) The streptococcal cell wall is first weakened, (b) thereby allowing the membrane to extrude through the hole generated by PlyC. (Source: Nelson et al., 2001)

PlyC to prevent or eliminate upper respiratory colonization by group A streptococci *in vivo* was tested. In the first set of experiments, group A streptococci was pre-mixed with either 1,000 U of PlyC or buffer *in vitro* and then was simultaneously applied orally and nasally to mice. After 24 hours post-infection, none of the endolysin-treated mice (n = 5) were colonized with group A streptococci, while all of the buffer-treated mice (n = 5) were colonized ($P < 0.01$). At the conclusion of the 7 day experiment, daily swabs of each mouse resulted in the detection of only a single colony from the endolysin-treated mice. In a second set of mouse experiments, animals were orally pre-treated with 250 U of either crude (n = 10) or purified (n = 11) PlyC prior to challenge with ~10^7 group A streptococci. The prophylactic application of PlyC was able to reduce streptococcal colonization from 70.5% (n = 17) in endolysin-treated mice to 28.5% (n = 21) in control animals after 24 hours ($P < 0.03$). The protection offered by the crude (3/10 infected) and purified (3/11 infected) endolysin treatment were similar and, with the exception of one mouse, all of the colonized endolysin-treated mice displayed low CFU counts (1-11 colonies). The CFU counts for the infected endolysin-treated animals either remained low or bacterial colonization was eliminated after 48 hours, whereas all of CFU counts for the buffer-treated mice increased at 48 hours. In the third mouse experiment, mice (n = 9) were first heavily colonized by group A streptococci (> 300 CFU per swab) for a total of four days. The infected animals were then orally treated with either a single 500 U dose of PlyC and then monitored for the next 48 hours for bacterial reduction. Swabs taken 2 hours post-treatment indicated that streptococci were completely eliminated from the mucosa of all nine mice. However, swabs taken 24 and 48 hours post-treatment revealed positive cultures for three mice, with one ultimately dying.

Molecular, Biochemical and Structural Characterization of PlyC

Prior to 2006, not much was known about the biochemical and structural properties of the endolysin derived from the C_1 phage. Purifying PlyC from phage lysates followed by native polyacrylamide gel electrophoresis (PAGE) analysis showed the enzyme behaves as a single homogenous protein (Nelson et al., 2006a). However, when viewed by sodium dodecyl sulfate PAGE (SDS-PAGE), the purified PlyC sample was shown to consist of two protein products, a ~50 kDa heavy chain, termed PlyCA, and an 8 kDa light chain, termed PlyCB. N-terminal sequencing results dictated that both PlyCA (SKKYTQQQYE) and PlyCB (SKINVNVENV) polypeptides have unique sequences.

To identify the gene(s) encoding PlyC, a genetic screen was implemented. The C_1 phage genome was partially digested with the Tsp509I restriction endonuclease and the DNA fragments were then cloned into the pBAD24 expression vector. Screening the resulting *E. coli* expression library allowed for the identification of a single clone, labeled as pBAD24: *plyC*, that exhibited lytic activity towards group A streptococci. Expression and purification of PlyC from this construct yielded a bacteriolytically-active enzyme with identical properties to PlyC purified form phage lysates when analyzed by means of column chromatography as well as native and SDS-PAGE. The *plyC* clone was comprised of a 2.2 kb insert with putative operon encoding three ORFs, with ~100 bp of noncoding sequence flanking the 5' and 3' ends of the insert. The first predicted gene in the operon, *plyCB*, consists of a translated 72 amino acid (7.858 kDa predicted mass) polypeptide that matches the before mentioned N-terminal sequencing results for PlyCB. The second putative gene in the *plyC* operon is predicted to encode a 105 amino acid (12.569 kDa predicted mass) protein. This translated sequence showed strong sequence

homology to 31 endonucleases, many of which belong to the homing HNH endonuclease family. The genes encoding HNH endonucleases are known to exist within group I introns and confer mobility to their host intervening sequence by catalyzing a precise double-strand break in the cognate allele deficient of the intervening sequence (Chevalier and Stoddard, 2001). Due to the position of the putative endonuclease gene between *plyCB* and ORF3, this region of the operon was named *lil*, for lysin intergenic locus. The third ORF of the *plyC* operon, *plyCA*, comprises a 465 amino acid (50.366 kDa) polypeptide that corresponds to the size and N-terminal sequence of PlyCA.

Various *plyC*-related constructs were synthesized, cloned and expressed to understand what genetic elements are required for PlyC activity. When expressing *plyCB, lil* and *plyCA* individually, all of the translated products were devoid of lytic activity. PlyC expressed in a Δ*lil* background retained activity, although the residual activity was less than a third of the full-length *plyC* clone. Co-expressing *plyCA* (pBAD24: *plyCA*) and *plyCB* (pBAD33: *plyCB*) on separate expression plasmids yielded a functional PlyC holoenzyme. While the activity of PlyC clearly requires both *plyCB* and *plyCA*, the presence of *lil* is not imperative for producing an active endolysin. RT-PCR and Northern blot analysis both suggest that intron splicing does not take place in the *plyC* operon. As a result, the molecular functionality of *lil* is currently still not understood.

Gel filtration and sedimentation analysis of purified PlyC in 1971 suggested that the mass of the endolysin was 101-105 kDa (Fischetti et al., 1971), which was then further confirmed in 2001 (Nelson et al., 2001). To determine the stoichiometry of PlyCB:PlyCA subunits, PlyC was subjected to size-exclusion chromatography (SEC) coupled with in-line laser light-scattering (LS), UV and refractive index (RI)

measurements (Nelson et al., 2006a). Results from a total of 20 independent SEC experiments using purified PlyC at various concentrations (100-300 µg total) confirmed the endolysin holoenzyme structure is 114.0 kDa with a standard deviation of ± 0.4 kDa. Considering PlyCB and PlyCA have predicted masses of 7.858 and 50.366 kDa, respectively, the SEC-LS/UV/RI data predicted an 8.0 ± 0.005 PlyCB to 1.0 PlyCA model for the holoenzyme structure.

Proteomic analysis of the PlyCA polypeptide using the Pfam database (www.pfam.xfam.org) disclosed the presence of a putative C-terminal CHAP domain. One of the two hydrolytic activities displayed by CHAP domains of peptidoglycan hydrolases is that of an N-acetylmuramoyl-L-alanine amidase. Significantly, prior experiments, which entailed using thin layer chromatography to analyze *S. pyogenes* cell wall fragments digested by PlyC, revealed the endolysin exhibited amidase activity (Fischetti et al., 1972a). Seeing as cysteine is the one of two active-site residues conserved in CHAP domains, several thiol-reactive inhibitors were added to PlyC to observe whether or not these chemicals had an effect on enzyme activity. An oxidizing compound, dithiodipyridine, in addition to two sulfhydryl alkylating reagents, ethylmaleimide and iodoacetamide, significantly reduced the enzymatic activity of PlyC. When an excess of reducing agent was subsequently added to each PlyC sample, activity was partially rescued for the oxidized PlyC but not the alkylated samples. It was concluded from these biochemical experiments that PlyC consists of an active-site cysteine. Performing a sequence alignment of PlyCA against other known members of the CHAP domain family indicated that the most likely active-site residues were C333 and H420. To confirm whether these two amino acids were the active-site residues, SDM

was used. The mutants PlyC (PlyCA) C333S and PlyC (PlyCA) H420A each displayed less than 1% activity compared to wild-type PlyC, thereby confirming C333 and H420 are indeed the active-site residues. As a control, independently mutating three additional cysteine residues to serine (C268S, C345S and C404S) in PlyCA resulted in a PlyC mutant that displayed activity that resembled that of wild-type. Therefore, these results confirm the presence of a CHAP domain within PlyCA.

PlyCA alone lacks the ability to lyse streptococcal cells and thus requires the presence of the eight PlyCB subunits. With this understanding, PlyCB was hypothesized to serve as the CBD of the holoenzyme that directs PlyCA to the streptococcal cell wall for peptidoglycan hydrolysis. To test this, PlyC, PlyC (PlyCA) C333S and PlyCB were each purified and fluorescently labeled, added to bacteria and visualized for cell binding via fluorescence microscopy. Notably, PlyCB eluted from gel filtration at ~60 kDa, suggesting that it forms a self-assembled octomer. When gel filtration was repeated in the presence of 0.1% SDS, PlyCB eluted as an ~8 kDa monomer. Labeled wild-type PlyC not only retained its binding properties, but the sample was still catalytically active and therefore lysed all of the streptococcal cells before they could be mounted on a microscope. PlyC (PlyCA) C333S (Fig. 1-4a) and PlyCB (Fig. 1-4b) were both able to successfully fluorescently label *S. pyogenes* cells, but not other bacterial species tested (e.g. *S. agalactiae*, *S. mutans* and *S. aureus*) (Fig. 1-4c), indicating that PlyCB acts as the CBD of the PlyC holoenzyme.

Recently, a 3.3-Å X-ray crystal structure of the PlyC holoenzyme was published (Fig. 1-5) (McGowan et al., 2012). As suggested by previous structural studies, the crystal structure of PlyC consisted of nine distinct subunits. Eight identical PlyCB

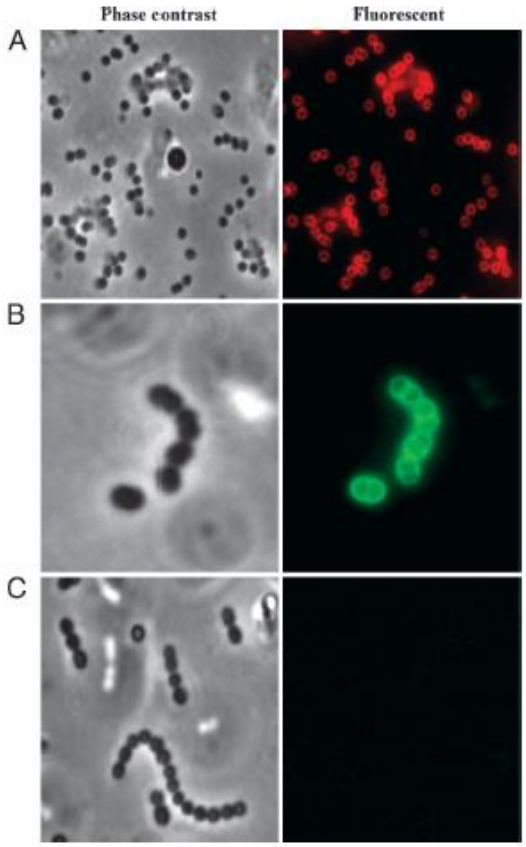

Figure 1-4. PlyCB acts as the cell wall binding domain of PlyC. Fifty micrograms of labeled protein was added to 1 ml of various bacterial cells, washed two times and viewed under both phase-contrast and fluorescent light sources. (a) PlyC (PlyCA) C333S cross-linked with Alexa Fluor 568 specifically labels *S. pyogenes*. (b) PlyCB labeled with Alexa Fluor 488 specifically labels *S. pyogenes*; thus PlyCB directs cell wall binding for PlyC. (c) Bacterial species insensitive to PlyC (*S. agalactiae* (shown), *S. mutans* and *S. aureus* (not shown)) are resistant to labeling by PlyCB-Alex Fluor 488. All panels were viewed through a 100x magnification oil-immersion objective lens with a 2x magnifier (200x total). Additionally, B was digitally zoomed 2x, for a final magnification of 400x. (Source: Nelson et al., 2006b)

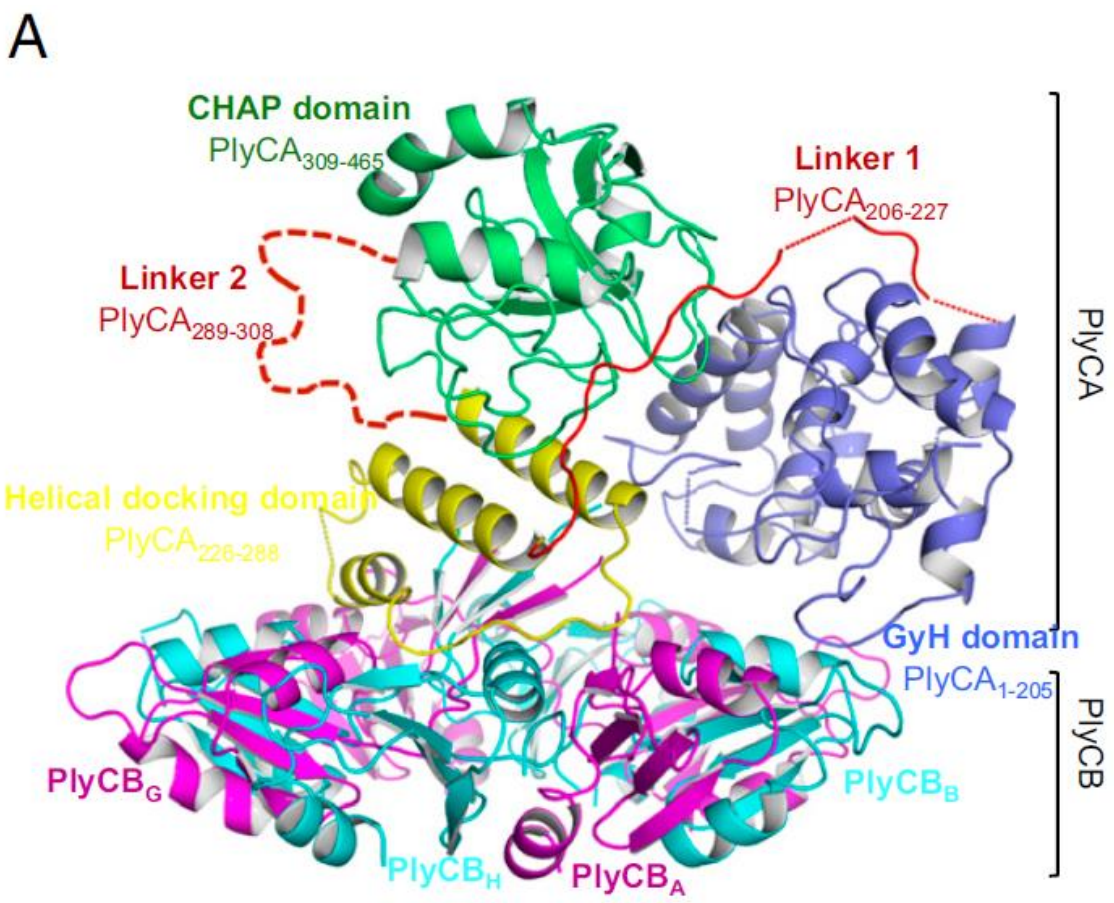
A
CHAP domain
PlyCA309-465
Linker 1
PlyCA206-227
Linker 2
PlyCA289-308
PlyCA
Helical docking domain
PlyCA226-288
GyH domain
PlyCA1-205
PlyCB
PlyCBG
PlyCBB
PlyCBH
PlyCBA

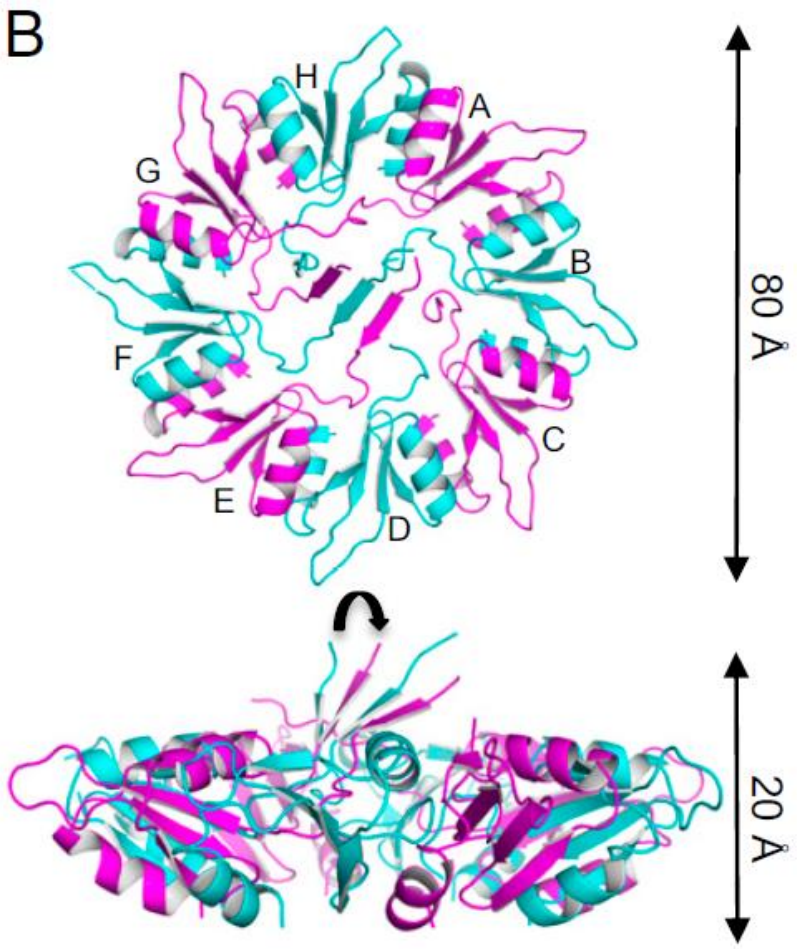

Figure 1-5. X-ray crystal structure of PlyC. (a) The 3.3-Å X-ray crystal structure of PlyC whereby PlyCB monomers are colored alternatively with magenta/cyan and labeled monomers A-H. The PlyCA subunit is colored by domain as indicated. The Cα atoms of the model show the N-terminal residues 1-205 in light blue, the disordered linker 1 (residues 206-227) in red, the helical structure (residues 226-288) that docks PlyCA to PlyCB in yellow, the second disordered linker 2 (residues 289-308) in a dashed red line, and the CHAP domain (residues 309-465) in green. Regions of disordered/absent density are depicted by dashed lines. (b) The PlyCB CBD alone colored alternatively in magenta/cyan and labeled A-H. (Source: McGowan et al., 2012)

monomers interact through protein-protein interactions to form a symmetrical octomeric complex, which serves as the CBD of the holoenzyme (Fig. 1-5, magenta and cyan). The ninth subunit, PlyCA, consists of a previously unknown N-terminal glycosol hydrolase (GyH) domain (Fig. 1-5a, light blue) linked via linker 1 to a central helical docking domain (Fig. 1-5a, yellow). This centralized domain is responsible for interacting with the PlyCB CBD to form the holoenzyme structure. The carboxyl end of the helical docking domain of PlyCA is then linked via linker 2 to the C-terminal CHAP domain (Fig. 1-5a, green).

Stimulated by the unexpected finding of an N-terminal GyH in PlyCA, a series of biochemical assays were performed to determine whether or not the GyH domain is functional and, if so, elucidate if this domain displays synergism with the C-terminal CHAP domain and consequently identify the active-site residues and hydrolytic mechanism (amidase or glycosidase) of the domain. To first assess if the GyH domain is enzymatically active and synergistic with the CHAP domain, a PlyCΔCHAP (i.e. PlyC holoenzyme with CHAP domain deletion) construct was synthesized, expressed, purified to homogeneity and assayed for lytic activity against *S. pyogenes* using turbidity reduction assays. Additionally, other PlyC constructs were expressed, purified and assayed for activity, including PlyC, PlyCA alone, CHAP alone and PlyCΔGyH (i.e. PlyC holoenzyme with GyH domain deletion). In these particular experiments, 44 nM of each protein was added to *S. pyogenes* in an individual well of a 96-well microtiter plate and the OD_{600} was monitored at 37°C every 6 seconds for 10 minutes, with a loss in OD correlating to enzyme-specific lytic activity. PlyCΔGyH and PlyCΔCHAP each displayed < 1% of wild-type activity, and complementing PlyCΔCHAP with purified CHAP did not

restore wild-type activity. PlyC at a 1 nM concentration was still considerably more active than 44 nM PlyCΔCHAP complimented with 44 nM CHAP. Altogether, these kinetic results show that, in the context of the holoenzyme, the GyH and CHAP domains are both hydrolytically active and act together cooperatively to generate the robust lytic mechanism of PlyC.

VAST and DALI searches showed that the enzymatically-active N-terminal GyH domain of PlyCA is homologous to class IV family 19 chitinases, which cleave β-1,4 glycosidic bonds of unbranched chains of N-acetylglucosamine polymers. To determine the lytic mechanism of this domain and to confirm the amidase activity affiliated with the C-terminal CHAP domain of PlyCA, two separate biochemical assays were used to analyze free sugar (glycosidase activity) (Spiro, 1966) and amine (amidase activity) (Snyder and Sobocinski, 1975) release that occurs as a result of PlyC hydrolysis of purified streptococcal peptidoglycan. PlyC, PlyCA only and PlyCB octomer only were used as controls and purified streptococcal peptidoglycan was used as a substrate. To assess the contribution of the CHAP domain, an active-site mutant, PlyC (PlyCA) C333S, was used. To analyze the contribution of the GyH domain, four putative catalytic center mutants, PlyC (PlyCA) E78A, N87A, H88A and N104A, were used. Results showed that PlyC exhibits elevated glycosidase activity and mutating any of the putative GyH domain catalytic residues or surrounding residues reduced activity ~85%. Additionally, the CHAP domain active-site knockout, PlyC (PlyCA) C333S, also displayed a dramatic reduction in glycosidase activity, further supporting the idea that the CHAP domain and GyH domain work together synergistically. Combining the CHAP domain active-site knockout, PlyCA (C333S), independently with each of the putative catalytic residues of

the GyH domain consequently eradicated all glycosidase activity associated with PlyC. Similar biochemical assays were then used to quantitate amidase activity. As expected, PlyC (PlyCA) C333S provoked a complete loss in amidase activity. Mutations to the putative catalytic residues of the GyH also promoted significant losses in amidase activity, although the reduction was not as severe as the CHAP active-site mutant. Combining the PlyCA (C333S) mutation with each of the GyH putative catalytic residue mutations yielded a PlyC construct devoid of all amidase activity. Conjointly, the results of these two biochemical experiments suggest that PlyCA exhibits both amidase and glycosidase activity, and additionally provide further evidence that both the GyH and CHAP domains act together cooperatively.

Transient Shelf Life of PlyC Caused by the Thermolability of PlyCA

There are several characteristics associated with PlyC that makes this particular translational antimicrobial a potentially valuable alternative to classical antibiotics. First, the immense bacteriolytic activity unique to PlyC allows this enzyme to rapidly clear streptococcal colonization when utilized as a disinfectant, prophylactic and therapeutic. Secondly, as is the case with most Gram-positive endolysins, the high selectivity of these enzymes inhibits the non-specific killing of commensal bacteria. This reduction in chemotherapeutic toxicity helps prevent harmful side effects from occurring. However, contrary to other endolysins, PlyC can target and lyse a variety of streptococcal species that cause both human (e.g. *S. pyogenes*) and animal (e.g. *S. equi*, *S. uberis* and *Streptococcus porcinus*) health complications. Group A streptococcus, *S. pyogenes*, is the major streptococcal human pathogen that can cause an assortment of acute (e.g.

pharyngitis, scarlet fever, impetigo and cellulitis) and invasive (e.g. necrotizing fasciitis, myositis and toxic shock syndrome) suppurative infections. *S. equi*, *S. uberis* and *S. porcinus* are causative agents for equine strangles, bovine mastitis and swine lymphadenitis, respectively. An antimicrobial, like PlyC, that encompasses the ability to target and expeditiously eliminate both human and animal pathogens is vastly desirable for commercialization, especially as an alternative therapy for treating MDR infections.

A critical property of any chemotherapeutic agent relates to its intrinsic thermal stability. In congruence with the Arrhenius equation, which relates the rate of a chemical reaction to the temperature present in the system, the structural stability of a macromolecule directly correlates with its shelf life expectancy (Anderson and Scott, 1991). The Arrhenius equation is as followed:

$$k = A\exp(-E_A/RT)$$

where k is the rate constant, A is the frequency factor, E_A is activation energy, R is the universal gas constant and T is the temperature. As defined by the equation, high temperatures and low activation energy values favor larger rate constants, thus speeding up a chemical reaction. Considering both variables consist in an exponent, the effects of each on the reaction rate is substantial. Simplistically applying this equation to macromolecules, like proteins, for shelf life calculations elucidates two important trends. First, the shelf life of a chemotherapeutic is progressively shortened as the storage temperature increases. Secondly, chemotherapeutic shelf life continuously increases as the activation energy of kinetic inactivation or unfolding is elevated.

Heating experiments in 2004 involving PlyC demonstrated that the endolysin manifested modest thermal stability (Daniel Nelson, personal communication). In these

experiments, PlyC was incubated at temperatures ranging from 37°C-100°C for one hour in phosphate buffered saline (PBS). At the conclusion of the incubation, the structural integrity of the holoenzyme was visualized by both native and SDS-PAGE and the residual lytic activity was assayed by means of turbidity reduction assays. At temperatures exceeding 42°C, PlyC irreversibly precipitates to form high molecular weight complexes incapable of penetrating the native PAGE gel, rendering the enzyme inactivate.

Unpublished thermodynamic characterization of PlyC in 2008 by differential scanning calorimetry (DSC) revealed the endolysin has transient shelf life expectancy due to the thermolabile nature of the catalytic subunit, PlyCA (Fred Schwarz, personal communication). Altogether, the complete unfolding of the PlyC holoenzyme fulfills a five-state thermal transition model. The unfolding of PlyCA consists of an irreversible three-state thermal transition, with an initial unfolding event occurring at 46.2°C. PlyCA was further dissected to determine the thermodynamics of the N-terminal GyH and C-terminal CHAP domain. The catalytic subunit in a PlyCΔCHAP (PlyC holoenzyme with a PlyCA CHAP domain deletion) background exhibited a thermal transition temperature (T_G) 46.0°C, whereas the isolated CHAP domain had a T_G of 39.1°C. This suggests that the CHAP domain of PlyCA is the most heat-susceptible structural element in the EAD. Conversely to PlyCA, the octomeric PlyCB CBD is endogenously thermostable, displaying a three-state transition model with a T_G of 75.0°C. When the CBD unfolds, the PlyCB octomer first reversibly dissociates into individual monomers, followed by the irreversible unfolding of each PlyCB subunit.

The inferior inherent thermal stability of PlyCA and hence limited antimicrobial potential of PlyC makes the feasibility of developing the endolysin as a translational chemotherapeutic for industrial application challenging. While the database of thermally characterized endolysins is sparse, there are several examples of Gram-positive endolysins derived from mesophilic phages that display similar thermolability to that of PlyC. For example, heating the staphylococcal endolysin LysK to 42°C caused a 1,000 fold reduction in lytic activity against *S. aureus* (Filatova et al., 2010). Results from circular dichroism (CD) far-UV spectroscopy signified that the loss in enzymatic activity was accompanied by significant changes in the secondary structure of the protein. In addition to LysK, the thermal properties of the pneumococcal endolysins Cpl-1, Pal and Cpl-7 were investigated by DSC. Deconvolution of the excess heat capacity data for Cpl-1 and Pal showed both endolysins manifested three-state thermal transition models, with Cpl-1 (Sanz et al., 1993) and Pal (Varea et al., 2004) exhibiting respective T_G values of 43.5°C and 50.2°C. Analyzing the DSC-derived heat capacity thermogram of Cpl-7 revealed the unfolding of the enzyme consists of a four-state thermal transition, displaying a T_G of 50.4°C at the optimum pH for stability (Bustamante et al., 2012).

Protein Engineering Methodologies

Protein engineering constitutes a powerful tool for designing new enzymes or proteins with novel or desirable properties. At the beginning of the 1980s, the inability to alter macromolecular chemistry was viewed as a significant hindrance in the field of biochemistry. Without the capability of modifying macromolecular surface chemistries, elucidating relationships between structure and activity was particularly difficult,

especially in the field of enzymology. The principles that govern enzyme catalysis were well understood (Knowles and Albery, 1977) and the quantity of solved enzyme X-ray crystal structures was continually expanding (Campbell, 2002). Together, this information provided the framework hypothesizing enzymatic mechanisms of action in which particular roles could be assigned to functional groups that were identified in the active sites. In order to test these hypotheses, scientists would attempt to chemically modify these functional groups of interest using laborious techniques with limited range and poor specificity. However, the development of SDM changed everything in the field of biochemistry. The first reported use of this technology, for the purpose of mutating a gene encoding an enzyme with a known mechanism to yield a final protein product with a defined amino acid substitution, was documented in 1982 for a tyrosyl-transfer RNA synthetase (TyrRS) (Winter et al., 1982) and β-lactamase (Dalbadie-McFarland et al., 1982; Sigal et al., 1982). Mutating one or two amino acids eventually expanded to changing entire loops and even entire domains. This production of modified proteins to study their corresponding properties fueled the formation of a new field, termed protein engineering.

Currently, a variety of protein engineering approaches can be exploited to protein catalysis, specificity, folding and stability. Bioengineering methodologies tailored towards increasing protein thermal stability can be employed to address the innate instability of Gram-positive endolysins. Although there are no documented examples of thermostabilizing endolysins to date, there are numerous examples where the stability of other enzymes was significantly augmented. Engineering desirable properties to enzymes can be achieved using either rationale-based (e.g. sequence comparison, structure-guided

SDM or *in silico* computational modeling) or random techniques (e.g. random mutagenesis, gene shuffling or directed evolution).

Rationale-based Methods for Protein Thermostabilization

Protein stability is dependent on a multitude of both local and distant intermolecular and intramolecular interactions. Engineering enhanced stability to proteins generally requires combining multiple thermostabilizing amino acid mutations that individually have a small effect on stability. In many cases, the mechanism of stability for each residue mutation is unique and therefore combining numerous advantageous mutations can be additive to induce pronounced enhancements in protein stability (Akasako et al., 1995; Ohage and Steipe, 1999; Pantoliano et al., 1989; Serrano et al., 1993; Shih and Kirsch, 1995; von der Osten et al., 1993).

Rational protein engineering methods collectively involve replacing amino acids at specific sites of the protein that are selected based on prior mechanistic or structural knowledge. One distinct advantage of rationale-based methodologies relative to random techniques is that only a small number of protein variants must be examined. A number of rational methods have been validated to improve protein stability, including sequence and structure comparisons between related mesophilic and thermophilic proteins, structure-guided SDM and *in silico* computational modeling.

Comparing amino acid sequences or three-dimensional structures between related mesophilic and thermophilic proteins can allow for the identification of critical residues or regions that enhance thermal stability. One systematic study compared the translated sequences corresponding to the cold shock proteins derived from the mesophile *Bacillus*

subtilis and the thermophile *Bacillus caldolyticus* (Perl et al., 2000). Despite only 12 of the 67 residues differ between the two protein sequences, the difference in structural stability is significant (15.8 kJ/mol at 70°C). Systematically introducing all 12 of the varying residues from the *B. caldolyticus* enzyme into the *B. subtilis* enzyme by SDM revealed that the difference in thermal stability between the two enzymes can be assimilated to just two amino acid mutations (E3R, E66L) located on the surface of the enzyme. The respective electrostatic and hydrophobic interaction contributions of E3R and E66L were able to convert the mesophilic enzyme into a modified highly thermostable form. In another study, the structures of the closely related mesophilic *Clostridium beijerinckii* alcohol dehydrogenase (CBADH) and the hyperthermophilic *Thermoanaerobacter brockii* alcohol dehydrogenase (TBADH) were directly compared in an attempt to identify structural differences that may contribute to the disparity in thermal stability (Bogin et al., 1998). While these two enzymes have 75% sequence identity, TBADH and CBADH differ greatly in stability, with TBADH and CBADH losing 50% activity at 93.8°C and 63.8°C, respectively. Analysis of the two protein structures suggested that the eight extra proline residues of TBADH, some of which are in apparent critical sites, could be potential thermostability factors. Due to the rigidity and hence low intrinsic entropy, proline is a common amino acid residue found in thermophilic proteins, especially in loop and turn structures. Using SDM, proline residues were individually substituted in place of the eight residues in CBADH that were spatially analogous to their endogenous location in TBADH. Of the eight individual proline mutants characterized, five of the eight improved the thermal stability of the enzyme,

with the most significant increase in melting temperature (T_m) observed with the S24P (ΔT_m = +3.9°C) and L316P (ΔT_m = +10.8°C) mutations.

An alternative rationale-based protein engineering strategy consists of using previously solved protein structures as a platform to incorporate modifications that are hypothesized to be stabilizing. There are several general strategies for stabilizing proteins that have been validated, including "entropic stabilization" (i.e. rigidification) by glycine → alanine or Xxx → proline mutations or the insertion of disulfide bridges (Clarke and Fersht, 1993; Mansfeld et al., 1997; Matsumura et al., 1989; Matthews et al., 1987), "helix capping" by introducing residues that interact with the alpha-helix dipole (Marshall et al., 2002; Nicholson et al., 1991; Nicholson et al., 1988; Sali et al., 1988; Serrano and Fersht, 1989), other types of helix optimization (e.g. replacing residues in left-handed helical structures with glycine or asparagines) (Blaber et al., 1993; Serrano et al., 1992), formation of additional salt-bridge interactions (Makhatadze et al., 2003; Pace et al., 2000; Schwehm et al., 2003; Serrano et al., 1990; Strop and Mayo, 2000; Sun et al., 1991; Waldburger et al., 1995), and the introduction of clusters of aromatic-aromatic interactions (Anderson et al., 1993; Burley and Petsko, 1985; Puchkaev et al., 2003; Serrano et al., 1991). Furthermore, conserved characteristics of proteins encoded by thermophiles and hyperthermophiles have provided insight into how these macromolecules adapt to the stressful elevated temperature environments they are exposed to. Thermophilic proteins typically consist of (Renugopalakrishnan et al., 2005):

- Reduced glutamine composition, glycine → alanine, lysine → arginine (Tekaia et al., 2002)

- Arginine and tyrosine are more frequent while cysteine and serine are less frequent, longer α-helices with lower proline composition (Cooper et al., 1992)
- Polar residues form extra hydrogen bonds with each subunit (Dalhus et al., 2002)
- Charged residues form extra ionic interactions between dimer-dimer interface (Facchiano et al., 1998; Vieille and Zeikus, 2001)
- Higher number of alanine and aromatic residues (Hakulinen et al., 2003)
- Decrease in β branched residues (valine, isoleucine, threonine) (Facchiano et al., 1998)
- Larger threonine:serine ratio in β-strands (Hakulinen et al., 2003)
- Increase of charged residues on the protein surface, especially arginine

Proteins derived from hyperthermophiles typically consist of:

- Reduced glutamine and increased glutamic acid levels (Tekaia et al., 2002)
- Salt bridges that rigidify the protein structure (Kumar et al., 2000a)
- Larger number of isoleucine (Facchiano et al., 1998)
- Decrease in glycine residues in α-helices (Hakulinen et al., 2003)

Comparing mesophilic proteins to their homologous thermophilic counterparts have revealed that nature has employed several structural strategies for achieving high stability. The high conservation of the hydrophobic core of mesophilic and thermophilic protein homologs has led to the realization that the surface and surface electrostatics of a protein are more important for thermal stability than originally thought (Eijsink et al., 1995; Hoseki et al., 1999; Machius et al., 2003; Martin et al., 2002; Martin et al., 2001; Perl et al., 2000; Perl and Schmid, 2001; Vieille and Zeikus, 2001). Also, large electrostatic interaction networks and a higher oligomerization state tend to be favored

for thermostabilization (Clantin et al., 2001; Maeda et al., 2002; Thoma et al., 2000; Vetriani et al., 1998; Vieille and Zeikus, 2001; Walden et al., 2001; Xiao and Honig, 1999). Collectively, unique compositional and structural characteristics of proteins originating from thermophiles and hyperthermophiles can be incorporated into mesophilic homologues for the purpose of engineering progressed stability.

Computational screening methods have been developed to measure the effect that amino acid mutations have on protein stability through the estimation of Gibbs free energy ($\Delta\Delta G$) values. These algorithms use either biophysical models of amino acid interactions (Kellogg et al., 2011; Seeliger and de Groot, 2010; Worth et al., 2011; Yin et al., 2007), statistical analyses of available proteins and corresponding thermodynamic properties (Dehouck et al., 2011; Guerois et al., 2002; Johnston et al., 2011), machine learning methods (Capriotti et al., 2008; Tian et al., 2010), or a combination thereof (Li et al., 2012; Masso and Vaisman, 2010) to estimate the effect a mutation has on stability. Some examples of algorithms that have been successfully exploited to increase protein stability are CC/PBSA (Benedix et al., 2009), EGAD (Pokala and Handel, 2005), I-mutant 2.0 (Capriotti et al., 2005), Rosetta (Dantas et al., 2007; Kellogg et al., 2011; Leaver-Fay et al., 2011) and FoldX (Guerois et al., 2002). Independent evaluation of these computational methods suggested that they are highly efficient and display moderate accuracy (Potapov et al., 2009).

Results from third-party testing showed the FoldX protein folding algorithm performed with useful accuracy across all protein types, with a correlation coefficient r of 0.5 between estimated and experimental $\Delta\Delta G$ values (Khan and Vihinen, 2010; Potapov et al., 2009). FoldX uses an empirical potential from a weighted combination of physical

energy terms (e.g. van der Waals interactions, hydrogen bonding, electrostatics and solvation), statistical energy terms and structural descriptors (Guerois et al., 2002; Schymkowitz et al., 2005b). The parameters used in the potential were determined by fitting experimental $\Delta\Delta G$ values for 339 point mutants from a total of nine different proteins, resulting in a respective correlation coefficient and standard deviation between the predicted and experimental data of 0.8 and 0.75 kcal/mol (Guerois et al., 2002).

FoldX was applied to the structure of Cel7A chimeric fungal cellobiohydrolase I (CBH I), as well as 39 different fungal CBH I crystal structures, in order to identify mutations that are predicted to be stabilizing for the majority of the CBH I structures (Komor et al., 2012). The *in silico* screening combined with a consensus sequence analysis using a total of 41 CBH I sequences ultimately generated a final combined mutant with a T_{50} (i.e. temperature at which the enzyme loses 50% activity after a 10 minute incubation) increase of 4.7°C. The stabilized chimeric Cel7A mutant comprised an overall T_{50} of 72.1°C, which is 9.2°C higher than that of the most stable native CBH I. This improvement in stability also increased the optimal temperature for activity from 50°C to 60°C. In an independent study, the automated computer algorithm PERLA and the FoldX empirical force field were used to improve the thermal stability of a multimeric tumor necrosis factor (TNF)-related apoptosis-inducing ligand (TRAIL) (van der Sloot et al., 2004). Stabilization of the TRAIL trimer was accomplished by two mutations the caused both intra- and inter-subunit modifications, resulting in a T_m increase of 8°C. Consequently, the thermostabilized TRAIL protein was shown to be biologically active after a 73°C incubation for 1 hour.

Random Methods for Protein Thermostabilization

The use of rational protein engineering methods for improving stability are often limited because structural and mechanistic understanding of the protein is often required, the library size tested is limited and there is inherent difficulty in predicting distinct amino acid mutations that are thermally advantageous, even if the crystal structure is known. Moreover, although extensive proteomic and structural studies have yielded protein properties that are believed to enhance thermal stability, findings from independent studies tend to be contradictory, making it difficult, if not impossible, to identify universal thermostabilization strategies. For example, Jaenicke and Bohm state that the optimization of atomic packing contributes to protein thermostability whereas Karshikoff and Ladenstein indicate that there is little disparity between the atomic packing of mesophilic and thermophilic proteins (Jaenicke and Bohm, 1998; Karshikoff and Ladenstein, 1998). After performing a systematic analysis of the structural distribution of amino acids between 20 families of homologous mesophilic and thermophilic proteins, Pack and Yoo state there is no difference in the occurrence of the amino acid cysteine between the samples, which contradicts the findings of Kumar *et al.* who observed a significant decrease in cysteine residues in thermophilic proteins when performing a statistical analysis between 18 families of homologous mesophilic and thermophilic proteins (Kumar et al., 2000b; Pack and Yoo, 2004). While analyzing the difference between 16 different families of homologous mesophilic and thermophilic proteins, the Argos group found that hydrogen bonding was the most important stabilizing factor for thermophilic proteins (Vogt and Argos, 1997; Vogt et al., 1997). Conversely, Szilágyi and Závodszky compared the structures of 25 different families of

homologous mesophilic and thermophilic proteins and found no significant difference in hydrogen bonding (Szilagyi and Zavodszky, 2000).

Accordingly, alternative methods have been designed that involve randomly mutating individual amino acids to each of the other 19 naturally occurring amino acids. The resulting mutant library is then screened in order to identify mutations that are beneficial to the stability of the protein. Random methods are often preferred to rational methods due to two reasons. First, the size and genetic diversity of the libraries produced when using random methods are significantly greater than that of the SDM mutant pool produced for rationale-based methodologies. Larger and more diverse libraries allow for the possibility of identifying stabilizing mutations that would have been otherwise overlooked if using structure-guided rational methods. Secondly, random bioengineering methodologies require minimal understanding of the structure and function of the protein of interest. Along these lines and contrary to most rational methods, an understanding of the mechanism of stabilization is not required when a stabilizing mutation is identified during the screening process. In general, stabilizing mutations selected by random mutagenesis approaches are scattered throughout the entire protein (typically near the surface) and their effects are not always understood on the basis of generally accepted principles of protein stability (van den Burg and Eijsink, 2002).

Random mutagenesis strategies involve methods for generating diversity either throughout an entire DNA sequence or to explicit regions along the sequence (e.g. saturation or localized/region-specific mutagenesis) (Neylon, 2004). These strategies can generally be classified into groups of enzymatic and chemistry- or cell-based approaches, as well as their combinations. Enzymatic strategies often exploit the properties of DNA

modifying enzymes, such as DNA polymerase. For example, natural or engineered defective DNA polymerase enzymes with low fidelity are often used in a random mutagenesis technique known as epPCR. The error rates for these enzymes can be modulated by unbalancing nucleotide concentrations, altering pH, changing the divalent cation(s) used in the reaction and/or varying the number of heating cycles (Cadwell and Joyce, 1992; Shafikhani et al., 1997). Chemical methods can either directly or indirectly (e.g. oligonucleotide synthesis) modify DNA to provoke nucleotide mutations. Traditionally, chemical DNA-modifying strategies have been employed for *in vivo* mutagenesis of plasmids and genomes of bacteria and eukaryotes, using chemicals such as ethyl methane sulfonate (EMS), methylnitronitrosoguanidine (MNNG) and ethylnitrosourea (ENU) (Rasila et al., 2009). Conversely, only few chemicals have been validated to successfully modify DNA *in vitro* (Smith, 1985), including EMS (Lai et al., 2004) and hydroxylamine hydrochloride (Kaur and Sharma, 2006; Stellwagen and Craig, 1997; Wong et al., 2006b). Cell-based mutagenesis strategies are based on the increased rate of DNA replication errors. These elevated mutation rates observed in these methods are caused by either environmental/physiological stress (e.g. exposure to ionizing radiation or ultraviolet light) or defective replication/repair functions in cells (e.g. bacterial mutator strains with deficient DNA repair pathway genes). Using this strategy, mutations are randomly introduced during *in vivo* replication of the gene of interest that is comprised within an appropriate replicative vector. The *E. coli* strain XL1-Red, which lacks the three primary DNA repair pathways *mutS*, *mutT* and *mutD* (Greener et al., 1996), is an example of a validated cell-based system that is commercially available for random mutagenesis (Belanger et al., 2005; Bornscheuer et al., 1999; Callanan et al.,

2007; Henke and Bornscheuer, 1999; Lu et al., 2001). Alternatively, homology-dependent and -independent *in vitro* genetic shuffling methods have proven to be an effective approach for randomly mutagenizing proteins (Brakmann, 2001).

Firefly luciferase, which catalyzes the oxidation of a benzothiazole substrate (e.g. beetle luciferin) in the presence of magnesium ions, adenosine triphosphate (ATP) and oxygen, is an extremely sensitive genetic reporter widely used in molecular biology (Deluca, 1976; Gould and Subramani, 1988). Besides being utilized as a genetic reporter, the North American firefly luciferase is used extensively for measuring microbial contamination as well as bioluminescence-based technologies as an alternative to more conventional screening methods. Unfortunately, the applicability of the enzyme was limited due to its native *in vitro* and *in vivo* instability. To address this concern, the North American firefly luciferase gene, *luc*, was subjected to random mutagenesis in hopes of identifying potential thermostabilizing mutations (White et al., 1996). The gene was first cloned into an expression vector and then chemically-treated with hydroxylamine, transformed into *E. coli* and plated. After overnight incubation at 37°C, the bacterial colonies were transferred to a new agar plate by nylon filters, followed by incubation at 37°C for 2-4 hours. The nylon filters were removed and soaked in D-luciferin to assay for residual luciferase activity. One particular clone was identified that displayed a substantial increase in kinetic stability. This mutant, encoding a single glutamate to lysine mutation at position 354, allowed the luciferase enzyme to retain 80% activity after the 37°C incubation, whereas the wild-type enzyme was devoid of activity. Saturation mutagenesis was then performed on residue position 354 to investigate whether any of the remaining 18 possible amino acids were thermally advantageous. Half-life studies at

40°C confirmed the most stabilizing mutations at 354 were E354K and E354R, each of which exhibited a 12 fold increase in kinetic stability over wild-type. This prompted the authors to hypothesize that the side-chain size, hydrophobicity and charge characteristics are all important contributors to the overall stability of the enzyme at position 354.

The laboratory approach to Darwinian evolution of biological macromolecules, often referred to as directed evolution, is the most commonly exploited protein engineering method for augmenting enzyme stability (Lutz and Patrick, 2004). Evolutionary methods used for protein engineering require generating extensively diverse and voluminous variant libraries of an initial lead candidate enzyme by *in vitro* random mutagenesis and recombination (Fig. 1-6) (Arnold et al., 2001; Love, 2008). From this immense mutant pool, a highly selective screening process is required for identifying variants with improved thermal properties. Multiple iterations of this two-step process are often required for the biosynthesis of enzyme mutants with significantly progressed structural stability (Brakmann, 2001). While the number of thermostabilized enzymes using directed evolution methods is vast, some notable studies using this approach include the construction of subtilisin variants with an up to 1,200 fold increase in kinetic stability at 60°C as well as a ~23°C improvement in thermal stability (Wintrode et al., 2001; Zhao and Arnold, 1999), an esterase depicting a 14°C increase in T_m (Giver et al., 1998), a galactose oxidase with a 4°C increase in thermal stability (Sun et al., 2001) and a cold-shock protein with a 28°C augmentation in T_m (Martin et al., 2001).

Purpose of Research

Findings from several studies involving the thermal characterization of Gram-

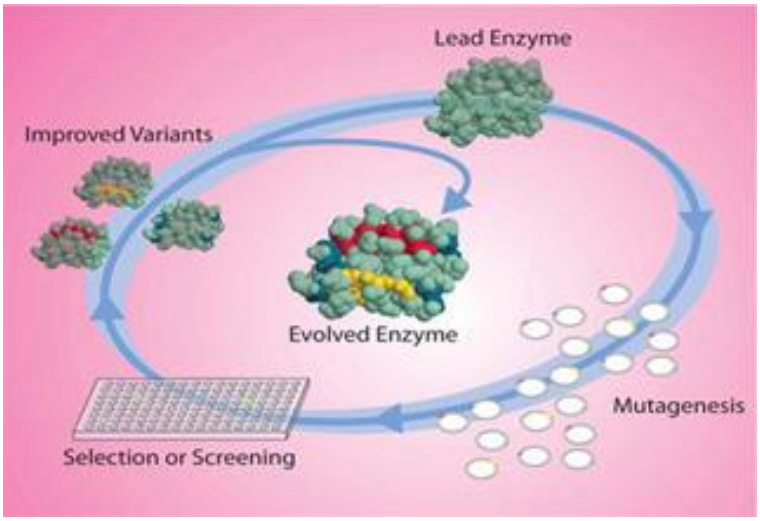

Figure 1-6. Directed evolution methodology overview. The two essential steps for directed evolution protein engineering approaches are: (1) generating an extensive mutant library by *in vitro* random mutagenesis and recombination that is exceedingly diverse, and (2) utilizing a stringent screening process in order to select enzyme variants that display desired properties. This two-step process is repeated multiple times followed by genetic recombination to yield the final evolved enzyme(s). (Source: Love, 2008)

positive endolysins derived from mesophilic phage revealed these enzymes generally lack intrinsic thermal stability. With a long-term goal of developing endolysins as novel alternative translational antimicrobials to classical antibiotics, their unstable nature limits their antimicrobial potential and subsequently makes the feasibility of developing these enzymes for industrial application challenging due to transient shelf life expectancy. This dissertation focuses on using rational and/or random bioengineering methods for increasing the kinetic, structural and thermodynamic stability of the streptococcal-specific endolysin PlyC. By doing so, one would generate an antimicrobial with an elongated shelf life that would increase the prospect of commercialization, as well as providing validated thermostabilizing engineering strategies that can then be further applied to other heat-labile endolysins. A rationale-based computational screening analysis is first described in this dissertation that involves using the protein folding algorithms FoldX and Rosetta for the purpose of identifying thermostabilizing mutations specific to the thermolabile CHAP domain of PlyC (Chapter II). Next, the development of a novel directed evolution methodology is discussed that is comprised of an epPCR step followed by an extensively optimized screening process to ultimately elucidate amino acid mutations that improve the kinetic stability of any bacteriolytic enzyme (Chapter III). Finally, this directed evolution protocol was then applied to PlyC with a goal of further validating the methodology by significantly improving the structural stability and antimicrobial potential of the endolysin (Chapter IV).

Chapter II

Increasing the Stability of the Bacteriophage Endolysin PlyC Using Rationale-Based FoldX Computational Modeling

Ryan D. Heselpoth[1], Yizhou Yin[1,2], John Moult[1,3] and Daniel C. Nelson[1,4]

[1]Institute for Bioscience and Biotechnology Research, 9600 Gudelsky Drive, Rockville, MD 20850, USA; Computational Biology, Bioinformatics and Genomics; [2]Biological Sciences Graduate Program; University of Maryland, College Park, MD 20742, USA; [3]Department of Cell Biology and Molecular Genetics, University of Maryland, 1109 Microbiology Building, College Park, MD 20742, USA; [4]Department of Veterinary Medicine, University of Maryland, 8075 Greenmead Drive, College Park, MD 20742, USA

This chapter has been submitted for publication.

Abstract

Endolysins are bacteriophage-derived peptidoglycan hydrolases that induce host cell lysis and progeny virion release late in the lytic bacteriophage infection cycle. When expressed and purified as a recombinant protein, endolysins extrinsically lyse susceptible Gram-positive pathogens, thus representing a novel alternative antimicrobial approach to antibiotics. While the streptococcal endolysin PlyC has been validated *in vitro* and *in vivo* for its therapeutic efficacy, the inherent thermosusceptible structure of the enzyme correlates to transient shelf life expectancy, thereby hindering the feasibility of developing the enzyme as an antimicrobial. Here we thermostabilized the CHAP domain of the PlyCA catalytic subunit of PlyC using a FoldX-driven computational protein engineering approach. Ten mutants were selected as potentially increasing thermodynamic stability using a combination of FoldX, Rosetta and visual inspection. One of these mutants, PlyC (PlyCA) T406R, predicted by FoldX and Rosetta to produce stabilizing $\Delta\Delta G$ values of -1.05 and -1.29 kcal/mol, respectively, was shown experimentally to significantly increase the stability of the PlyC endolysin. This mutant is expected to introduce a new hydrogen bond between the C-terminal CHAP domain R406 and the Q106 side-chain of the N-terminal GyH domain, likely stabilizing the PlyCA subunit to account for the observed increase in melting temperature of ≥ 2.2°C and the 16 fold improved kinetic fitness at 45°C due to the 11 kcal/mol enhancement in the activation energy (E_A) of PlyCA unfolding.

Introduction

Endolysins, also termed phage lysins or enzybiotics, are bacteriophage-encoded peptidoglycan hydrolases (Nelson et al., 2006a). During a lytic phage replication cycle within the host bacterium, endolysins are expressed and accumulate in the cytosol in a fully folded and active conformation. The exact moment of cell lysis is then highly regulated by holins, hydrophobic membrane proteins that generate pore-forming complexes on the cytoplasmic membrane, providing cytosolic endolysins access to their peptidoglycan substrate (Wang et al., 2000; Young, 1992). The endolysin then degrades the peptidoglycan upon direct contact due to the hydrolysis of key covalent bonds within the cell wall structure, resulting in osmotic lysis and liberation of intracellular progeny virions. With this mechanistic understanding, the exogenous application of a purified recombinant endolysin to susceptible Gram-positive bacteria produces the same bacteriolytic phenotype without the presence of the bacteriophage or holins and thus represents an alternative antimicrobial to treat antibiotic resistant bacterial infections (Fischetti et al., 2006).

PlyC is an endolysin derived from the streptococcal C_1 lytic bacteriophage that has been validated *in vitro* for its bacteriolytic efficacy against groups A (GAS), C (GCS) and E (GES) streptococci and *in vivo* for its ability to protect mice from streptococcal challenge (Krause, 1957; Nelson et al., 2001). When added to GAS (*Streptococcus pyogenes*) *in vitro,* 10 ng of PlyC was able to cause a 7 log decrease in colony forming units in 5 s, making this endolysin ~100 fold more active than any other characterized endolysin to date (Nelson et al., 2001). Unlike other endolysins, which are single gene products consisting of one or more enzymatically active domains (EAD) and a cell wall

binding domain (CBD), PlyC consists of a novel multimeric structure with nine distinct subunits (McGowan et al., 2012; Nelson et al., 2006a). Eight identical PlyCB monomers interact to form a symmetrical octomeric ring structure that serves as the CBD of the holoenzyme. The ninth subunit, PlyCA, functions as the EAD of the endolysin and consists of an active N-terminal glycosol hydrolase (GyH) domain that is linked to a central helical docking domain. The helical docking domain is responsible for interacting with the PlyCB octomer to form the holoenzyme structure. The carboxyl end of the helical docking domain is linked to an active C-terminal cysteine, histidine-dependent amidohydrolase/peptidase (CHAP) domain that functions as an *N*-acetylmuramoyl-L-alanine amidase (Fischetti et al., 1972b; Nelson et al., 2006a). The PlyCA N-terminal GyH domain acts synergistically with the C-terminal CHAP domain to generate the robust bacteriolytic mechanism of the enzyme (McGowan et al., 2012).

Thermodynamic characterization of PlyC by means of differential scanning calorimetry (DSC) showed that the PlyCB octomer is endogenously thermostable, displaying a thermal transition temperature (T_G) of 75.0°C, whereas the PlyCA EAD is thermosusceptible, with an T_G of 46.2°C (F. Schwarz, personal communication). While the dissociation of the PlyCB octomer into isolated monomers is a reversible thermodynamic process, the unfolding of the individual PlyCA and PlyCB monomers is an irreversible event, which is supported by their inability to refold after being heat-denatured. The C-terminal CHAP domain of PlyCA was shown to have a T_G of 39.1°C when isolated, compared to a T_G of 46.0°C associated with PlyCAΔCHAP in a PlyCΔCHAP background (i.e. PlyC holoenzyme with a PlyCA C-terminal CHAP domain deletion), suggesting that the CHAP domain of PlyCA is the most heat-labile structural

component of the PlyC holoenzyme.

Although the number of thermodynamically characterized endolysins is limited, there are examples of endolysins that display similar structural instability to that of PlyC. For example, the *Staphylococcus aureus* endolysin LysK as well as the *Streptococcus pneumoniae* endolysins Cpl-1, Pal and Cpl-7 are devoid of activity or unfold at 42.0°C, 43.5°C, 50.2°C and 50.4°C, respectively (Bustamante et al., 2012; Filatova et al., 2010; Sanz et al., 1993; Varea et al., 2004). In congruence to the Arrhenius equation, the thermolability of PlyC and other endolysins correlates to a short-term therapeutic shelf life expectancy (Anderson and Scott, 1991).

A number of computational methods have proven partially effective at identifying single amino acid substitutions that result in increased thermodynamic stability of a protein (Cheng et al., 2006; Gilis and Rooman, 2000; Guerois et al., 2002; Parthiban et al., 2007; Parthiban et al., 2006; Schymkowitz et al., 2005a; Zhou and Zhou, 2002). One example is FoldX (Guerois et al., 2002; Schymkowitz et al., 2005a; Schymkowitz et al., 2005b), which uses an empirical potential derived from a weighted combination of physical energy terms (e.g. van der Waals interactions, hydrogen bonding, electrostatics and solvation), statistical energy terms and structural descriptors. Parameters in the potential were obtained by fitting to experimental $\Delta\Delta G$ values for 339 point mutants in nine different proteins (Guerois et al., 2002), yielding a correlation coefficient and standard deviation between the predicted and experimental data of 0.8 and 0.75 kcal/mol, respectively. The resulting potential gave similar agreement against a further set of 625 point mutants in 27 proteins not used in training, with a respective correlation coefficient and standard deviation of 0.8 and 0.84 kcal/mol between predicted and experimentally

calculated $\Delta\Delta G$ values. In third-party testing, FoldX has been shown to perform with useful accuracy across all protein structure types, yielding a correlation coefficient of 0.5 between estimated and experimental $\Delta\Delta G$ (Khan and Vihinen, 2010; Potapov et al., 2009). Rosetta was developed primarily for designing proteins with desirable properties, including new protein folds (Kuhlman et al., 2003), novel enzymatic activity (Jiang et al., 2008; Rothlisberger et al., 2008) and modified substrate specificity (Ashworth et al., 2006). The ddG module also provides a means of estimating $\Delta\Delta G$ for point mutations (Kellogg et al., 2011).

Here we aim to engineer enhanced stability of a thermolabile bacteriolytic enzyme using computational modeling. Using the PlyC holoenzyme structure as the template, our engineering strategy was to apply the FoldX and Rosetta algorithms together, in addition to subsequent visual inspection, to the C-terminal CHAP domain of PlyCA. By doing so, we were able to identify one point mutant, PlyC (PlyCA) T406R, which was shown experimentally to thermostabilize the PlyC holoenzyme structure and thereby improve the shelf life expectancy and feasibility of developing the endolysin as a translational antimicrobial.

Materials and Methods

Computational Modeling of PlyC Mutants

Initial atomic co-ordinates were taken from the PlyC holoenzyme X-ray crystal structure (Protein Data Bank ID 4F88). Due to the relatively low (3.30 Å) resolution of the structure, polypeptide backbones and side-chains were adjusted using Rosetta Relax

(Raman et al., 2009), followed by another round of side-chain orientation optimization using the FoldX3.0 RepairPDB command (Guerois et al., 2002; Schymkowitz et al., 2005b). The resulting co-ordinates were then processed with FoldX3.0 PositionScan to obtain estimated changes in folding free energy ($\Delta\Delta G_{FoldX}$) for all of the 2945 possible CHAP domain point mutants (155 total CHAP domain residues multiplied by the 19 alternative natural amino acids).. The structural environments of those mutations with a predicted $\Delta\Delta G_{FoldX} \leq$ -1 kcal/mol were then manually inspected to remove those judged likely to introduce unfavorable structural alterations. Finally, the remaining mutants were processed through the Rosetta ddg_monomer application (Kellogg et al., 2011) to yield the PlyC candidate mutant list for experimental study.

Bacterial Strains and Culture Conditions

S. pyogenes D471 (group A streptococcus) was maintained and grown in Todd Hewitt broth supplemented with 1% yeast extract as previously described (Nelson et al., 2001; Nelson et al., 2003). *E. coli* strains DH5α and BL21(DE3)pLysS (Novagen) were grown in Luria-Bertani (LB) broth at 37°C in a shaking incubator unless otherwise stated. When needed, ampicillin (100 μg/ml) was added to the media.

Cloning and Site-directed Mutagenesis

The *plyC* operon was cloned into pBAD24 as previously described (Nelson et al., 2006a). Site-directed mutagenesis was performed using the Phusion Site-Directed Mutagenesis Kit (Thermo Scientific). Mutations were introduced into the middle of the 30 nucleotide forward phosphorylated oligonucleotide primer for each mutant, with the

reverse primer being complimentary to the next 30 nucleotides upstream (Eurofins Scientific). The standard 50 µl PCR reaction mixture consisted of 1 ng of pBAD24:*plyC*, 1x Phusion HF Buffer, 0.2 mM dNTP, 0.5 µM of each primer and 1 U of Phusion DNA polymerase. The thermocycler heating conditions consisted of 98°C for 30 s, 25x (98°C for 10 s; 65°C for 30 s; 72°C for 4 min) and 72°C for 5 min. The resulting PCR products were then ligated and transformed into *E. coli* DH5α. Mutations were confirmed by nucleotide sequencing (Macrogen USA).

Protein Expression and Purification

E. coli BL21(DE3)pLysS harboring the wild-type and mutant pBAD24:*plyC* expression constructs were grown to mid-log phase in 1.5L LB supplemented with ampicillin in a 4L baffled Erlenmeyer flask. Protein expression was induced with 0.25% L-arabinose at 37°C overnight. The cells were harvested the following morning at 7,000 RPM, resuspended in PBS, pH 7.25, supplemented with 1 mM phenylmethanesulfonyl fluoride (Sigma-Aldrich) and sonicated on ice for 15 min. The insoluble cell debris from the cell lysate was pelleted at 13,000 RPM for 1 h at 4°C. The soluble endolysins were then purified as previously described (Nelson et al., 2001). Protein solubility and purity was assessed on a 4-15% gradient sodium dodecyl sulfate polyacrylamide gel electrophoresis (SDS-PAGE) gel (Laemmli, 1970).

In vitro Endolysin Activity on *S. pyogenes*

Spectrophotometric-based turbidity reduction assays were performed to determine the bacteriolytic activity of each endolysin investigated. An overnight culture of *S.*

pyogenes D471 was harvested at 4,000 RPM for 15 min, washed once with PBS, pH 7.2, and resuspended to an OD_{600} = 2.0. In a flat-bottomed 96-well plate, the purified endolysin at an initial concentration of 8.84 µM (1 µg/µl) was serial diluted in 100 µl of PBS buffer. An equal volume of bacteria was then mixed with the different enzyme concentrations and the OD_{600} was monitored kinetically on a SpectraMax 190 microplate spectrophotometer (Molecular Devices) every 6 s for 30 min at 37°C. The amount of time (s) to decrease the initial OD_{600} by 50% was then plotted against the enzyme molar concentration and fit with a one-phase exponential decay curve. 1 U of enzyme activity was equated to the amount of endolysin (µg) required to decrease the OD_{max} by 50% in 15 min. Each independent turbidity reduction assay was performed in triplicate.

Circular Dichroism (CD) Spectroscopy

A Chirascan CD spectrometer (Applied Photophysics) equipped with a thermoelectrically controlled cell holder was used for all CD experiments. For secondary structure far-UV analysis, the endolysins were at a 0.1 mg/ml concentration in 20 mM sodium phosphate buffer, pH 7.0. CD spectra were obtained in the far-UV range (190-260 nm) in a 1 mm path length quartz cuvette at 1 nm steps with 5 second signal averaging per data point. Spectra were collected in triplicate, followed by averaging, baseline subtraction, smoothing and conversion to mean residue ellipticity (MRE) by the Pro-Data software (Applied Photophysics). Secondary structure prediction was performed using the Provencher and Glockner method provided by DICHROWEB (Provencher and Glockner, 1981; Whitmore and Wallace, 2004). Melting experiments were performed by heating the endolysins at a 1 mg/ml concentration in 20 mM sodium

phosphate buffer, pH 7.0, from 20°C to 95°C at 1°C/min. MRE was monitored at 222 nm in a 1 mm path length quartz cuvette at 0.5°C steps with 5 second signal averaging per data point. The melting data was smoothed, normalized and fit with a Boltzmann sigmoidal curve. The first derivative of the melting curve was then taken to determine the temperature ($T_{1/2}$) at which the folded and unfolded state of the PlyCA subunit was at equilibrium. This temperature was defined as the minimum in the first derivative graph (Fallas and Hartgerink, 2012).

Differential Scanning Calorimetry

DSC experiments were performed on a Nano DSC differential scanning calorimeter (TA Instruments) at a constant pressure of 3 atm. All samples were degassed for at least 15 minutes prior to the experiment. The sample and reference cells consist of an optimal operational volume of 0.3 ml and were calibrated with equal volumes of 20 mM sodium phosphate buffer, pH 7.0, by means of three consecutive heating/cooling cycles from 15°C to 105°C and 105°C to 15°C at 1°C/min. The endolysins were then heated from 15°C to 105°C at a 1°C/min heating rate in 20 mM sodium phosphate buffer, pH 7.0, using a final protein concentration of 1 mg/ml followed by immediate cooling from 105° to 15°C at 1°C/min. Data analysis by means of baseline subtraction and curve fitting was performed by the NanoAnalyze software (TA Instruments).

Calculating the Activation Energy of PlyCA Unfolding

The rate constant *k* for PlyCA unfolding was derived from the corresponding DSC thermograms using the equation

$$k = vC_p/(Q_t\text{-}Q)$$

where v (K/min) is the scan rate, C_p the excess heat capacity, Q_t the total heat of the process and Q the heat evolved at a given temperature, T. The activation energy, E_A, is determined by measuring the value of k at several temperatures and then using the Arrhenius equation $k = A\exp(-E_A/RT)$. That is, the corresponding Arrhenius plot, ln k versus $1/T$, is used to calculate E_A by using the equation

$$m = -E_A/R$$

where m stands for the slope of the Arrhenius plot and R stands for the gas constant.

45°C Kinetic Stability Assay

The various endolysins investigated were incubated in a 45°C hot plate in PBS, pH 7.2, at a 44 nM (5 μg/ml) concentration for a total of 3 hours. At 20 minute increments, a 400 μl aliquot of the heated enzyme was removed and incubated on ice for 5 minutes. Three adjacent wells of a 96-well plate were then filled with 100 μl of the cooled enzyme, followed by the addition of an equal volume of *S. pyogenes* D471 (see *In Vitro* Endolysin Activity on *S. pyogenes* for cell preparation). The residual lytic activity of the endolysin was analyzed via turbidity reduction assay by monitoring the OD_{600} every 6 s for 20 min. The activity of the endolysin was equated to the V_{max} (milli-OD units per min) corresponding to the linear portion of the resulting killing curve. Residual lytic activity was normalized to the activity displayed in the absence of heat treatment.

Results

Prediction of Stabilizing Mutations of the PlyCA CHAP Domain

FoldX was applied to the C-terminal CHAP domain of PlyCA (CHAP is comprised of PlyCA amino acids 309-465; however, atomic co-ordinates were only available for residues 310-464), substituting each of the possible 19 alternative natural amino acids at each residue position, so generating a library of 2945 PlyC mutants. Most of the mutations analyzed (n = 2453) were predicted by FoldX to have either destabilizing or neutral effects on stability, resulting in a $\Delta\Delta G_{FoldX} \geq 0$ kcal/mol ($\Delta\Delta G_{FoldX} = \Delta G_{mut} - \Delta G_{wt}$) (Fig. 2-1). All of the mutants (n = 92) that had a $\Delta\Delta G_{FoldX} \leq -1$ kcal/mol were visually inspected, resulting in the elimination of another 61 mutants that appear to modify the PlyC structure in an unfavorable manner. Examples of these disadvantageous structure changes are disruption of salt-bridge and dipole interactions, replacement of salt-bridge interactions with weaker dipole interactions, generation of cavities in the hydrophobic core by the introduction of an amino acid with a smaller side-chain, exposure of hydrophobic side-chains at the surface and disruption of the active site.

The impact of the mutations encoded by the remaining 31 mutants was analyzed by the Rosetta ddg monomer algorithm (Kellogg et al., 2011) to further evaluate likely stabilizing potential (Fig. 2-2). Rosetta predicted 12 of the 31 mutants to be destabilizing ($\Delta\Delta G_{Rosetta} > 0.01$ kcal/mol) and these were eliminated from further consideration (Fig. 2-2, triangles). An additional mutant, PlyC (PlyCA) Q332H, has a predicted mildly destabilizing $\Delta\Delta G_{Rosetta}$ of 0.01 kcal/mol, but was retained since it is in an interesting

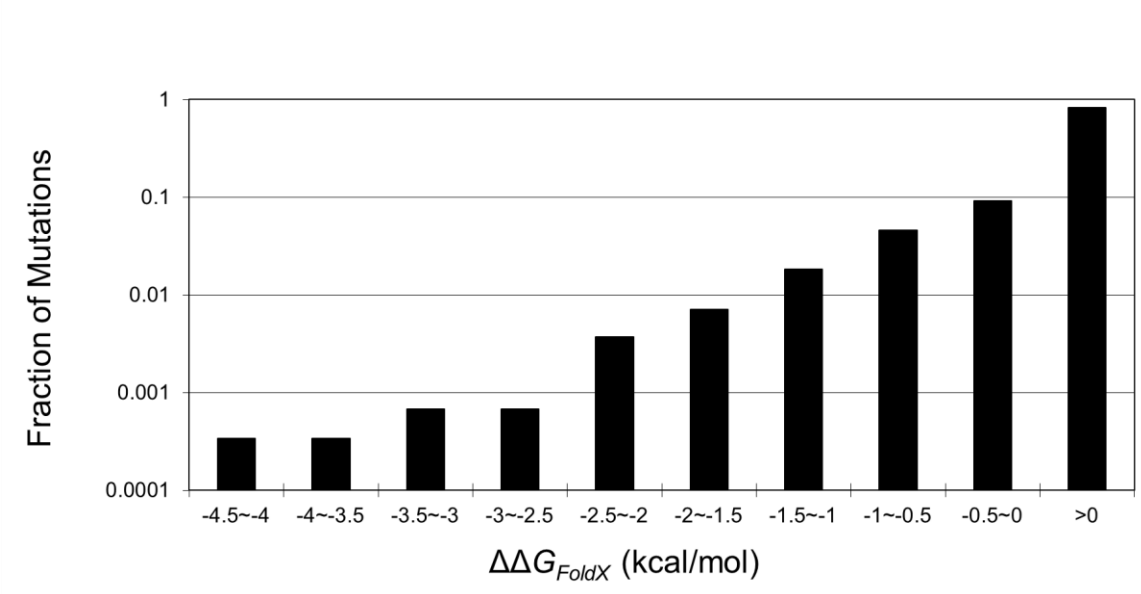

Figure 2-1. Log distribution of the predicted change in folding free energy ($\Delta\Delta G_{FoldX}$) for all 2945 possible PlyCA CHAP domain point mutants calculated with FoldX 3.0 PositionScan. Mutations with $\Delta\Delta G_{FoldX} < 0$ are expected to increase protein stability. Only a small portion of mutations are predicted to be stabilizing.

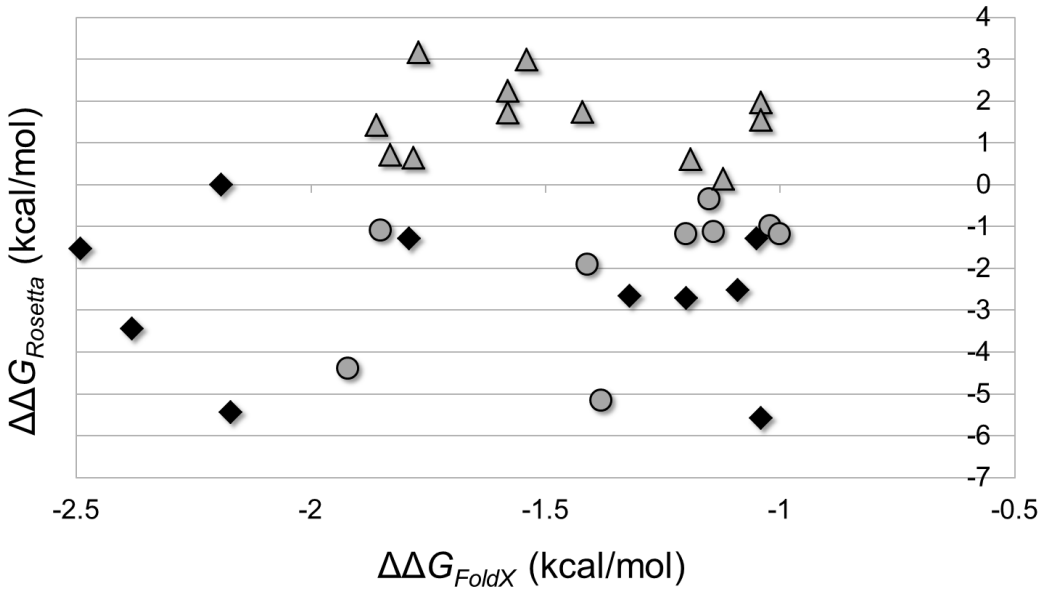

Figure 2-2. Comparison between the $\Delta\Delta G_{FoldX}$ and $\Delta\Delta G_{Rosetta}$ values of the final 31 mutant candidates retained after manual curation. 12 of these remaining mutants displayed a $\Delta\Delta G_{Rosetta} > 0.01$ kcal/mol and were not further considered (triangles). Of the remaining 19 mutants (circles and diamonds), 10 were selected for experimentally characterization (diamonds). All of the final candidates had predicted $\Delta\Delta G \leq 0.01$ kcal/mol values by both FoldX and Rosetta algorithms.

location, adjacent to the active site cysteine of the CHAP domain, C333. Although mutations near the active site generally induce activity defects, there are several documented instances where such mutations improve overall thermal stability (Daude et al., 2013; Kanaya et al., 1996; Zhi et al., 1991). In addition to Q332H, the PlyC (PlyCA) mutants D330Y, Q332V, C345T, D375Y, T381Y, V384Y, C404I, T406R and T421I were also selected as candidates for experimental study, on the basis of predicted $\Delta\Delta G <$ 0 kcal/mol by both of FoldX and Rosetta (Fig. 2-2, diamonds, Table 2-1). These final 10 candidates consisted of mutations located either near the CHAP domain active site (D330Y, Q332H, Q332V), in the hydrophobic core (C404I and T421I), at the surface and predicted to form an intra-domain hydrogen bond (V384Y) and at the surface, predicted to form an inter-domain interaction with the N-terminal GyH domain (C345T, D375Y, T381Y, T406R). The other nine mutants with FoldX and Rosetta $\Delta\Delta G < 0$ kcal/mol values were omitted from further characterization (Fig. 2-2, circles). These had similar structural locations to those selected, and were hypothesized to employ analogous stabilizing mechanisms so that inclusion would not improve the diversity of the candidate pool.

Protein Solubility, Purity and Secondary Structure Determination

PlyC (PlyCA) mutants Q332H, Q332V, C345T, D375Y, V384Y, C404I and T406R all expressed as soluble holoenzymes and were purified to homogeneity based on SDS-PAGE analysis (Fig. 2-3). PlyC (PlyCA) D330Y and T381Y did not express and therefore were excluded from further characterization (data not shown). SDS-PAGE and far-UV CD secondary structure analysis of purified PlyC (PlyCA) T421I showed a mixed

Table 2-1. List of the final 10 FoldX PlyC mutant candidates, including the specific mutation within the PlyCA CHAP domain (column 1), the location of the mutation (column 2) and the calculated ΔΔ*G* (kcal/mol) values by the FoldX (column 3) or Rosetta (column 4) algorithms.

PlyC Construct	Location	$\Delta\Delta G_{FoldX}$ (kcal/mol)	$\Delta\Delta G_{Rosetta}$ (kcal/mol)
Wild-type	--------	--------	--------
D330Y	Near the active site	-1.09	-2.51
Q332H	Near the active site	-2.19	0.01
Q332V	Near the active site	-1.79	-1.29
C345T	Surface with potential domain-domain interaction	-1.20	-2.70
D375Y	Surface with potential domain-domain interaction	-2.49	-1.53
T381Y	Surface with potential domain-domain interaction	-1.32	-2.65
V384Y	Surface with potential intra-domain hydrogen bond	-1.04	-5.57
C404I	Hydrophobic core	-2.17	-5.44
T406R	Surface with potential domain-domain interaction	-1.05	-1.29
T421I	Hydrophobic core	-2.38	-3.43

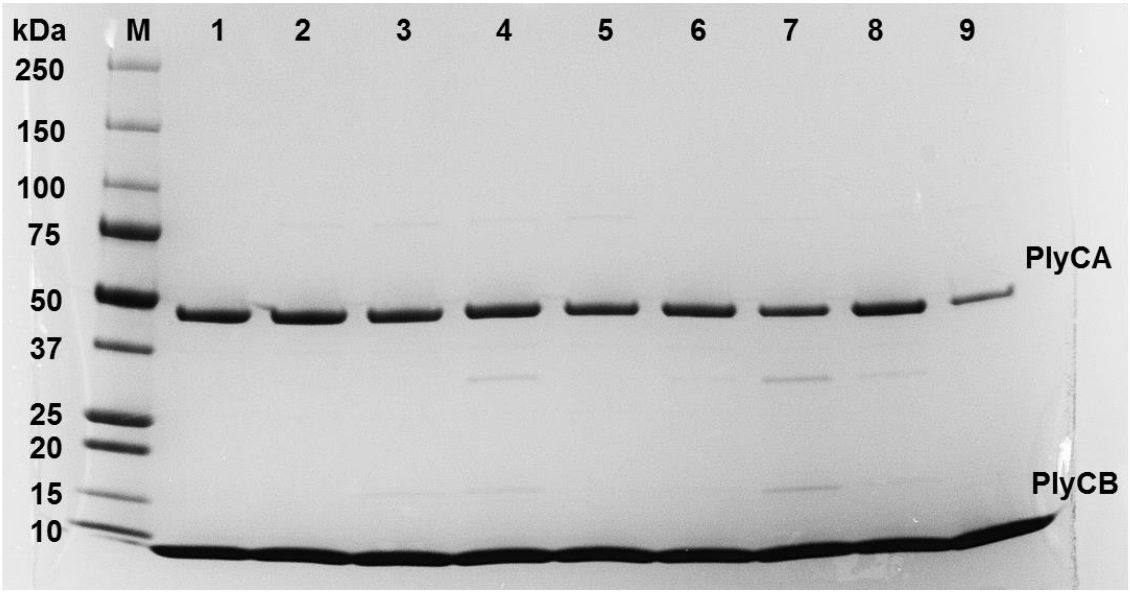

Figure 2-3. SDS-PAGE analysis of the FoldX PlyC mutants. The solubility and purity of each of the mutants was analyzed on a 4-15% gradient SDS-PAGE gel. The various lanes correlate to: (M) Molecular weight standard, (1) Wild-type, (2) Q332H, (3) Q332V, (4) C345T, (5) D375Y, (6) V384Y, (7) C404I, (8) T406R and (9) T421I. Protein expression was not observed for D330Y and T381Y and therefore both were excluded from the gel.

population of holoenzyme and uncomplexed PlyCB octomer structures (data not shown). To overcome this issue, a C-terminal 6x His-tag was added to PlyCA T421I. This mutant was expressed and purified in the same way as the other PlyC mutants, with two alterations; protein expression was induced at 18°C instead of 37°C, and there was an addition of a final immobilized metal affinity chromatography (IMAC) step using a 5 ml Bio-Scale Mini Profinity IMAC Cartridge (Bio-Rad) to remove uncomplexed PlyCB octomers.

Protein secondary structure analysis was performed using far-UV CD. The CD spectra for all of the proteins analyzed were represented in terms of mean residue ellipticity (MRE) as a function of wavelength (Fig. 2-4a). All eight of the purified PlyC mutants displayed no deviation in secondary structure when compared to that of wild-type. The far-UV spectra resembles that of an α/β folded protein, displaying ellipticity minima at 208 nm and 220 nm, and ellipticity maxima at 195 nm (Greenfield and Fasman, 1969; Kelly et al., 2005). Secondary structure composition analysis results depict highly homologous regular α-helical (±1.1%), distorted α-helical (±1.2%), regular β-sheet (±1.0%), distorted β-sheet (±0.5%), turn (±0.7%) and unordered (±0.7%) structures when comparing wild-type to the eight FoldX mutants (Table 2-2). The normalized root mean square deviation (NRMSD) measures the goodness-of-fit between back-calculated spectra (spectra extrapolated using the CONTIN method for soluble proteins with known crystal structures) and experimental spectra. All of the NRMSD values are < 0.1, suggesting that the back-calculated and experimental spectra are in close agreement. Thus, none of the point mutations introduced significantly affected the secondary structure of the holoenzyme.

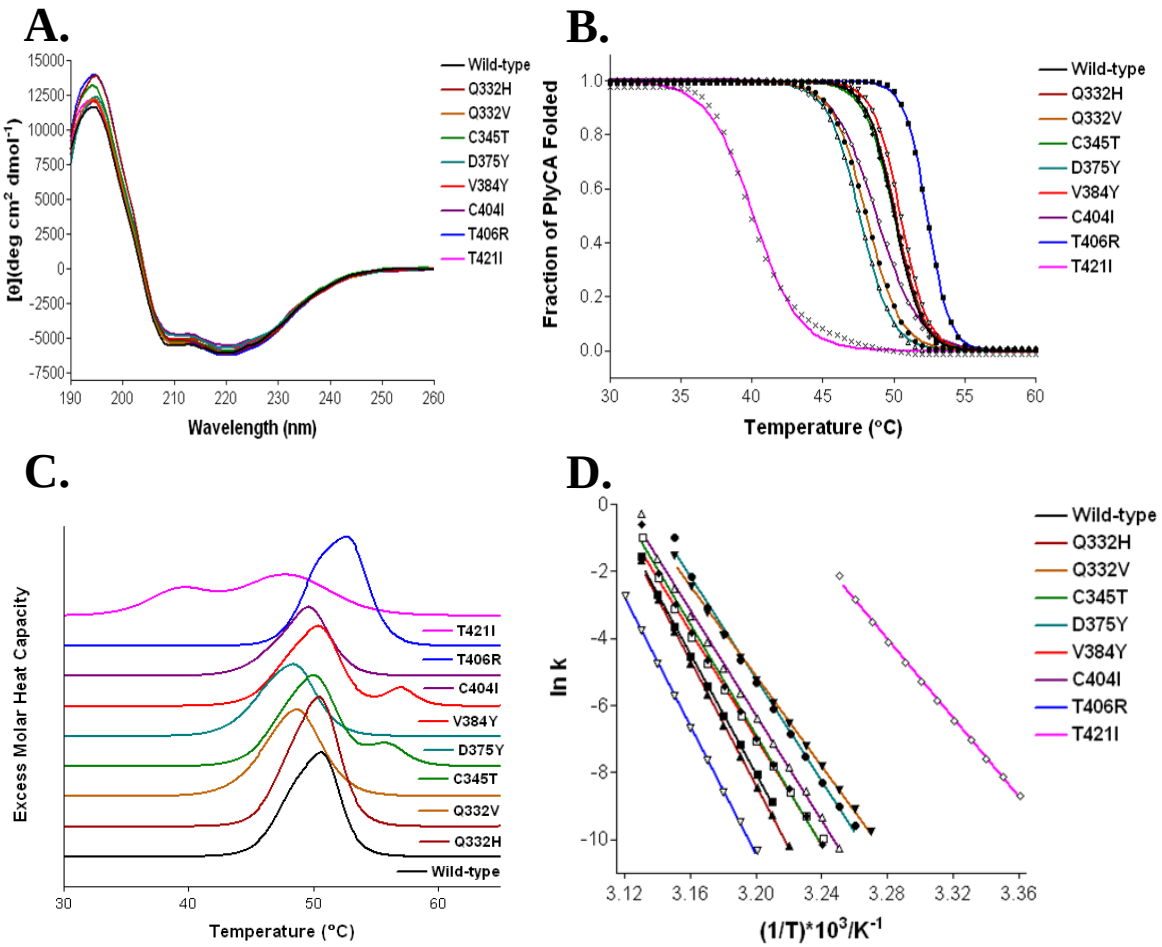

Figure 2-4. Secondary structure and thermal stability determination. (a) The secondary structure of each of the FoldX PlyC mutant was analyzed by far-UV CD spectroscopy between the wavelengths of 190-260 nm. The mean residue ellipticity [θ] (deg cm^2 $dmol^{-1}$) was plotted against wavelength (nm) for each mutant, with all of the resulting spectra being overlaid for comparative purposes. The thermal stability of each mutant was then analyzed by means of (b) CD and (c) DSC in 20 mM phosphate buffer pH 7.0 at a protein concentration of 1 mg/ml using a heating rate of 1°C/min. Using the calorimetric data, the rate constant (*k*) for each FoldX PlyC mutant was calculated and plotted against the inverse of the temperature ((1/T)*10^3/K^{-1}) in order to determine the E_A of PlyCA unfolding.

Table 2-2. Far-UV CD protein secondary structure estimation using the CONTIN deconvolution method. Calculations were made for regular α-helix (α_R), distorted α-helix (α_D), regular β-strand (β_R), distorted β-strand (β_D), turn and unordered structures.

PlyC Construct	α_R	α_D	β_R	β_D	Turns	Unordered	Total	NRMSD
Wild-type	11.5%	12.3%	17.5%	10.2%	20.7%	27.9%	100.1%	0.066
Q332H	12.1%	11.6%	18.3%	10.4%	20.2%	27.3%	99.9%	0.063
Q332V	11.5%	11.7%	17.9%	10.5%	20.7%	27.8%	100.1%	0.069
C345T	12.0%	11.4%	18.1%	10.4%	20.3%	27.8%	100.0%	0.094
D375Y	10.9%	11.6%	18.4%	10.7%	21.0%	27.5%	100.1%	0.080
V384Y	11.2%	11.2%	18.4%	10.5%	20.5%	28.0%	99.8%	0.079
C404I	10.7%	11.3%	18.5%	10.7%	20.7%	28.1%	100.0%	0.084
T406R	12.6%	11.7%	18.1%	10.3%	20.0%	27.2%	99.9%	0.078
T421I	11.2%	11.1%	18.5%	10.6%	20.5%	28.0%	99.9%	0.098

Kinetic Analysis of Bacteriolytic Activity against S. pyogenes

To assess the bacteriolytic activity of each PlyC mutant, the purified enzymes were incubated with *S. pyogenes* D471 at different molar concentrations and the resulting activity was elucidated by turbidity reduction assays. There were no activity defects observed with the PlyC (PlyCA) C345T, D375Y and V384Y mutants, displaying 1.13, 1.03 and 1.23 fold increases in activity when compared to wild-type, respectively (Table 2-3). PlyC (PlyCA) mutants C404I and T406R exhibited a moderate loss in activity, exhibiting a respective 2.2 and 2.1 fold decrease in activity. Significant activity deficiencies were observed with the PlyC (PlyCA) Q332H, Q332V and T421I mutants, of 3.6, 9.1 and 16.7 fold reduction in activity, respectively.

Circular Dichroism Thermal Stability Analysis

Equal molar concentrations of the PlyC mutant enzymes were subjected to CD melting experiments to determine the temperature ($T_{1/2}$) at which the apparent folded and unfolded fractions of the mutagenized PlyCA subunits in the context of the holoenzyme structure were in equilibrium (Fig. 2-4b). When monitoring the loss of α-helical secondary structure, PlyCA qualitatively exhibits a single, cooperative structural transition that is not reversed on cooling. PlyC (PlyCA) mutations Q332V, C345T, D375Y, C404I and T421I were destabilizing, decreasing the $T_{1/2}$ of the catalytic subunit by 1.98°C, 0.07°C, 2.45°C, 0.99°C and 10.41°C, respectively, compared to wild-type ($T_{1/2}$ = 50.09°C) (Table 2-4). The PlyC (PlyCA) mutants Q332H and V384Y slightly stabilized PlyCA by 0.08°C and 0.39°C, respectively. PlyC (PlyCA) T406R was significantly beneficial to the thermal fitness of the enzyme, augmenting the $T_{1/2}$ of

Table 2-3. Bacteriolytic activity quantitation by means of *S. pyogenes* turbidity reduction assay.

PlyC Construct	Lytic Activity (U/ml)	Relative Lytic Activity
Wild-type	45350	1.00
Q332H	12730	0.28
Q332V	4950	0.11
C345T	51180	1.13
D375Y	46550	1.03
V384Y	55560	1.23
C404I	16000	0.45
T406R	21550	0.48
T421I	2880	0.06

Table 2-4. Comparison of $T_{1/2}$ values derived from the CD melting experiments.

PlyC Construct	$T_{1/2}$ (°C)	$\Delta T_{1/2}$ (°C)
Wild-type	50.09	-
Q332H	50.17	+0.08
Q332V	48.11	-1.98
C345T	50.02	-0.07
D375Y	47.64	-2.45
V384Y	50.48	+0.39
C404I	49.10	-0.99
T406R	52.36	+2.27
T421I	39.68	-10.41

PlyCA by 2.27°C.

Differential Scanning Calorimetry

To validate the CD stability analysis, the thermodynamic stability of each PlyC mutant was investigated by DSC at equal molar concentrations (Fig. 2-4c). Contrary to the CD thermal analysis of PlyCA, which qualitatively suggests PlyCA irreversibly unfolds in a cooperative manner, DSC analysis of the FoldX mutants depicts PlyCA unfolding non-cooperatively in a three-state, and in some cases, four-state, thermal transition model. Heating the protein samples from 15°C to 105°C followed by immediate cooling from 105°C to 15°C did not result in the refolding of the PlyCA subunit for each PlyC construct investigated.

Consistent with CD results, PlyC (PlyCA) mutants Q332V, C345T, D375Y, C404I and T421I were less thermostable than wild-type (T_G = 48.27°C, ΔH_{VH} = 171.23 kcal/mol) when analyzed by DSC, encompassing a 1.33°C, 0.27°C, 2.01°C, 0.52°C and 9.03°C decrease in PlyCA T_G and a 20.73 kcal/mol, 12.84 kcal/mol, 15.22 kcal/mol, 17.47 kcal/mol and 49.86 kcal/mol reduction in ΔH_{VH}, respectively (Table 2-5). PlyC (PlyCA) mutants Q332H and V384Y displayed marginable increases in thermodynamic stability, with an increase in PlyCA T_G of 0.20°C and 0.23°C, and a 5.84 kcal/mol and 2.73 kcal/mol gain in ΔH_{VH} , respectively. The T406R mutation produces a more notable improvement in PlyCA, increasing T_G and ΔH_{VH} by 2.21°C and a 21.45 kcal/mol, respectively.

Using the wild-type PlyC and mutant calorimetric traces, the PlyCA thermal transitions were kinetically modeled to construct Arrhenius plots by using the rate

Table 2-5. Calorimetric determination of PlyCA T_G (columns 2-4) and the corresponding ΔH_{VH} values (columns 5-7).

PlyC Construct	T_{G1} (°C)	T_{G2} (°C)	T_{G3} (°C)	ΔH_{VH1} (kcal/mol)	ΔH_{VH2} (kcal/mol)	ΔH_{VH3} (kcal/mol)
Wild-type	48.27	50.67		171.23	205.09	
Q332H	48.47	50.74		177.07	211.87	
Q332V	46.94	49.28		150.50	192.22	
C345T	48.00	50.45	55.56	158.39	205.09	193.50
D375Y	46.26	48.78		156.01	181.05	
V384Y	48.50	50.79	57.05	173.96	212.65	252.90
C404I	47.72	49.99		153.76	203.14	
T406R	50.48	53.05		192.68	211.38	
T421I	39.24	45.75	49.64	121.37	113.83	118.01

constants for at least nine different temperatures in order to derive E_A values of unfolding (Fig. 2-4d). The calculated E_A for PlyC (PlyCA) Q332V, C345T, D375Y, V384Y, C404I and T421I were lower than that of wild-type PlyC (178 kcal/mol) (Table 2-6). In contrast, PlyC (PlyCA) Q332H and T406R displayed a respective increase in E_A of 7 kcal/mol and 11 kcal/mol.

45°C Kinetic Inactivation Analysis

The rate of PlyCA kinetic inactivation was monitored for wild-type PlyC and the lead FoldX mutant candidate, PlyC (PlyCA) T406R, at 45°C for a total of 3 hours. For this particular assay, the unfolding of PlyCA is directly correlated with the loss of bacteriolytic activity as a function of temperature and time. The loss in activity is not associated with the unfolding of the PlyCB binding domain of PlyC due to the inherent thermal stability of the octomeric CBD complex of the CBD (F. Schwarz, personal communication). The heat-labile nature of wild-type PlyC promoted rapid PlyCA unfolding at 45°C, resulting in a half-life ($t_{1/2}$) of 17.84 min (Fig. 2-5, squares). Conversely, PlyC (PlyCA) T406R mutant improved the kinetic fitness of PlyCA at 45°C 16 fold when compared to wild-type, displaying an extrapolated $t_{1/2}$ increase to 286.09 minutes (Fig. 2-5, inverted triangles).

Discussion

The PlyC endolysin is the most active phage-derived peptidoglycan hydrolase characterized to date and has been validated *in vitro* and *in vivo* for its antimicrobial efficacy against a wide-range of streptococcal species known to cause a variety of animal

Table 2-6. Determination of the PlyCA E_A (kcal/mol) of unfolding from applying a kinetic model to the calorimetric data.

PlyC Construct	E_A (kcal/mol)	R^2
Wild-type	178	0.9982
Q332H	185	0.9989
Q332V	133	0.9982
C345T	164	0.9956
D375Y	152	0.9961
V384Y	158	0.9963
C404I	156	0.9960
T406R	189	0.9992
T421I	117	0.9989

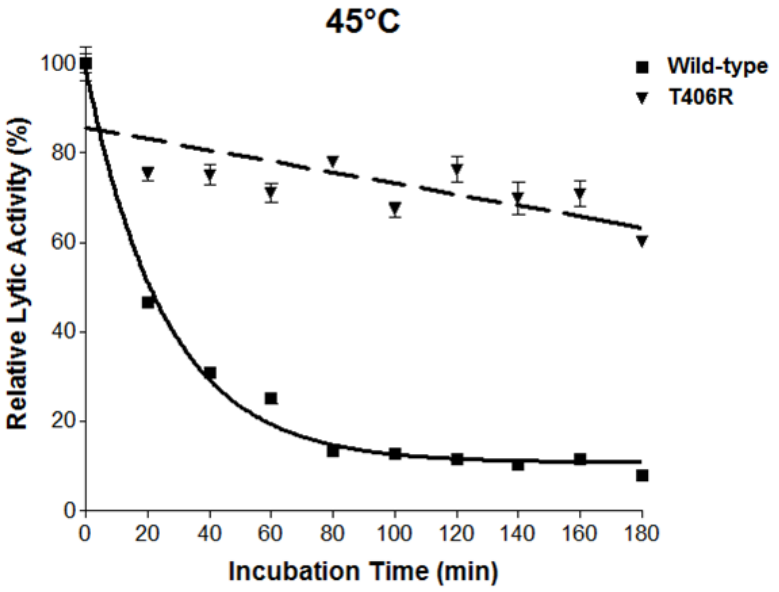

Figure 2-5. Kinetic stability of wild-type PlyC and PlyC (PlyCA) T406R at 45°C. Equal molar concentrations of wild-type PlyC and PlyC (PlyCA) T406R were incubated at 45°C for a total of 3 hours. At 20 minute increments, the residual lytic activity of each enzyme was monitored by means of turbidity reduction assay. The activity of each was normalized to the lytic activity displayed by the unheated sample.

and human health complications (Hoopes et al., 2009; Nelson et al., 2001; Nelson et al., 2006a). With a long-term goal of developing PlyC as a novel antimicrobial disinfectant, prophylactic and therapeutic, the poor thermal stability, and hence transient shelf life, makes the feasibility of proceeding forward with the developmental process challenging. Here we show for the first time the ability to engineer increased stability *in silico* to a phage endolysin through the use of the FoldX algorithm. Considering the complexity of the novel nine subunit structure of PlyC in conjunction with the endogenous thermal stability of the PlyCB CBD, we decided to focus our engineering efforts on the most thermolabile structural component of the PlyCA EAD, which was previously shown to be the C-terminal CHAP domain.

Although the structural integrity of all eight of the final CHAP domain mutant holoenzymes analyzed remained intact (Fig. 2-3 and Fig. 2-4a, Table 2-2), endolysin turbidity reduction activity titers showed that while the C404I and T406R mutations respectively caused considerable 2.2 and 2.1 fold decreases in activity, the Q332H, Q332V and T421I mutations to the CHAP domain generated significant activity defects that correlated to a >70% loss in activity (Table 2-3). Considering the PlyCA CHAP domain has active site residues at C333 and H420 (Nelson et al., 2006a), it was not surprising to observe major perturbations to the catalytic efficiency of the enzyme when introducing amino acid mutations adjacent to either of the two active site residues.

After being subjected to CD and DSC thermal stability analysis, the lead FoldX mutant candidate was PlyC (PlyCA) T406R, which displayed a $\geq$ 2.2°C increase in PlyCA stability with a 21.45 kcal/mol gain in ΔH_{VH} (Fig. 2-4b and c, Table 2-4 and 2-5). The T406R mutation is located on the CHAP domain surface and is hypothesized to

promote an inter-domain interaction between the C-terminal CHAP domain and the N-terminal GyH domain of the PlyCA subunit. Modeling the T406R mutation into the CHAP domain shows how the longer arginine side-chain allows the formation of a stabilizing hydrogen bond with the polar Q106 side-chain located on the surface of the N-terminal GyH domain of PlyCA (Fig. 2-6). The suspected PlyCA stabilizing inter-domain interaction engineered by the T406R mutation also resulted in an increase in kinetic fitness. This finding is consistent with a kinetic model based on the calorimetric traces provided by DSC. The resulting Arrhenius plots show the T406R mutation results in a PlyCA unfolding E_A of 189 kcal/mol, an 11 kcal/mol increase in E_A compared to wild-type (Fig. 2-4d, Table 2-6). Moreover, the T406R mutation promotes an extrapolated 16 fold augmentation in PlyCA kinetic stability at 45°C (Fig. 2-5). Although PlyC (PlyCA) T406R had an overall reduction in bacteriolytic activity when compared to the endogenous activity of wild-type PlyC, a common observation when thermostabilizing biomolecules (Arnold et al., 2001; Beadle and Shoichet, 2002; Giver et al., 1998; Meiering et al., 1992; Mukaiyama et al., 2006; Shoichet et al., 1995; Yutani et al., 1987), the residual activity displayed by the mutant nonetheless remains more potent than that of any other characterized endolysin.

Engineering inter-domain interactions is a commonly practiced strategy for thermostabilizing proteins (Choudhury et al., 2010; Wakabayashi and Fay, 2013; Wozniak-Knopp and Ruker, 2012). As suggested by the results from the thermal characterization and molecular modeling of PlyC (PlyCA) T406R, the hypothesized thermostabilizing inter-domain hydrogen bond would link the N-terminal GyH and C-terminal CHAP domains together. Increased stability likely arises from the enthalpic gain

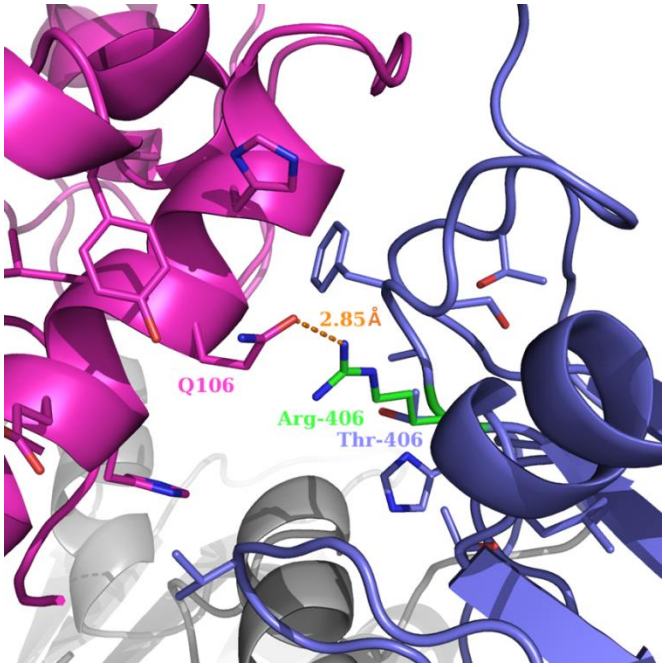

Figure 2-6. Local structure around wild-type PlyCA T406 with the proposed conformation of the mutant T406R superimposed. The crystal structure of the wild-type PlyCA T406 residue (blue sticks) and the model of the PlyCA mutant residue T406R (green sticks) are shown together with the surrounding residues. The predicted additional hydrogen bond between Q106 of the N-terminal GyH domain and R406 of the C-terminal CHAP domain introduced by the T406R mutation is shown as orange dots. Parts of the polypeptide backbone of the PlyCA N-terminal GyH domain (magenta) and the C-terminal CHAP domain (blue) are also shown.

associated with the new hydrogen bond.

With respect to the effectiveness of the FoldX algorithm for estimating CHAP domain mutant $\Delta\Delta G$ values, it should be born in mind that these calculations are based on a relatively low resolution 3.3-Å X-ray crystal structure. The $\Delta\Delta G$ estimates derived from FoldX did yield one very useful and non-obvious candidate that significantly increased the stability of PlyCA, at the expense of some extra experimental work on non-useful ones. There may of course be other potentially useful mutations that the procedure used here overlooked.

While the increase in thermodynamic and kinetic stability are important findings from a computational-based engineering approach for improving the stability of phage endolysins, additional engineering efforts can be employed to the PlyC endolysin to further evolve the enzyme's thermal fitness. For instance, instead of solely focusing on the C-terminal CHAP domain, FoldX modeling could be directed towards the N-terminal GyH domain. Despite the CHAP domain (T_G = 39.1°C) being more thermosusceptible than the PlyCAΔCHAP subunit (T_G = 46.0°C), this may not be the case when the thermodynamics of each are analyzed in the context of the holoenzyme. Supplementary to rationale-based computational bioengineering methodologies, structure-guided site-directed mutagenesis could be implemented to improve the thermal stability of PlyC. Due to the high conservation of the protein core when comparing a wide-range of homologous mesophilic and hyperthermophilic protein structures, various stabilization strategies that have been implemented typically focus on the polar surface areas of the protein (Vieille and Zeikus, 2001). Replacing residues in left-handed helical structures with glycine or asparagines, introducing proline residues in turn and loop structures, promoting the

formation of nonlocal surface ion pairs, and anchoring loop structures to the protein surface by the addition of a disulfide bridge are all strategies that have been successfully exploited for increasing the thermal stability of proteins (Kawamura et al., 1996; Kimura et al., 1992; Matthews et al., 1987; Sanz-Aparicio et al., 1998; Van den Burg et al., 1998). Since protein stability can be increased through the sequential addition of individual adaptive mutations, advantageous mutations elucidated through different engineering strategies can be combined to further enhance the thermal stability of the endolysin in an additive nature.

Acknowledgements

We would like to respectively thank Amanda Altieri and Robert G. Brinson for their technical assistance when using the CD spectrometer and DSC. We are also thankful for the insight and advice provided by Philip N. Bryan regarding the thermodynamic and kinetic analysis experiments. Finally, we are grateful to the National Institute of Standards and Technology for access to DSC instrumentation.

Author contributions: R.D.H, J.M. and D.C.N. conceived the experiments; Y.Y. and J.M. performed the computational experiments and analyzed the data; R.D.H. performed the biological, biochemical and biophysical experiments and analyzed the data; J.M and D.C.N. planned and supervised the project. R.D.H. wrote the article.

Funding: This work was supported by grants from the United States Department of Defense (DM102823) and the Maryland Agriculture Experiment Station to DCN.

Chapter III

A New Screening Method for the Directed Evolution of Thermostable Bacteriolytic Enzymes

Ryan D. Heselpoth[1] and Daniel C. Nelson[1,2]

[1]Institute for Bioscience and Biotechnology Research, 9600 Gudelsky Drive, Rockville, MD 20850, USA; [2]Department of Veterinary Medicine, University of Maryland, 8075 Greenmead Drive, College Park, MD 20742, USA

This chapter has been published as follows:

Heselpoth, R.D., Nelson, D.C. A New Screening Method for the Directed Evolution of Thermostable Bacteriolytic Enzymes. J. Vis. Exp. (69), e4216, doi:10.3791/4216 (2012).

Link to video article: http://www.jove.com/video/4216

Abstract

Directed evolution is defined as a method to harness natural selection in order to engineer proteins to acquire particular properties that are not associated with the protein in nature. Literature has provided numerous examples regarding the implementation of directed evolution to successfully alter molecular specificity and catalysis (Jackel et al., 2008). The primary advantage of utilizing directed evolution instead of more rational-based approaches for molecular engineering relates to the volume and diversity of variants that can be screened (Liu et al., 2009). One possible application of directed evolution involves improving structural stability and the corresponding thermodynamic properties associated with bacteriolytic proteins, such as endolysins. Endolysins, often called enzybiotics for their therapeutic potential, are an emerging enzyme-based class of antimicrobials that hydrolyze critical covalent bonds in the peptidoglycan (i.e. cell wall) of susceptible Gram-positive bacteria species, resulting in cellular lysis (Fischetti, 2008; Fischetti et al., 2006; Loessner, 2005). The subject of our directed evolution study involves the PlyC endolysin, which is composed of PlyCA and PlyCB subunits (Nelson et al., 2006b). When purified and added extrinsically, the PlyC holoenzyme lyses group A streptococci (GAS) as well as other streptococcal groups in a matter of seconds and furthermore has been validated *in vivo* against GAS (Loeffler et al., 2001). Significantly, monitoring residual enzyme kinetics after elevated temperature incubation provides distinct evidence that PlyC loses lytic activity abruptly at 45°C, suggesting a short therapeutic shelf life, which may limit additional development of this enzyme. Further studies reveal the lack of thermal stability is only observed for the PlyCA subunit, whereas the PlyCB subunit is stable up to ~90°C (unpublished observation). According to

the Arrhenius equation, which relates the rate of a chemical reaction to the temperature present in the particular system, an increase in thermostability will correlate with an increase in shelf life expectancy (Anderson and Scott, 1991). Toward this end, directed evolution has been shown to be a useful tool for altering the thermodynamics of various molecules in nature but never has this particular technology been exploited successfully for the study of bacteriolytic proteins. In this video, we employ the use of an error-prone DNA polymerase followed by an optimized novel screening process using a 96-well microtiter plate format to identify mutations to the PlyCA subunit of the PlyC streptococcal endolysin that correlate to an increase in enzyme thermostability. Results after just one round of random mutagenesis suggest the methodology is generating thermodynamically advanced PlyC variants that retain more than twice the residual activity when compared to wild-type (WT) PlyC after elevated temperature treatment.

Protocol

1. Determining Optimal Heating Conditions

First, one must experimentally determine the optimal incubation temperature and time to use for the heating step in the assay. For our PlyC model, it is important to note that *E. coli* co-transformed with *plyCA* and *plyCB* genes on separate expression plasmids has been shown to form a fully functional PlyC holoenzyme (Nelson et al., 2006b). The 96-well microtiter plate preparation as well as cell growth conditions and the subsequent replica plating technique were adapted from examples provided in the literature (Kim et al., 2000; Koutsioulis et al., 2008; McCarthy et al., 2004; Ren et al., 2009; Tsuzuki et al., 2005). Using 30 minutes as the predetermined heat treatment time, the optimal incubation temperature for PlyC was elucidated by the following steps:

1.1) Transform the expression construct pBAD24:*plyCA* (Amp^r) into the competent *E. coli* strain DH5α pBAD33:*plyCB* (Cm^r).

1.2) Plate the transformants on a Luria-Bertani (LB) agar plate supplemented with ampicillin (100 μg/ml) and chloramphenicol (35 μg/ml). Incubate the plates overnight at 37°C.

1.3) With a sterile toothpick, inoculate an individual colony into each row of wells (Fig. 3-1a) in a sterile, clear, flat-bottomed 96-well, lidded microtiter plate that contains 200 μl of LB supplemented with ampicillin and chloramphenicol.

1.4) Securely place the 96-well microtiter plate on a 37°C shaking incubator and grow the bacteria overnight at 300 RPM.

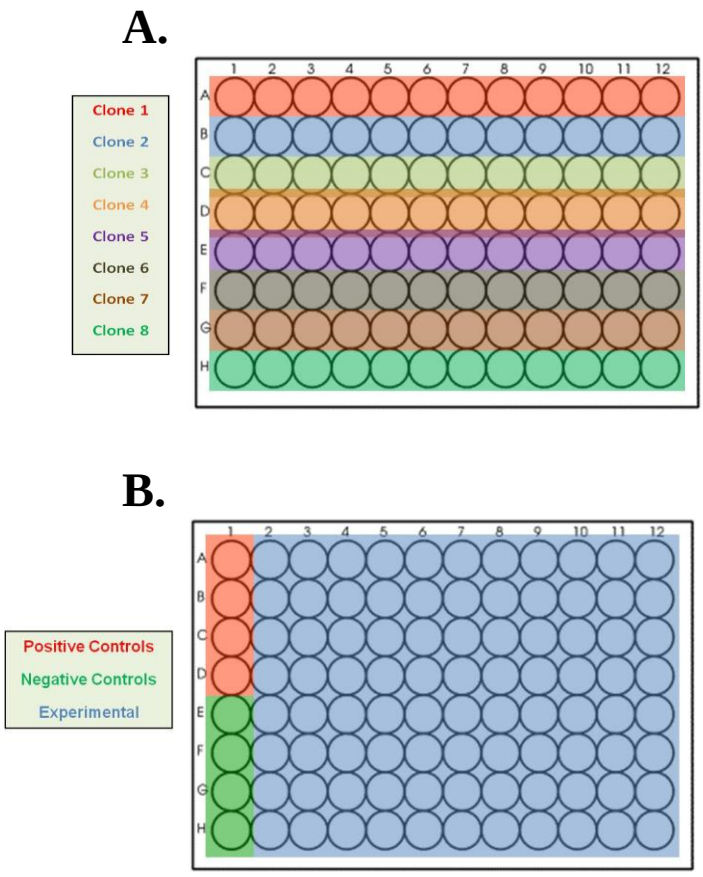

Figure 3-1. 96-well microtiter plate templates for directed evolution assay. (a) The microtiter plate schematic during the determination of the optimal heating conditions consists of inoculating a single WT PlyC clone into each row of the microtiter plate. (b) The microtiter plate schematic during mutant screening consists of inoculating each well in column 1 with a unique WT PlyC clone as well as inoculating each well in columns 2-12 with a distinct PlyC mutant clone. Wells A1-D1 are designated for the positive controls, which consist of WT PlyC constructs not exposed to non-permissible temperature incubation. Wells E1-H1 are designated for the negative controls, which consist of WT PlyC constructs that are exposed to non-permissible temperature incubation.

1.5) Retrieve the 96-well microtiter plate from the 37°C shaking incubator and replica plate to a new 96-well microtiter plate as follows:

a. Add 180 µl of LB supplemented with ampicillin and chloramphenicol to each well of the replica plate.

b. Transfer 20 µl of bacteria from the original plate to the corresponding wells in the replica plate. This should result in an initial optical density between 0.3-0.5.

1.6) Securely place the replica plate on the 37°C shaking incubator and incubate the plate for 1 hour at 300 RPM, then add the inductant. In the case of our pBAD expression systems, the inductant is 0.25% arabinose. Other expression systems may require different inductants. Place the plate back on the 37°C shaking incubator and shake at 300 RPM for an additional 4 hours to allow for protein expression.

1.7) Once protein expression has concluded, retrieve the replica plate and pellet the bacteria by placing the 96-well microtiter plate in a refrigerated centrifuge that contains a swinging-bucket rotor which fits 96-well microtiter plates. Centrifuge at 3000 RPM for 10 minutes at room temperature.

1.8) Remove the media supernatant with a vacuum apparatus being careful not to disturb the pelleted bacteria in order to minimize the chances of cross-contamination or sample loss.

1.9) Lyse the cells by adding 50 µl of B-PER II Bacterial Protein Extraction Reagent to each well. Incubate the plate at room temperature for 20 minutes.

1.10) Increase the volume in each well to 120 µl by adding 70 µl of phosphate buffered saline (PBS) pH 7.2.

1.11) Pellet the insoluble cellular debris by spinning the plate at 3000 RPM for 10 minutes at 4°C in the refrigerated centrifuge.

1.12) Transfer 110 µl of the soluble crude lysate to the corresponding wells of a 96-well thermocycler plate.

1.13) Using 30 minutes as the predetermined incubation time, expose the soluble lysates currently residing in the 96-well thermocycler plate to a broad gradient temperature range spanning 15°-20°C. Note, the goal is to determine what temperature your particular enzyme loses > 95% catalytic activity.

1.14) After incubation, incubate the 96-well thermocycler plate at 4°C for 5 minutes and transfer 100 µl of the soluble lysates from the 96-well thermocycler plate to their corresponding well location in the final 96-well microtiter plate.

1.15) With a 12-channel multipipettor, add 100 µl of GAS strain D471 to each well. Note, D471 cells are originally lyophilized from overnight cultures and resuspended with PBS pH 7.2 to obtain an OD_{600} of ~1.5.

1.16) Immediately place the 96-well plate in the microplate spectrophotometer and monitor the enzyme kinetics by measuring the O_{D600} every 15 seconds for 20 minutes. The lowest temperature incubation that corresponded to wells that lacked a change in optical density ($\Delta OD \leq 0.1$) is defined as the non-permissive temperature.

After a broad temperature screen is performed to identify the non-permissive temperature, the above steps can be repeated over a more narrow range of temperatures (5°-10°C) to elucidate the precise non-permissive temperature for the enzyme of interest. Note, the non-permissive temperature identified in this assay may be different than the melting temperature elucidated by other means due to differences in volume, concentration, etc.

2. Generating the Mutant Library

The creation of the mutant library to be screened involves randomly incorporating mutations with minimal nucleotide bias in the *plyCA* gene using the GeneMorph II Random Mutagenesis Kit as follows:

2.1) Nucleotide primers with similar melting temperatures (T_m) between 55°-72°C were designed with the restriction sites of choice to the 5' and 3' ends of the *plyCA* gene.

2.2) Since the desired mutation rate is 2-3 nucleotides per *plyCA* (1.4 kb), we utilized the PCR reaction component concentrations as well as the thermocycler conditions recommended by the manufacturer for low mutation frequencies (0-4.5 per kb).

2.3) Clone the mutagenized *plyCA* genes into the expression vector pBAD24.

2.4) Transform the constructs into a DH5α pBAD33:*plyCB* background and plate transformants on LB agar plates supplemented with ampicillin and chloramphenicol.

2.5) Additionally, transform and plate DH5α pBAD33:*plyCB* with the expression vector pBAD24 containing the WT *plyCA* gene. Colonies from this plate will serve as the controls during thermostability screening.

3. 96-Well Microtiter Plate Preparation and Cell Growth Conditions

3.1) Fill each well of a 96-well microtiter plate with 200 µl of LB supplemented with ampicillin and chloramphenicol.

3.2) Following the microtiter plate schematic (Fig. 3-1b), carefully select an individual colony from the overnight agar plates with a sterilized toothpick and inoculate the bacteria in the designated well of the 96-well microtiter plate. It is essential to ensure only one colony per well is inoculated.

3.3) Shake the securely anchored 96-well microtiter plate at 300 RPM overnight at 37°C.

4. Replica Plating, Protein Expression Induction and Lysate Preparation

4.1) Follow steps 1.5-1.11 from the section titled "Determining the optimal heating conditions" with one modification. Store the original plate at 4°C after the replica plating step has concluded.

4.2) After step 1.11, transfer 110 µl of the soluble crude lysate to the corresponding wells of a 96-well thermocycler plate except for the positive control wells A1-D1. With regard to the positive control lysates (i.e. lysates that are not heated), transfer 100 µl of the lysates to the corresponding wells in

a new 96-well microtiter plate that will serve as the final assay plate for the experiment.

5. Soluble Lysate Heat Treatment

5.1) Heat the negative control and mutant soluble lysates currently confined in the 96-well thermocycler plate in the thermocycler for 30 minutes at the optimized non-permissive incubation temperature determined in step 1.

5.2) After non-permissive temperature incubation, incubate the 96-well thermocycler plate at 4°C for 5 minutes.

5.3) Transfer 100 µl of the soluble lysates from the 96-well thermocycler plate to their identical well locations in the final 96-well microtiter assay plate already containing the positive control soluble lysates.

5.4) With a 12-channel multipipettor, add 100 µl of GAS strain D471 to each well. Immediately place the plate in the microplate spectrophotometer.

5.5) Monitor the enzyme kinetics by measuring the OD_{600} every 15 seconds for 20 minutes.

a. We defined a thermostable PlyC variant as a construct that can decrease the original optical density by 50 percent in less than 900 seconds at the non-permissive temperature. Additionally, the positive controls (i.e. non-heated, WT PlyC) need to display WT catalytic activity ($t_{1/2} \leq 100$ seconds) and the negative controls (i.e. heated, WT PlyC) should be devoid of activity.

5.6) Once a thermostable PlyC variant is identified, the original plate stored at 4°C is retrieved and bacteria from the individual well specific to the mutant of interest is inoculated into fresh LB media supplemented with ampicillin and chloramphenicol. The inoculum is then grown overnight at 37°C.

5.7) Plasmid DNA was extracted and purified from the culture and submitted for sequencing to identify the nucleotide mutations that inferred enhanced thermodynamic properties to PlyCA. Additionally, a small aliquot from the overnight culture was supplemented with 10% glycerol and stored at -80°C for further use.

Representative Results

Over 6000 PlyC mutants were screened for increased thermodynamic properties. A total of 35 mutants with potentially increased thermostability were identified, selected and sequenced. Genomic analysis, summarized in Table 3-1, suggest that of the 35 candidates, 7 of the constructs contained WT PlyCA sequences at the level of translation, corresponding to false positives identified by the assay. Of the remaining 28 candidates, the mutation range was from 1 to 6 nucleotide mutations with an average mutation rate of 2.75 nucleotides per *plyCA* gene, which was in the 2-3 nucleotide mutation range we were targeting. At the translational level, this particular nucleotide mutation range and frequency yielded an amino acid mutation range of 1 to 5 amino acids, with an average mutation rate of 1.9 amino acid mutations per PlyCA polypeptide. Of the 28 candidates with at least one amino acid mutation, four of these mutant constructs were randomly chosen for further characterization to validate that the extensive screening process of the

Table 3-1. Candidate Pool Genomic Analysis

Total Round 1 Candidates	35
Candidates with WT PlyCA Sequence	7
Candidates with ≥1 Amino Acid Mutation	28
Average Nucleotide Mutation Rate (nt/*plyCA*)	2.75
Nucleotide Mutation Range (nt)	1-6
Average Amino Acid Mutation Rate (AA/PlyCA)	1.9
Amino Acid Mutation Range (AA)	1-5

directed evolution methodology was indeed functioning properly. The mutant PlyC enzymes were purified to > 95% homogeneity based on SDS-PAGE analysis as previously described (Loeffler et al., 2001; Nelson et al., 2006b). Enzyme kinetics of WT PlyC and each of the four PlyC mutants were characterized at equal molar concentrations after incubating the purified enzymes at various elevated temperatures. Activity was monitored after the addition of D471 GAS by measuring the optical density at 600 nm every 15 seconds for 20 minutes. Activity was defined as the residual maximum velocity of the enzyme after heat incubation. Of the four candidates randomly selected for further characterization, mutant 29C3 showed the most enhanced thermodynamic properties (data not shown).

WT PlyC and 29C3 showed no significant difference in activity at room temperature (25°C) as depicted in the first set of bars in Fig. 3-2. However, after a short-term incubation for 30 minutes from temperatures ranging from 45°-50°C, the activity of 29C3 was substantially greater than the activity specific to the WT construct at each temperature point. For example, after a 30 minute incubation at 45.2°C, WT PlyC lost 50% of its activity whereas 29C3 showed no significant decrease in activity when compared to the activity displayed at room temperature.

Long-term incubation studies comparing the residual activity of both WT PlyC and 29C3 were additionally performed at 35°C and 40°C involving the measurement of residual activity at 24 and 48 hour time points. At 35°C, 29C3 displayed 41% and 176% higher activity than WT PlyC at 24 and 48 hour incubation time points, respectively (Fig.

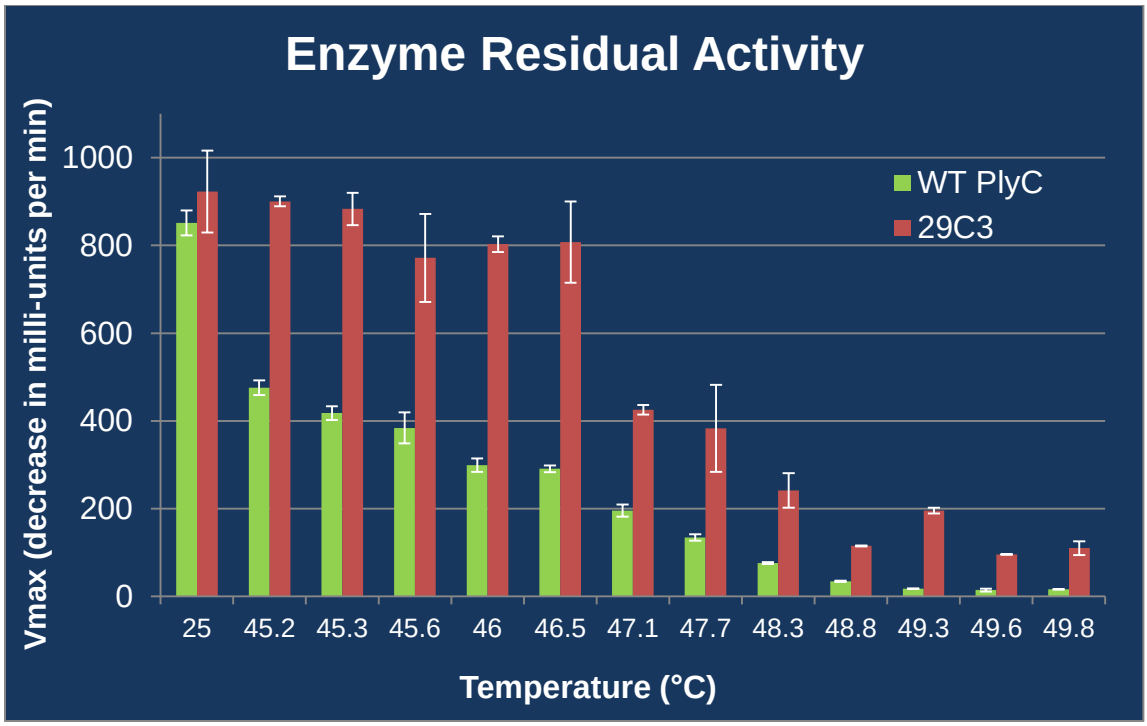

Figure 3-2. Residual activity kinetic analysis comparing WT PlyC and 29C3. Enzymes were purified to homogeneity and incubated at equal molar concentrations at either room temperature or at a temperature gradient ranging from 45°-50°C. Enzymatic activity correlates with the maximum velocity displayed after specific temperature incubation.

3-3a). At 40°C, 29C3 displayed 28% and 107% higher activity than WT PlyC at 24 and 48 hour incubation time points, respectively (Fig. 3-3b). The residual activity of WT PlyC and 29C3 were also monitored every 20 minutes for a total of 3 hours at 45°C. WT PlyC was only able to retain 21% activity after a 3 hour incubation at this temperature whereas 29C3 was able to retain 46% activity, resulting in 29C3 displaying more than twice the thermostability when compared to WT PlyC (Fig. 3-4).

Discussion

This protocol, outlined in Fig. 3-5, presents a 96-well microtiter plate methodology that allows one to utilize directed evolution to increase the thermodynamic properties of any bacteriolytic protein. Through the use of an error-prone DNA polymerase, one can introduce random mutations that increase the overall thermostability of the translated bacteriolytic molecule of interest, which is typically due to molecular reorganizations consisting of increasing electrostatic, disulfide bridge and hydrophobic interactions that generate improved molecular packing, enhanced modifications of surface charge networks or reinforcement of a higher oligomerization state (Eijsink et al., 2005; Kumar and Nussinov, 2001). After the introduction of nucleotide mutations, an extensive screening procedure was then used to identify mutations that enhanced thermostability. The representative results presented here were based on one round of random mutagenesis. In reality, it has been suggested that at least three successive rounds of random mutagenesis, each using the most robust mutant as the lead enzyme, followed by DNA shuffling is appropriate for these types of directed evolution thermostability studies (Liu et al., 2009).

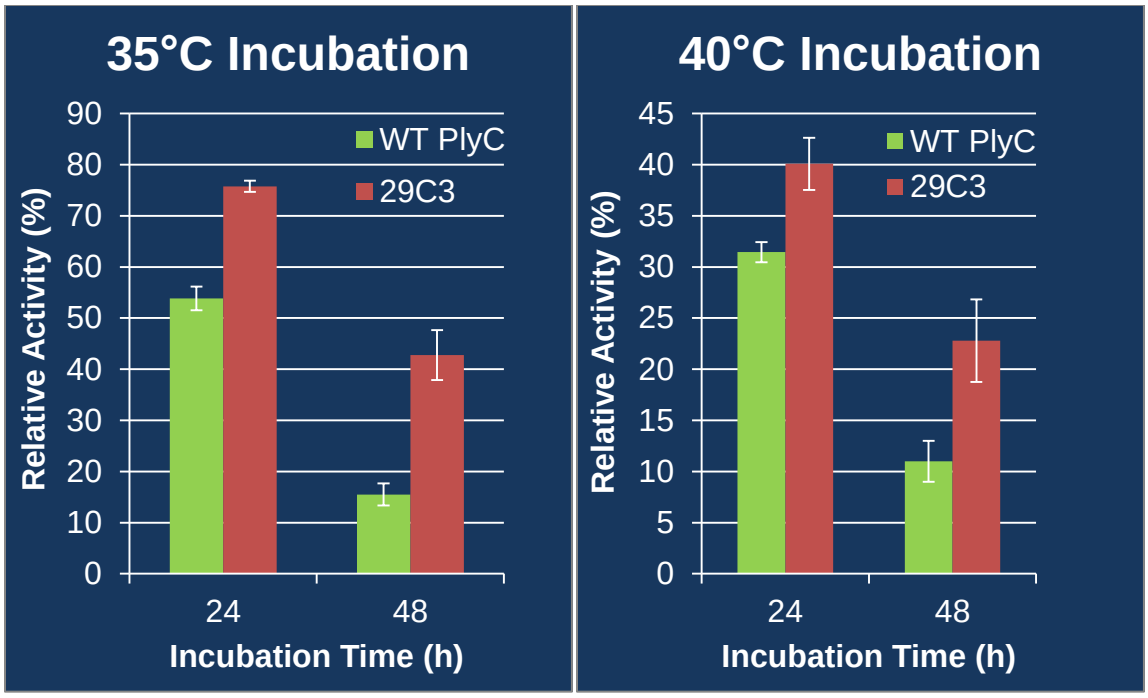

Figure 3-3. Residual activity kinetic analysis comparing WT PlyC to 29C3 at 35°C and 40°C. Equal molar concentrations of purified WT PlyC and 29C3 were incubated at (a) 35°C or (b) 40°C. The residual enzyme activity was measured at 24 and 48 hour time points. The activity displayed by each construct was normalized to the maximum velocity displayed at time point zero.

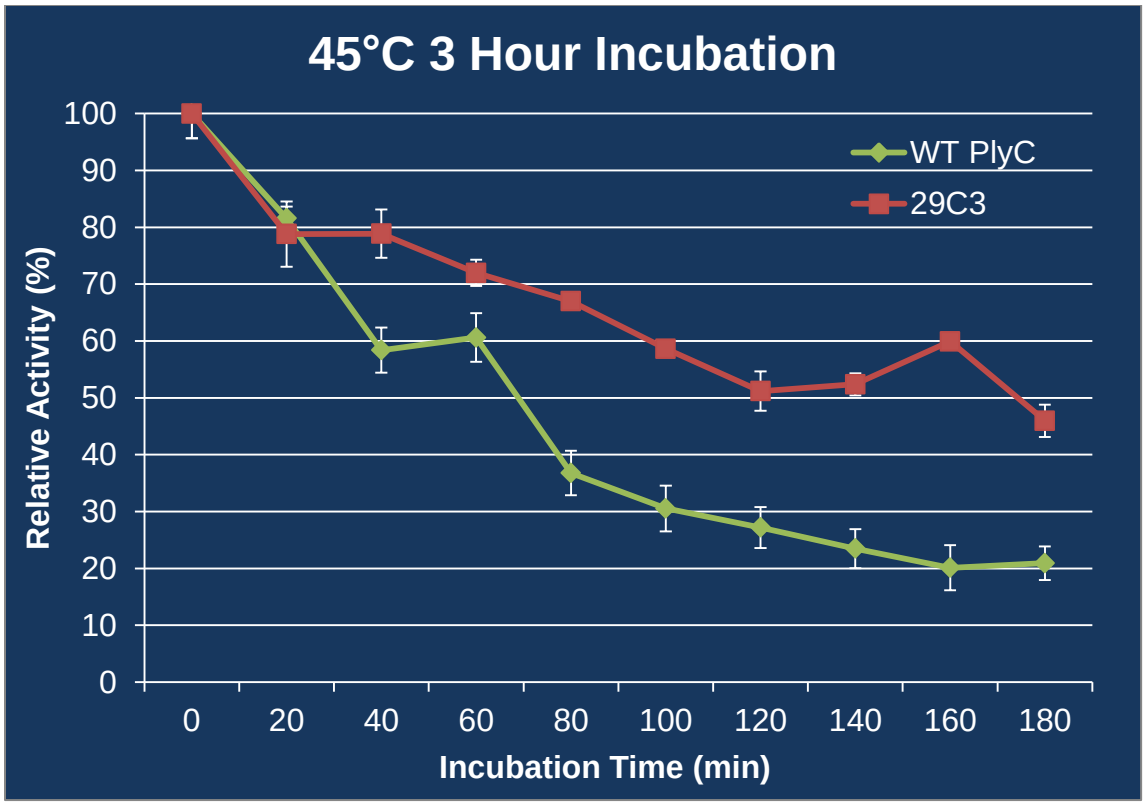

Figure 3-4. Residual activity kinetic analysis comparing WT PlyC to 29C3 at 45°C. Equal molar concentrations of purified WT PlyC and 29C3 were incubated at 45°C and the residual enzyme activity was measured every 20 minutes for 3 hours. The activity displayed by each construct was normalized to the maximum velocity displayed at time point zero.

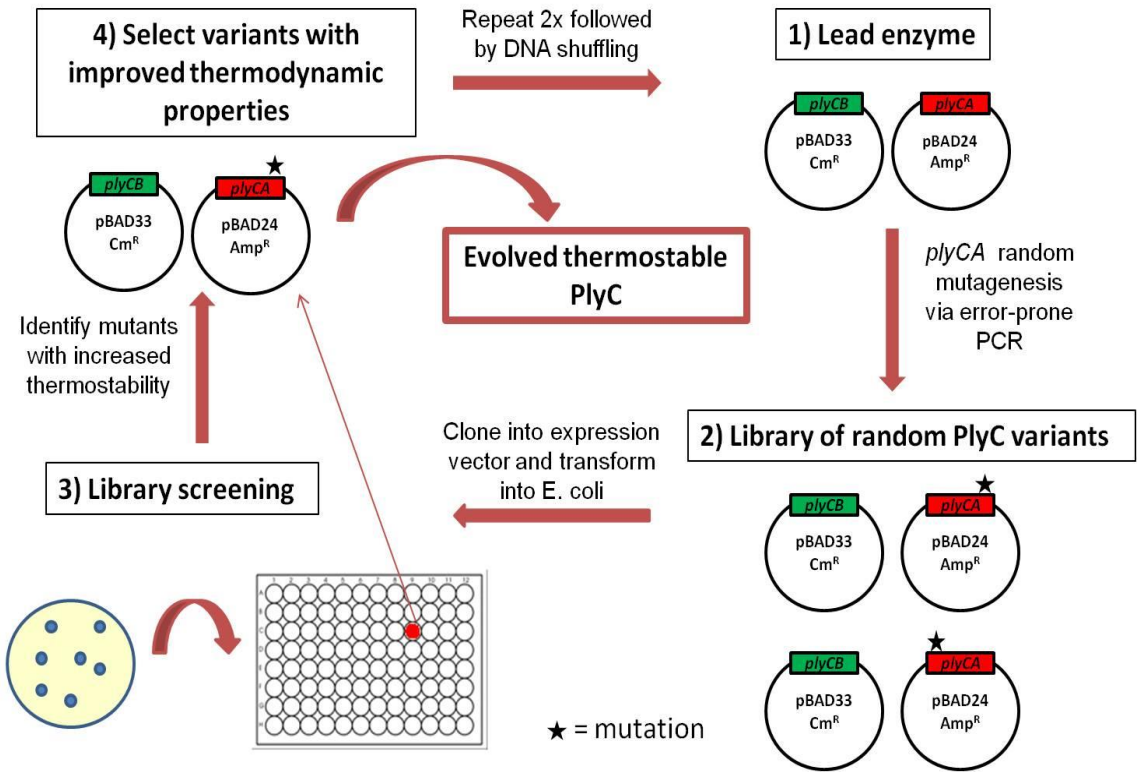

Figure 3-5. Directed evolution assay methodology. In random mutagenesis, one starts with the lead enzyme, which would be WT PlyC for the first round. A library of PlyC mutants containing random unbiased nucleotide mutations to the *plyCA* gene is then constructed, cloned into the expression vector pBAD24 and transformed into the *E. coli* strain DH5α already containing pBAD33:*plyCB.* Individual transformants are inoculated into their own specific well of a 96-well microtiter plate. Through an extensive screening process, individual PlyC mutants that are catalytically active after incubation at a non-permissible temperature are classified as mutants with enhanced thermodynamic properties. After performing genomic analysis on the candidate pool, the chosen specific mutations are then incorporated into the *plyCA* gene by means of site-directed mutagenesis and this particular *plyC* construct consequently becomes the lead enzyme for

the next round of random mutagenesis. Overall, there are three complete rounds of random mutagenesis followed by DNA shuffling resulting in a thermodynamically evolved bacteriolytic molecule.

While the methodology presented here is specific to implementing increased thermostability to PlyC, this same methodology can additionally be employed to enhance thermostability to other bacteriolytic proteins with some minor alterations to variables such as buffers, mutation rates, heating conditions and expression systems. One critical variable associated with this assay relates to the nucleotide mutation rate of the error-prone DNA polymerase. We chose to use the error-prone Mutazyme II DNA polymerase in our directed evolution assay due to experimental evidence suggesting this particular enzyme displays the least amount of bias with regards to which nucleotides are randomly incorporated into the gene of interest when compared to other random mutagenesis techniques such as use of hydroxylamine, mutator *E. coli* strains and other error-prone DNA polymerases (Rasila et al., 2009). In general, lower mutation rates tend to be more desirable for two reasons. First, engineering thermostability to proteins typically consist of relatively few amino acid substitutions. High mutation rates can cause dramatic structural alterations to particular molecules that can conclusively result in structural misfolding and functional discrepancies. For example, the incorporation of glycine and proline residues can disrupt alpha helical secondary structures (Wong et al., 2006a). Second, high nucleotide mutation rates increase the chances of incorporating premature stop codons, resulting in truncated molecules that are biologically inactive. In general, lower mutation rates are preferred because lower error rates result in the accumulation of adaptive mutations while higher mutation rates generate neutral or deleterious mutations (Arnold et al., 2001).

For each round of random mutagenesis, another critical variable that one must optimize involves the incubation temperature used during the screening process.

Selection of the experimental non-permissive temperature is relatively challenging. One needs to utilize an incubation temperature that is not too temperate (≤ 1°C higher than lowest non-permissive temperature) and conversely not too harsh (≥ 3°C higher than lowest non-permissive temperature). The ideal temperature we decided to use in this particular assay was a moderate 2°C higher than the experimentally determined non-permissive temperature. Choosing a temperature that is too mild will result in a much higher false positive identification rate than the ~20% we observed (Table 3-1) when using a moderate incubation temperature. Furthermore, using an incubation temperature that is too harsh could ultimately result in the inability to identify mutants with significantly enhanced thermostability. For example, using an incubation temperature of ≥ 3°C would have resulted in the inability to identify the thermodynamically promising 29C3 mutant as well as the majority of the other candidates selected during the first round of screening. In summation, we provide a protocol for engineering bacteriolytic proteins to acquire enhanced thermodynamic properties. Moreover, this same assay, without the heating steps, can be used to screen for mutations that increase catalytic activity. Augmenting both catalytic activity and increased thermostability is an important developmental hurdle facing any therapeutic enzyme. While the details of this protocol are specific to the endolysin PlyC, the methodology can be adapted to any bacteriolytic protein with only a few alterations. We presented preliminary results from only the first round of mutagenesis which validates that this assay is indeed functional, resulting in the implementation and identification of mutations that generate an increase in molecular thermostability of significant magnitude.

Acknowledgements

The authors wish to thank Emilija Renke and Janet Yu for technical assistance. DCN is supported by grants from the United States Department of Defense (DR080205, DM102823, OR09055, and OR090059). RDH is supported by a grant from the Maryland Agriculture Experiment Station and an NIH Training Grant in Cell and Molecular Biology.

Chapter IV

Directed Evolution of the Thermosusceptible Bacteriophage Endolysin PlyC

Ryan D. Heselpoth[1] and Daniel C. Nelson[1,2]

[1]Institute for Bioscience and Biotechnology Research, 9600 Gudelsky Drive, Rockville, MD 20850, USA and [2]Department of Veterinary Medicine, University of Maryland, 8075 Greenmead Drive, College Park, MD 20742, USA

This chapter is being edited and formatted for imminent submission.

Abstract

Bacteriophage-derived peptidoglycan hydrolases, termed endolysins, have been successfully exploited as an alternative antimicrobial to traditional antibiotics. One disconcerting property affiliated with many endolysins derived from mesophilic bacteriophage is the poor intrinsic thermal stability of their structures. The thermolability and subsequent abbreviated shelf life expectancy limits the antimicrobial potential of these enzymes. To overcome this challenge, directed evolution was applied to the heat-sensitive catalytic subunit, PlyCA, of the streptococcal-specific PlyC endolysin to improve its structural stability. After screening a total of 18,000 mutants, the lead candidate was the mutant PlyC (PlyCA) N211H. This mutation, which is located in the linker structure that conjoins the N-terminal GyH domain with the central helical docking domain, appeared to thermostabilize PlyCA by forming electrostatic interactions with E113 and D150 of the GyH domain. These interactions improved the thermodynamic stability of PlyCA by respectively increasing the thermal transition temperature (T_G) and van't Hoff enthalpy (ΔH_{VH}) of the subunit by 4.10°C and 19.97 kcal/mol. PlyCA was also kinetically stabilized, exhibiting an activation energy (E_A) of PlyCA unfolding increase of 17.52 kcal/mol. At pH 7.2-7.3, thermally-induced kinetic inactivation of PlyC (PlyCA) N211H decreased 18.8 fold at 45°C. When combining a previously identified stabilizing mutation, T406R, with N211H, the thermal stability augmentation was additive. PlyC (PlyCA) N211H T406R displayed a PlyCA ΔT_G and $\Delta(\Delta H_{VH})$ of +7.46°C and +22.60 kcal/mol over wild-type PlyC, respectively, while also demonstrating a 28.72 kcal/mol increase in PlyCA E_A of unfolding.

Introduction

Antibiotic misuse and overuse has stimulated bacteria to rapidly develop resistance. In combination with the extensive dissemination of these antibiotic-resistant microorganisms, the loss in antimicrobial efficacy of antibiotics has subsequently caused health and economic implications globally, thus prompting a definitive need for alternative antimicrobial approaches. One such alternative is a class of translational antimicrobials known as endolysins. Endolysins, also termed phage lysins or enzybiotics, are bacteriophage-derived peptidoglycan hydrolases that coordinate host cell lysis at the completion of progeny virion assembly (Lopez et al., 1997; Nelson et al., 2006a; Wang et al., 2000). Late in the lytic phage infection cycle, the endolysin is translocated from the cytosol to the peptidoglycan structure of the host bacterium by holins, which are pore-forming hydrophobic proteins encoded by the phage that oligomerize on the inner membrane of the host bacterium. Upon direct contact with the peptidoglycan, the endolysin cleaves one or more essential covalent bonds in the cell wall structure, resulting in bactericidal osmotic lysis and progeny virion liberation. Due to the extrinsic accessibility to the peptidoglycan structure, purified recombinant endolysins have been validated both *in vitro* and *in vivo* for their antimicrobial efficacy against Gram-positive pathogens when extrinsically applied and thus serve as a novel alternative to classical antibiotics (Fischetti, 2005, 2008; Fischetti et al., 2006; Loessner, 2005).

PlyC is a streptococcal-specific endolysin that can lyse a range of bacterial species known to cause severe human (e.g. *Streptococcus pyogenes*) and animal (e.g. *Streptococcus equi*) health complications (Nelson et al., 2001). Unlike other endolysins, PlyC is uniquely encoded by an operon and consists of a novel multimeric protein

structure with nine distinct subunits (McGowan et al., 2012; Nelson et al., 2006a). Eight identical PlyCB monomers interact through protein-protein interactions to form the octomeric cell wall binding domain (CBD) of the holoenzyme. The CBD dictates the lytic specificity of an endolysin by binding to a species-specific cell wall-associated epitope. The ninth subunit, PlyCA, serves as the enzymatically active domain (EAD) of the endolysin responsible for peptidoglycan hydrolysis. PlyCA is comprised of a catalytically-active N-terminal glycosol hydrolase (GyH) domain that is linked to a central helical docking domain. The helical docking domain is responsible for interacting with the PlyCB octomer, thereby promoting the formation of the holoenzyme structure. The carboxyl end of the helical docking domain is linked to a catalytically-active C-terminal cysteine, histidine-dependent amidohydrolase/peptidase (CHAP) domain that functions as an N-acetylmuramoyl-L-alanine amidase (Fischetti et al., 1972a). The GyH domain acts synergistically with the CHAP domain to generate the potent bacteriolytic mechanism of the enzyme. PlyC has been characterized *in vitro* to be several orders of magnitude more active than any other endolysin to date (McGowan et al., 2012; Nelson et al., 2001).

Despite the promising aforementioned antimicrobial characteristics of PlyC, one attribute that significantly hinders its antimicrobial potential relates to the inherent structural stability of the enzyme. Thermodynamic characterization of PlyC by differential scanning calorimetry (DSC) revealed the PlyCB octomer is endogenously thermostable, displaying a thermal transition temperature (T_G) temperature of 75.85°C, whereas the PlyCA EAD conversely displayed a thermolabile T_G of 48.27°C at pH 7.0 (Chapter II). Calorimetric unfolding and refolding studies depict that, while the

dissociation of the PlyCB octomer is a reversible process, the unfolding of the individual PlyCA and PlyCB monomers is irreversible (F. Schwartz, personal communication). The thermolability associated with PlyC seems to be a common trend when compared to other thermally characterized Gram-positive endolysins derived from mesophilic bacteriophage. For example, the *Staphylococcus aureus* endolysin LysK and the *Streptococcus pneumoniae* endolysins Cpl-1, Pal and Cpl-7, are kinetically inactivated and/or unfold at 42.0°C, 43.5°C, 50.2°C and 50.4°C, respectively (Bustamante et al., 2012; Filatova et al., 2010; Sanz et al., 1993; Varea et al., 2004). The thermosusceptible nature of endolysins, such as PlyC, is problematic because, in congruence with the Arrhenius equation, poor structural stability directly correlates with abbreviated shelf life (Anderson and Scott, 1991).

There exists a wide-range of protein engineering methodologies that have been successfully exploited to alter the molecular properties of proteins, ranging from rationale-based techniques such as computational modeling, sequence homology comparisons and structure-guided site-directed mutagenesis, to random approaches such as directed evolution (Antikainen and Martin, 2005). Directed evolution is a laboratory-based bioengineering approach that utilizes the concept of Darwinian evolution to alter various macromolecular properties (Lutz and Patrick, 2004). The two key steps of directed evolution are generating molecular diversity followed by the use of a screening process to identify variants that display progressed fitness. After several iterations of mutagenesis, screening and amplification of selected mutants with enhanced properties, beneficial mutations can accumulate in true Darwinian evolution (Jackel et al., 2008). In addition to isolating enzyme variants from thermophilic organisms and rationale-based

techniques, directed evolution is commonly exploited for engineering increased protein stability. Directed evolution is often preferred to other engineering strategies due to the level of diversification and size of the mutant pool screened. Moreover, neither structural information nor an understanding of the molecular mechanism for increased fitness are required to design and implement directed evolution experiments (Arnold et al., 2001; Cherry and Fidantsef, 2003; Eijsink et al., 2004; Lutz and Patrick, 2004; Matthews, 1995; Robertson and Steer, 2004; Schiraldi and De Rosa, 2002; Turner, 2003; van den Burg, 2003; Vieille and Zeikus, 2001; You and Arnold, 1994; Zhao et al., 2002).

Here we aim to increase the stability of PlyC by means of directed evolution in order to extend the shelf life and thus improve the antimicrobial potential of the enzyme. We previously developed and validated a novel directed evolution protocol that first utilizes the error-prone polymerase chain reaction (epPCR) to randomly incorporate mutations into a bacteriolytic enzyme. This step is followed by an extensive screening process that effectively identifies mutations that improve the kinetic stability of a bacteriolytic enzyme, such as an endolysin, without compromising its native catalytic efficiency (Heselpoth and Nelson, 2012). At the time, we screened a total of 6,000 PlyC mutants and presented experimental results to validate the protocol. Here, we extend the screening to 18,000 PlyC variants, kinetically and biophysically characterize the lead enzyme candidate, perform site-directed mutagenesis to elucidate the stabilizing mechanism, and finally combine these results with a point mutant from rational design experiments to further optimize the thermostability of PlyC.

Materials and Methods

Bacterial Strains and Culture Conditions

S. pyogenes D471 (group A streptococcus) was stored at -80°C and routinely grown in THY (Todd Hewitt broth, 1% wt/vol yeast extract) at 37°C. *E. coli* strains DH5α, DH5α pBAD33: *plyCB* and BL21(DE3)pLysS (Novagen) were grown in Luria-Bertani (LB) broth at 37°C in a shaking incubator unless otherwise stated. When needed, ampicillin (100 μg/ml) and/or chloramphenicol (35 μg/ml) were added to the media.

Molecular Cloning of PlyC Structural and Directed Evolution Constructs

The *plyC* operon is composed of the structural gene for PlyCB, a non-coding intergenic locus termed the lysin intergenic locus, or *lil*, and the structural gene for PlyCA. *plyCB* and *plyCA* were cloned into pBAD24 as previously described (Nelson et al., 2006a). *gyh* was amplified with the forward primer 5'-CTTCTTCAATTGATTATGAGTAAGAAGTATACACAACAACAATACG and reverse primer 5'-CCCTCTAGATTAATGGTGATGATGATGATGAATTGAACCACCTG. *chap* was amplified with the forward primer 5'-CTTCTTCAATTGATTATGTCACCAGGTCAAAACGATTTAGGGTCG and reverse primer 5'-CCCTCTAGATTATTTAAATGTTATCAAACCAGTTAGTG. *plyCΔgyh* was constructed by overlap extension PCR with three sets of primers. The first gene construct, *plyCB+lil*, was amplified with the forward primer 5'-CTTCTTCAATTGATTATGAGCAAGATTAATGTAAACGTAG and reverse primer

5’-CTTCTCTCTGTTAGCTTCCATTAAATAAATTCTCCCTTTC. The second gene construct, *plyCAΔgyh*, was amplified with the forward primer 5’-GAAAGGGAGAATTTATTTAATGGAAGCTAACAGAGAGAAG and reverse primer 5’-CCCTCTAGATTATTTAAATGTTATCAAACCAGTTAGTGTTG. *plyCB+lil* and *plyCAΔgyh* were then fused together with the forward primer 5’-CTTCTTCAATTGATTATGAGCAAGATTAATGTAAACGTAG and reverse primer 5’-CCCTCTAGATTATTTAAATGTTATCAAACCAGTTAGTGTTG to generate the full-length *plyCΔgyh* construct. *plyCΔchap* was amplified with the forward primer 5’-CTTCTTCAATTGATTATGAGCAAGATTAATGTAAACGTAG and reverse primer 5’-GGGTCTAGATTA AACGGTCGGTTTGTCTGGG. *plyCΔΔ* was amplified with the forward primer 5’-CTTCTTCAATTGATTATGAGCAAGATTAATGTAAACGTAG and reverse primer 5’-CCCTCTAGA TTAGTGATGGTGATGGTGATGCGATCCCTGTAAGTTAACATCAGC. The standard 50 µl PCR reaction mixture consisted of 1 ng of template (pBAD24: *plyC* for all constructs except for *plyCΔΔ*, which required the use of pBAD24: *plyCΔgyh*), 1x Q5 reaction buffer (New England Biolabs), 0.2 mM dNTP mix, 0.5 µM of each primer and 1 U of Q5 DNA polymerase (New England Biolabs). The thermocycler heating conditions consisted of 98°C for 30 s, 35x (98°C for 10 s; 60°C for 30 s; 72°C for 30 s/kb) and 72°C for 2 min. The PCR products were then double digested with MfeI and XbaI restriction endonucleases and ligated into pBAD24 using the EcoRI and XbaI restriction sites of the vector.

Site-directed mutagenesis was performed using the Phusion Site-Directed Mutagenesis Kit (Thermo Scientific). Mutations were introduced into the middle of the

30 nucleotide forward phosphorylated oligonucleotide primer for each mutant, with the reverse primer being complimentary to the next 30 nucleotides upstream. The standard 50 µl PCR reaction mixture consisted of 1 ng of pBAD24:*plyC* , 1x Phusion HF buffer, 0.2 mM dNTP, 0.5 µM of each primer and 1 U of Phusion DNA polymerase. The thermocycler heating conditions consisted of 98°C for 30 s, 25x (98°C for 10 s; 65°C for 30 s; 72°C for 4 min) and 72°C for 5 min. The mutagenized PCR products were then ligated and transformed into *E. coli* DH5α. Mutations were confirmed by nucleotide sequencing (Macrogen USA).

Error-prone PCR (epPCR) using Mutazyme II (Agilent Technologies) was applied to *plyCA* at a low mutation rate of 2-3 nucleotides per *plyCA* gene. The standard 50 µl epPCR reaction mixture consisted of 3 µg of pBAD24: *plyCA* (750 ng of target DNA), 1x Mutazyme II reaction buffer, 0.2 mM dNTP mix, 0.5 µM of each primer (forward primer 5'-CTTCTTCAATTGATTATGAGTAAGAAGTATACACAACAACAATACG and reverse primer 5'-CCCTCTAGATTATTTAAATGTTATCAAACCAGTTAGTGTTG) and 0.05 U of Mutazyme II DNA polymerase. The thermocycler heating conditions consisted of 95°C for 2 min, 30x (95°C for 30 s; 60°C for 30 s; 72°C for 2 min) and 72°C for 10 min. The mutant *plyCA* library was then double digested with MfeI and XbaI restriction endonucleases and ligated into pBAD24 using the EcoRI and XbaI restriction sites of the vector. The resulting pBAD24: *plyCA* mutant constructs were then transformed into *E. coli* DH5α harboring pBAD33: *plyCB* and then plated on LB agar plates supplemented with ampicillin (100 µg/ml) and chloramphenicol (35 µg/ml).

Protein Expression and Purification

With the exception of the protein expression during directed evolution screening, all of the endolysin constructs investigated were initially expressed in *E. coli* BL21(DE3)pLysS. Bacterial cells were grown in 1.5L LB supplemented with ampicillin (100 µg/ml) to mid-log phase in a 4L Erlenmeyer flask. Protein expression was induced using 0.25% L-arabinose at 37°C for 4 h. Cells were then harvested at 7,000 RPM for 15 min at 25°C, resuspended in 75 ml of phosphate buffered saline (PBS), pH 7.2, supplemented with 1 mM phenylmethanesulfonyl fluoride (Sigma-Aldrich), and sonicated on ice for 15 min. The insoluble cellular debris was pelleted at 13,000 RPM for 1 h at 4°C. The soluble endolysin constructs were purified as previously mentioned (Nelson et al., 2001). Protein solubility and purity was analyzed on a 4-15% gradient sodium dodecyl sulfate polyacrylamide gel electrophoresis (SDS-PAGE) gel (Laemmli, 1970).

Directed Evolution Genetic Diversification and Screening Methodology

The directed evolution methodology was previously described (Heselpoth and Nelson, 2012). Briefly, epPCR was applied to the PlyCA subunit of PlyC at a low mutation rate. The resulting mutant library was cloned into pBAD24 and transformed into *E. coli* DH5α pBAD33: *plyCB*. Thermostabilized PlyC mutants encoded by the transformants were subsequently identified using a novel, optimized screening methodology.

Thermal Inactivation Experiments

Wild-type PlyC and various PlyC mutants were incubated in a 45°C heat block in PBS, pH 7.2-7.3, at a 44 nM (5 μg/ml) concentration for a total of 3 hours. At 20 minute increments, a 400 μl aliquot of the heated enzyme was removed and immediately incubated on ice for 5 minutes. Three adjacent wells of a 96-well microtiter plate were then filled with 100 μl of the cooled enzyme, followed by the addition of an equal volume of *S. pyogenes* D471. Streptococcal cells used in this study were grown as previously described (see *Bacterial Strains and Culture Conditions*), then harvested at 4,000 RPM for 15 minutes, washed once with PBS, pH 7.2-7.3, and resuspended in PBS buffer to an OD_{600} = 2.0. The residual lytic activity of the endolysin was analyzed via turbidity reduction assay by monitoring the OD_{600} every 6 s for 20 min. The activity of the endolysin was equated to the V_{max} corresponding to linear portion of the resulting killing curve. Residual lytic activity was normalized to the activity displayed in the absence of heat treatment.

Circular Dichroism (CD) Spectroscopy

Far-UV and thermal denaturation CD experiments were conducted using a Chirascan CD spectrometer (Applied Photophysics). To determine protein secondary structure composition, the various PlyC constructs were analyzed at 0.1 mg/ml in 20 mM sodium phosphate buffer, pH 7.0. Using a 1 mm path length quartz cuvette, far-UV CD spectra (190-260 nm) were taken at 20°C using 1 nm steps with 5 second signal averaging per data point. Spectra were collected in triplicate, followed by averaging, baseline subtraction, smoothing and conversion to mean residue ellipticity (MRE) by the

Pro-Data software (Applied Photophysics). Thermal denaturation experiments consisted of monitoring the MRE at 222 nm for the protein samples as they were heated from 20°C to 95°C at 1°C/min. Samples were at a 1 mg/ml concentration in 20 mM sodium phosphate buffer, pH 6.0-8.0, and the MRE was measured at 0.5°C steps with 5 s signal averaging per data point. The data was smoothened, normalized and fit with a Boltzmann sigmoidal curve. The first derivative of the denaturation curve was then taken to determine the temperature ($T_{1/2}$) at which the folded and unfolded PlyCA subunit population was at equilibrium (Fallas and Hartgerink, 2012).

Differential Scanning Calorimetry

The thermally-induced unfolding thermodynamics of the protein samples were measured using a Nano DSC differential scanning calorimeter (TA Instruments). All samples were degassed for at least 20 minutes prior to the experiment and maintained at 3 atm during calorimetric analysis. The sample and reference cells were initially calibrated with equal volumes of 20 mM sodium phosphate buffer, pH 6.0-8.0, using three consecutive heating/cooling cycles at 1°C/min consisting of a temperature range of 15°C to 105°C. The protein samples at 8.84 μM were heated from 15°C to 105°C at a 1°C/min heating rate in 20 mM sodium phosphate buffer, pH 6.0-8.0, and immediately cooled over the same temperature range at 1°C/min. Baseline subtraction and curve fitting was performed by the NanoAnalyze software (TA Instruments).

Bacteriolytic Activity Quantitation against *S. pyogenes*

Turbidity reduction assays were performed to determine the bacteriolytic activity

of wild-type PlyC and PlyC (PlyCA) N211H. In a 96-well microtiter plate, the purified endolysin at an initial concentration of 8.84 μM (1 μg/μl) was two-fold serial diluted in 100 μl of PBS, pH 7.2-7.3, buffer. An equal volume of *S. pyogenes* D471 (see *Thermal Inactivation Experiments* for cell preparation) was then mixed with the different enzyme concentrations and the OD_{600} was monitored by means of a turbidity reduction assay every 6 s for 30 min at 37°C. The amount of time (s) to decrease the OD_{max} by 50% was then plotted against the enzyme molar concentration and fit with a one-phase exponential decay curve. 1 U of enzyme activity was equated to the amount of endolysin (μg) required to decrease the OD_{max} by 50% in 15 min. Each independent turbidity reduction assay was performed in triplicate.

Constructing Arrhenius Plots for Calculating Activation Energy of PlyCA Unfolding

The rate constant *k* for PlyCA unfolding was derived from the corresponding DSC thermograms using the equation

$$k = \nu C_p/(Q_t-Q)$$

where ν (K/min) is the scan rate, C_p the excess heat capacity, Q_t the total heat of the process and Q the heat evolved at a given temperature, T. The activation energy, E_A, is determined by measuring the value of k at several temperatures and then using the Arrhenius equation $k = A\exp(-E_A/RT)$. That is, the corresponding Arrhenius plot, ln k versus $1/T$, is used to calculate E_A by using the equation

$$\mathrm{m} = -E_A/R$$

where m stands for the slope of the Arrhenius plot and R stands for the gas constant.

Results

Thermodynamic Analysis of the Structural Components of PlyC

Results from a previous DSC analysis of several PlyC constructs, including PlyC, PlyCB, PlyCA, CHAP domain only and PlyCAΔCHAP (in a PlyCΔCHAP background), advocated the CHAP domain being the most unstable structural element of PlyCA (F. Schwartz, personal communication). Preliminary observations from a more recent study suggested the CHAP and GyH domains (isolated or in the context of the holoenzyme) are thermodynamically similar. Without an obvious region to target, epPCR was applied to the entire PlyCA subunit during the initial round of directed evolution (Heselpoth and Nelson, 2012).

To further confirm the absence of a specific region in PlyCA that is responsible for intrinsic instability of the subunit, a more complete thermodynamic analysis of the various structural components comprised by the PlyC holoenzyme was constructed. Eight different PlyC constructs (PlyC, PlyCA, PlyCB, GyH domain, CHAP domain, PlyCΔGyH, PlyCΔCHAP, PlyCΔΔ) were expressed and purified to homogeneity based on SDS-PAGE analysis (Fig. 4-1, Table 4-1). The protein samples were then subjected to T_G analysis at equal molar concentrations by DSC in 20 mM sodium phosphate buffer pH 7.0. Results from the calorimetric experiments show the complete unfolding of the PlyC holoenzyme fulfills a five-state thermal transition model, with the unfolding of PlyCA and PlyCB each displaying two thermal transitions. When the PlyCA N-terminal GyH domain and C-terminal CHAP domain are isolated, the stability of the individual domains

Table 4-1. List of different PlyC constructs thermodynamically characterized by DSC.

PlyC Construct	Description	PlyCA Amino Acids	PlyCB Amino Acids
PlyC	Full-length PlyC holoenzyme	1-465 (50 kDa)	1-72 (8 kDa)
PlyCA	PlyCA EAD only	1-465 (50 kDa)	-------
PlyCB	PlyCB CBD octomer only	-------	1-72 (8 kDa)
GyH Domain	PlyCA N-terminal GyH domain only	1-205 (23 kDa)	-------
CHAP Domain	PlyCA C-terminal CHAP domain only	300-465 (18 kDa)	-------
PlyCΔGyH	PlyC holoenzyme with the PlyCA GyH domain deleted	226-465 (26 kDa)	1-72 (8 kDa)
PlyCΔCHAP	PlyC holoenzyme with the PlyCA CHAP domain deleted	1-298 (33 kDa)	1-72 (8 kDa)
PlyCΔΔ	PlyC holoenzyme with PlyCA GlyH and CHAP domain deletions	226-288 (7 kDa)	1-72 (8 kDa)

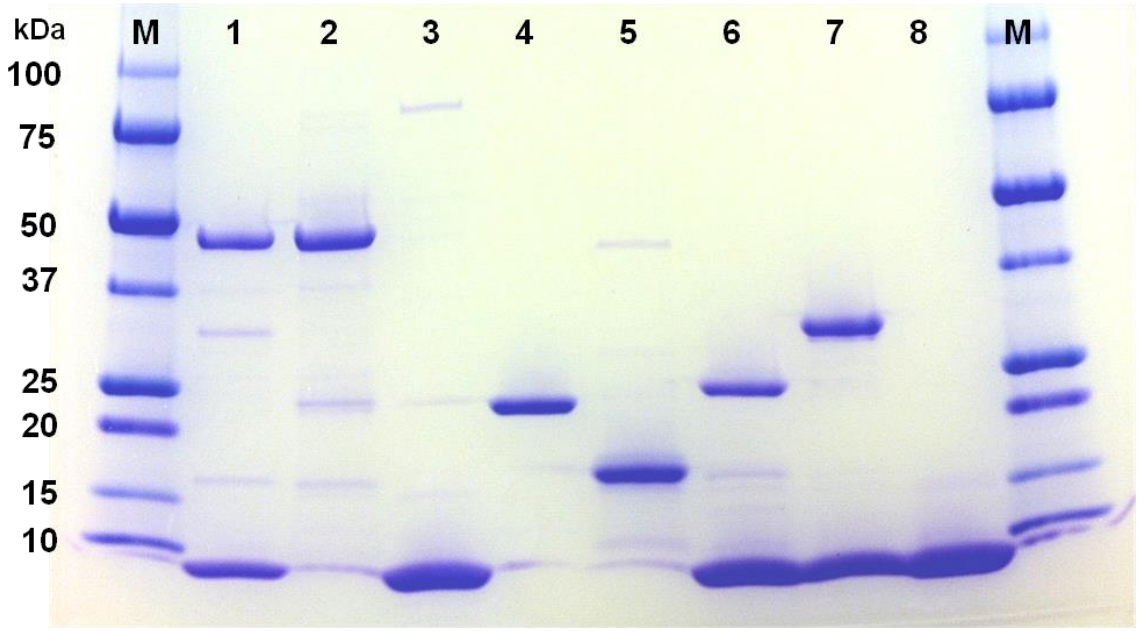

Figure 4-1. SDS-PAGE analysis of the PlyC structural constructs. The solubility and purity of each of the protein samples was analyzed on a 4-15% gradient SDS-PAGE gel. The various lanes correlate to: (M) Molecular weight standard, (1) PlyC holoenzyme (composed of a 50 kDa PlyCA and 8 x 8 kDa identical PlyCB subunits), (2) PlyCA, (3) PlyCB, (4) GyH domain, (5) CHAP domain, (6) PlyCΔGyH, (7) PlyCΔCHAP and (8) PlyCΔΔ (note, the 7 kDa helical docking domain of PlyCA is indistinguishable from the 8 kDa PlyCB monomer by SDS-PAGE).

were highly similar, depicting a ΔT_G of ±0.07°C (Table 4-2). When each individual domain is linked to the central helical docking domain of PlyCA and simultaneously complexed to the PlyCB octomer, PlyCAΔGyH (GyH deletion) was stabilized by 1.34°C while PlyCAΔCHAP (CHAP deletion) was conversely destabilized by 0.43°C when compared to the stability of full-length PlyCA (T_G = 48.27°C) complexed to the CBD. When directly comparing the stability of PlyCAΔGyH to PlyCAΔCHAP when complexed to the PlyCB CBD, the ΔT_G was ±1.77°C. A decisive unfolding thermal transition for the isolated central helical docking of PlyCA when bound to the PlyCB CBD was not detected in the temperature range tested and therefore a distinct thermal transition temperature could not be assigned to this structural component of PlyCA. Due to comparable stability profiles of the uncomplexed and complexed GyH and CHAP domains ($\Delta T_G \leq 2$°C) coupled with the unknown stability of the central helical docking domain, the focus of epPCR step of the PlyC directed evolution study continued to be the entire PlyCA subunit.

Directed Evolution Screening Synopsis

Overall, 18,000 PlyC mutants were screened for enhanced kinetic stability over a total of 3 rounds of directed evolution (Fig. 4-2). For round 1, the lead candidate and template for epPCR was wild-type *plyCA*. 6,000 mutants were screened at 35°C and 35 candidates were chosen for re-screening in order to remove false positives and identify a lead candidate. The lead *plyCA* mutant candidate from round 1 was then subjected to epPCR and subsequently 75 mutant candidates were chosen for re-screening after initially screening 6,000 second generation mutants at 42°C. Finally, the lead *plyCA*

Table 4-2. DSC T_G comparative analysis of PlyCA (columns 2 and 3) and PlyCB (columns 4 and 5) thermal transitions exhibited by the PlyC structural components.

PlyC Construct	PlyCA		PlyCB	
	T_{G1} (°C)	T_{G2} (°C)	T_{G3} (°C)	T_{G4} (°C)
PlyC	48.27	50.67	75.85	79.32
PlyCA	45.92	48.41	--------	--------
PlyCB	--------	--------	75.44	77.00
GyH Domain	47.74	49.44	--------	--------
CHAP Domain	47.81	50.14	--------	--------
PlyCΔGyH	49.61	56.77	73.90	75.73
PlyCΔCHAP	47.84	50.22	76.26	79.52
PlyCΔΔ	NA	NA	74.23	76.59

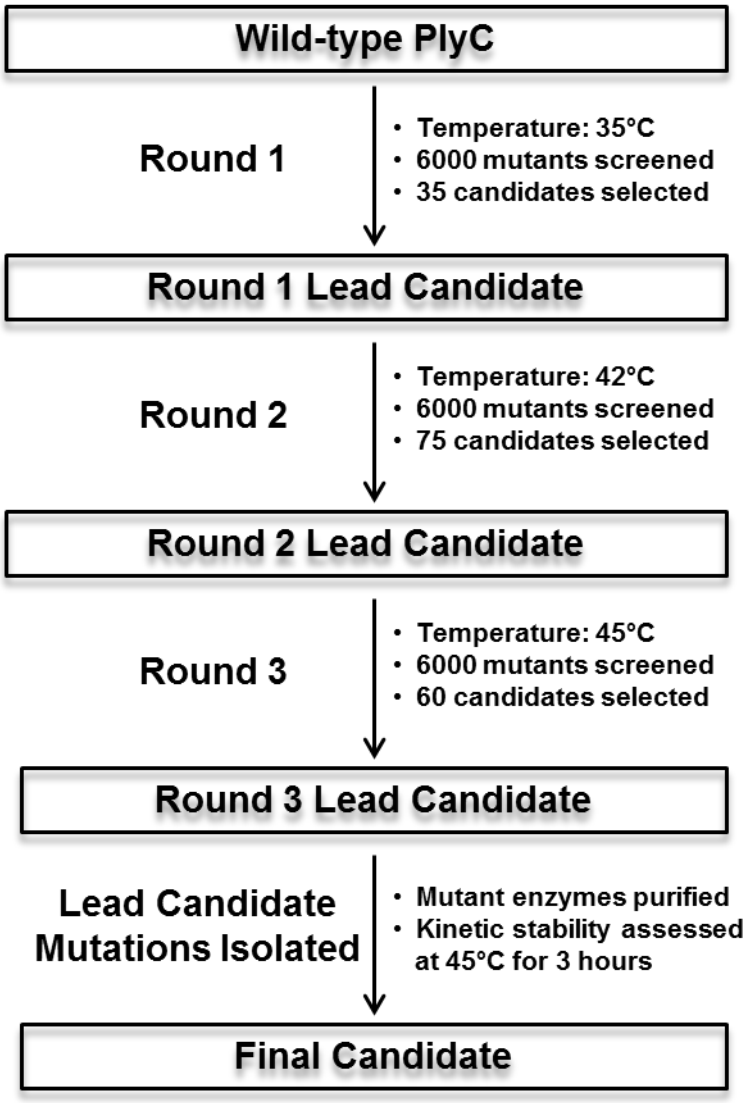

Figure 4-2. Flowchart of the PlyC directed evolution methodology. A total of 18,000 PlyC mutants were screened at non-permissive temperatures over three rounds of directed evolution followed. The four amino acid mutations comprised by the round 3 lead candidate were isolated, with the most kinetically stable construct being labeled as the final stabilized variant for further characterization.

mutant candidate from round 2 served as a template for epPCR for round 3 of directed evolution. Another 6,000 mutants were then screened at 45°C, with 60 candidates being identified for re-screening. The lead candidate at the conclusion of directed evolution was termed PlyC 33D2, which encodes the four PlyCA amino acid mutations N211H, S224N, G249C and A407S.

The kinetic stability PlyC 33D2 was further dissected to determine if one or more of the amino acid mutations encoded by the mutant were responsible for the stability enhancement. To answer this question, wild-type PlyC, PlyC 33D2 and the four individual 33D2 point mutants (N211H, S224N, G249C, A497S) were constructed, expressed and purified to homogeneity for kinetic stability analysis (Fig. 4-3, lanes 1-6). The purified enzymes were incubated at equal molar concentrations for a total of 3 hours at 45°C. The residual activity was determined at 20 minute increments and normalized to the activity displayed when the sample was devoid of heat-treatment. At 45°C, the PlyC 33D2 mutant displays a half-life ($t_{1/2}$) of 44.59 min, which correlates to a 2.5 fold increase in kinetic stability when compared to the 17.84 min $t_{1/2}$ of wild-type PlyC (Fig. 4-4a, Table 4-3). When four 33D2 point mutations were isolated, mutants S224N, G249C and A407S displayed similar $t_{1/2}$ values. None of the three mutants were able to fully rescue the kinetic stability phenotype displayed by the PlyC 33D2 mutant (Fig. 4-4b, Table 4-3). Nonetheless, all three mutants displayed kinetic stability phenotypes that represented marginable improvements over wild-type. Conversely, the N211H mutation significantly improved the kinetic fitness of the enzyme nearly 19 fold, raising the $t_{1/2}$ from 17.84 min to an extrapolated 335.04 min. When directly comparing the stability of 33D2 to the isolated N211H point mutant, the N211H mutant exhibits a $t_{1/2}$ that is 7.5 fold higher.

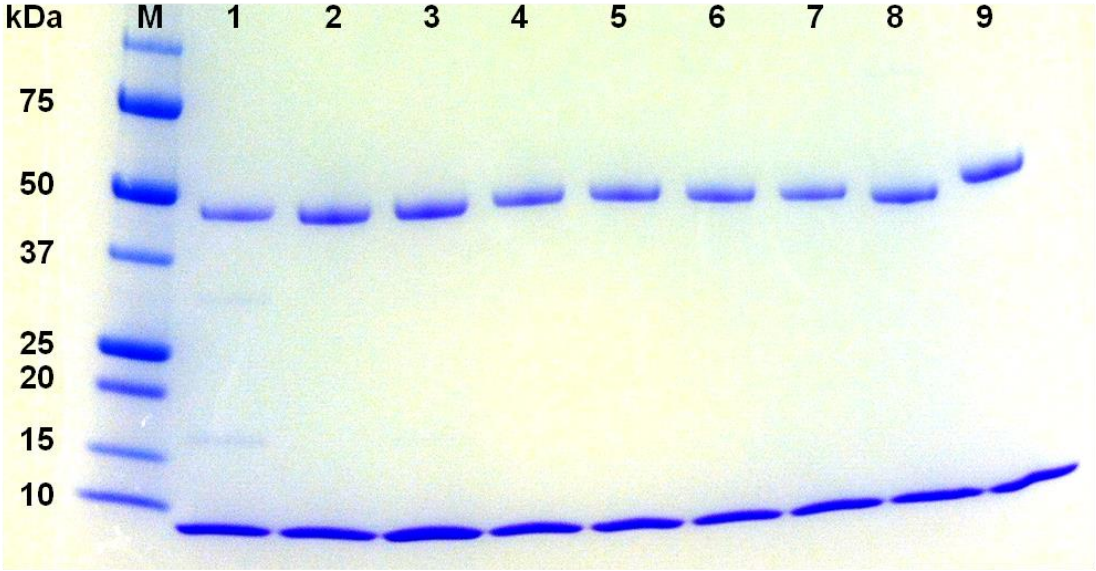

Figure 4-3. SDS-PAGE analysis of PlyC 33D2 constructs and PlyC (PlyCA) N211 charge mutants. The solubility and purity of each of the mutants was analyzed on a 4-15% gradient SDS-PAGE gel. The various lanes correlate to: (M) Molecular weight standard, (1) PlyC, (2) PlyC 33D2, (3) PlyC (PlyCA) N211H, (4) S224N, (5) G249C, (6) A407S, (7) N211A, (8) N211K and (9) N211D.

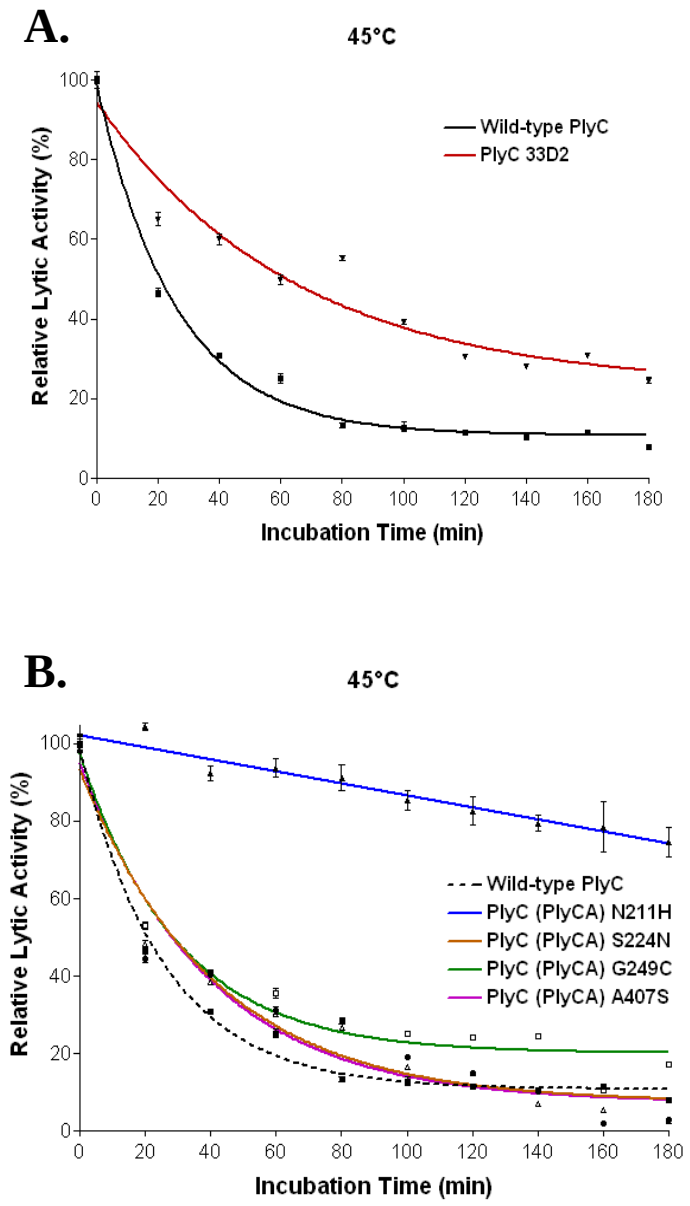

Figure 4-4. Kinetic stability of the directed evolution round 3 lead candidate, PlyC 33D2, and the isolated PlyC 33D2 point mutations. The rate of kinetic inactivation of wild-type PlyC at 45°C was compared to that of either (a) the round 3 lead candidate PlyC 33D2 or (b) the individual point mutants encoded by the PlyC 33D2 mutant. The enzymes were incubated at equal molar concentrations in PBS, pH 7.2-7.3, with the residual lytic activity being analyzed every 20 min for a total of 3 h.

Table 4-3. Kinetic stability comparison at 45°C between wild-type PlyC, PlyC 33D2 and the isolated point mutations collectively encoded by PlyC 33D2.

PlyC Construct	$t_{1/2}$ (min)	Relative Kinetic Stability	R^2
Wild-type	17.84	1.0	0.99
33D2	44.59	2.5	0.93
N211H	**335.04**	**18.8**	**0.94**
S224N	28.26	1.6	0.93
G249C	20.85	1.2	0.96
A407S	27.26	1.5	0.96

This suggests that in a PlyC (PlyCA) N211H background, the combination of the N211H mutation with one or more of the other pre-existing 33D2 mutations is destabilizing. As a result, PlyC (PlyCA) N211H served as the final directed evolution lead candidate for further analysis.

Structural and Thermodynamic Stability of the Directed Evolution Lead Candidate

The structural and thermodynamic stability of both wild-type PlyC and PlyC (PlyCA) N211H were next investigated. CD thermal denaturation experiments revealed both wild-type PlyC and PlyC (PlyCA) N211H display a single PlyCA unfolding structural transition corresponding to a $T_{1/2}$ of 50.09°C and 51.61°C, respectively (Fig. 4-5a). These results dictate that the N211H point mutant improved the structural stability of PlyCA by 1.52°C. DSC analysis of each holoenzyme confirmed the findings from the CD experiments, with PlyCA N211H (T_G = 50.26°C, van't Hoff enthalpy of unfolding (ΔH_{VH}) = 199.25 kcal/mol) displaying a respective T_G and ΔH_{VH} increase of 1.99°C and 28.02 kcal/mol when compared to wild-type PlyCA (T_G = 48.27°C, ΔH_{VH} = 171.23 kcal/mol) (Fig. 4-5b). In addition to exhibiting intensified kinetic stability, results from two independent biophysical experimental approaches suggest that PlyC (PlyCA) N211H has enhanced structural and thermodynamic stability when compared to wild-type.

Protonated H211 Employs a Charge-Mediated Stabilizing Mechanism

While biochemical and biophysical experiments demonstrated that the N211H mutation improved PlyCA thermal stability, it is unknown how this particular point mutation is mechanistically accomplishing this enhanced stability phenotype.

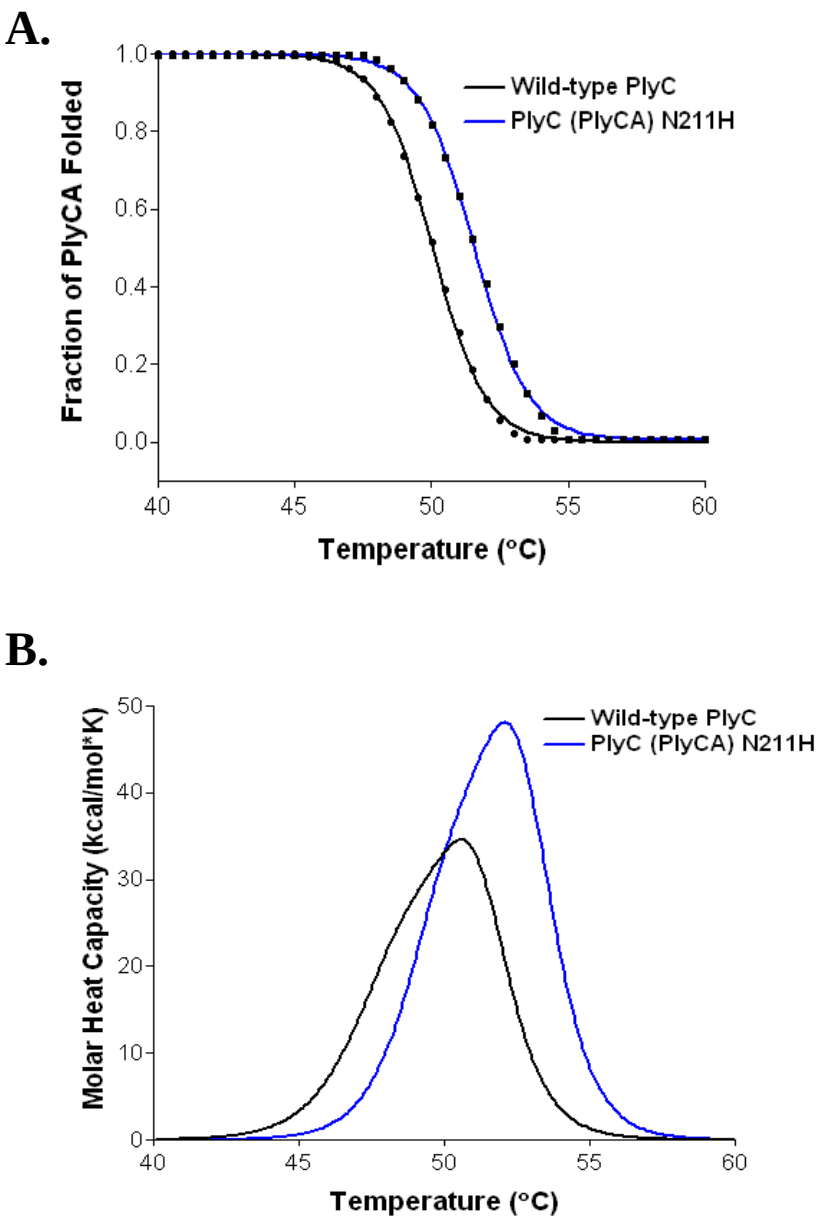

Figure 4-5. Biophysical thermal analysis of wild-type PlyC and PlyC (PlyCA) N211H. The structural and thermodynamic stability of both holoenzymes were characterized at equal molar concentrations by (a) CD thermal denaturation experiments or (b) DSC in 20 mM phosphate buffer, pH 7.0, using a heating rate of 1°C/min. The structural and thermal transitions depicted correspond to the unfolding of the PlyCA subunit.

Considering the mutation consisted of substituting an asparagine with a histidine, and hence, replacing a polar neutral amino acid with a polar basic amino acid, we hypothesized that the possible addition of the protonated side-chain of the histidine at this particular structural location within PlyCA could be increasing the stability of the subunit in a charge-mediated manner.

To first test this hypothesis, we performed a charge-dependent kinetic stability analysis focusing on residue 211 of PlyCA. The three mutants analyzed, PlyC (PlyCA) N211A (neutral charge), N211K (positive charge) and N211D (negative charge), were expressed and purified to homogeneity based on SDS-PAGE analysis (Fig. 4-3, lanes 7-9). The neutral charge mutant PlyC (PlyCA) N211A displayed a $t_{1/2}$ at 45°C that mimics the kinetic stability exhibited by wild-type (Fig. 4-6, Table 4-4). The positively charged mutant PlyC (PlyCA) N211K, which resembles the charge properties of the N211H point mutant, was kinetically stabilized 14.5 fold over wild-type. Reversing the charge of the residue 211 side-chain with the point mutation PlyC (PlyCA) N211D was significantly deleterious, decreasing the kinetic stability 2.5 fold when compared to wild-type. Therefore, replacing N211 with a positively charged basic amino acid at residue position 211, such as N211H and N211K, improves the overall kinetic fitness of the catalytic subunit at elevated temperatures in a charge-dependent fashion.

To further establish the charge-dependence for stability, we investigated the structural and thermodynamic stability of the various charge mutants. Results from CD thermal denaturation experiments of PlyC (PlyCA) N211A, N211K and N211D produced $\Delta T_{1/2}$ values of +0.01°C, +1.12°C and -3.99°C, respectively, when compared to the 50.09°C $T_{1/2}$ of wild-type PlyC (Fig. 4-7a, Table 4-5). DSC analysis of the three charge

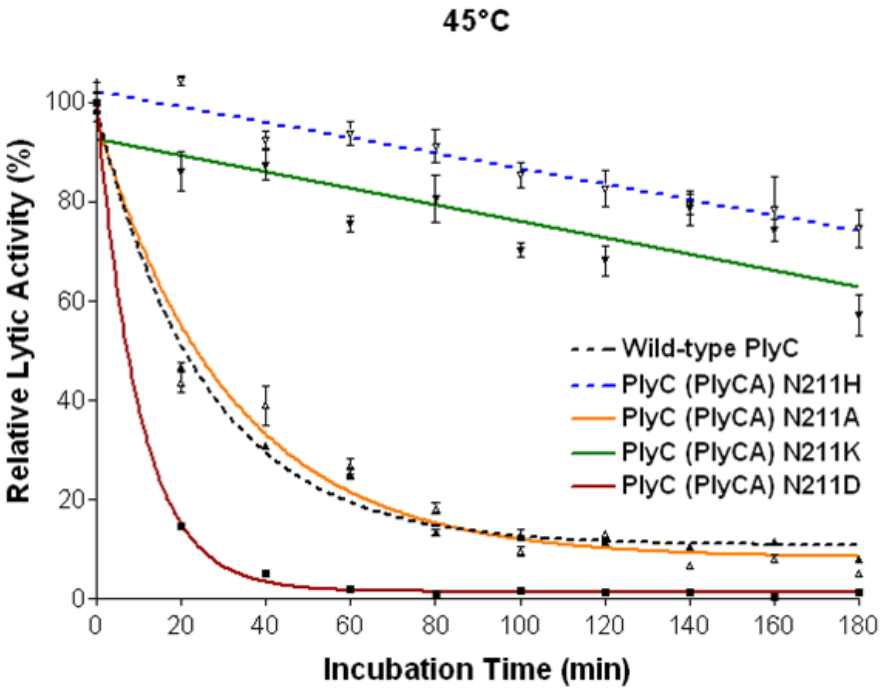

Figure 4-6. Kinetic half-life calculation for charge-specific PlyC (PlyCA) N211 mutants. The rate of kinetic inactivation at 45°C was elucidated for the mutants PlyC (PlyCA) N211A, N211K and N211D. The enzymes were incubated at equal molar concentrations in PBS, pH 7.2-7.3, with the residual lytic activity being analyzed every 20 min for a total of 3 h.

Table 4-4. Kinetic stability comparison at 45°C between the charge-specific N211 mutants.

PlyC Construct	$t_{1/2}$ (min)	Relative Kinetic Stability	R^2
Wild-type	17.84	1.0	0.99
N211H	**335.04**	**18.8**	**0.94**
N211A	21.96	1.2	0.96
N211K	**258.83**	**14.5**	**0.71**
N211D	7.03	0.4	0.99

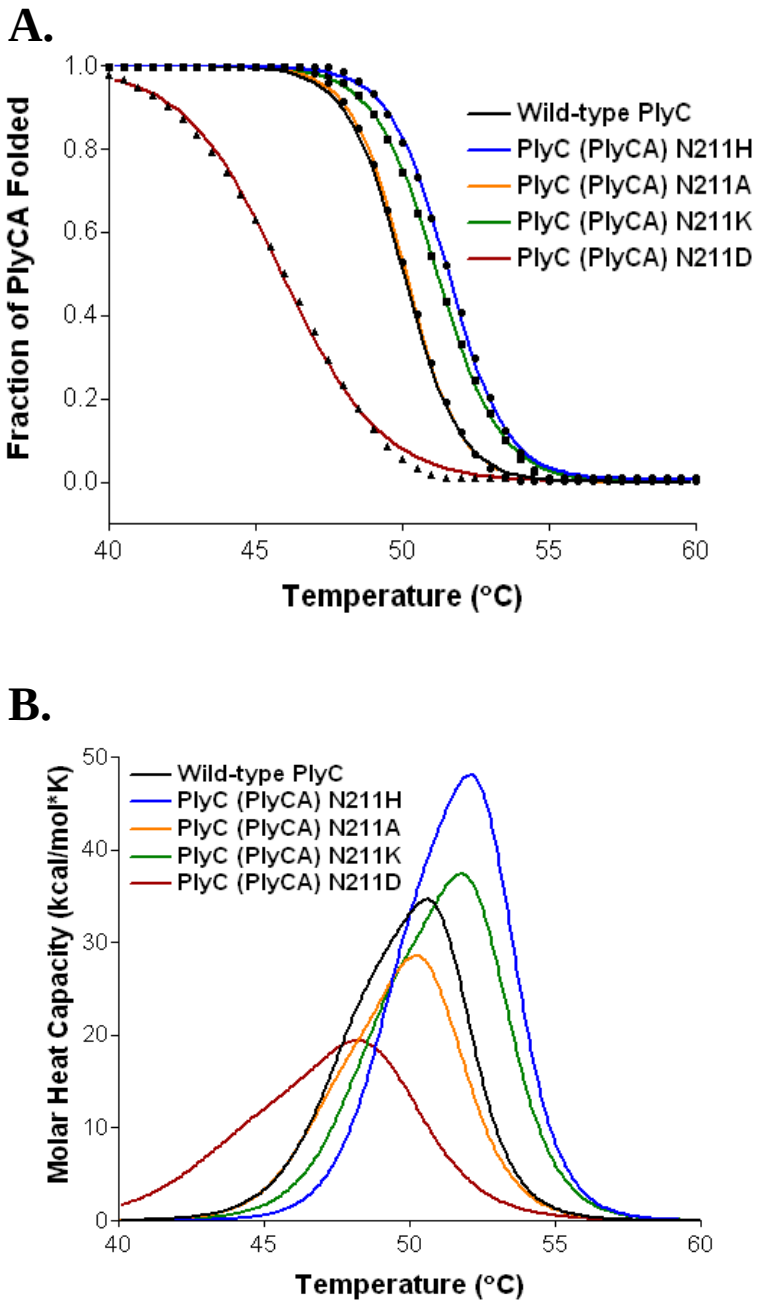

Figure 4-7. CD and DSC thermal analysis of charge-specific PlyC (PlyCA) N211 mutants. The structural and thermodynamic stability of PlyC (PlyCA) N211A, N211K and N211D were determined at equal molar concentrations by (a) CD thermal denaturation experiments or (b) DSC in 20 mM phosphate buffer, pH 7.0, using a heating rate of 1°C/min. The structural and thermal transitions depicted correspond to the unfolding of the PlyCA subunit.

Table 4-5. Thermal stability associated with the different N211 charge mutants of PlyCA as explicated by means of CD thermal denaturation experiments (columns 2 and 3) and DSC (columns 4-7). Data displayed correlates to the PlyCA subunit only.

PlyC	Circular Dichroism		Differential Scanning Calorimetry			
Construct	$T_{1/2}$ (°C)	$\Delta T_{1/2}$ (°C)	T_{G1} (°C)	T_{G2} (°C)	ΔH_{VH1} (kcal/mol)	ΔH_{VH2} (kcal/mol)
Wild-type	50.09	-----	48.27	50.67	171.23	205.09
N211H	51.61	+1.52	50.26	52.46	199.25	240.14
N211A	50.10	+0.01	47.78	50.45	186.38	205.45
N211K	51.21	+1.12	49.61	52.16	170.97	223.74
N211D	46.10	-3.99	45.19	48.63	117.22	161.61

mutants supports the findings of the CD thermal denaturation experiments. The thermally-induced PlyCA unfolding thermal transitions for PlyC (PlyCA) N211A, N211K and N211D consisted of a respective ΔT_G values of -0.49°C, +1.34°C and -3.08°C and a $\Delta(\Delta H_{VH})$ of +15.15 kcal/mol, -0.26 kcal/mol and -54.01 kcal/mol. (Fig. 4-7b, Table 4-5). Collectively, the CD and calorimetric results suggest that the increased structural and thermodynamic stability of PlyC (PlyCA) N211H is mediated through a charge-dependent mechanism.

Considering PlyC (PlyCA) N211H improves the stability of the enzyme due to the cationic properties of the protonated H211 side-chain, we hypothesized that altering the protonated state of this residue will have significant implications on stability. To address this hypothesis, we analyzed the structural and thermodynamic stability of both wild-type PlyC and PlyC (PlyCA) N211H in 20 mM phosphate buffer, pH 6.0-8.0. At pH 6.0, which represents the pH environment in our study where the mutated PlyCA N211H side-chain is at its most protonated state, CD thermal denaturation results showed that PlyCA N211H exhibits a $\Delta T_{1/2}$ of +3.45°C when compared to wild-type PlyC (Fig. 4-8a). Results from CD thermal denaturation experiments at pH 6.5, 7.0, 7.5 and 8.0 revealed that PlyC (PlyCA) N211H consisted of a respective $\Delta T_{1/2}$ of +3.28°C, +1.52°C, +0.19°C and +0.06°C. The same trend was observed after carrying out calorimetric experiments at pH 6.0-8.0. At pH 6.0, PlyC (PlyCA) N211H displayed a ΔT_{G1} and ΔH_{VH1} of +4.10°C +19.97 kcal/mol and a ΔT_{G2} and ΔH_{VH2} of +4.44°C and +29.58 kcal/mol over wild-type (Fig. 4-8b and c). When compared to the T_G values of wild-type PlyCA at pH 6.5, 7.0, 7.5 and 8.0, the PlyCA N211H ΔT_{G1} is +3.20°C, +1.99°C, +0.48°C and +0.21°C, while the ΔT_{G2} is +2.97°C, +1.79°C, +0.33°C and 0.17°C, respectively. Therefore, the stability of

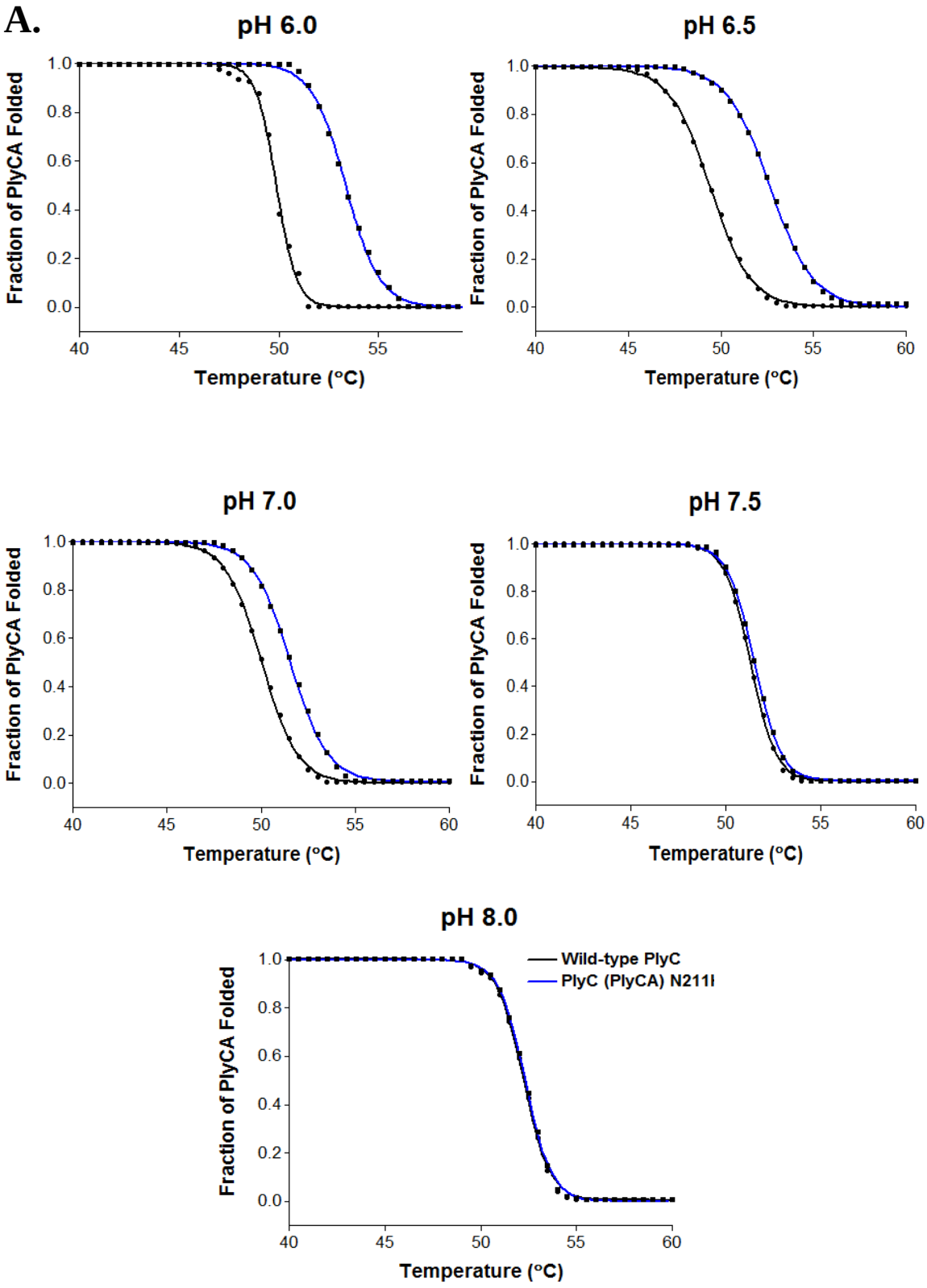
A.
pH 6.0
pH 6.5
pH 7.0
pH 7.5
pH 8.0
Fraction of PlyCA Folded
Temperature (°C)
Wild-type PlyC
PlyC (PlyCA) N211I

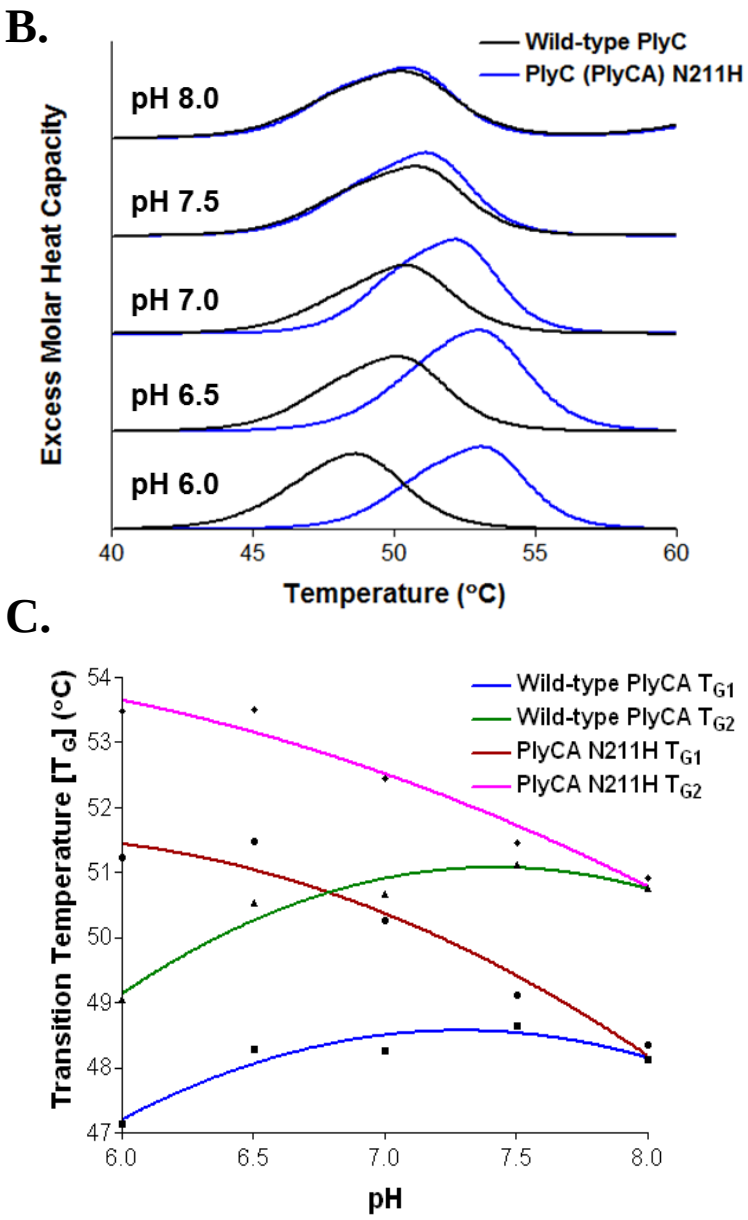

Figure 4-8. pH-dependent thermal stability of wild-type PlyC and PlyC (PlyCA) N211H. The stability of the two endolysins was investigated as a function of pH using biophysical thermal analysis. Equal molar concentrations of the enzymes were heated at a 1°C/min rate in 20 mM phosphate buffer, pH 6.0-8.0. The resulting (a) CD thermal denaturation data, (b) overlaid DSC thermograms and (c) T_G vs pH plots specific to the unfolding of PlyCA are shown.

PlyC (PlyCA) N211H increasingly mimics that of wild-type as you increase the pH of the system as a direct result of transitioning the H211 side-chain from a positive to neutral charged state.

H211 Electrostatically Interacts with E113 and D150 of the GyH Domain

Experimental results suggest the protonated H211 side-chain of the PlyC (PlyCA) N211H mutant is stabilizing the catalytic subunit, but it remains elusive how the positive charge at this particular location within the structure is stabilizing. One possibility is H211, which is located at the beginning of the flexible linker structure that interconnects the N-terminal GyH domain to the central helical docking domain (Fig. 4-9a and b), is forming a favorable electrostatic interaction with another localized amino acid residue. With this in mind, three acidic amino acids (E113, D150 and D208) within a 10-15 Å radius of H211 were identified as potential electrostatic interaction partners (Fig. 4-9c).

To determine if E113, D150 or D208 forms a stabilizing charge-mediated interaction with H211 of PlyCA, a mutational CD and DSC thermal analysis was undertaken. The PlyC (PlyCA) E113A, D150A and D208A point mutants in a ± N211H background were expressed and purified to homogeneity based on SEC (data not shown) and SDS-PAGE analysis (Fig. 4-10, lanes 1-6). The CD and DSC heating experiments consisted of two steps. The first step involves analyzing the thermal stability of PlyC (PlyCA) E113A, D150A and D208A. The next step consisted of inserting the N211H mutation into a PlyC (PlyCA) E113A, D150A or D208A background to determine whether the N211H could provoke the same augmentation in structural and thermodynamic stability observed when all three acidic residues were present. Results

A.

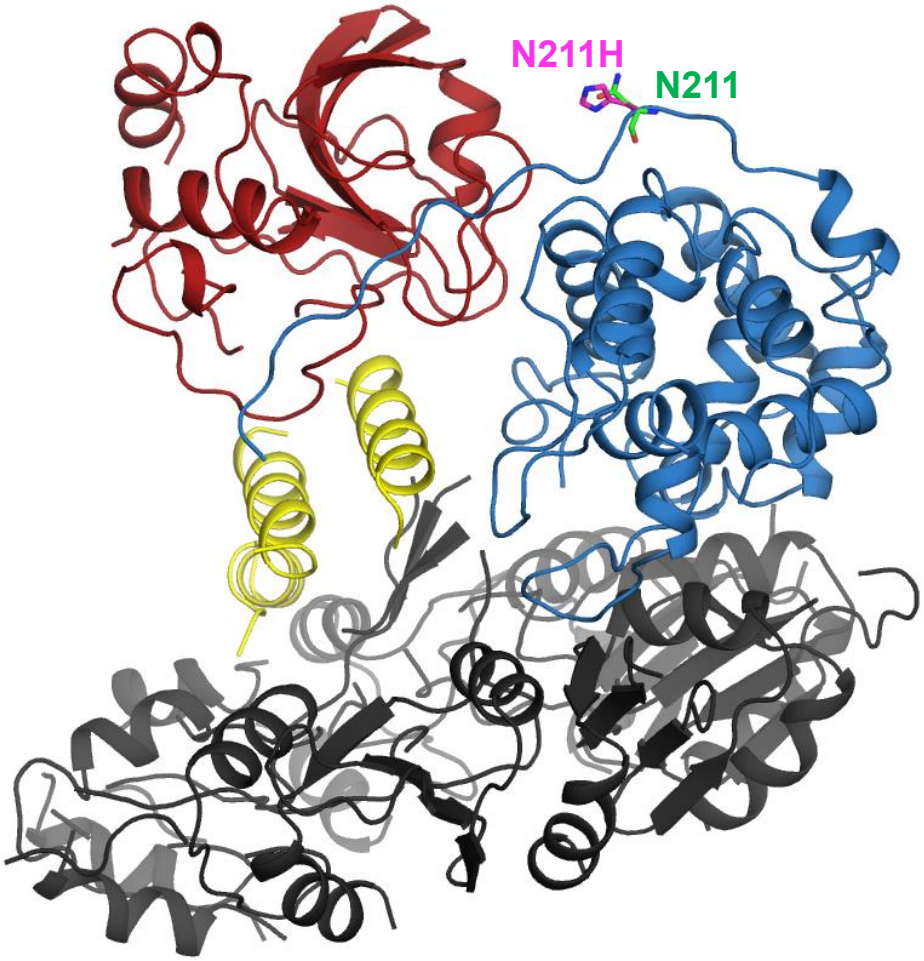

GyH Domain
Helical Docking Domain
CHAP Domain

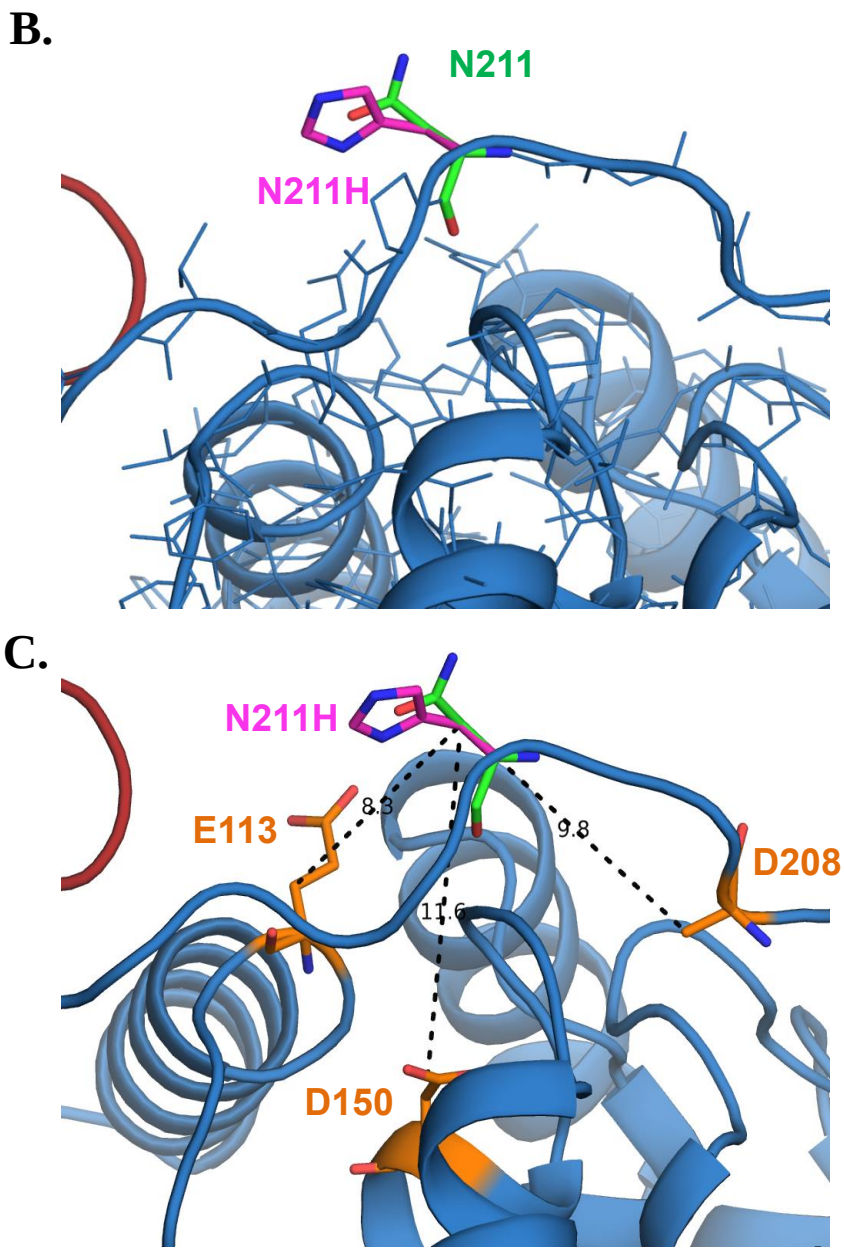

Figure 4-9. Modeling H211 into the 3.3-Å crystal structure of PlyC. The PlyC holoenzyme structure consists of eight identical PlyCB monomers that interact to form the octomeric CBD structure (a, gray). The N-terminal GyH domain (blue) of the PlyCA subunit is linked to a central helical docking domain (a, yellow). The carboxyl end of the central helical docking domain is linked to the C-terminal CHAP domain (red). The H211

residue (pink sticks) was modeled into the PlyCA subunit and was shown superimposed with the endogenous N211 residue (green sticks). The superimposed H211 residue is shown (a) macroscopically with the holoenzyme viewable or (b) zoomed-in on the N-terminal region of PlyCA. The hypothesized β-carbon side-chain distance between H211 and the three nearby acidic residues in the GyH domain that are hypothesized to electrostatically interact are illustrated (orange sticks).

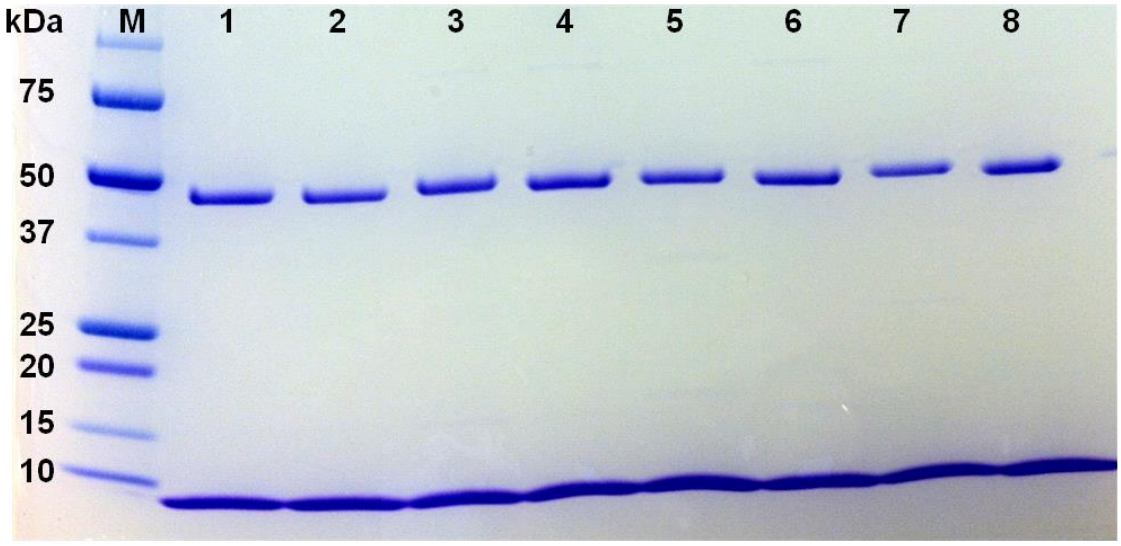

Figure 4-10. SDS-PAGE analysis of the putative H211 electrostatic interaction mutants. The solubility and purity of each of the construct was analyzed on a 4-15% gradient SDS-PAGE gel. The various lanes correlate to: (M) Molecular weight standard, (1) PlyC (PlyCA) E113A, (2) E113A N211H, (3) D150A, (4) D150A N211H, (5) D208A, (6) D208A N211H, (7) E113A D150A and (8) E113A D150A N211H.

from CD thermal denaturation experiments showed that PlyC (PlyCA) E113A, D150A and D208A displayed PlyCA $T_{1/2}$ values of 49.34°C, 50.76°C and 50.91°C, respectively (Fig. 4-11a, b and c). When the N211H mutation was added to these three mutants, PlyCA was stabilized by 0.92°C, 0.80°C and 1.31°C, respectively (Fig. 4-11a, b and c). A similar trend was observed when using DSC to analyze the thermodynamic stability of the aforementioned mutants. Adding N211H to PlyC (PlyCA) E113A, D150A or D208A increased the respective T_G values of PlyCA by 0.60°C, 0.39°C and 1.86°C. With PlyC (PlyCA) N211H displaying improvements in PlyCA $T_{1/2}$ and T_G of 1.52°C and 1.99°C over wild-type PlyC, mutating the D208 residue had little effect on the stabilizing potential of H211. Alternatively, while H211 could still improve the stability of PlyCA in an E113A or D150A background, the absence of either acidic residue significantly impeded the full stabilizing potential of H211.

Collectively, results from the thermal analysis imply that while E113, D150 and D208 all seem to electrostatically interact with H211, the PlyCA subunit is mainly stabilized by the simultaneous additive electrostatic interactions formed between E113-H211 and D150-H211. To determine if this is true, the effect of H211 on PlyCA stability was evaluated in an E113A D150A background. The double mutant PlyC (PlyCA) E113A D150A and triple mutant PlyC (PlyCA) E113A D150A N211H were expressed and purified to homogeneity based on SDS-PAGE analysis (Fig. 4-10, lanes 7-8). Elucidating the structural stability of PlyC (PlyCA) E113A D150A and E113A D150A N211H by CD thermal denaturation experiments revealed both constructs encompass comparable PlyCA $T_{1/2}$ values of 50.72°C and 50.69°C, respectively (Fig. 4-11d). DSC experiments validated the CD results, with PlyC (PlyCA) E113A D150A and PlyC

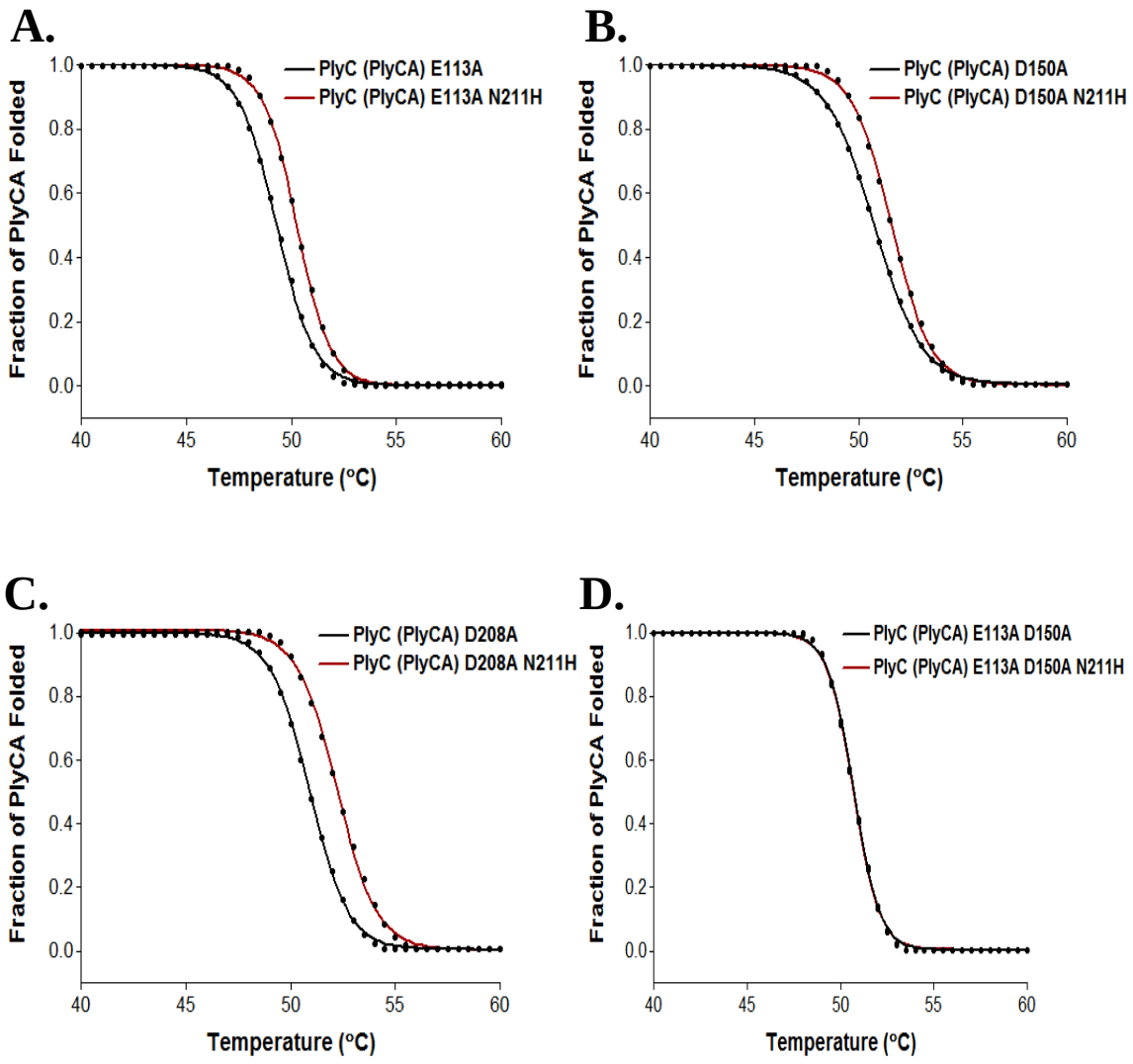

Figure 4-11. Structural stability determination for the acidic amino acid candidate mutants in a ± N211H background. CD thermal denaturation experiments were conducted to determine the structural stability of (a) PlyC (PlyCA) E113A, (b) D150A, (c) D208A and (d) E113A D150A in a ± N211H background. All experiments were performed at equal molar concentrations in 20 mM phosphate buffer, pH 7.0, using a heating rate of 1°C/min. The structural transitions correspond to the unfolding of the PlyCA subunit.

(PlyCA) E113A D150A N211H exhibiting a near identical PlyCA T_G of 47.52°C and 47.59°C, respectively. Therefore, without the presence of both E113 and D150, the H211 has no effect on the structural or thermodynamic stability of PlyCA.

Bacteriolytic Activity Comparison Between Wild-type PlyC and PlyC (PlyCA) N211H

An inverse relationship between activity and stability is commonly observed when engineering progressed thermal stability to macromolecules, especially at reduced temperatures. The activity displayed by thermophilic enzymes at lower temperatures is regularly compromised when compared to their psychrophilic or mesophilic homologs (Giver et al., 1998; Meiering et al., 1992; Shoichet et al., 1995; Somero, 1975). To overcome an unwanted activity-stability trade-off, the screening component of the directed evolution protocol was designed to identify kinetically stabilized bacteriolytic enzyme variants that retain their original catalytic efficiency.

To confirm the bacteriolytic activity of the thermostabilized PlyC (PlyCA) N211H mutant was comparable to that of wild-type, serial dilutions of each enzyme were prepared and measured for lytic activity against *S. pyogenes* by means of turbidity reduction assay (Fig. 4-12). The time (s) to decrease the OD_{max} by 50% for each enzyme at the various molar concentrations tested were nearly identical, correlating to lytic activities of 45350 and 51950 U/ml for wild-type PlyC and PlyC (PlyCA) N211H, respectively. The introduction of the N211H mutation to PlyCA did not result in any loss in enzymatic activity while simultaneously stabilizing the enzyme.

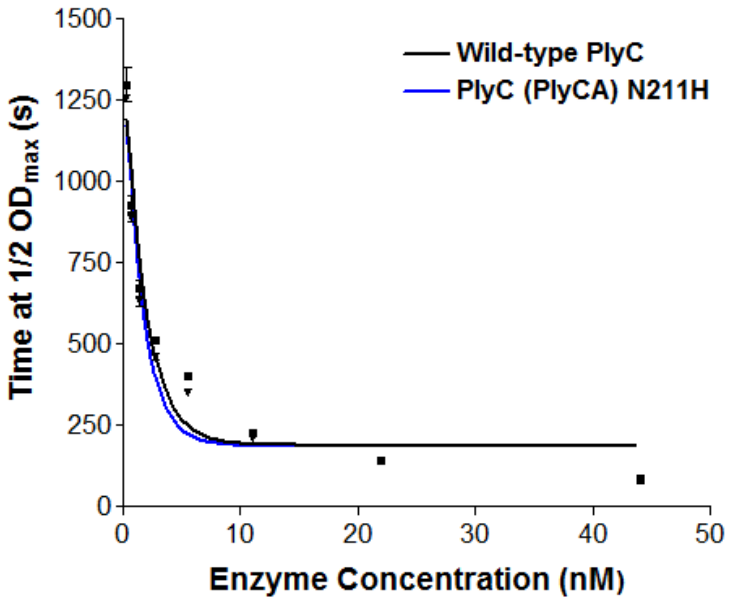

Figure 4-12. Bacteriolytic activity evaluation against *S.pyogenes in vitro*. The lytic activity of wild-type PlyC and PlyC (PlyCA) N211H against *S. pyogenes* D471 in PBS, pH 7.2-7.3, was compared by means of turbidity reduction assay. The time (s) at which the OD_{max} was reduced by 50% was plotted against the corresponding enzyme concentration (nM) to formulate the lytic activity of the enzyme (U/ml).

Combining Beneficial Mutations from Different Engineering Approaches is Additively Thermostabilizing

Previously we reported results from a computational-based bioengineering study where we utilized the FoldX and Rosetta protein folding algorithms to successfully improve the thermal stability of PlyC (Chapter II). The identified CHAP domain point mutant T406R thermostabilized the PlyCA subunit by ≥ 2.2°C in 20 mM sodium phosphate buffer, pH 7.0, translating to a 21.45 kcal/mol improvement in ΔH_{VH}, an 11 kcal/mol progression in the E_A of PlyCA unfolding and a 16 fold decrease in kinetic inactivation at 45°C. H211 and its hypothesized electrostatic interaction partners, E113 and D150, are located independently within PlyCA when compared to R406 and its predicted inter-domain hydrogen bonding partner Q106 (Fig. 4-13). With this in mind, we next investigated whether combining PlyC (PlyCA) N211H and PlyC (PlyCA) T406R could have additive ramifications on the thermal stability of PlyC.

Wild-type PlyC, PlyC (PlyCA) N211H and PlyC (PlyCA) N211H T406R were expressed and purified to homogeneity based on SDS-PAGE analysis (Fig. 4-14a). The thermodynamic stability of the three enzymes was analyzed at equal molar concentrations by DSC in 20 mM sodium phosphate buffer, pH 6.0. As described previously, the N211H mutant improved the respective T_G and ΔH_{VH} values by 4.1°C and 19.97 kcal/mol at pH 6.0 when compared to wild-type (Fig. 4-8 and 4-14b, Table 4-6). Combining the N211H and T406R mutations had additive effects with respect to the thermodynamic stability of the enzyme, enhancing the T_G and ΔH_{VH} of the double mutant by 7.46°C and 22.60 kcal/mol when compared to wild-type, respectively (Fig. 4-14b). The double mutant also exhibited a 3.36°C and 2.63 kcal/mol improvement over PlyC (PlyCA) N211H.

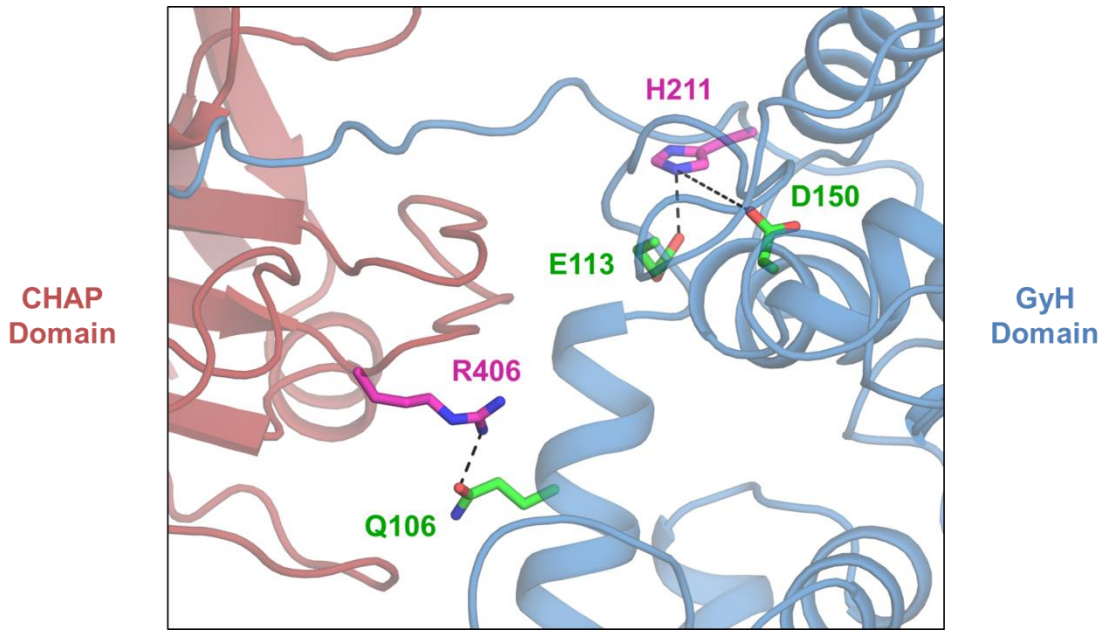

Figure 4-13. Modeling H211 and R406 into the PlyCA subunit. The H211 residue (pink sticks, top) was modeled into the linker structure stemming from the GyH domain (blue), with the proposed electrostatic interactions with E113 and D150 (green sticks, top) depicted. The R406 residue (pink sticks, bottom) was modeled onto the surface of the CHAP domain (red), with the hypothesized inter-domain hydrogen bond with Q106 (green sticks, bottom) of the GyH domain shown.

A.

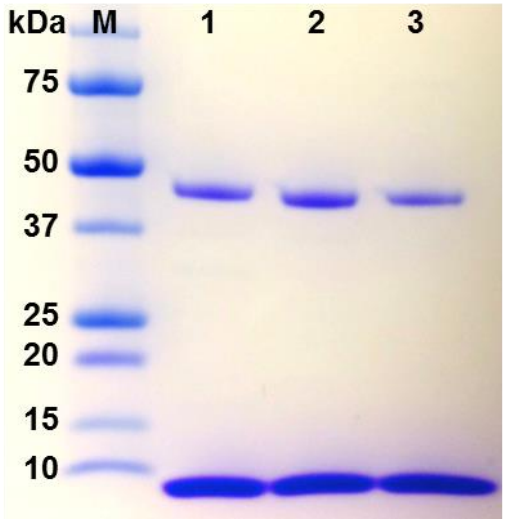
kDa
M
1
2
3
75
50
37
25
20
15
10

B.

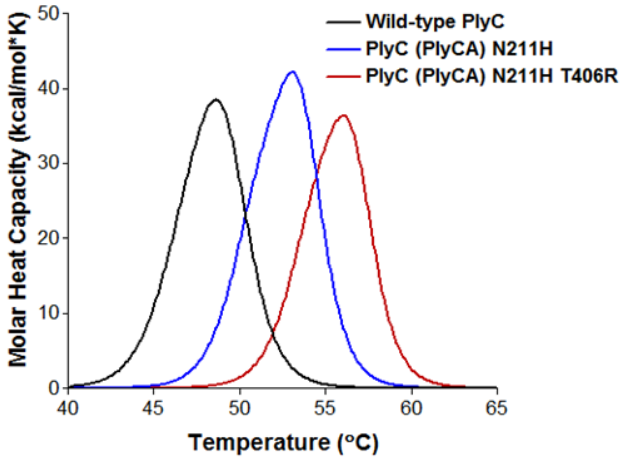
Wild-type PlyC
PlyC (PlyCA) N211H
PlyC (PlyCA) N211H T406R
Molar Heat Capacity (kcal/mol*K)
Temperature (°C)

C.

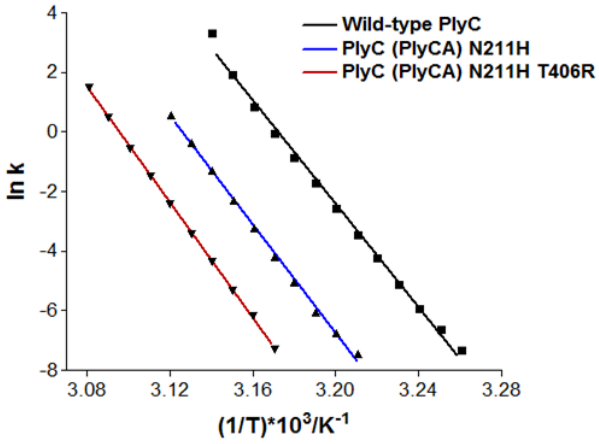
Wild-type PlyC
PlyC (PlyCA) N211H
PlyC (PlyCA) N211H T406R
ln k
(1/T)*10³/K⁻¹

Figure 4-14. Thermodynamic and kinetic stability of PlyC (PlyCA) N211H T406R. The solubility and purity of wild-type PlyC (a, lane 1), PlyC (PlyCA) N211H (a, lane 2) and N211H T406R (a, lane 3) were analyzed on a 4-15% gradient SDS-PAGE gel. The thermodynamic stability of wild-type PlyC (b, black trace), PlyC (PlyCA) N211H (b, blue trace) and N211H T406R (b, red trace) was dissected by DSC in 20 mM phosphate buffer, pH 6.0, using a heating rate of 1°C/min. The unfolding of the PlyCA subunit is shown. Using the PlyCA calorimetric data, the rate constant (*k*) for was calculated for the various samples and the ln k was then plotted against the inverse of the temperature ($(1/T)*10^3/K^{-1}$) to generate Arrhenius plots for elucidating PlyCA E_A values of unfolding. The Arrhenius plot for the catalytic subunits for wild-type PlyC (c, black), PlyC (PlyCa) N211H (c, blue) and N211H T406R (c, red) are shown.

Table 4-6. Calorimetric (columns 2-5) and kinetic (columns 6 and 7) stability analysis of PlyC (PlyCA) N211H T406R. Data displayed correlates to the PlyCA subunit only.

PlyC Construct	T_{G1} (°C)	T_{G2} (°C)	ΔH_{VH1} (kcal/mol)	ΔH_{VH2} (kcal/mol)	E_A (kcal/mol)	R^2
Wild-type	47.14	49.05	165.11	201.16	162.93	0.99
N211H	51.24	53.49	185.08	230.74	180.45	0.99
N211H T406R	54.60	56.57	187.71	242.82	191.65	0.99

Next, the unfolding kinetics of PlyCA were elucidated by constructing Arrhenius plots using the PlyCA calorimetric data from wild-type PlyC, PlyC (PlyCA) N211H and PlyC (PlyCA) N211H T406R. The natural log of the rate constant, k, was plotted against the inverse of the temperature to determine the E_A of PlyCA unfolding. When compared to wild-type PlyC at pH 6.0, the N211H mutation increased the E_A of PlyCA unfolding by 17.52 kcal/mol (Fig. 4-14c, Table 4-6). The N211H T406R double mutant had additive implications on the kinetic fitness of the holoenzyme, improving the respective E_A of PlyCA unfolding by 28.72 kcal/mol and 11.20 kcal/mol over wild-type and PlyC (PlyCA) N211H.

Discussion

Meager inherent thermal stability appears to be a common characteristic associated with endolysins derived from mesophilic bacteriophage (Bustamante et al., 2012; Filatova et al., 2010; Sanz et al., 1993; Varea et al., 2004). With a long-term goal of developing these enzymes as a translational antimicrobial for industrial application, the Arrhenius equation advocates the poor structural stability of endolysins correlates to transient shelf life expectancy, thereby impeding the feasibility of furthering the development of the antimicrobial (Anderson and Scott, 1991). Despite exhibiting a highly robust bacteriolytic mechanism and being validated *in vitro* and *in vivo* against a variety of streptococcal species known to generate both human and animal health complications (Hoopes et al., 2009; Nelson et al., 2001; Nelson et al., 2006a), the thermolabile structure of the streptococcal endolysin PlyC hinders its antimicrobial potential due to the 48.27°C T_G comprised by the EAD of the enzyme.

The lead candidate at the summation of directed evolution screening was the point mutant PlyC (PlyCA) N211H. The H211 residue is located at the beginning of the linker structure that interconnects the N-terminal GyH domain to the central helical docking domain (Fig. 4-9a and b). This mutation increased the kinetic stability of the enzyme 18.8 fold at 45°C in PBS, pH 7.2-7.3 (Fig. 4-4b), and improved the T_G by 4.10°C and the E_A of PlyCA unfolding by 17.52 kcal/mol in 20 mM phosphate buffer, pH 6.0 (Fig. 4-8b and c, Fig. 4-14c). Moreover, the PlyC (PlyCA) N211H mutant did not manifest any reduction in bacteriolytic activity when compared to wild-type PlyC (Fig. 4-12). This was an important finding because there is typically a significant trade-off between enzymatic activity and thermal stability when thermostabilizing proteins (Arnold et al., 2001; Beadle and Shoichet, 2002; Giver et al., 1998; Meiering et al., 1992; Mukaiyama et al., 2006; Yutani et al., 1987).

Based on side-chain distance estimations, there were three initial acidic amino acid candidates (E113, D150 and D208) that could feasibly interact electrostatically with the protonated H211 side-chain. While other electrostatic interactions with H211 could be stabilizing, such as alpha helical dipole, solvation and van der Waals interactions, we simplistically hypothesized for these experiments that an electrostatic attraction between H211 and a nearby anionic acidic residue could be the primary molecular interaction responsible for the improved thermal stability of the directed evolution lead candidate. The similar $\Delta T_{1/2}$ values depicted by PlyC (PlyCA) N211H (when compared to wild-type) (Fig. 4-5a) and PlyC (PlyCA) D208A N211H (when compared to PlyC (PlyCA) D208A) (Fig. 4-11c) ultimately eradicated D208 as a primary stabilizing electrostatic partner for H211. Nonetheless, it is probable D208 and N211H electrostatically interact

with each other; however most significant stabilization effects are greatest when the two interacting residues are distant in sequence. If D208 and N211H are indeed interacting, the close sequence proximity of the two would have little effect on the global stability of the PlyCA subunit. Adding N211H to a PlyC (PlyCA) E113A or D150A background only partially restored the $\Delta T_{1/2}$ value exhibited by PlyC (PlyCA) N211H over wild-type (Fig. 4-5a, 4-11a and b). When both E113 and D150 were simultaneously mutated, H211 had no effect on the structural (Fig. 4-11d) or thermodynamic stability (data not shown) when added to a PlyC (PlyCA) E113A D150A background. This finding infers both E113 and D150 electrostatically interact with H211 to considerably intensify the thermal stability of PlyCA in an additive manner. The electrostatic fields formed between the cationic H211 and the anionic E113 and D150 residues most likely anchored a segment of the linker to the surface of the GyH domain. As a result, the enthalpic gains associated with this molecular reorganization could account for the improvement in thermal stability.

While the formation of an electrostatic field between E113-H211 and D150-H211 seems to be the likely mechanism of stabilization, the possibility of a salt-bridge interaction between either E113-N211H or D150-N211H cannot be completely ruled out. Although the estimated distance between E113-N211H and D150-N211H are comparable, a salt-bridge interaction between D150-N211H is improbable because D150 is not as flexible as E113 and appears to have an unfavorable structural conformation. Conversely, E113 could possibly form a salt-bridge given the normal torsional freedom of the E113 and H211 side-chains.

Combining the mutation comprised by the directed evolution lead candidate, N211H, with the mutation derived from the lead candidate from a previous rationale-based *in silico* screen (Chapter II), T406R, had additive effects on the thermal stability of the enzyme (Fig. 4-13 and 4-14, Table 4-7). While the N211H mutation appears to improve the stability of PlyCA by promoting favorable electrostatic interactions in the N-terminal region of the subunit, the C-terminal CHAP domain T406R mutation was hypothesized to stabilize PlyCA through the formation of an inter-domain hydrogen bond with Q106 of the N-terminal GyH domain (Chapter II). The PlyC (PlyCA) N211H T406R double mutant featured T_G, ΔH_{VH} and PlyCA unfolding E_A improvements over wild-type PlyC and PlyC (PlyCA) N211H of 7.46°C, 22.60 kcal/mol, 28.72 kcal/mol, and 3.36°C, 2.63 kcal/mol, 11.20 kcal/mol at pH 6.0, respectively. This finding was not unexpected because the different stabilizing mechanisms employed by H211 and R406 would be seemingly unaffected when both mutations were simultaneously present due to the independent locations and unique interaction partners associated with the two mutations.

Using the PlyC X-ray crystal structure as a guide (McGowan et al., 2012), future rationale-based engineering efforts could be implemented to further stabilize PlyCA. Seeing as H211 possibly improved the thermal fitness of PlyCA through electrostatic interactions with E113 and D150, these charge-based interactions can be substituted with a stronger, more enthalpically favorable covalent interaction. An inter-domain covalent bond could also be engineered to replace the hypothesized stabilizing hydrogen bond formed between Q106 of the GyH domain and R406 of the CHAP domain. Alternative thermostabilization strategies include rigidifying PlyCA turn and loop structures through

glycine → alanine or Xxx → proline mutations, inserting intra-domain disulfide bonds and salt-bridges, "helix capping" by introducing amino acids that interact with the alpha-helix dipole, replacing residues in left-handed helical structures with glycine or asparagines, or engineering clusters of aromatic-aromatic interactions (Anderson et al., 1993; Burley and Petsko, 1985; Clarke and Fersht, 1993; Kawamura et al., 1996; Kimura et al., 1992; Makhatadze et al., 2003; Mansfeld et al., 1997; Marshall et al., 2002; Matsumura et al., 1989; Matthews et al., 1987; Nicholson et al., 1991; Nicholson et al., 1988; Pace et al., 2000; Puchkaev et al., 2003; Sali et al., 1988; Schwehm et al., 2003; Serrano et al., 1991; Serrano and Fersht, 1989; Serrano et al., 1990; Strop and Mayo, 2000; Sun et al., 1991; Waldburger et al., 1995).

Acknowledgements

We would like to thank D. Travis Gallagher for constructing the PlyC structure images. We are also grateful to the National Institute of Standards and Technology for allowing us to use their differential scanning calorimeter.

Author contributions: R.H and D.N. conceived the experiments; R.H performed the biological, biochemical and biophysical experiments and analyzed the data; D.N. planned and supervised the project. R.H. wrote the article.

Funding: This work was supported by grants from the United States Department of Defense (DM102823) and the Maryland Agriculture Experiment Station.

Chapter V

Discussion and Future Directions

Discussion

The CDC conservatively estimates that antibiotic-resistant bacteria annually cause at least 2 million illnesses and 23,000 deaths domestically, with combined national economic ramifications totaling $55 billion (Roberts et al., 2009). The morbidity and mortality affiliated with these microorganisms will increase as drug-resistance continuously becomes more prevalent. In addition to the persistent loss in antimicrobial efficacy, antibiotic use has instigated illnesses and deaths associated with a number of opportunistic pathogens. For instance, the nonspecific killing of commensal bacteria that comprise the colonic microflora by broad spectrum antibiotics has directly aided to the pathogenicity of *C. difficile*, a microorganism that causes 250,000 illnesses and 14,000 deaths annually in the United States. Consequently, the CDC has assigned *C. difficile* as an urgent threat to human health.

Endolysins derived from lytic phage have been shown experimentally to be suitable alternative chemotherapeutics to classical antibiotics. The antimicrobial efficacy of these enzymes have been demonstrated *in vitro* and/or *in vivo* against a variety of Gram-positive pathogens (e.g. *L. monocytogenes, S. aureus, S. pneumoniae, S. pyogenes, B. anthracis*, etc.) known to cause serious health complications and economic distress. The uses of endolysins have been implicated for a variety of applications, including medicine, food safety and agriculture. Unlike antibiotics, resistance to these translational antimicrobials has not been documented to date, thereby rendering both antibiotic-

sensitive and –resistant bacterial species susceptible to these enzymes. Moreover, the high specificity of the CBD modules of endolysins allows them to be utilized in antimicrobial strategies that only target pathogenic bacteria of interest. This prevents toxicity issues that arise from indirect harming of the commensal microflora and eukaryotic cells and hence removes the possibility of obtaining antimicrobial-induced secondary infections.

As antibiotic resistance becomes more widespread, the pressure to transition endolysins from discovery to the developmental phase will to continue to expand in parallel. An assortment of engineering techniques explicit to optimizing the therapeutic potential of these enzymes has been described in the literature. Rationale-based engineering techniques, such as chimeragenesis (Croux et al., 1993b; Diaz et al., 1990) and structure-guided SDM (Low et al., 2011; Resch et al., 2011b), and random techniques, like directed evolution (Cheng and Fischetti, 2007), have been demonstrated to effectively enhance the catalytic kinetics and/or alter lytic specificity and biochemical characteristics (pH-, salt- and divalent cation-dependence) of endolysin EADs. Importantly, constructing chimeric endolysins with multiple EADs encompassing different peptidoglycan cut site specificities is an engineering strategy currently being employed to reduce the risk of bacterial resistance formation. Endolysin CBDs are also being subjected to chimeragenesis (Croux et al., 1993a; Diaz et al., 1991; Donovan et al., 2006a; Schmelcher et al., 2011) and structure-guided SDM (Diez-Martinez et al., 2013) for the purpose of improving binding kinetics and modifying endolysin catalysis and selectivity for therapeutic and diagnostic applications.

Besides properties attributable to the catalysis and binding of these enzymes, structural thermal stability is another characteristic associated with endolysins that is critical to their antimicrobial potential and development. In correspondence with the Arrhenius equation, which relates the rate of a chemical reaction to activation energy and temperature, the stability of a macromolecule directly equates to shelf life (Anderson and Scott, 1991). Elucidating the thermal properties of several Gram-positive endolysins derived from mesophilic phages revealed these enzymes appear to be relatively unstable and thus possess transient shelf life expectancies (Bustamante et al., 2012; Filatova et al., 2010; Sanz et al., 1993; Varea et al., 2004). While the intrinsic thermolability is an obvious trend for the several endolysins that have been thermally characterized, this list is far from extensive and thus currently assigning instability as a universal property to all endolysins would not be statistically justified. Furthermore, there are examples of Gram-positive endolysins derived from mesophilic phage that are thermodynamically and/or kinetically stable. For example, heating experiments involving four different *Listeria* endolysins revealed that several of these enzymes were kinetically thermoresistant (Fig. 5-1). Three of the four endolysins exhibited > 50% residual lytic activity after 50°C incubation (HPL118, HPL500 and HPL511; Fig. 5-1a, b and c) and remained catalytically active after incubating at 90°C (HPL118, HPL511 and HPLP35; Fig. 5-1a, b and d). In a set of experiments specific to elucidating the thermal characteristics of the *B. anthracis* endolysin PlyG, thermodynamic analysis of PlyG by means of DSC showed the enzyme irreversibly unfolds to fit a three-state thermal transition model, with a thermostable T_G of 63.53°C (Fig. 5-2a). In addition, heating PlyG for 10 minutes in pH 6.0 buffer resulted in the endolysin retaining ≥ 50% activity at temperatures ≤ 70°C, as

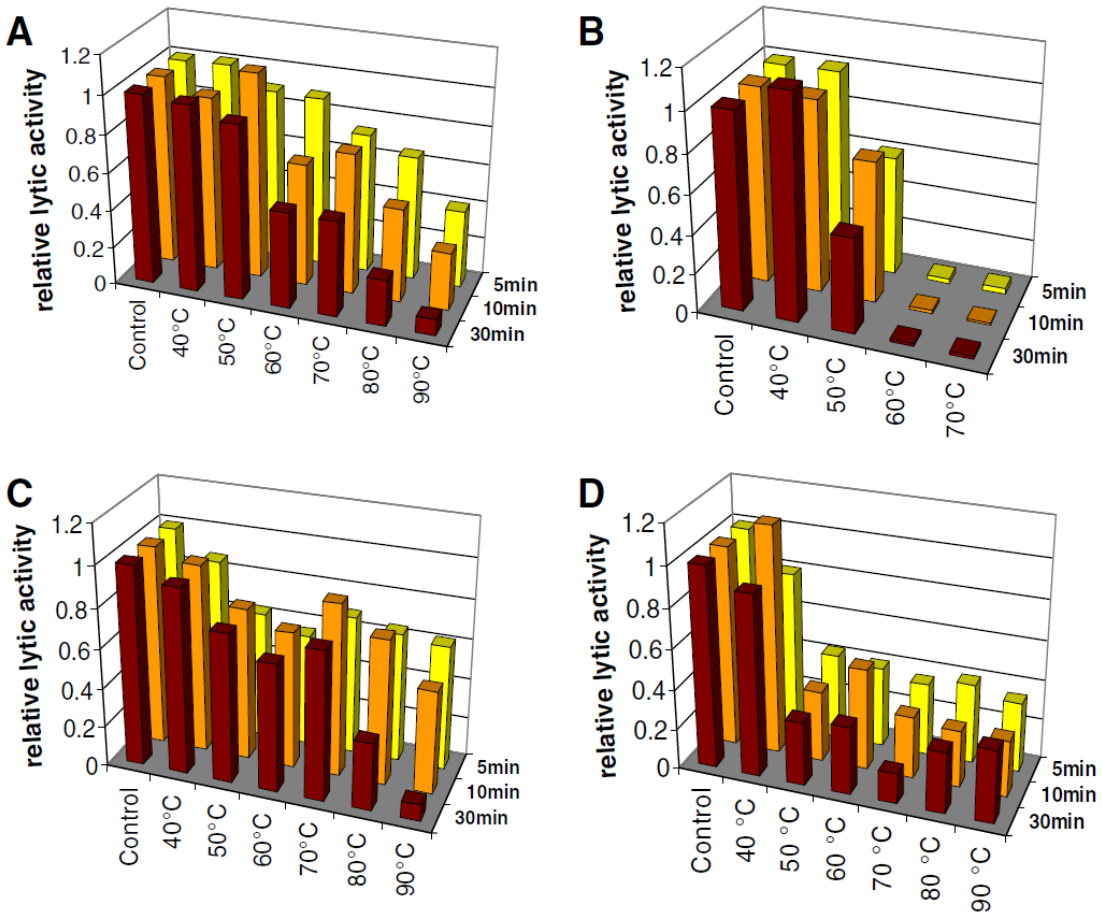

Figure 5-1. Kinetic stability of different *Listeria* endolysins. *L. monocytogenes* endolysins (a) HPL118, (b) HPL500, (c) HPL511 and (d) HPLP35 were incubated at different temperatures for 5, 10 or 30 minutes, cooled on ice and then assayed for residual activity by means of turbidity reduction assays. Lytic activity values are expressed relative to the control (non-heat treated enzyme). (Source: Schmelcher et al., 2012c)

A.

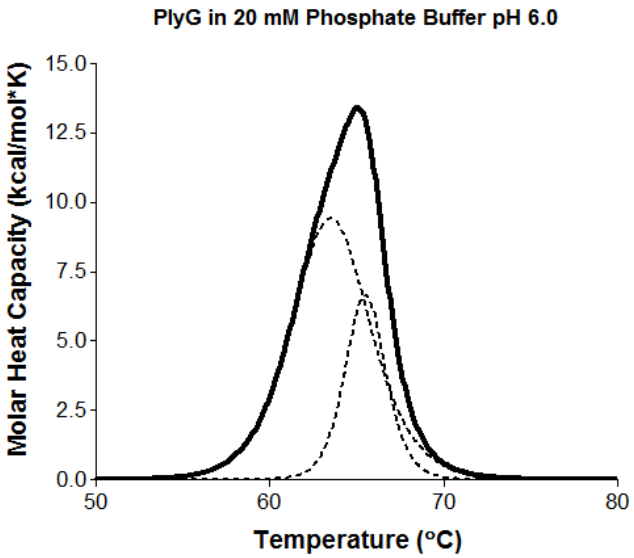

B.

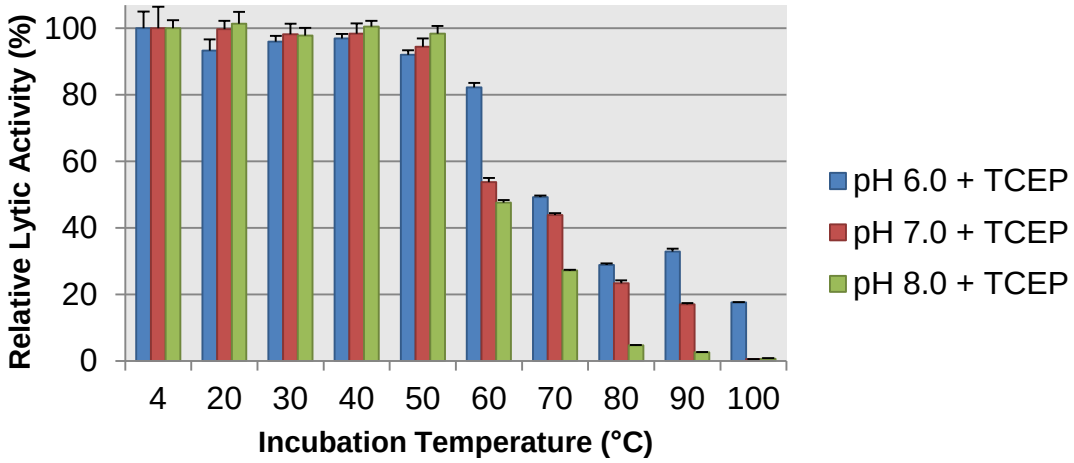

Figure 5-2. Thermodynamic and kinetic stability of *B. anthracis* endolysin PlyG. (a) The thermodynamics of PlyG were investigated using DSC. The enzyme at 0.5 mg/ml was heated in 20 mM sodium phosphate buffer pH 6.0 from 15°C to 105°C at 1°C/min. (b) PlyG in 50 mM sodium phosphate buffer pH 6.0-8.0 supplemented with 200 mM NaCl and 10 mM tris-(2-carboxyethyl)phosphine (TCEP) was heated at various temperatures for 10 minutes, cooled on ice and then assayed for residual lytic activity by turbidity reduction assay. Data was normalized to the activity displayed by the unheated sample at each pH.

well as 18% activity after being heated-treated at 100°C (Fig. 5-2b). Nevertheless, when collectively comparing the stability of endolysins that have been at least partially thermally characterized, endolysins like PlyG and the several thermoresistant *Listeria* endolysins (HPL118, HPL500, HPL511, HPLP35) appear to be evolutionary outliers. Overall, a number of characterized thermolabile endolysins with validated antimicrobial efficacy exist (e.g. Cpl-1, Pal, Cpl-7 and PlyC), with more undoubtedly being discovered in the coming years. To this end, effective strategies geared towards thermostabilizing bacteriolytic enzymes are needed from a commercialization perspective.

Prior to the bioengineering studies mentioned in Chapters II-IV in this dissertation, there were no published studies definitive to the discipline of modifying the structure of peptidoglycan hydrolases (i.e. endolysins, autolysins and exolysins) to improve stability. Thermodynamic characterization of PlyC in 2008 revealed that, while the CBD of the enzyme (i.e. the PlyCB octomer) exhibited a T_G of 75.0°C and thus was endogenously thermostable, the EAD (i.e. PlyCA) was relatively unstable, comprising a T_G of 46.2.0°C. Results from comparing the thermodynamics of the isolated C-terminal CHAP domain of the EAD to that of PlyCAΔCHAP in a PlyCΔCHAP background suggested the CHAP domain was the most heat-susceptible structural constituent of PlyCA. With concentration on the thermosusceptible EAD of the streptococcal endolysin PlyC, the work presented in this dissertation focuses on independently subjecting a phage endolysin to two established protein engineering methodologies with the overall goal of increasing the stability. Using the 2008 PlyC thermodynamic data in combination with the solved X-ray crystal structure of the holoenzyme as a guide, the first engineering strategy consisted of applying a rationale-based *in silico* computational screening method

that utilized the FoldX and Rosetta protein folding algorithms to identify thermodynamically beneficial mutations to the C-terminal CHAP domain of the catalytic subunit of PlyC (Chapter II). Next, a novel directed evolution protocol was constructed specific to thermostabilizing bacteriolytic enzymes, with PlyC being used as the enzyme of choice (Chapter III). Preliminary results from a more recent (2012) and thorough thermodynamic analysis of PlyC suggested that the N-terminal GyH and C-terminal CHAP domains had similar thermal properties. Without an obvious region of PlyCA to focus on, the entire PlyCA subunit was targeted when initially constructing this novel directed evolution protocol. Once the random mutagenesis and screening components were validated following one round of screening, the methodology was then expanded to additional rounds of screening to further elucidate stabilizing mutations to PlyCA (Chapter IV).

While the rational and random protein engineering methods used were successful at enhancing the thermodynamic and kinetic stability of PlyC, using this particular endolysin for these studies was far from ideal. We ultimately decided on using PlyC for several reasons. First, our lab possessed the clone for expressing this particular endolysin and had extensive experience working with the enzyme. Secondly, the molecular, biochemical and biophysical characteristics of PlyC were explicated through previous and current experiments, as well as ongoing collaborations. Third, the 3.3-Å crystal structure of the enzyme had been solved, providing the structural insight and atomic coordinates necessary for formulating thermostabilizing engineering methodologies. However, devising effective strategies was difficult and laborious due to the complexity of the nine subunit structure and the presence of multiple catalytic domains that together

deploy a synergistic bacteriolytic mechanism. Using a traditional Gram-positive endolysin with the simplistic monomeric architecture of an N-terminal EAD linked to a C-terminal CBD would have made designing and performing engineering experiments more straightforward and efficient. For example, when using computational protein folding algorithms to simulate the folding of highly complex proteins, such as PlyC, there is a greater propensity for folding and subsequent atomic interaction inaccuracies, causing imprecise free energy predictions. Accordingly, stabilizing mutations may be overlooked or a more voluminous list of candidates may need to be experimentally characterized in order to identify beneficial mutations. In a more simplistic system, such as a monomeric endolysin, free energy values calculated by simulating the three-dimensional folding of the protein will be more reliable. This would decrease the chances of excluding potentially stabilizing mutations during computational screening and additionally limit the number of incorrectly identified candidates for experimental characterization.

Expanding to the directed evolution screening methodology created in Chapter III, using a traditional monomeric Gram-positive endolysin instead of PlyC would have simplified the protocol. Due to PlyC being composed of PlyCB and PlyCA subunits, it was necessary to utilize a dual expression system. This first required making a stable and highly competent *E. coli* DH5α strain harboring the expression construct pBAD33: *plyCB*, for which mutagenized pBAD24: *plyCA* constructs were then transformed into. Unfortunately, as a direct consequence of co-expressing PlyCA and PlyCB on separate and unique expression plasmids, the resulting holoenzyme population displays significant activity defects compared to PlyC expressed in a pBAD24: *plyC* background. The dual

expression system could have been avoided by applying epPCR to *plyCA* and then re-inserting the gene into the context of the *plyC* operon. However, due the absence of intrinsic endonuclease restriction sites at the 5' and 3' ends of *plyCA*, this would have required additional overlap-extension PCR (OE-PCR) steps. Not only is this more time consuming, but DNA recombination techniques further increase the chances of incorporating additional unwanted nucleotide mutations in the *plyC* operon. Alternatively, a co-expression system could have been avoided altogether using a single subunit protein, and, with the exception of targeting specific regions of the enzyme for epPCR, subsequent OE-PCR steps could be omitted as well.

The kinetics pertaining to the EAD and CBD modules of endolysins along with the CBD specificity can be altered by modifying the directed evolution methodology discussed in Chapter III. Amending the directed evolution protocol for increasing the bacteriolytic kinetics of an endolysin by either amplifying the catalytic efficiency of the EAD or, since it is believed endolysins bind irreversibly to their explicit cell wall ligand to prevent other potential host cells from being lysed (Loessner et al., 2002), enhancing CBD binding affinity, can be achieved through three alterations. First, the heating step initially installed in the methodology would be removed since you would no longer be screening for variants with improved kinetic stability. Second, epPCR can be applied to the full-length endolysin gene or to the individual domains. Finally, the criteria used for identifying enzyme variants with increased catalytic efficiency after turbidity reduction kinetic analysis would have to be adapted. Previously, the screening component of the directed evolution protocol was formulated for identifying kinetically stabilized PlyC variants, with the criteria being that a heat-treated endolysin had to

spectrophotometrically lyse at least half of the *S. pyogenes* population (i.e. ≥ 50% reduction of the initial OD_{600}) in less than 900 seconds. To transition from screening for kinetic stability to catalytic efficiency, one would need to first obtain a reasonable estimation of the amount of time (seconds) required for the wild-type endolysin to achieve a spectrophotometric-based 50% reduction in cell population. After this value is identified, then one would select a time point considerably lower to serve as the baseline criteria for discerning endolysin mutants with or without significantly progressed catalytic efficiency. For example, if the wild-type pneumococcal endolysin Cpl-1 was able to lyse half of the *S. pneumoniae* cell population in 1000 seconds, then one could progressively identify Cpl-1 variants with improved catalytic efficiency by using the screening requirements of:

- Round 1: 50% decrease in initial OD_{600} in less than 800 seconds
- Round 2: 50% decrease in initial OD_{600} in less than 600 seconds
- Round 3: 50% decrease in initial OD_{600} in less than 400 seconds
- Round 4: 50% decrease in initial OD_{600} in less than 200 seconds
- Shuffle kinetically advantageous mutations, final evolved Cpl-1 variant(s) must display a 50% decrease in initial OD_{600} in less than 100 seconds

Adjusting the directed evolution methodology for generating endolysin variants with revised bacterial specificity can also be accomplished by introducing several changes to the protocol. Once again the heating step would be removed since the focus of the screening portion of the protocol is not geared towards identifying stabilized enzyme variants. Next, epPCR would be applied to the CBD of the endolysin and the resulting

mutagenized PCR products would be genetically combined with the rest of the endolysin gene through either OE-PCR or utilizing endogenous endonuclease restriction sites at the polar ends of the CBD gene. The last modification focuses on the assay used to determine bacterial lysis. Considering the objective is to identify endolysin variants that display altered lytic specificity, one could use spot-on-lawn (i.e. plate lysis) assays (e.g. Fig. 5-3) (Donovan et al., 2006a; Schuch et al., 2002) as an alternative to spectrophotometric turbidity reduction assays. These assays consist of plating exponentially growing target bacterial cells on an agar plate, followed by spotting the endolysin on the air-dried plate. Incubating the plates overnight allows for the growth of the bacterial lawn. If the endolysin spotted on the agar plate is active against the bacteria, then the antimicrobial activity will be represented by a clear lysis zone.

Chimeragenesis is an alternative engineering approach that can be adequately applied to Gram-positive endolysins due to their modular composition. Domain swapping has proven to be practical for refining the kinetics and specificity of both the EAD and CBD modules (Croux et al., 1993a, b; Diaz et al., 1990, 1991; Donovan et al., 2006a; Schmelcher et al., 2011), however this practice has never been utilized for the purpose of improving the thermal stability of endolysins. In order for chimeragenesis to be effective, the thermal stability of the EAD and CBD modules that comprise the unstable endolysin of interest need to be understood. This can be achieved by expressing and purifying the individual domains separately, followed by thermal characterization (e.g. CD, DSC, differential scanning fluorimetry (DSF) or spectrophotometric-based assays measuring protein aggregation at OD_{360} as a function of temperature). If a thermosusceptible domain is identified, then this domain can be deleted and replaced with a more stable EAD

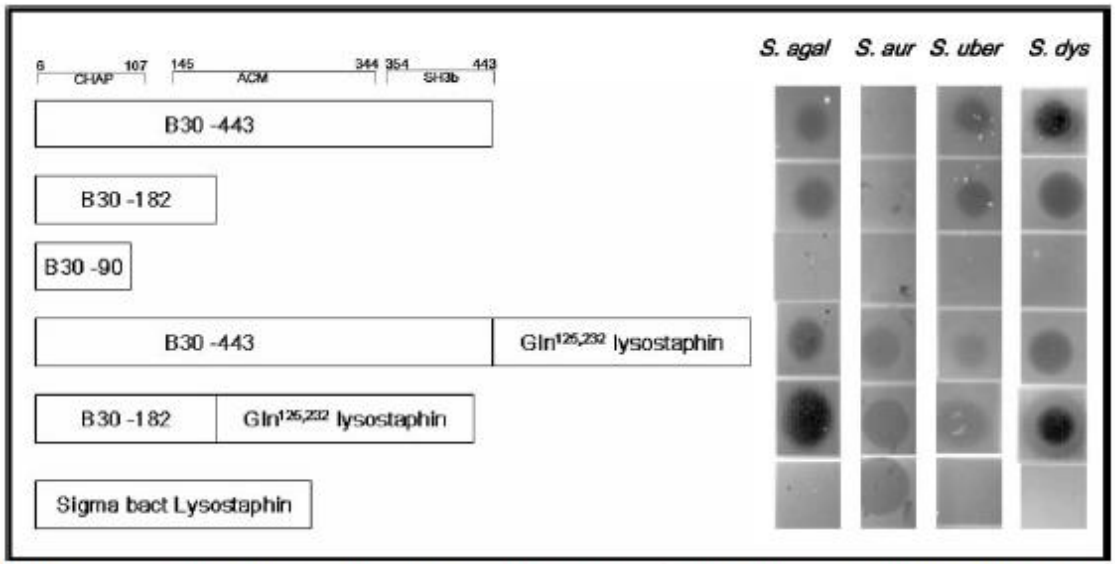

Figure 5-3. Plate lysis assay example. The GBS B30 endolysin and *S. aureus* exolysin lysostaphin were fused together to expand the lytic specificity of the antimicrobial. Crude *E. coli* lysates were prepared from cells harboring the various pET21a-derived expression vectors. Spots of cleared lawn represent lysis of the target organisms. Lysostaphin was spotted as a control. B30-90 is an inactive truncation of B30 and thus served as a negative control. *S. agal*, *S. agalactiae*; *S. aur*, *S. aureus*; *S. uber*, *S. uberis*; *S. dys*, *S. dysgalactiae*. (Source: Donovan et al., 2006a)

originating from any peptidoglycan hydrolase or a CBD specific to the target bacterial species.

The scarcity of characterized thermostable EAD and CBD modules from mesophilic phage currently limits the practicality of the chimeragenesis approach for thermostabilizing endolysins. One way to address this limitation is to utilize peptidoglycan hydrolases derived from thermophilic phage or bacteria. These enzymes and their catalytic domains can be identified from literature (if characterized) or bioinformatic sources (if uncharacterized), such as the National Center for Biotechnology Information (NCBI) and Pfam databases. Once a thermophilic peptidoglycan hydrolase is selected as a candidate, the gene encoding the enzyme can be synthetically constructed to use as a template for chimeragenesis. For example, the following six catalytic domains were identified from thermophilic bacteria or phage as possessing similar size (~20 kDa) and putative cell wall hydrolytic activities to EADs derived from phage endolysins (Table 5-1). Future chimeragenesis approaches could utilize these or similar domains for thermostabilizing endolysins (Appendix D).

Although the general theme of this dissertation was to progress the intrinsic structural stability of phage endolysins, stabilizing chemical components for protein formulations need to also be considered, including polyols, sugars, amino acids, salts, polymers/proteins, surfactants and preservatives. Polyols and sugars act through a preferential exclusion mechanism and were initially exploited by pharmaceuticals in 1993 (Timasheff, 1993). The preferential exclusions of the polyols and sugars from the protein promotes a stronger protein hydration, which then minimizes the energetically unfavorable surface exposure of hydrophobic regions of the protein due to denser protein

Table 5-1. List of thermophilic peptidoglycan hydrolase catalytic domain candidates.

Species	Type of Peptidoglycan Hydrolase	Hydrolytic Activity	Catalytic Domain Size
Thermosinus carboxydivorans sp. Nor1	Autolysin or exolysin	Glucosaminidase	18 kDa
Geobacillus sp. Y412MC10	Autolysin or exolysin	Glucosaminidase or amidase	18 kDa
Dictyoglomus thermophilum H-6-12	Autolysin or exolysin	Amidase	20 kDa
Pseudomonas aeruginosa phage ΦKMV	Part of the extensible phage tail	Muramidase	19 kDa
Pseudomonas aeruginosa phage ΦKZ	Part of phage needle-like puncturing device	Muramidase	19 kDa
Geobacillus phage E2 GVE2	Endolysin	Amidase	27 kDa

packing. Moreover, this preferential exclusion reduces the chemical potential of the protein and thus lessens the risk of oxidation (Kendrick et al., 1997). Sugars can additionally improve protein stability by removing metal salts from solution in order to prevent these metals from acting as antioxidants, or to decrease chemical degradation processes catalyzed by metal ions (Lam et al., 1997). Furthermore, polyols and sugars have shown to be effective cryoprotectants and lyoprotectants, with the concentrations of each determining the degree of stabilization. Proteins can be stabilized during freeze-thawing by including lactose, glycerol, xylitol, sobitol and mannitol at molar concentrations of 0.5-1.0 M (Carpenter et al., 1990), as well as sucrose, maltose, glucose and inositol (Carpenter et al., 1986). When freeze-drying protein samples, sugars can act as a water replacement by providing hydroxyl functions to the protein (Crowe et al., 1993a, b; Schule et al., 2008). Disaccharides (e.g. trehalose, sucrose, maltose and lactose) are equal to or better lyoprotectants than monosaccharides (e.g. glucose and galactose). In particular, the tendency of sucrose and trehalose to form amorphous cakes makes them superlative bulking agents when freeze-drying protein samples (Arakawa and Prestrelski, 1993; Chang et al., 1996).

Amino acid additives (e.g. histidine, arginine and glycine) stabilize proteins using a variety of mechanisms. For example, several amino acids were shown to stabilize pig heart mitochondrial malate dehydrogenase by preferential exclusion (Jensen et al., 1996), histidine was able to prevent oxidation of papain (Kanazawa et al., 1994), and cysteine and (partially) methionine were able to increase the stability of recombinant human Ciliary Neurotrophic Factor and recombinant human Nerve Growth Factor (Knepp et al.,

1996). Other amino acids used as formulation excipients include proline, lysine, glutamic acid and arginine mixtures.

The stabilizing potential of salts depends on several factors, including the type and concentration of salt, the nature of the ionic interactions and the charged residues that comprise the protein of interest (Kohn et al., 1997). By increasing the ionic strength of a solution, protein stability can be augmented by enhancing the strength of hydrophobic interactions. Additionally, salts can be preferentially excluded from proteins, making their structures more compact and stable. Buffer salts are a required component of protein storage solutions for the purpose of maintaining pH values best for retention of the native state of the protein.

Hydrophilic polymers (e.g. PEGs, polysaccharides and inert proteins) nonspecifically interact with the proteins to induce steric hindrance and enhance protein assembly. Hydrophobic moieties of various polymers (e.g. those comprised by PEGs and Pluronics) alter surface activity by decreasing the water surface tension, which suppresses protein aggregation caused by surface absorption. Other mechanisms of stability affiliated with the use of polymers/proteins include preferential exclusion and decreased protein flexibility provoked by enhanced viscosity (Wang, 1999).

Pharmaceutical companies commonly use surfactants in protein formulations to compete for interfaces that could possibly cause unfolding and aggregation (Piatigorsky et al., 1977). These interfaces are mainly between the aqueous protein solution on the side of container walls, stoppers (coated or uncoated), ice-crystals from freezing or storage, filter materials, tubes and air-water interfaces. Surfactants can also act as artificial chaperones to promote protein refolding when the unfolding event is reversible

(Rozema and Gellman, 1996). Examples of surfactants include Tween 20 and 80, Brij 35, Triton X-10, Pluronic F127 and SDS.

Approximately 25% of all protein formulations include preservatives that prevent microbial growth, particularly for multi-dose, single container formulations. M-cresol, phenol and benzyl alcohol are the most widely used antimicrobial agents. These antimicrobial are typically used independently, although insulin-protamine suspension products, for example, contain both m-cresol and phenol. However, many times these compounds are not compatible with the protein itself, often promoting aggregation (Hutchings et al., 2013), as well as the particular processing and packaging materials.

Summary and Conclusions

In this dissertation, rationale-based (Chapter II) and directed evolution (Chapters III and IV) protein engineering methods were applied to streptococcal endolysin PlyC with the goal of improving the thermal stability of the enzyme. The motivation behind this work was to elongate the shelf life expectancy to enhance the antimicrobial potential of the endolysin for industrial application. Guided by previously elucidated structural and biophysical data, mutations were computationally modeled into the thermolabile C-terminal CHAP domain of the PlyCA subunit using the protein folding algorithm FoldX in order to identify mutants that are thermodynamically advantageous (Chapter II). Next, a novel directed evolution methodology was developed and validated for improving the kinetic stability of bacteriolytic enzymes (Chapter III). This directed evolution protocol was devised for identifying enzyme variants that concurrently exhibit progressed kinetic stability while maintaining wild-type catalytic efficiency. As a means to further validate

the methodology, several rounds of directed evolution were then applied to PlyC in order to significantly enhance the thermal properties of the enzyme (Chapter IV).

In conclusion, it has been determined that:

1) Computationally screening thermolabile regions of endolysins, such as the C-terminal CHAP domain of PlyCA, using the FoldX algorithm in combination with Rosetta and visual inspection can effectively identify stabilizing mutations. For example, the PlyC (PlyCA) T406R mutant, which is hypothesized to generate an enthalpic gain due to an inter-domain hydrogen bond formed between the side-chains of Q106 of the GyH domain and R406 of the CHAP domain, displayed a 2.27°C increase in thermodynamic stability, 16 fold decrease in thermally-induced kinetic inactivation at 45°C and an 11 kcal/mol improvement in E_A of PlyCA unfolding. These types of *in silico* strategies can be applied to specific regions or the entire subunit of other endolysins for increasing thermal stability.
2) Directed evolution methodologies can be devised to significantly augment the stability of bacteriolytic enzymes while preserving their native catalytic efficiency. The validated directed evolution protocol we developed consists of several steps, including:
    - Determining the optimal heating conditions to use during screening
    - Generating the mutant library using, for example, epPCR with a desired low nucleotide mutation rate
    - 96-well microtiter plate preparation and subsequent cell growth conditions
    - Replica plating, protein expression induction and lysate preparation
    - Soluble lysate heat treatment and residual enzyme activity analysis

Although multiple rounds are generally used in directed evolution studies, implementing only one round of epPCR and screening can result in the identification of mutants with decidedly improved kinetic stability and wild-type catalytic activity. For example, when compared to wild-type, the PlyC 29C3 mutant exhibited a ~2 fold decrease in thermally-induced kinetic inactivation at 45°C, while showing no significant difference in lytic activity at room temperature.

3) Expanding the directed evolution methodology to incorporate multiple rounds of mutagenesis and screening can yield bacteriolytic enzymes with considerably evolved kinetic and thermodynamic stability. Screening a total of 18,000 mutants over three rounds of directed evolution yielded a lead candidate, termed PlyC 33D2. Isolating the four amino acid mutations that comprised this construct subsequently produced a final thermally evolved PlyC variant, termed PlyC (PlyCA) N211H, with a 4.10°C increase in T_G, an 18.8 fold enhancement in kinetic stability at 45°C and a 17.52 kcal/mol gain in E_A of PlyCA unfolding. The H211 residue appears to stabilize the EAD of PlyC through the enthalpic gains generated by anchoring a segment of the flexible linker 1 structure to the surface of the GyH domain. This hypothesized structural alteration seems to be induced by electrostatic interactions formed between E113, D150 and H211.

4) Combining thermally advantageous mutations identified from independent bioengineering techniques can additively enhance the stability of bacteriolytic enzymes. Using PlyC as an example, combining the stabilizing mutations N211H (directed evolution) and T406R (FoldX computational screening) resulted in a

double mutant (i.e. PlyC (PlyCA) N211H T406R) that displayed additive improvements in both thermodynamic (+7.46°C ΔT_G) and kinetic (+28.72 kcal/mol ΔE_A of PlyCA unfolding) stability.

Future Research

Computational Screening of the GyH and Helical Docking Domains of PlyCA

Considering how effective it was to utilize protein folding algorithms to identify thermostabilizing mutations to the C-terminal CHAP domain of PlyCA, I would like to expand the *in silico* screening to the other regions of the subunit, namely the N-terminal GyH domain and the central helical docking domain. When initially designing computational screening strategies specific for PlyC, it was believed that the CHAP domain was the most heat-labile domain of PlyCA and thus was an obvious region to target. With a more detailed thermodynamic understanding of the PlyC holoenzyme structure, it appears the GyH and CHAP domains have similar thermodynamic stability. As such, the thermostability engineering potential for the GyH domain is comparable to that of CHAP. Modeling mutations into the central helical docking domain could also be thermodynamically rewarding. The helical docking domain interacts with four adjacent PlyCB N-termini to promote the formation of the holoenzyme structure. Computationally screening this domain could reveal mutations that generate stabilizing inter-domain or intra-domain interactions.

Further Structural Characterization and Thermostabilization Strategies using PlyC (PlyCA) N211H, T406R and N211H T406R

A combination of biochemical and biophysical experimental approaches has been used in an attempt to understand the mechanism of stability for the PlyCA mutations N211H and T406R. It is believed that H211 stabilizes PlyCA by electrostatically interacting with E113 and D150, whereas R406 is hypothesized to form an inter-domain hydrogen bond with Q106 of the GyH domain. To structurally determine the stabilizing molecular interactions associated with H211 and R406, I plan on collaborating with Travis Gallagher at the National Institute of Standards and Technology (NIST) to obtain an X-ray crystal structure of PlyC (PlyCA) N211H T406R. Elucidating these mechanisms can be helpful for devising future structure-guided rational engineering strategies for PlyC and other endolysins.

Additional engineering strategies can be directed towards PlyC (PlyCA) N211H T406R to continue enhancing the thermal stability of the endolysin. With potential interaction partners for both H211 and R406 being identified, these interactions can be strengthened through the insertion of disulfide bonds. For example, with H211 hypothesized to electrostatically interact with E113 and D150, the constructs PlyC (PlyCA) N211C E113C or PlyC (PlyCA) N211C D150C can be synthesized to substitute the weaker electrostatic interaction with a stronger covalent interaction. Furthermore, a PlyC (PlyCA) Q106C T406C construct can be made in an attempt to covalently link the GyH and CHAP domains, although this may not be feasible due to the distance between the two mutagenized cysteine side-chains. In terms of the PlyC (PlyCA) N211H mutant, the electrostatic interaction formed between H211, E113 and D150 most likely anchors a

segment of the linker 1 structure to the surface of the GyH domain. To this end, future engineering studies can focus on decreasing the flexibility of the linker 1 and linker 2 structures of PlyCA. This can be accomplished several ways, including substituting the highly flexible glycine and serine residues that comprise these linkers with proline residues, anchoring the linkers to the surfaces of either the GyH or CHAP domains by engineered disulfide bonds, or deleting amino acids to shorten the linker structures. Finally, additional rounds of directed evolution can be applied to PlyC (PlyCA) N211H T406R.

Applying Chimeragenesis to Other Gram-Positive Endolysins

Preliminary experimental results show chimeragenesis can be an efficient engineering strategy for increasing the thermal stability of Gram-positive endolysins (Appendix D). Unfortunately, while the gain in stability is significant, the complex synergistic bacteriolytic mechanism employed by PlyC makes this endolysin a poor candidate for chimeric engineering. Without the simultaneous presence of fully-functional GyH and CHAP domains, PlyC displays < 1% activity compared to wild-type. Thus, removing both domains and inserting a foreign thermostable catalytic domain in their place results in a streptococcal endolysin with drastically reduced lytic activity. Traditional Gram-positive endolysins that constitute a single EAD would be better suited for this protein engineering approach. First, I would like to thermodynamically characterize the EAD and CBD modules from a variety of Gram-positive endolysins. For the endolysins that are comprised of an EAD that is significantly less stable than the CBD, I would construct chimeras substituting the native EAD with one of the several

thermostable catalytic domain candidates, such as Nor1, PlyG EAD and Ply511 EAD. The resulting chimeras would then be biochemically and biophysically characterized in order to obtain a more complete understanding of their kinetic and thermodynamic characteristics.

Appendix A

Sequence Information for Constructs used in

Dissertation-Related Studies

pBAD24: *plyC*

Insert Sequence (2213 nucleotides)

GAAGTAATTTCCATTCTTGAAAACGTCGCATGGTACTTACCAGTGCCAAAGAAACTGCT
AAATGTTTTAGCACAATTTAAAGAAATAGAAAATGAGGTAAAATCAAATGAGCAAGATT
AATGTAAACGTAGAAAATGTTTCTGGTGTACAAGGTTTCCTATTCCATACCGATGGAAA
AGAAAGTTACGGTTATCGTGCTTTTATTAACGGAGTTGAAATTGGTATTAAAGACATTG
AAACCGTACAAGGATTTCAACAAATTATACCGTCTATCAATATTAGTAAGTCTGATGTA
GAGGCTATCAGAAAGGCTATGAAAAAGTAATGATTGAGGAGTGGGTCAAGCACCCCTCC
CTCAATTACTATATAAGTAGTTATGGCAGGGTGAAAAACTCTAAAGGTTTAATAATGAA
ACAACACATATGCAATGGTTATAAGCGAATTAAATTAGTAAAGGACGGTATAAAAAAGA
ATTACTATGTTCATCGCTTAGTTGCAGAAACATTCATACCTAAACTACATGTTGACTAT
GTTGTACATCATATTGACCATGATAAACTAAACAACTGGGTACATAACTTAGAATGGTG
TCATTATCAAACTAACCTATTATATGAAAGGGAGAATTTATTTAATGAGTAAGAAGTAT
ACACAACAACAATACGAAAAATATTTAGCACAACCAGCAAATAACACATTTGGGTTATC
ACCTCAACAGGTTGCTGATTGGTTTATGGGTCAAGCTGGTGCTAGGCCTGTTATTAACT
CGTATGGGGTAAATGCTAGTAATTTAGTATCAACGTACATACCTAAAATGCAGGAATAC
GGTGTATCATATACACTATTCTTAATGTATACTGTCTTTGAGGGAGGCGGCGCAGGTAA
TTGGATTAATCATTACATGTACGATACGGGGTCTAATGGATTAGAGTGTTTGGAACACG
ATTTACAATACATACATGGCGTCTGGGAAACTTATTTTCCACCAGCTTTATCTGCGCCA
GAATGTTACCCAGCTACGGAAGATAACGCAGGTGCTTTAGATAGATTTTATCAATCGCT
ACCAGGCCGAACATGGGGTGATGTTATGATACCTAGTACAATGGCTGGTAATGCTTGGG
TATGGGCTTATAACTATTGTGTTAACAACCAAGGGGCTGCCCCATTAGTTTACTTTGGC
AATCCATACGATAGTCAAATTGATAGCTTGCTTGCAATGGGAGCTGACCCGTTTACAGG
TGGTTCAATTACAGGTGATGGAAAAAATCCTAGTGTTGGCACTGGGAATGCTACCGTTT
CTGCTAGCTCGGAAGCTAACAGAGAGAAGTTAAAGAAAGCCCTAACAGATTTATTCAAC
AACAACCTAGAACATCTATCAGGTGAATTCTACGGTAACCAAGTGTTGAATGCTATGAA
ATACGGCACTATCCTGAAATGTGATTTAACAGATGACGGACTTAATGCCATTCTTCAAT
TAATAGCTGATGTTAACTTACAGACTAACCCTAACCCAGACAAACCGACCGTTAAATCA
CCAGGTCAAAACGATTTAGGGTCGGGGTCTGATAGAGTTGCAGCAAACTTAGCCAATGC
ACAGGCGCAAGTCGGTAAGTATATTGGTGACGGTCAATGTTATGCTTGGGTTGGTTGGT
GGTCAGCTAGGGTATGTGGTTATTCTATTTCATACTCAACAGGTGACCCAATGCTACCG
TTAATTGGTGATGGTATGAACGCTCATTCTATCCATCTTGGTTGGGATTGGTCAATCGC
AAATACTGGTATTGTTAACTACCCAGTTGGTACTGTTGGACGCAAGGAAGATTTGAGAG
TCGGCGCGATATGGTGCGCTACAGCATTCTCTGGCGCTCCGTTTTATACAGGACAATAC
GGCCATACTGGTATCATTGAAAGCTGGTCAGATACTACCGTTACAGTCTTAGAACAAAA
CATTTTAGGGTCACCAGTTATACGCAGCACCTATGACCTTAACACATTCCTATCAACAC

TAACTGGTTTGATAACATTTAAATAAAAAAGAAGAGACTGTAAAGTCTCTTTTCTTATT
TTATAATGACGTTATTAACAACTGTGTTATTAATCATGTCACTTTCTTTGTGCCATAAC
CTTACACCTGCTTCAAACAAAGCTCTTAACATATTCATATGCCCAGTGTCTACGTTAGG
AAGAGTCCATATTCCCTTGAATTGAACCCA

Protein Sequence (Holoenzyme is 1032 AA, 113.11 kDa)

PlyCB (71 AA in monomer, 7.86 kDa/568 AA in octomer, 62.75 kDa)

SKINVNVENVSGVQGFLFHTDGKESYGYRAFINGVEIGIKDIETVQGFQQIIPSINISK
SDVEAIRKAMKK

PlyCA (464 AA, 50.37 kDa)

SKKYTQQQYEKYLAQPANNTFGLSPQQVADWFMGQAGARPVINSYGVNASNLVSTYIPK
MQEYGVSYTLFLMYTVFEGGGAGNWINHYMYDTGSNGLECLEHDLQYIHGVWETYFPPA
LSAPECYPATEDNAGALDRFYQSLPGRTWGDVMIPSTMAGNAWVWAYNYCVNNQGAAPL
VYFGNPYDSQIDSLLAMGADPFTGGSITGDGKNPSVGTGNATVSASSEANREKLKKALT
DLFNNNLEHLSGEFYGNQVLNAMKYGTILKCDLTDDGLNAILQLIADVNLQTNPNPDKP
TVKSPGQNDLGSGSDRVAANLANAQAQVGKYIGDGQCYAWVGWWSARVCGYSISYSTGD
PMLPLIGDGMNAHSIHLGWDWSIANTGIVNYPVGTVGRKEDLRVGAIWCATAFSGAPFY
TGQYGHTGIIESWSDTTVTVLEQNILGSPVIRSTYDLNTFLSTLTGLITFK

Primers and Template

plyC operon was cloned into pBAD24 while Dan was at Rockefeller University.

Notes

plyC operon with 5’ and 3’ UTRs was cloned into pBAD24 using SmaI and HindIII restriction sites.

pBAD33: *plyCB*

Insert Sequence (219 nucleotides)

ATGAGCAAGATTAATGTAAACGTAGAAAATGTTTCTGGTGTACAAGGTTTCCTATTCCA
TACCGATGGAAAAGAAAGTTACGGTTATCGTGCTTTTATTAACGGAGTTGAAATTGGTA
TTAAAGACATTGAAACCGTACAAGGATTTCAACAAATTATACCGTCTATCAATATTAGT
AAGTCTGATGTAGAGGCTATCAGAAAGGCTATGAAAAAGTAA

Protein Sequence (71 AA in monomer, 7.86 kDa/568 AA in octomer, 62.75 kDa)

SKINVNVENVSGVQGFLFHTDGKESYGYRAFINGVEIGIKDIETVQGFQQIIPSINISK
SDVEAIRKAMKK

Primers and Template

PlyCB KpnI F 5’ CCCGGTACCATGAGCAAGATTAATGTAAACG 3’
PlyCB XbaI R 5’ CCCTCTAGATTACTTTTTCATAGCCTTTCTG 3’

Template: pBAD24:*plyC*

Notes

plyCB was cloned into pBAD33 using KpnI and XbaI restriction sites.

pBAD24: *plyCA*

Insert Sequence (1398 nucleotides)

ATGAGTAAGAAGTATACACAACAACAATACGAAAAATATTTAGCACAACCAGCAAATAA
CACATTTGGGTTATCACCTCAACAGGTTGCTGATTGGTTTATGGGTCAAGCTGGTGCTA
GGCCTGTTATTAACTCGTATGGGGTAAATGCTAGTAATTTAGTATCAACGTACATACCT
AAAATGCAGGAATACGGTGTATCATATACACTATTCTTAATGTATACTGTCTTTGAGGG
AGGCGGCGCAGGTAATTGGATTAATCATTACATGTACGATACGGGGTCTAATGGATTAG
AGTGTTTGGAACACGATTTACAATACATACATGGCGTCTGGGAAACTTATTTTCCACCA
GCTTTATCTGCGCCAGAATGTTACCCAGCTACGGAAGATAACGCAGGTGCTTTAGATAG
ATTTTATCAATCGCTACCAGGCCGAACATGGGGTGATGTTATGATACCTAGTACAATGG
CTGGTAATGCTTGGGTATGGGCTTATAACTATTGTGTTAACAACCAAGGGGCTGCCCCA
TTAGTTTACTTTGGCAATCCATACGATAGTCAAATTGATAGCTTGCTTGCAATGGGAGC
TGACCCGTTTACAGGTGGTTCAATTACAGGTGATGGAAAAAATCCTAGTGTTGGCACTG
GGAATGCTACCGTTTCTGCTAGCTCGGAAGCTAACAGAGAGAAGTTAAAGAAAGCCCTA
ACAGATTTATTCAACAACAACCTAGAACATCTATCAGGTGAATTCTACGGTAACCAAGT
GTTGAATGCTATGAAATACGGCACTATCCTGAAATGTGATTTAACAGATGACGGACTTA
ATGCCATTCTTCAATTAATAGCTGATGTTAACTTACAGACTAACCCTAACCCAGACAAA
CCGACCGTTAAATCACCAGGTCAAAACGATTTAGGGTCGGGGTCTGATAGAGTTGCAGC
AAACTTAGCCAATGCACAGGCGCAAGTCGGTAAGTATATTGGTGACGGTCAATGTTATG
CTTGGGTTGGTTGGTGGTCAGCTAGGGTATGTGGTTATTCTATTTCATACTCAACAGGT
GACCCAATGCTACCGTTAATTGGTGATGGTATGAACGCTCATTCTATCCATCTTGGTTG
GGATTGGTCAATCGCAAATACTGGTATTGTTAACTACCCAGTTGGTACTGTTGGACGCA
AGGAAGATTTGAGAGTCGGCGCGATATGGTGCGCTACAGCATTCTCTGGCGCTCCGTTT
TATACAGGACAATACGGCCATACTGGTATCATTGAAAGCTGGTCAGATACTACCGTTAC
AGTCTTAGAACAAAACATTTTAGGGTCACCAGTTATACGCAGCACCTATGACCTTAACA
CATTCCTATCAACACTAACTGGTTTGATAACATTTAAATAA

Protein Sequence (464 amino acids, 50.37 kDa)

SKKYTQQQYEKYLAQPANNTFGLSPQQVADWFMGQAGARPVINSYGVNASNLVSTYIPK
MQEYGVSYTLFLMYTVFEGGGAGNWINHYMYDTGSNGLECLEHDLQYIHGVWETYFPPA
LSAPECYPATEDNAGALDRFYQSLPGRTWGDVMIPSTMAGNAWVWAYNYCVNNQGAAPL
VYFGNPYDSQIDSLLAMGADPFTGGSITGDGKNPSVGTGNATVSASSEANREKLKKALT
DLFNNNLEHLSGEFYGNQVLNAMKYGTILKCDLTDDGLNAILQLIADVNLQTNPNPDKP
TVKSPGQNDLGSGSDRVAANLANAQAQVGKYIGDGQCYAWVGWWSARVCGYSISYSTGD
PMLPLIGDGMNAHSIHLGWDWSIANTGIVNYPVGTVGRKEDLRVGAIWCATAFSGAPFY
TGQYGHTGIIESWSDTTVTVLEQNILGSPVIRSTYDLNTFLSTLTGLITFK

Primers and Template

PlyCA MfeI F 5’ CTTCTTCAATTGATTATGAGTAAGAAGTATACACAACAACAATACG 3’
PlyCA XbaI R 5’ CCCTCTAGATTATTTAAATGTTATCAAACCAGTTAGTGTTG 3’

Template: pBAD24:*plyC*

Notes

plyCA was cloned into pBAD24 using EcoRI and XbaI restriction sites.

pBAD24: *chap*

Insert Sequence (504 nucleotides)

ATGTCACCAGGTCAAAACGATTTAGGGTCGGGGTCTGATAGAGTTGCAGCAAACTTAGC
CAATGCACAGGCGCAAGTCGGTAAGTATATTGGTGACGGTCAATGTTATGCTTGGGTTG
GTTGGTGGTCAGCTAGGGTATGTGGTTATTCTATTTCATACTCAACAGGTGACCCAATG
CTACCGTTAATTGGTGATGGTATGAACGCTCATTCTATCCATCTTGGTTGGGATTGGTC
AATCGCAAATACTGGTATTGTTAACTACCCAGTTGGTACTGTTGGACGCAAGGAAGATT
TGAGAGTCGGCGCGATATGGTGCGCTACAGCATTCTCTGGCGCTCCGTTTTATACAGGA
CAATACGGCCATACTGGTATCATTGAAAGCTGGTCAGATACTACCGTTACAGTCTTAGA
ACAAAACATTTTAGGGTCACCAGTTATACGCAGCACCTATGACCTTAACACATTCCTAT
CAACACTAACTGGTTTGATAACATTTAAATAA

Protein Sequence (167 amino acids, 17.89 kDa)

MSPGQNDLGSGSDRVAANLANAQAQVGKYIGDGQCYAWVGWWSARVCGYSISYSTGDPM
LPLIGDGMNAHSIHLGWDWSIANTGIVNYPVGTVGRKEDLRVGAIWCATAFSGAPFYTG
QYGHTGIIESWSDTTVTVLEQNILGSPVIRSTYDLNTFLSTLTGLITFK

Primers and Template

chap was cloned into pBAD24 by Todd Hoopes.

Notes

chap was cloned into pBAD24 using SmaI and HindIII restriction sites.

pBAD24: *glycosidase* (3' 6x His-tag)

Insert Sequence (636 nucleotides)

ATGAGTAAGAAGTATACACAACAACAATACGAAAAATATTTAGCACAACCAGCAAATAA
CACATTTGGGTTATCACCTCAACAGGTTGCTGATTGGTTTATGGGTCAAGCTGGTGCTA
GGCCTGTTATTAACTCGTATGGGGTAAATGCTAGTAATTTAGTATCAACGTACATACCT
AAAATGCAGGAATACGGTGTATCATATACACTATTCTTAATGTATACTGTCTTTGAGGG
AGGCGGCGCAGGTAATTGGATTAATCATTACATGTACGATACGGGGTCTAATGGATTAG
AGTGTTTGGAACACGATTTACAATACATACATGGCGTCTGGGAAACTTATTTTCCACCA
GCTTTATCTGCGCCAGAATGTTACCCAGCTACGGAAGATAACGCAGGTGCTTTAGATAG
ATTTTATCAATCGCTACCAGGCCGAACATGGGGTGATGTTATGATACCTAGTACAATGG
CTGGTAATGCTTGGGTATGGGCTTATAACTATTGTGTTAACAACCAAGGGGCTGCCCCA
TTAGTTTACTTTGGCAATCCATACGATAGTCAAATTGATAGCTTGCTTGCAATGGGAGC
TGACCCGTTTACAGGTGGTTCAATTCATCATCATCATCACCATTAA

Protein Sequence (211 AA, 23.55 kDa)

MSKKYTQQQYEKYLAQPANNTFGLSPQQVADWFMGQAGARPVINSYGVNASNLVSTYIP
KMQEYGVSYTLFLMYTVFEGGGAGNWINHYMYDTGSNGLECLEHDLQYIHGVWETYFPP
ALSAPECYPATEDNAGALDRFYQSLPGRTWGDVMIPSTMAGNAWVWAYNYCVNNQGAAP
LVYFGNPYDSQIDSLLAMGADPFTGGSIHHHHHH

Primers and Template

PlyCA MfeI F- 5' CTTCTTCAATTGATTATGAGTAAGAAGTATACACAACAACAATACG 3'
Glycosidase XbaI R- 5'
CCCTCTAGATTAATGGTGATGATGATGATGAATTGAACCACCTG 3'

Template: pBAD24:*plyCA*

Notes

glycosidase domain of PlyCA (AA 1-205) was cloned into pBAD24 using EcoRI and XbaI restriction sites with a 3' 6x His-tag. The *glycosidase* gene is also referred to as *gyh* in Chapter IV of this dissertation.

pBAD24: *plyCΔglycosidase*

Insert Sequence (1252 nucleotides)

ATGAGCAAGATTAATGTAAACGTAGAAAATGTTTCTGGTGTACAAGGTTTCCTATTCCA
TACCGATGGAAAAGAAAGTTACGGTTATCGTGCTTTTATTAACGGAGTTGAAATTGGTA
TTAAAGACATTGAAACCGTACAAGGATTTCAACAAATTATACCGTCTATCAATATTAGT
AAGTCTGATGTAGAGGCTATCAGAAAGGCTATGAAAAAGTAATGATTGAGGAGTGGGTC
AAGCACCCCTCCCTCAATTACTATATAAGTAGTTATGGCAGGGTGAAAAACTCTAAAGG
TTTAATAATGAAACAACACATATGCAATGGTTATAAGCGAATTAAATTAGTAAAGGACG
GTATAAAAAAGAATTACTATGTTCATCGCTTAGTTGCAGAAACATTCATACCTAAACTA
CATGTTGACTATGTTGTACATCATATTGACCATGATAAACTAAACAACTGGGTACATAA
CTTAGAATGGTGTCATTATCAAACTAACCTATTATATGAAAGGGAGAATTTATTTAATG
GAAGCTAACAGAGAGAAGTTAAAGAAAGCCCTAACAGATTTATTCAACAACAACCTAGA
ACATCTATCAGGTGAATTCTACGGTAACCAAGTGTTGAATGCTATGAAATACGGCACTA
TCCTGAAATGTGATTTAACAGATGACGGACTTAATGCCATTCTTCAATTAATAGCTGAT
GTTAACTTACAGACTAACCCTAACCCAGACAAACCGACCGTTAAATCACCAGGTCAAAA
CGATTTAGGGTCGGGGTCTGATAGAGTTGCAGCAAACTTAGCCAATGCACAGGCGCAAG
TCGGTAAGTATATTGGTGACGGTCAATGTTATGCTTGGGTTGGTTGGTGGTCAGCTAGG
GTATGTGGTTATTCTATTTCATACTCAACAGGTGACCCAATGCTACCGTTAATTGGTGA
TGGTATGAACGCTCATTCTATCCATCTTGGTTGGGATTGGTCAATCGCAAATACTGGTA
TTGTTAACTACCCAGTTGGTACTGTTGGACGCAAGGAAGATTTGAGAGTCGGCGCGATA
TGGTGCGCTACAGCATTCTCTGGCGCTCCGTTTTATACAGGACAATACGGCCATACTGG
TATCATTGAAAGCTGGTCAGATACTACCGTTACAGTCTTAGAACAAAACATTTTAGGGT
CACCAGTTATACGCAGCACCTATGACCTTAACACATTCCTATCAACACTAACTGGTTTG
ATAACATTTAAATAA

Protein Sequence (Holoenzyme is 809 AA, 88.87 kDa)

PlyCB (71 AA in monomer, 7.86 kDa/568 AA in octomer, 62.75 kDa)

SKINVNVENVSGVQGFLFHTDGKESYGYRAFINGVEIGIKDIETVQGFQQIIPSINISK
SDVEAIRKAMKK

PlyCAΔGlycosidase (241 AA, 26.13 kDa)

MEANREKLKKALTDLFNNNLEHLSGEFYGNQVLNAMKYGTILKCDLTDDGLNAILQLIA
DVNLQTNPNPDKPTVKSPGQNDLGSGSDRVAANLANAQAQVGKYIGDGQCYAWVGWWSA
RVCGYSISYSTGDPMLPLIGDGMNAHSIHLGWDWSIANTGIVNYPVGTVGRKEDLRVGA
IWCATAFSGAPFYTGQYGHTGIIESWSDTTVTVLEQNILGSPVIRSTYDLNTFLSTLTG
LITFK

Primers and Template

PlyCB MfeI F 5’ CTTCTTCAATTGATTATGAGCAAGATTAATGTAAACGTAG 3’
lil+PlyCAΔChitinase F 5’ GAAAGGGAGAATTTATTTAATGGAAGCTAACAGAGAGAAG 3’

lil+PlyCAΔChitinase R 5’ CTTCTCTCTGTTAGCTTCCATTAAATAAATTCTCCCTTTC 3’
PlyCA XbaI R 5’ CCCTCTAGATTATTTAAATGTTATCAAACCAGTTAGTGTTG 3’

Template: pBAD24:*plyC*

Notes

plyCΔglycosidase was cloned into pBAD24 using EcoRI and XbaI restriction sites. Amino acids 1-225 (includes initial methionine) were deleted from PlyCA, which correlates to the glycosidase domain dictated by the crystal structure of PlyC. The two PCR products (*plyCB*+*lil*+First 20 nucleotides of helical docking domain, last 20 nucleotides of *lil*+*plyCAΔglycosidase*) were fused together by means of overlap extension PCR.

pBAD24: *plyCΔchap*

Insert Sequence (1425 nucleotides)

ATGAGCAAGATTAATGTAAACGTAGAAAATGTTTCTGGTGTACAAGGTTTCCTATTCCA
TACCGATGGAAAAGAAAGTTACGGTTATCGTGCTTTTATTAACGGAGTTGAAATTGGTA
TTAAAGACATTGAAACCGTACAAGGATTTCAACAAATTATACCGTCTATCAATATTAGT
AAGTCTGATGTAGAGGCTATCAGAAAGGCTATGAAAAAGTAATGATTGAGGAGTGGGTC
AAGCACCCCTCCCTCAATTACTATATAAGTAGTTATGGCAGGGTGAAAAACTCTAAAGG
TTTAATAATGAAACAACACATATGCAATGGTTATAAGCGAATTAAATTAGTAAAGGACG
GTATAAAAAAGAATTACTATGTTCATCGCTTAGTTGCAGAAACATTCATACCTAAACTA
CATGTTGACTATGTTGTACATCATATTGACCATGATAAACTAAACAACTGGGTACATAA
CTTAGAATGGTGTCATTATCAAACTAACCTATTATATGAAAGGGAGAATTTATTTAATG
AGTAAGAAGTATACACAACAACAATACGAAAAATATTTAGCACAACCAGCAAATAACAC
ATTTGGGTTATCACCTCAACAGGTTGCTGATTGGTTTATGGGTCAAGCTGGTGCTAGGC
CTGTTATTAACTCGTATGGGGTAAATGCTAGTAATTTAGTATCAACGTACATACCTAAA
ATGCAGGAATACGGTGTATCATATACACTATTCTTAATGTATACTGTCTTTGAGGGAGG
CGGCGCAGGTAATTGGATTAATCATTACATGTACGATACGGGGTCTAATGGATTAGAGT
GTTTGGAACACGATTTACAATACATACATGGCGTCTGGGAAACTTATTTTCCACCAGCT
TTATCTGCGCCAGAATGTTACCCAGCTACGGAAGATAACGCAGGTGCTTTAGATAGATT
TTATCAATCGCTACCAGGCCGAACATGGGGTGATGTTATGATACCTAGTACAATGGCTG
GTAATGCTTGGGTATGGGCTTATAACTATTGTGTTAACAACCAAGGGGCTGCCCCATTA
GTTTACTTTGGCAATCCATACGATAGTCAAATTGATAGCTTGCTTGCAATGGGAGCTGA
CCCGTTTACAGGTGGTTCAATTACAGGTGATGGAAAAAATCCTAGTGTTGGCACTGGGA
ATGCTACCGTTTCTGCTAGCTCGGAAGCTAACAGAGAGAAGTTAAAGAAAGCCCTAACA
GATTTATTCAACAACAACCTAGAACATCTATCAGGTGAATTCTACGGTAACCAAGTGTT
GAATGCTATGAAATACGGCACTATCCTGAAATGTGATTTAACAGATGACGGACTTAATG
CCATTCTTCAATTAATAGCTGATGTTAACTTACAGACTAACCCTAACCCAGACAAACCG
ACCGTTTAA

Protein Sequence (Holoenzyme is 865 AA, 95.23 kDa)

PlyCB (71 AA in monomer, 7.86 kDa/568 AA in octomer, 62.75 kDa)

SKINVNVENVSGVQGFLFHTDGKESYGYRAFINGVEIGIKDIETVQGFQQIIPSINISK
SDVEAIRKAMKK

PlyCAΔCHAP (297 AA, 32.5 kDa)

SKKYTQQQYEKYLAQPANNTFGLSPQQVADWFMGQAGARPVINSYGVNASNLVSTYIPK
MQEYGVSYTLFLMYTVFEGGGAGNWINHYMYDTGSNGLECLEHDLQYIHGVWETYFPPA
LSAPECYPATEDNAGALDRFYQSLPGRTWGDVMIPSTMAGNAWVWAYNYCVNNQGAAPL
VYFGNPYDSQIDSLLAMGADPFTGGSITGDGKNPSVGTGNATVSASSEANREKLKKALT
DLFNNNLEHLSGEFYGNQVLNAMKYGTILKCDLTDDGLNAILQLIADVNLQTNPNPDKP
TV

Primers and Template

PlyCB MfeI F 5’ CTTCTTCAATTGATTATGAGCAAGATTAATGTAAACGTAG 3’
PlyCA CHAPless XbaI R 5’ GGGTCTAGATTAAACGGTCGGTTTGTCTGGG 3’

Template: pBAD24:*plyC*

Notes

plyCΔchap was cloned into pBAD24 using EcoRI and XbaI restriction sites. Amino acids 299-464 (including the initial methionine) were deleted from PlyCA. This results in the removal of the CHAP domain beginning with the start site lysine 299 as predicted by means of proteolysis (trypsin digest).

pBAD24: *plyCΔΔ* (3’ 6x His-tag)

Insert Sequence (747 nucleotides)

ATGAGCAAGATTAATGTAAACGTAGAAAATGTTTCTGGTGTACAAGGTTTCCTATTCCA
TACCGATGGAAAAGAAAGTTACGGTTATCGTGCTTTTATTAACGGAGTTGAAATTGGTA
TTAAAGACATTGAAACCGTACAAGGATTTCAACAAATTATACCGTCTATCAATATTAGT
AAGTCTGATGTAGAGGCTATCAGAAAGGCTATGAAAAAGTAATGATTGAGGAGTGGGTC
AAGCACCCCTCCCTCAATTACTATATAAGTAGTTATGGCAGGGTGAAAAACTCTAAAGG
TTTAATAATGAAACAACACATATGCAATGGTTATAAGCGAATTAAATTAGTAAAGGACG
GTATAAAAAAGAATTACTATGTTCATCGCTTAGTTGCAGAAACATTCATACCTAAACTA
CATGTTGACTATGTTGTACATCATATTGACCATGATAAACTAAACAACTGGGTACATAA
CTTAGAATGGTGTCATTATCAAACTAACCTATTATATGAAAGGGAGAATTTATTTAATG
GAAGCTAACAGAGAGAAGTTAAAGAAAGCCCTAACAGATTTATTCAACAACAACCTAGA
ACATCTATCAGGTGAATTCTACGGTAACCAAGTGTTGAATGCTATGAAATACGGCACTA
TCCTGAAATGTGATTTAACAGATGACGGACTTAATGCCATTCTTCAATTAATAGCTGAT
GTTAACTTACAGGGATCGCATCACCATCACCATCACTAA

Protein Sequence (Holoenzyme is 640 AA, 70.9 kDa)

PlyCB (71 AA in monomer, 7.86 kDa/568 AA in octomer, 62.75 kDa)

SKINVNVENVSGVQGFLFHTDGKESYGYRAFINGVEIGIKDIETVQGFQQIIPSINISK
SDVEAIRKAMKK

PlyCAΔΔ (72 AA, 8.2 kDa)

MEANREKLKKALTDLFNNNLEHLSGEFYGNQVLNAMKYGTILKCDLTDDGLNAILQLIA
DVNLQGSHHHHHH

Primers and Template

PlyCB MfeI F 5’ CTTCTTCAATTGATTATGAGCAAGATTAATGTAAACGTAG 3’
DeltaDelta 6His 5’
CCCTCTAGATTAGTGATGGTGATGGTGATGCGATCCCTGTAAGTTAACATCAGC 3’

Template: pBAD24:*plyCΔΔ*

Notes

plyCΔΔ 6x His-tag was cloned into pBAD24 using EcoRI and XbaI restriction sites. Amino acids 1-225 corresponding to the N-terminal glycosidase domain and linker 1 were deleted from PlyCA as well as amino acids 289-465 that encode the linker 2 and C-

terminal CHAP domain. A 6x His-tag (GSHHHHHH) was fused to the C-terminus of the PlyCAΔΔ polypeptide.

pBAD24: *nor1* (3’ 6x His-tag)

Insert Sequence (480 nucleotides)

ATGACACCGGATGAATTTATTGCATGGCTGGGTCCGGTTGCACAGCGTGTTTGTCGTAA
ATATGGTCTGCCTGCAAGCGTTTGTATTGCACAGGGTGCACTGGAAAGCGGTTGGGGTC
GTTATGTTATTGGTGAATATAACCTGTTTGGTCGTAAAGCAGTTGCCGGTGATAAAAGC
ATTACCGTTACCACCCAAGAATACATTAATGGTGAATGGGTGACCATCAACGATGAGTT
CAAAGATTATGATAGCCTGGATGAAGCCGTTGAAGATTGGTGTGTTCTGATGACCGAAG
AACCGGCATATGCAGATGCACTGGCAGTTTGGCAAGAAACCCATGATGTTGAACAGTTT
GTTCGTACCATGGGTCCGGTTTATGCAACCGATCCGGAATATGCAGATAAAGTTCTGGC
AACCATTCGTGCAAATGATCTGACCCAGTATGATGAAGTTATGGCACATCATCATCATC
ACCATTAA

Protein Sequence (159 AA, 18.03 kDa)

MTPDEFIAWLGPVAQRVCRKYGLPASVCIAQGALESGWGRYVIGEYNLFGRKAVAGDKS
ITVTTQEYINGEWVTINDEFKDYDSLDEAVEDWCVLMTEEPAYADALAVWQETHDVEQF
VRTMGPVYATDPEYADKVLATIRANDLTQYDEVMAHHHHHH

Primers and Template

None, GeneArt cloned *nor1* into pBAD24.

Notes

nor1 was cloned into pBAD24 using EcoRI and XbaI restriction sites. *nor1* contains a 3’ 6x His-tag.

pBAD24: *plyCΔΔnor1_N* (3' 6x His-tag)

Insert Sequence (1263 nucleotides)

ATGAGCAAGATTAATGTAAACGTAGAAAATGTTTCTGGTGTACAAGGTTTCCTATTCCA
TACCGATGGAAAAGAAAGTTACGGTTATCGTGCTTTTATTAACGGAGTTGAAATTGGTA
TTAAAGACATTGAAACCGTACAAGGATTTCAACAAATTATACCGTCTATCAATATTAGT
AAGTCTGATGTAGAGGCTATCAGAAAGGCTATGAAAAAGTAATGATTGAGGAGTGGGTC
AAGCACCCCTCCCTCAATTACTATATAAGTAGTTATGGCAGGGTGAAAAACTCTAAAGG
TTTAATAATGAAACAACACATATGCAATGGTTATAAGCGAATTAAATTAGTAAAGGACG
GTATAAAAAAGAATTACTATGTTCATCGCTTAGTTGCAGAAACATTCATACCTAAACTA
CATGTTGACTATGTTGTACATCATATTGACCATGATAAACTAAACAACTGGGTACATAA
CTTAGAATGGTGTCATTATCAAACTAACCTATTATATGAAAGGGAGAATTTATTTAATG
ACACCGGATGAATTTATTGCATGGCTGGGTCCGGTTGCACAGCGTGTTTGTCGTAAATA
TGGTCTGCCTGCAAGCGTTTGTATTGCACAGGGTGCACTGGAAAGCGGTTGGGGTCGTT
ATGTTATTGGTGAATATAACCTGTTTGGTCGTAAAGCAGTTGCCGGTGATAAAAGCATT
ACCGTTACCACCCAAGAATACATTAATGGTGAATGGGTGACCATCAACGATGAGTTCAA
AGATTATGATAGCCTGGATGAAGCCGTTGAAGATTGGTGTGTTCTGATGACCGAAGAAC
CGGCATATGCAGATGCACTGGCAGTTTGGCAAGAAACCCATGATGTTGAACAGTTTGTT
CGTACCATGGGTCCGGTTTATGCAACCGATCCGGAATATGCAGATAAAGTTCTGGCAAC
CATTCGTGCAAATGATCTGACCCAGTATGATGAAGTTATGGCAACAGGTGATGGAAAAA
ATCCTAGTGTTGGCACTGGGAATGCTACCGTTTCTGCTAGCTCGGAAGCTAACAGAGAG
AAGTTAAAGAAAGCCCTAACAGATTTATTCAACAACAACCTAGAACATCTATCAGGTGA
ATTCTACGGTAACCAAGTGTTGAATGCTATGAAATACGGCACTATCCTGAAATGTGATT
TAACAGATGACGGACTTAATGCCATTCTTCAATTAATAGCTGATGTTAACTTACAGGGA
TCGCATCACCATCACCATCACTAA

Protein Sequence (812 AA, 89.76 kDa)

PlyCB (71 AA in monomer, 7.86 kDa/568 AA in octomer, 62.75 kDa)

SKINVNVENVSGVQGFLFHTDGKESYGYRAFINGVEIGIKDIETVQGFQQIIPSINISK
SDVEAIRKAMKK

PlyCAΔΔNor1_N with 6x His-tag (244 AA, 27.01 kDa)

MTPDEFIAWLGPVAQRVCRKYGLPASVCIAQGALESGWGRYVIGEYNLFGRKAVAGDKS
ITVTTQEYINGEWVTINDEFKDYDSLDEAVEDWCVLMTEEPAYADALAVWQETHDVEQF
VRTMGPVYATDPEYADKVLATIRANDLTQYDEVMATGDGKNPSVGTGNATVSASSEANR
EKLKKALTDLFNNNLEHLSGEFYGNQVLNAMKYGTILKCDLTDDGLNAILQLIADVNLQ
GSHHHHHH

Primers and Template

PlyCB MfeI F 5' CTTCTTCAATTGATTATGAGCAAGATTAATGTAAACGTAG 3'

DeltaDelta 6His XbaI R 5’
CCCTCTAGATTAGTGATGGTGATGGTGATGCGATCCCTGTAAGTTAACATCAGC 3’

Template: pBAD24: *plyCΔΔ_nor1* N-terminal fusion w/linker 1

Notes

plyCΔΔnor1_N was cloned into pBAD24 using EcoRI and XbaI restriction sites. Nor1 was fused to the N-terminus of the helical docking domain of PlyCA by the endogenous 22 amino acid linker 1 of PlyCA. A 6x His-tag was added to the C-terminus of the PlyCAΔΔNor1_N polypeptide.

pBAD24: *ply511* EAD only (5' 6x His-tag)

Insert Sequence (564 nucleotides)

ATGCGTGGTAGCCATCATCATCACCATCATGGTAGCATGGTGAAATATACCGTGGAAAA
CAAAATCATTGCAGGTCTGCCGAAAGGTAAACTGAAAGGTGCAAATTTTGTGATCGCAC
ATGAAACCGCAAATAGCAAAAGCACCATTGATAACGAAGTGAGCTATATGACCCGCAAC
TGGAAAAATGCCTTTGTTACCCATTTTGTGGGTGGTGGTGGTCGTGTTGTTCAGGTTGC
AAATGTTAATTATGTTAGCTGGGGTGCAGGTCAGTATGCAAATAGCTATAGTTATGCAC
AGGTTGAACTGTGTCGTACCAGCAATGCAACCACCTTCAAAAAAGATTATGAGGTGTAT
TGTCAGCTGCTGGTTGATCTGGCAAAAAAAGCAGGTATTCCGATTACCCTGGATAGCGG
TAGCAAAACCAGCGATAAAGGTATCAAAAGCCATAAATGGGTTGCCGATAAACTGGGTG
GCACCACCCATCAGGATCCGTATGCATATCTGAGCAGCTGGGGTATTAGCAAAGCACAG
TTTGCAAGCGATCTGGCCAAAGTTAGCGGTTAA

Protein Sequence (187 AA, 20.44 kDa)

MRGSHHHHHHGSMVKYTVENKIIAGLPKGKLKGANFVIAHETANSKSTIDNEVSYMTRN
WKNAFVTHFVGGGGRVVQVANVNYVSWGAGQYANSYSYAQVELCRTSNATTFKKDYEVY
CQLLVDLAKKAGIPITLDSGSKTSDKGIKSHKWVADKLGGTTHQDPYAYLSSWGISKAQ
FASDLAKVSG

Primers and Template

Ply511 MfeI F 5' CTTCTTCAATTGATTATGCGTGGTAGCCATCATC 3'
Ply511 EAD XbaI R 5' CCCTCTAGATTAACCGCTAACTTTGGCCAGATCGCTTGCAAAC 3'

Template: pMA-T: *ply511*

Notes

ply511 EAD only contains amino acids 1-175 of Ply511 and was cloned into pBAD24 using EcoRI and XbaI restriction sites. There was a 5' 6x His-tag added to *ply511* EAD using the amino acid sequence (MRGSHHHHHHGS) outlined by Loesnner *et al.* 1996. Modified *Listeria* Bacteriophage Lysin Genes (*ply*) Allow Efficient Overexpression and One-Step Purification of Biochemically Active Fusion Proteins. Appl. Environ. Microbiol. **62:** 3057-3060.

pBAD24: *plyCΔΔply511_N*

Insert Sequence (1311 nucleotides)

ATGAGCAAGATTAATGTAAACGTAGAAAATGTTTCTGGTGTACAAGGTTTCCTATTCCA
TACCGATGGAAAAGAAAGTTACGGTTATCGTGCTTTTATTAACGGAGTTGAAATTGGTA
TTAAAGACATTGAAACCGTACAAGGATTTCAACAAATTATACCGTCTATCAATATTAGT
AAGTCTGATGTAGAGGCTATCAGAAAGGCTATGAAAAAGTAATGATTGAGGAGTGGGTC
AAGCACCCCTCCCTCAATTACTATATAAGTAGTTATGGCAGGGTGAAAAACTCTAAAGG
TTTAATAATGAAACAACACATATGCAATGGTTATAAGCGAATTAAATTAGTAAAGGACG
GTATAAAAAAGAATTACTATGTTCATCGCTTAGTTGCAGAAACATTCATACCTAAACTA
CATGTTGACTATGTTGTACATCATATTGACCATGATAAACTAAACAACTGGGTACATAA
CTTAGAATGGTGTCATTATCAAACTAACCTATTATATGAAAGGGAGAATTTATTTAATG
GTGAAATATACCGTGGAAAACAAAATCATTGCAGGTCTGCCGAAAGGTAAACTGAAAGG
TGCAAATTTTGTGATCGCACATGAAACCGCAAATAGCAAAAGCACCATTGATAACGAAG
TGAGCTATATGACCCGCAACTGGAAAAATGCCTTTGTTACCCATTTTGTGGGTGGTGGT
GGTCGTGTTGTTCAGGTTGCAAATGTTAATTATGTTAGCTGGGGTGCAGGTCAGTATGC
AAATAGCTATAGTTATGCACAGGTTGAACTGTGTCGTACCAGCAATGCAACCACCTTCA
AAAAAGATTATGAGGTGTATTGTCAGCTGCTGGTTGATCTGGCAAAAAAAGCAGGTATT
CCGATTACCCTGGATAGCGGTAGCAAAACCAGCGATAAAGGTATCAAAAGCCATAAATG
GGTTGCCGATAAACTGGGTGGCACCACCCATCAGGATCCGTATGCATATCTGAGCAGCT
GGGGTATTAGCAAAGCACAGTTTGCAAGCGATCTGGCCAAAGTTAGCGGTGGTGGTAAT
ACCGGCACCGCACCGGCAAAACCGAGCACTCCGGCACCGAAACCGAGTACCCCGAGCAC
CAATAACAGAGAGAAGTTAAAGAAAGCCCTAACAGATTTATTCAACAACAACCTAGAAC
ATCTATCAGGTGAATTCTACGGTAACCAAGTGTTGAATGCTATGAAATACGGCACTATC
CTGAAATGTGATTTAACAGATGACGGACTTAATGCCATTCTTCAATTAATAGCTGATGT
TAACTTACAGTAA

Protein Sequence (828 AA, 90.86 kDa)

PlyCB (71 AA in monomer, 7.86 kDa/568 AA in octomer, 62.75 kDa)

SKINVNVENVSGVQGFLFHTDGKESYGYRAFINGVEIGIKDIETVQGFQQIIPSINISK
SDVEAIRKAMKK

PlyCAΔΔPly511_N (260 AA, 28.11 kDa)

MVKYTVENKIIAGLPKGKLKGANFVIAHETANSKSTIDNEVSYMTRNWKNAFVTHFVGG
GGRVVQVANVNYVSWGAGQYANSYSYAQVELCRTSNATTFKKDYEVYCQLLVDLAKKAG
IPITLDSGSKTSDKGIKSHKWVADKLGGTTHQDPYAYLSSWGISKAQFASDLAKVSGGG
NTGTAPAKPSTPAPKPSTPSTNNREKLKKALTDLFNNNLEHLSGEFYGNQVLNAMKYGT
ILKCDLTDDGLNAILQLIADVNLQ

Primers and Template

PlyCB MfeI F 5’ CTTCTTCAATTGATTATGAGCAAGATTAATGTAAACGTAG 3’

lil/Ply511 F 5’ GAAAGGGAGAATTTATTTAATGGTGAAATATACCGTGGAAAAC 3’
lil/Ply511 R 5’ GTTTTCCACGGTATATTTCACCATTAAATAAATTCTCCCTTTC 3’
Ply511/Dock F 5’ CGAGTACCCCGAGCACCAATAACAGAGAGAAGTTAAAG 3’
Ply511/Dock R 5’ CTTTAACTTCTCTCTGTTATTGGTGCTCGGGGTACTCG 3’
Dock R 5’ CCCTCTAGATTACTGTAAGTTAACATCAGCTATTAATTGAAG 3’

Template: pBAD24: *plyC* and pMA-T: *ply511*

Notes

plyCΔΔply511_N was cloned into pBAD24 using EcoRI and XbaI restriction sites. Ply511 EAD was fused to the N-terminus of the helical docking domain of PlyCA by the 25 amino acid proline-rich linker derived from Ply511. Three PCR products (*plyCB*+*lil*+first 20 nucleotides of *ply511*, last 20 nucleotides of *lil*+*ply511* EAD+first 20 nucleotides of helical docking domain, last 20 nucleotides of *ply511* EAD+helical docking domain) were fused together by means of overlap extension PCR to yield the full-length *plyCΔΔply511_N* construct.

pBAD24: *plyG* (5’ 6x His-tag)

Insert Sequence (737 nucleotides)

ATGCGTGGTAGCCATCATCATCACCATCATGGTAGCATGGAAATCCAGAAAAAACTGGT
TGATCCGAGCAAATATGGCACCAAATGTCCGTATACCATGAAACCGAAATATATCACCG
TGCACAACACCTATAATGATGCACCGGCAGAAAATGAAGTGAGCTATATGATTAGCAAC
AACAACGAGGTGAGCTTTCATATTGCCGTGGATGATAAAAAAGCCATTCAGGGTATTCC
GCTGGAACGTAATGCATGGGCATGTGGTGATGGTAATGGTAGCGGTAATCGTCAGAGCA
TTAGCGTTGAAATCTGCTATAGTAAAAGCGGTGGTGATCGTTATTACAAAGCCGAAGAT
AATGCCGTTGATGTTGTTCGTCAGCTGATGAGCATGTATAACATTCCGATTGAAAATGT
GCGTACCCATCAGAGCTGGTCAGGTAAATATTGTCCGCATCGTATGCTGGCCGAAGGTC
GTTGGGGTGCATTTATTCAGAAAGTGAAAAATGGTAATGTGGCAACCACCAGTCCGACC
AAACAGAACATTATTCAGAGCGGTGCCTTTAGCCCGTATGAAACACCGGATGTTATGGG
TGCACTGACCTCACTGAAAATGACCGCAGATTTTATTCTGCAGAGTGATGGTCTGACCT
ACTTTATTAGCAAACCGACCAGTGATGCACAGCTGAAAGCAATGAAAGAATATCTGGAT
CGTAAAGGTTGGTGGTATGAAGTGAAATAA

Protein Sequence (245 AA, 27.67 kDa)

MRGSHHHHHHGSMEIQKKLVDPSKYGTKCPYTMKPKYITVHNTYNDAPAENEVSYMISN
NNEVSFHIAVDDKKAIQGIPLERNAWACGDGNGSGNRQSISVEICYSKSGGDRYYKAED
NAVDVVRQLMSMYNIPIENVRTHQSWSGKYCPHRMLAEGRWGAFIQKVKNGNVATTSPT
KQNIIQSGAFSPYETPDVMGALTSLKMTADFILQSDGLTYFISKPTSDAQLKAMKEYLD
RKGWWYEVK

Primers and Template

PlyG EcoRI F 5’ CCGGAATTCATTATGCGTGGTAGCCATCATCATC 3’
PlyG XbaI R 5’ CCCTCTAGATTATTTCACTTCATACCACCAACC 3’

Template: pMA-T: *plyG*

Notes

plyG was cloned into pBAD24 using EcoRI and XbaI restriction sites. There was a 5’ 6x His-tag added to *plyG* using the amino acid sequence (MRGSHHHHHHGS) outlined by Loesnner *et al.* 1996. Modified *Listeria* Bacteriophage Lysin Genes (*ply*) Allow Efficient Overexpression and One-Step Purification of Biochemically Active Fusion Proteins. Appl. Environ. Microbiol. **62:** 3057-3060.

pBAD24: *plyG* EAD only (5’ 6x His-tag)

Insert Sequence (519 nucleotides)

ATGCGTGGTAGCCATCATCATCACCATCATGGTAGCATGGAAATCCAGAAAAAACTGGT
TGATCCGAGCAAATATGGCACCAAATGTCCGTATACCATGAAACCGAAATATATCACCG
TGCACAACACCTATAATGATGCACCGGCAGAAAATGAAGTGAGCTATATGATTAGCAAC
AACAACGAGGTGAGCTTTCATATTGCCGTGGATGATAAAAAAGCCATTCAGGGTATTCC
GCTGGAACGTAATGCATGGGCATGTGGTGATGGTAATGGTAGCGGTAATCGTCAGAGCA
TTAGCGTTGAAATCTGCTATAGTAAAAGCGGTGGTGATCGTTATTACAAAGCCGAAGAT
AATGCCGTTGATGTTGTTCGTCAGCTGATGAGCATGTATAACATTCCGATTGAAAATGT
GCGTACCCATCAGAGCTGGTCAGGTAAATATTGTCCGCATCGTATGCTGGCCGAAGGTC
GTTGGGGTGCATTTATTCAGAAAGTGAAAAATGGTAATGTGGCATAA

Protein Sequence (172 AA, 19.44 kDa)

MRGSHHHHHHGSMEIQKKLVDPSKYGTKCPYTMKPKYITVHNTYNDAPAENEVSYMISN
NNEVSFHIAVDDKKAIQGIPLERNAWACGDGNGSGNRQSISVEICYSKSGGDRYYKAED
NAVDVVRQLMSMYNIPIENVRTHQSWSGKYCPHRMLAEGRWGAFIQKVKNGNVA

Primers and Template

PlyG EcoRI F 5’ CCGGAATTCATTATGCGTGGTAGCCATCATCATC 3’
PlyG EAD XbaI R 5’ CCCTCTAGATTATGCCACATTACCATTTTTCACTTTC 3’

Template: pMA-T: *plyG*

Notes

plyG EAD was cloned into pBAD24 using EcoRI and XbaI restriction sites. There was a 5’ 6x His-tag added to *plyG* EAD using the amino acid sequence (MRGSHHHHHHGS) outlined by Loesnner *et al.* 1996. Modified *Listeria* Bacteriophage Lysin Genes (*ply*) Allow Efficient Overexpression and One-Step Purification of Biochemically Active Fusion Proteins. Appl. Environ. Microbiol. **62:** 3057-3060.

pBAD24: *plyG* CBD only (5’ 6x His-tag)

Insert Sequence (272 nucleotides)

ATGCGTGGTAGCCATCATCATCACCATCATGGTAGCAATGGTAATGTGGCAACCACCAG
TCCGACCAAACAGAACATTATTCAGAGCGGTGCCTTTAGCCCGTATGAAACACCGGATG
TTATGGGTGCACTGACCTCACTGAAAATGACCGCAGATTTTATTCTGCAGAGTGATGGT
CTGACCTACTTTATTAGCAAACCGACCAGTGATGCACAGCTGAAAGCAATGAAAGAATA
TCTGGATCGTAAAGGTTGGTGGTATGAAGTGAAATAA

Protein Sequence (90 AA, 10.1 kDa)

MRGSHHHHHHGSNGNVATTSPTKQNIIQSGAFSPYETPDVMGALTSLKMTADFILQSDG
LTYFISKPTSDAQLKAMKEYLDRKGWWYEVK

Primers and Template

PlyG CBD EcoRI F 5’
CCGGAATTCATTATGCGTGGTAGCCATCATCATCACCATCATGGTAGCAATGGTAATGT
GGCAACCACCAGTCCG 3’
PlyG XbaI R 5’ CCCTCTAGATTATTTCACTTCATACCACCAACC 3’

Template: pMA-T: *plyG*

Notes

plyG CBD was cloned into pBAD24 using EcoRI and XbaI restriction sites. There was a 5’ 6x His-tag added to *plyG* CBD using the amino acid sequence (MRGSHHHHHHGS) outlined by Loesnner *et al.* 1996. Modified *Listeria* Bacteriophage Lysin Genes (*ply*) Allow Efficient Overexpression and One-Step Purification of Biochemically Active Fusion Proteins. Appl. Environ. Microbiol. **62:** 3057-3060.

Appendix B

SDM Primers for PlyC FoldX Computational Screening Studies (Chapter II)

D330Y F 5' [Phos]CGGTAAGTATATTGGTTACGGTCAATGTTATG 3'
D330Y R 5' [Phos]ACTTGCGCCTGTGCATTGGCTAAGTTTGCTGC 3'

Q332H F 5' [Phos]TATTGGTGACGGTCACTGTTATGCTTGGGTT 3'
Q332H R 5' [Phos]TACTTACCGACTTGCGCCTGTGCATTGGC 3'

Q332V F 5' [Phos]ATATTGGTGACGGTGTATGTTATGCTTGGG 3'
Q332V R 5' [Phos]ACTTACCGACTTGCGCCTGTGCATTGGCTA 3'

C345T F 5' [Phos]GGTCAGCTAGGGTAACTGGTTATTCTATTTC 3'
C345T R 5' [Phos]ACCAACCAACCCAAGCATAACATTGACCGTC 3'

D375Y F 5' [Phos]ATCCATCTTGGTTGGTATTGGTCAATCGCAAA 3'
D375Y R 5' [Phos]AGAATGAGCGTTCATACCATCACCAATTAAC 3'

T381Y F 5' [Phos]GGTCAATCGCAAATTATGGTATTGTTAACTAC 3'
T381Y R 5' [Phos]AATCCCAACCAAGATGGATAGAATGAGCG 3'

V384Y F 5' [Phos]GCAAATACTGGTATTTATAACTACCCAGTTGG 3'
V384Y R 5' [Phos]GATTGACCAATCCCAACCAAGATGGATAGA 3'

C404I F 5' [Phos]GTCGGCGCGATATGGATTGCTACAGCATTCTC 3'
C404I R 5' [Phos]TCTCAAATCTTCCTTGCGTCCAACAGTACC 3'

T406R F 5' [Phos]CGATATGGTGCGCTAGAGCATTCTCTGGCGC 3'
T406R R 5' [Phos]CGCCGACTCTCAAATCTTCCTTGCGTCC 3'

T421I F 5’ [Phos]GACAATACGGCCATATTGGTATCATTGAAAG 3’
T421I R 5’ [Phos]CTGTATAAAACGGAGCGCCAGAGAATGCTG 3’

Appendix C

SDM Primers for PlyC Directed Evolution Studies (Chapter IV)

N211H F 5’ [Phos]CAGGTGATGGAAAACATCCTAGTGTTGGCAC 3’
N211H R 5’ [Phos]TAATTGAACCACCTGTAAACGGGTCAGCTC 3’

S224N F 5’ [Phos]CTACCGTTTCTGCTAACTCGGAAGCTAACAG 3’
S224N R 5’ [Phos]CATTCCCAGTGCCAACACTAGGATTTTTTCC 3’

G249C F 5’ [Phos]CTAGAACATCTATCATGTGAATTCTACGGTAAC 3’
G249C R 5’ [Phos]GTTGTTGTTGAATAAATCTGTTAGGGCTTTC 3’

A407S F 5’ [Phos]GATATGGTGCGCTACATCATTCTCTGGCGC 3’
A407S R 5’ [Phos]GCGCCGACTCTAAATCTTCCTTGCGTCCAAC 3’

N211A F 5’ [Phos]CAGGTGATGGAAAAGCTCCTAGTGTTGGC 3’
N211A R 5’ [Phos]TAATTGAACCACCTGTAAACGGGTCAGCTCC 3’

N211D F 5’ [Phos]CAGGTGATGGAAAAGATCCTAGTGTTGGC 3’
N211D R 5’ [Phos]TAATTGAACCACCTGTAAACGGGTCAGCTCC 3’

N211K F 5’ [Phos]CAGGTGATGGAAAAAAACCTAGTGTTGGC 3’
N211K R 5’ [Phos]TAATTGAACCACCTGTAAACGGGTCAGCTCC 3’

N211R F 5’ [Phos]CAGGTGATGGAAAAAGGCCTAGTGTTGGC 3’
N211R R 5’ [Phos]TAATTGAACCACCTGTAAACGGGTCAGCTCC 3’

E113A F 5’ [Phos]CATGGCGTCTGGGCAACTTATTTTCCACC 3’
E113A R 5’ [Phos]TATGTATTGTAAATCGTGTTCCAAACACTC 3’

D150A F 5’ [Phos]GCCGAACATGGGGTGCTGTTATGATACCTAG 3’
D150A R 5’ [Phos]CTGGTAGCGATTGATAAAATCTATCTAAAGC 3’

D208A F 5’ [Phos]GTTCAATTACAGGTGCTGGAAAAAATCCTAG 3’
D208A R 5’ [Phos]CACCTGTAAACGGGTCAGCTCCCATTGCAAG 3’

D208A N211H F 5’ [Phos]GTTCAATTACAGGTGCTGGAAAACATCCTAG 3’
D208A N211H R 5’ [Phos]CACCTGTAAACGGGTCAGCTCCCATTGCAAG 3

Appendix D

Unpublished Dissertation-Related Preliminary Data

Chimeragenesis directed towards thermostabilizing Gram-positive endolysins is listed as a future goal in this dissertation; however, preliminary studies using this bioengineering strategy have already begun. While not fully developed into a complete chapter or publication, this appendix contains preliminary chimeragenesis studies involving the identification of thermostable EAD and CBD candidates (e.g. PlyG EAD/CBD and Nor1) and subsequently swapping these modules for their thermolabile counterparts from various Gram-positive endolysins. Here we focus on performing chimeragenesis on PlyC, where the GyH and CHAP domains are removed from the catalytic subunit and replaced with a thermostable catalytic domain.

As previously mentioned, our lab has recently investigated the thermal behavior of the PlyG endolysin. Thermodynamically characterizing the individual EAD and CBD modules of PlyG revealed that both domains are intrinsically thermostable, with the thermally-induced unfolding of the EAD and CBD each exhibiting a three-state thermal transition with respective T_G values of 65.40°C and 68.06°C (Fig. D-1). As a result, these two domains would represent excellent candidates for use in constructing thermostabilized endolysin chimeras. The PlyG EAD could replace a thermosusceptible EAD of any Gram-positive endolysin and the PlyG CBD can be substituted for unstable CBDs belonging to endolysins that target *B. anthracis*. To illustrate this concept, our lab constructed a PlyC chimera using the EAD derived from the *L. monocytogenes* endolysin Ply511, also known in the literature as HPL511, which is a catalytic domain described in

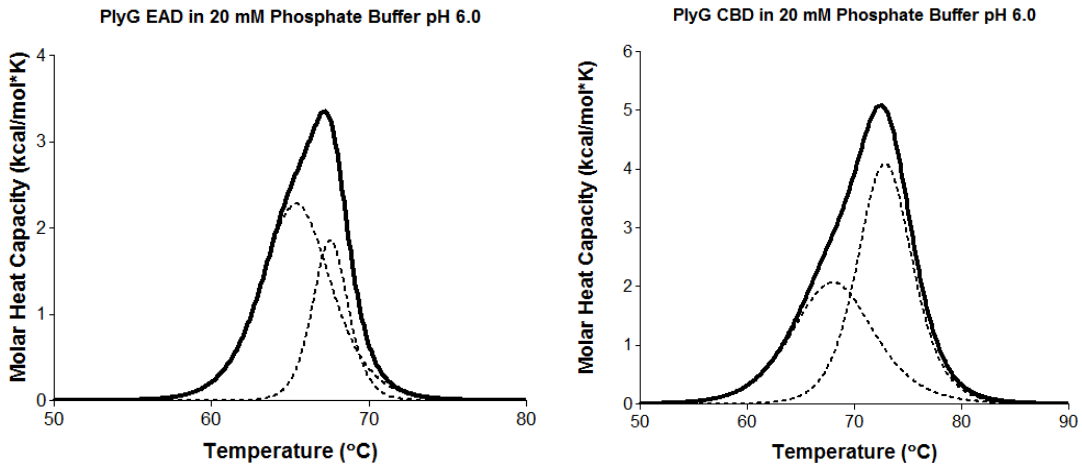

Figure D-1. DSC analysis of the isolated EAD and CBD of PlyG. The thermal properties of the purified EAD and CBD modules that constitute the *B. anthracis* endolysin PlyG were analyzed using DSC. The EAD (left) at 0.5 mg/ml and CBD (right) at 0.25 mg/ml were heated from 15°C to 105°C in 20 mM sodium phosphate buffer pH 6.0 using a heating rate of 1°C/min.

literature as being highly kinetically stable (Fig. 5-1c) (Schmelcher et al., 2012c). Using the PlyC crystal structure depicted in Fig. 1-8 as a guide, the N-terminal GyH domain, linker 1, linker 2 and the C-terminal CHAP domain were deleted from PlyCA. The Ply511 EAD was then N-terminally fused to the helical docking domain of PlyCA using the endogenous proline-rich linker of the Ply511 endolysin (i.e. the linker that naturally conjoins the EAD and CBD of Ply511). The resulting chimera, termed PlyCΔΔPly511_N, was then expressed, purified and thermally characterized. Kinetic inactivation analysis at 45°C showed that the PlyCΔΔPly511_N chimera still retained ~93% residual lytic activity at the conclusion of the 3 hour experiment, whereas wild-type PlyC, with a $t_{1/2}$ of 17.84 minutes, only maintained 5% residual activity after 3 hours (Fig. D-2). The thermodynamic stability of the isolated Ply511 EAD, which was still unknown, and PlyCΔΔPly511_N were elucidated using DSC. The thermally-induced unfolding of the Ply511 EAD exhibited a three-state thermal transition, with a T_G of 54.08°C (Fig. D-3a), while PlyCΔΔPly511_N exhibited a five-state thermal transition, with an EAD (i.e. PlyCAΔΔPly511_N) T_G of 54.21°C (Fig. D-3b). Considering the wild-type PlyCA subunit in a holoenzyme background yields a T_G of 48.27 at pH 7.0, the chimeric EAD subunit displayed a significant 5.94°C enhancement in thermodynamic stability.

With the limited availability of thermostable EAD candidates for chimeragenesis, a bioinformatic and literature search was conducted to identify additional peptidoglycan hydrolase catalytic domains from thermophilic bacteria or phage (Table 5-1). One peptidoglycan hydrolase catalytic domain candidate was encoded by the thermophile *Thermosinus carboxydivorans* strain Nor1, which is a bacterium that grows in the Norris

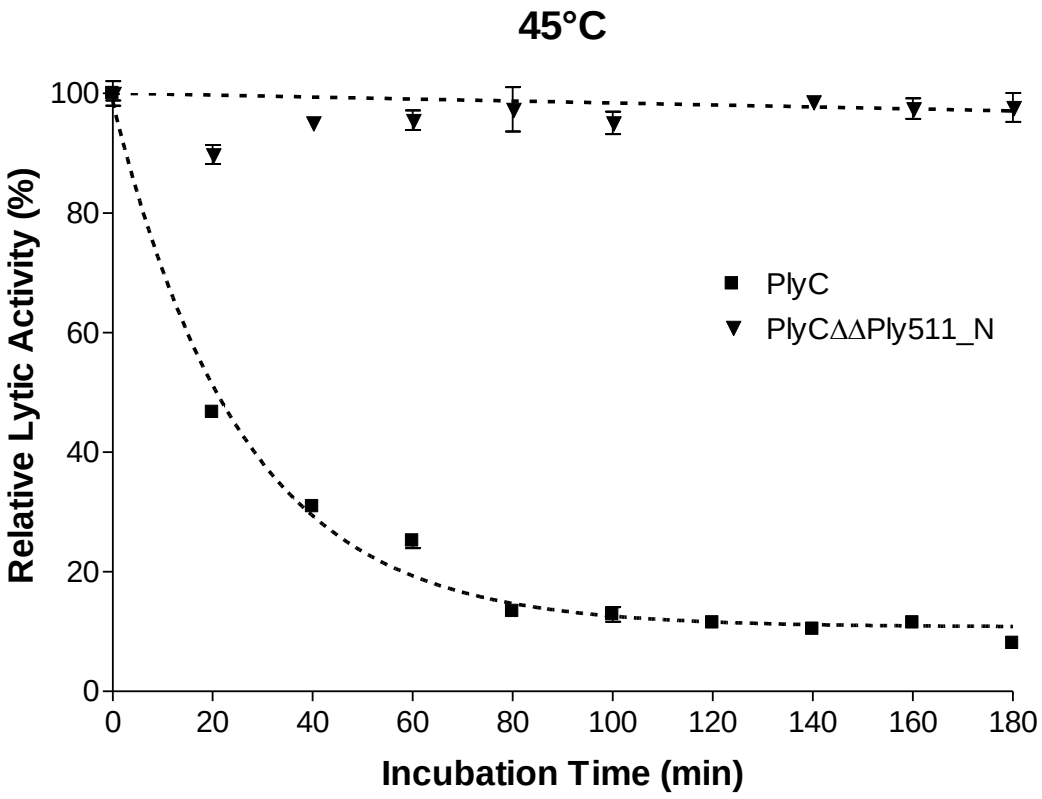

Figure D-2. Kinetic inactivation of wild-type PlyC and PlyCΔΔPly511_N at 45°C. PlyC (44 nM) in PBS pH 7.2 or PlyCΔΔPly511_N (1.1 μM) in Tris pH 8.0, 200 mM NaCl were incubated at 45°C for a total of 3 hours. At 20 minute time intervals, an aliquot of each sample was removed and cooled on ice. The heat-treated enzyme samples were then assayed for residual lytic activity against *S. pyogenes* in a turbidity reduction assay. The activity displayed by each sample was normalized to the activity displayed by an unheated control.

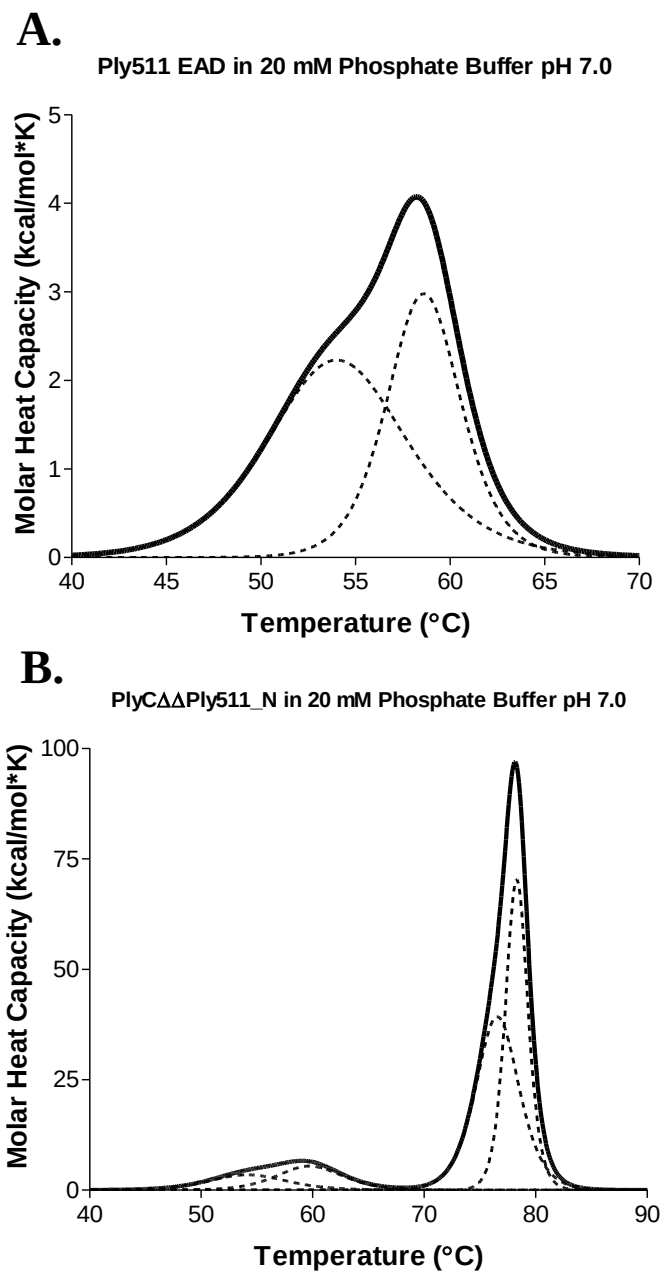

Figure D-3. Thermodynamic characterization of Ply511 EAD and PlyCΔΔPly511_N. The (a) isolated Ply511 EAD and (b) PlyCΔΔPly511_N chimera were thermodynamically investigated using DSC. Each enzyme at 1 mg/ml was heated from 15°C to 105°C in 20 mM sodium phosphate buffer pH 7.0 using a heating rate of 1°C/min.

Basin at Yellowstone National Park (Sokolova et al., 2004). This particular catalytic domain, termed Nor1, was experimentally shown by DSC to be exceedingly thermostable, with a T_G of 84.8°C (Fig. D-4a). In a PlyCΔΔ background (PlyC holoenzyme with PlyCA GyH domain, CHAP domain, and linker 1 or linker 2 deletions), Nor1 was fused N-terminally to the helical docking domain of PlyCA using linker 1. The resulting chimera, PlyCΔΔNor1_N, was then expressed, purified and thermally characterized. Results from a CD thermal denaturation experiment revealed the chimera had a resulting $T_{1/2}$ of 72.8°C (Fig. D-4b). Compared to wild-type PlyC, the chimera had $\Delta T_{1/2}$ improvement of ~23°C.

Chimeragenesis offers yet another powerful protein engineering tool to compliment rationale-based computational screening and directed evolution when seeking to increase the thermal stability of Gram-positive endolysins. This particular engineering methodology will become more practical as the list of thermostable EAD and CBD modules expands. Nonetheless, there are several EAD and CBD candidates currently available that can be utilized to significantly enhance the thermal stability of endolysins and thus increase their antimicrobial potential.

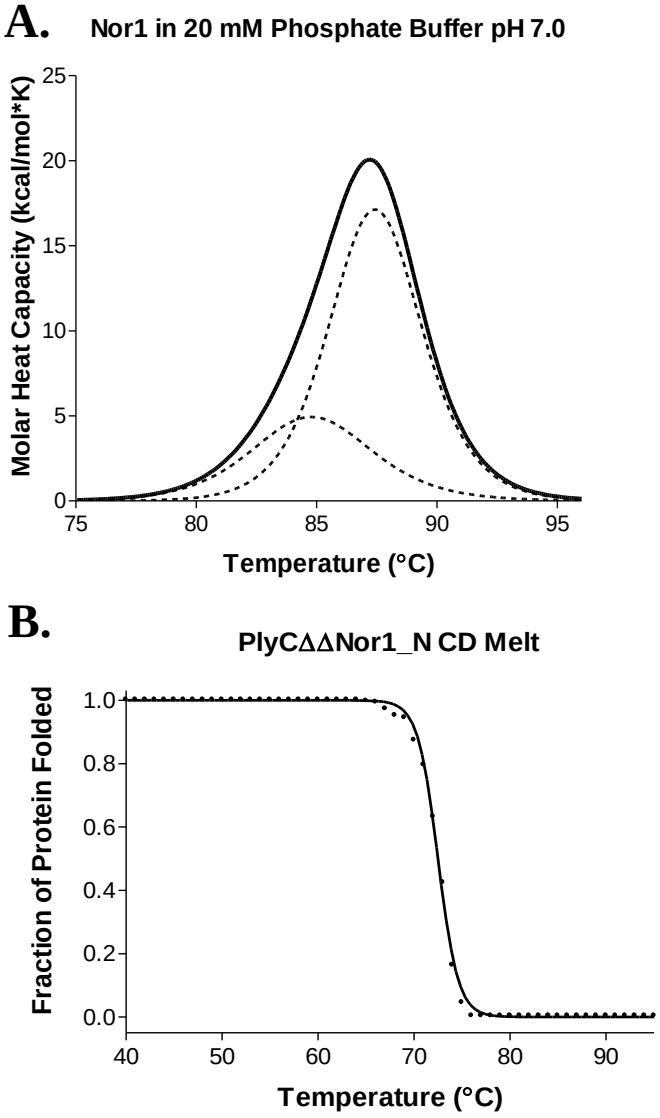

Figure D-4. Biophysical characterization of a thermostabilized streptococcal chimera endolysin. (a) Nor1 at 1 mg/ml was thermodynamically characterized by DSC in 20 mM sodium phosphate buffer from 15°C to 105°C using a heating rate of 1°C/min. (b) The thermal stability of 1 mg/ml PlyCΔΔNor1_N in 20 mM sodium phosphate buffer pH 7.0 was analyzed using CD spectroscopy by monitoring the α-helical content at 222 nm from 20°C to 95°C using a heating rate of 1°C/min.

Appendix E

List of Published or Submitted Co-Authored Manuscripts

High Throughput Structural Analysis of Yeast Ribosomes Using hSHAPE

This appendix contains the abstract for the following co-authored publication:

Jonathan A. Leshin, **Ryan Heselpoth**, Ashton Trey Belew, and Jonathan Dinman (2011). High throughput structural analysis of yeast ribosomes using hSHAPE. RNA Biol *8,* 478-487.

Abstract

Global mapping of rRNA structure by traditional methods is prohibitive in terms of time, labor and expense. High throughput selective 2' hydroxyl acylation analyzed by primer extension (hSHAPE) bypasses these problems by using fluorescently labeled primers to perform primer extension reactions, the products of which can be separated by capillary electrophoresis, thus enabling long read lengths in a cost effective manner. The data so generated is analyzed in a quantitative fashion using SHAPEFinder. This approach was used to map the flexibility of nearly the entire sequences of the 3 largest rRNAs from intact, empty yeast ribosomes. Mapping of these data onto near-atomic resolution yeast ribosome structures revealed the binding sites of known trans-acting factors, as well as previously unknown highly flexible regions of yeast rRNA.

Refinement of this technology will enable nucleotide-specific mapping of changes in rRNA structure depending on the status of tRNA occupancy, the presence or absence of other trans-acting factors, due to mutations of intrinsic ribosome components or extrinsic factors affecting ribosome biogenesis, or in the presence of translational inhibitors.

X-ray Crystal Structure of the Streptococcal Specific Phage Lysin PlyC

This appendix contains the abstract for the following co-authored publication:

Sheena McGowan, Ashley M. Buckle, Micheal S. Mitchell, James T. Hoopes, D. Travis Gallagher, **Ryan D. Heselpoth**, Yang Shen, Cyril F. Reboul, Ruby H. Law, Vincent A. Fischetti, James C. Whisstock, and Daniel C. Nelson (2012). X-ray Crystal Structure of the Streptococcal Specific Phage Lysin PlyC. Proc Natl Acad Sci U S A *109*, 12752-12757.

Abstract

Bacteriophages deploy lysins that degrade the bacterial cell wall and facilitate virus egress from the host. When applied exogenously, these enzymes destroy susceptible microbes and, accordingly, have potential as therapeutic agents. The most potent lysin identified to date is PlyC, an enzyme assembled from two components (PlyCA and PlyCB) that is specific for streptococcal species. Here the structure of the PlyC holoenzyme reveals that a single PlyCA moiety is tethered to a ring-shaped assembly of eight PlyCB molecules. Structure-guided mutagenesis reveals that the bacterial cell wall binding is achieved through a cleft on PlyCB. Unexpectedly, our structural data reveal that PlyCA contains a glycoside hydrolase domain in addition to the previously recognized cysteine, histidine-dependent amidohydrolases/peptidases catalytic domain. The presence of eight cell wall-binding domains together with two catalytic domains may explain the extraordinary potency of the PlyC holoenyzme toward target bacteria.

Crystal Structure of ORF210 from *E. coli* O157:H7 Phage CBA120 (TSP1), a Putative Tailspike Protein

This appendix contains the abstract for the following co-authored publication:

Chen Chen, Patrick Bales, Julia Greenfield, **Ryan D. Heselpoth**, Daniel C. Nelson, and Osnat Herzberg (2014). Crystal Structure of ORF210 from *E. coli* O157:H7 Phage CBA120 (TSP1), a Putative Tailspike Protein. PLoS One *9*, e93156.

Abstract

Bacteriophage tailspike proteins act as primary receptors, often possessing endoglycosidase activity toward bacterial lipopolysaccharides or other exopolysaccharides, which enable phage absorption and subsequent DNA injection into the host. Phage CBA120, a contractile long-tailed Viunalikevirus phage infects the virulent *Escherichia coli* O157:H7. This phage encodes four putative tailspike proteins exhibiting little amino acid sequence identity, whose biological roles and substrate specificities are unknown. Here we focus on the first tailspike, TSP1, encoded by the orf210 gene. We have discovered that TSP1 is resistant to protease degradation, exhibits high thermal stability, but does not cleave the O157 antigen. An immune-dot blot has shown that TSP1 binds strongly to non-O157:H7 *E. coli* cells and more weakly to *K. pneumoniae* cells, but exhibits little binding to *E. coli* O157:H7 strains. To facilitate structure-function studies, we have determined the crystal structure of TSP1 to a resolution limit of 1.8 Å. Similar to other tailspikes proteins, TSP1 assembles into

elongated homotrimers. The receptor binding region of each subunit adopts a right-handed parallel β helix, reminiscent yet not identical to several known tailspike structures. The structure of the N-terminal domain that binds to the virion particle has not been seen previously. Potential endoglycosidase catalytic sites at the three subunit interfaces contain two adjacent glutamic acids, unlike any catalytic machinery observed in other tailspikes. To identify potential sugar binding sites, the crystal structures of TSP1 in complexes with glucose, α-maltose, or α-lactose were determined. These structures revealed that each sugar binds in a different location and none of the environments appears consistent with an endoglycosidase catalytic site. Such sites may serve to bind sugar units of a yet to be identified bacterial exopolysaccharide.

Characterization of AlgMsp, an Alginate Lyase from *Microbulbifer* sp. 6532A

This appendix contains the abstract for the following co-authored manuscript that has been submitted for publication:

Steve M. Swift, Jeffrey W. Hudgens, **Ryan D. Heselpoth**, Patrick M. Bales, and Daniel C. Nelson. Characterization of AlgMsp, an Alginate Lyase from *Microbulbifer* sp. 6532A *(Submitted)*

Abstract

Alginate is a polysaccharide produced by certain seaweeds and bacteria that consists of mannuronic acid and guluronic acid residues. Seaweed alginate is used in food and industrial chemical processes, while the biosynthesis of bacterial alginate is associated with pathogenic *Pseudomonas aeruginosa*. Alginate lyases cleave this polysaccharide into short oligo-uronates and thus have the potential to be utilized for both industrial and medicinal applications. An alginate lyase gene, algMsp, from *Microbulbifer* sp. 6532A, was synthesized as an *E.coli* codon-optimized clone. The resulting 37 kDa recombinant protein, AlgMsp, was expressed, purified and characterized. The alginate lyase displayed highest activity at pH 8 and 0.2 M NaCl. Activity of the alginate lyase was greatest at 50°C; however the enzyme was not stable over time when incubated at 50°C. The alginate lyase was still highly active at 25°C and displayed little or no loss of activity after 24 hours at 25°C. The activity of AlgMsp was

not dependent on the presence of divalent cations. Comparing activity of the lyase against polymannuronic acid and polyguluronic acid substrates showed higher specific activity towards polymannuronic acid. However, AlgMSP exhibited greater binding affinity to the polyguluronic acid substrate. Prolonged AlgMsp-mediated degradation of alginate produced dimer, trimer, tetramer, and pentamer oligo-uronates.

Biochemical and Biophysical Characterization of PlyGRCS, a Bacteriophage Endolysin Active against Methicillin-Resistant *Staphylococcus aureus*

This appendix contains the abstract for the following co-authored manuscript that has been submitted for publication:

Sara B. Linden, Helena Zhang, **Ryan D. Heselpoth**, Yang Shen, Mathias Schmelcher, Fritz Eichenseher, and Daniel C. Nelson. Biochemical and Biophysical Characterization of PlyGRCS, a Bacteriophage Endolysin Active against Methicillin-Resistant *Staphylococcus aureus*. *(Submitted)*

Abstract

The increasing rate of resistance of pathogenic bacteria, such as *Staphylococcus aureus*, to classical antibiotics has driven research towards identification of other means to fight infectious disease. One particularly viable option is the use of bacteriophage-encoded peptidoglycan hydrolases, called endolysins or enzybiotics. These enzymes lyse the bacterial cell wall upon direct contact, are not inhibited by traditional antibiotic resistance mechanisms, and have already shown great promise in the areas of food safety, human health, and veterinary science. We have identified and characterized an endolysin, PlyGRCS, which displays dose-dependent antimicrobial activity against both planktonic and biofilm *S. aureus*, including methicillin-resistant *S. aureus* (MRSA). The host range for this enzyme includes all *S. aureus* and *S. epidermidis* strains tested, but not other

Gram-positive pathogens. The contributions of the PlyGRCS putative catalytic and cell wall binding domains were investigated through deletion analysis. The cysteine, histidine-dependent amidohydrolase/peptidase (CHAP) catalytic domain displayed activity by itself, though reduced, indicating the necessity of the binding domain for full activity. In contrast, the SH3_5 binding domain lacked activity but was shown to interact directly with the staphylococcal cell wall via fluorescent microscopy. Site-directed mutagenesis studies determined that the active-site residues in the CHAP catalytic domain were C29 and H92, and its catalytic functionality required calcium as a co-factor. Finally, biochemical assays coupled with mass spectrometry analysis determined that PlyGRCS displays both N-acetylmuramoyl-L-alanine amidase and D-alanyl-glycyl endopeptidase hydrolytic activities despite possessing only a single catalytic domain. These results indicate that PlyGRCS has the potential to become a revolutionary therapeutic option to combat bacterial infections.

HexNW is a Highly Thermostabile Glucosaminidase that Disperses *S. epidermidis* Biofilms

This appendix contains the abstract for the following co-authored manuscript that has been submitted for publication:

Patrick M. Bales, **Ryan D. Heselpoth**, and Daniel C. Nelson. HexNW is a Highly Thermostabile Glucosaminidase that Disperses *S. epidermidis* Biofilms. *(Submitted)*

Abstract

Staphylococcus epidermidis is a bacterium that is found on the skin of almost all humans but is capable of opportunistic infection (often by colonizing medical implant devices). When it does so, it normally survives by growing as a biofilm. Biofilm-forming bacteria are notoriously difficult to eradicate due to the resistance to antimicrobials and other stressors provided by the extracellular polymeric substance (EPS). Polysaccharide intercellular adhesin (PIA) is a major constituent of *Staphylococcus epidermidis* EPS and is made up of partially deacetylated β-1,6-*N*-acetylglucosamine. A bioinformatics search of putative hexosaminidases and glucosaminidases that may be able to break up *S. epidermidis* biofilms revealed an uncharacterized enzyme produced by *Neisseria wadsworthii*, henceforth referred to as HexNW. It was found to be active against a synthetic substrate containing *N*-acetylglucosamine and had a K_m of 1.13 mM and V_{max} of 22.06 pmols/sec, but it did not display activity against chitin-like substrates. In addition, HexNW was found to be highly thermostable by measuring enzymatic activity

after incubation at various temperatures and by performing circular dichroism and differential scanning calorimetry. Finally, HexNW was shown to be antagonistic to *S. epidermidis* biofilms by monitoring the release of amino sugars and colony-forming units from the surface of the biofilm. In addition, a 2-fold decrease in the minimum biofilm elimination concentration (MBEC) was observed when HexNW was used to supplement vancomycin treatment of a methicillin-resistant *S. epidermidis* strain.

Bibliography

Abraham, E.P., and Chain, E. (1940). An enzyme from bacteria able to destroy penicillin. Nature *146*, 837.

Akasako, A., Haruki, M., Oobatake, M., and Kanaya, S. (1995). High resistance of *Escherichia coli* ribonuclease HI variant with quintuple thermostabilizing mutations to thermal denaturation, acid denaturation, and proteolytic degradation. Biochemistry *34*, 8115-8122.

Aminov, R.I. (2010). A brief history of the antibiotic era: lessons learned and challenges for the future. Frontiers in microbiology *1*, 134.

Anderson, D.E., Hurley, J.H., Nicholson, H., Baase, W.A., and Matthews, B.W. (1993). Hydrophobic core repacking and aromatic-aromatic interaction in the thermostable mutant of T4 lysozyme Ser 117-->Phe. Protein Sci *2*, 1285-1290.

Anderson, G., and Scott, M. (1991). Determination of product shelf life and activation energy for five drugs of abuse. Clin Chem *37*, 398-402.

Andersson, D.I., and Hughes, D. (2010). Antibiotic resistance and its cost: is it possible to reverse resistance? Nature reviews Microbiology *8*, 260-271.

Antikainen, N.M., and Martin, S.F. (2005). Altering protein specificity: techniques and applications. Bioorg Med Chem *13*, 2701-2716.

Arakawa, T., and Prestrelski, S.J. (1993). Factors affecting short-term and long-term stabilities of proteins. Advanced drug delivery reviews *10*, 1-28.

Armelagos, G.J. (1969). Disease in ancient Nubia. Science *163*, 255-259.

Arnold, F.H., Wintrode, P.L., Miyazaki, K., and Gershenson, A. (2001). How enzymes adapt: lessons from directed evolution. Trends in biochemical sciences *26*, 100-106.

Arnoldi, M., Fritz, M., Bauerlein, E., Radmacher, M., Sackmann, E., and Boulbitch, A. (2000). Bacterial turgor pressure can be measured by atomic force microscopy. Physical review E, Statistical physics, plasmas, fluids, and related interdisciplinary topics *62*, 1034-1044.

Ashworth, J., Havranek, J.J., Duarte, C.M., Sussman, D., Monnat, R.J., Jr., Stoddard, B.L., and Baker, D. (2006). Computational redesign of endonuclease DNA binding and cleavage specificity. Nature *441*, 656-659.

Austrian, R., Douglas, R.M., Schiffman, G., Coetzee, A.M., Koornhof, H.J., Hayden-Smith, S., and Reid, R.D. (1976). Prevention of pneumococcal pneumonia by vaccination. Transactions of the Association of American Physicians *89*, 184-194.

Ayres, H.M., Payne, D.N., Furr, J.R., and Russell, A.D. (1998). Effect of permeabilizing agents on antibacterial activity against a simple *Pseudomonas aeruginosa* biofilm. Lett Appl Microbiol *27*, 79-82.

Babalova, E.G., Katsitadze, K.T., Sakvarelidze, L.A., Imnaishvili, N., Sharashidze, T.G., Badashvili, V.A., Kiknadze, G.P., Meipariani, A.N., Gendzekhadze, N.D., Machavariani, E.V., *et al.* (1968). [Preventive value of dried dysentery bacteriophage]. Zhurnal mikrobiologii, epidemiologii, i immunobiologii *45*, 143-145.

Banin, E., Brady, K.M., and Greenberg, E.P. (2006). Chelator-induced dispersal and killing of *Pseudomonas aeruginosa* cells in a biofilm. Appl Environ Microbiol *72*, 2064-2069.

Banin, E., Vasil, M.L., and Greenberg, E.P. (2005). Iron and *Pseudomonas aeruginosa* biofilm formation. Proc Natl Acad Sci U S A *102*, 11076-11081.

Bassett, E.J., Keith, M.S., Armelagos, G.J., Martin, D.L., and Villanueva, A.R. (1980). Tetracycline-labeled human bone from ancient Sudanese Nubia (A.D. 350). Science *209*, 1532-1534.

Beadle, B.M., and Shoichet, B.K. (2002). Structural bases of stability-function tradeoffs in enzymes. J Mol Biol *321*, 285-296.

Becker, S.C., Dong, S., Baker, J.R., Foster-Frey, J., Pritchard, D.G., and Donovan, D.M. (2009). LysK CHAP endopeptidase domain is required for lysis of live staphylococcal cells. FEMS Microbiol Lett *294*, 52-60.

Becker, S.C., Foster-Frey, J., and Donovan, D.M. (2008). The phage K lytic enzyme LysK and lysostaphin act synergistically to kill MRSA. FEMS Microbiol Lett *287*, 185-191.

Behring, E., and Kitasako, S. (1890). Ueber das Zustandekommen der Diphtherie-Immunitat undder Tetanus-Immunitat bei Thieren. Deutsche medizinische Wochenschrift *16*, 1113-1114.

Belanger, F., Theberge-Julien, G., Cunningham, P.R., and Brakier-Gingras, L. (2005). A functional relationship between helix 1 and the 900 tetraloop of 16S ribosomal RNA within the bacterial ribosome. Rna *11*, 906-913.

Benedix, A., Becker, C.M., de Groot, B.L., Caflisch, A., and Bockmann, R.A. (2009). Predicting free energy changes using structural ensembles. Nature methods *6*, 3-4.

Berlutti, F., Morea, C., Battistoni, A., Sarli, S., Cipriani, P., Superti, F., Ammendolia, M.G., and Valenti, P. (2005). Iron availability influences aggregation, biofilm, adhesion and invasion of *Pseudomonas aeruginosa* and *Burkholderia cenocepacia*. International journal of immunopathology and pharmacology *18*, 661-670.

Blaber, M., Zhang, X.J., and Matthews, B.W. (1993). Structural basis of amino acid alpha helix propensity. Science *260*, 1637-1640.

Blaser, M.J., and Bartlett, J.G. (2006). Letter to FDA Commissioner Andrew C. von Eschenbach, MD (Infectious Diseases Society of America).

Bogin, O., Peretz, M., Hacham, Y., Korkhin, Y., Frolow, F., Kalb, A.J., and Burstein, Y. (1998). Enhanced thermal stability of *Clostridium beijerinckii* alcohol dehydrogenase after strategic substitution of amino acid residues with prolines from the homologous thermophilic *Thermoanaerobacter brockii* alcohol dehydrogenase. Protein Sci *7*, 1156-1163.

Bogovazova, G.G., Voroshilova, N.N., Bondarenko, V.M., Gorbatkova, G.A., Afanas'eva, E.V., Kazakova, T.B., Smirnov, V.D., Mamleeva, A.G., Glukharev Iu, A., Erastova, E.I., *et al.* (1992). [Immunobiological properties and therapeutic effectiveness of preparations from *Klebsiella* bacteriophages]. Zhurnal mikrobiologii, epidemiologii, i immunobiologii, 30-33.

Bornscheuer, U.T., Altenbuchner, J., and Meyer, H.H. (1999). Directed evolution of an esterase: screening of enzyme libraries based on pH-indicators and a growth assay. Bioorg Med Chem *7*, 2169-2173.

Bortolussi, R. (2008). Listeriosis: a primer. CMAJ : Canadian Medical Association journal = journal de l'Association medicale canadienne *179*, 795-797.

Borysowski, J., and Gorski, A. (2010). Fusion to cell-penetrating peptides will enable lytic enzymes to kill intracellular bacteria. Medical hypotheses *74*, 164-166.

Borysowski, J., Weber-Dabrowska, B., and Gorski, A. (2006). Bacteriophage endolysins as a novel class of antibacterial agents. Exp Biol Med (Maywood) *231*, 366-377.

Boucher, H.W. (2008). Open public forum. In: FDA Anti-Infective Drugs Advistory Committee: Joint with Drug Safety and Risk Management Advisory Committee (Silver Spring, MD).

Brakmann, S. (2001). Discovery of superior enzymes by directed molecular evolution. Chembiochem *2*, 865-871.

Bramley, A.J., and Foster, R. (1990). Effects of lysostaphin on *Staphylococcus aureus* infections of the mouse mammary gland. Research in veterinary science *49*, 120-121.

Breukink, E., and de Kruijff, B. (2006). Lipid II as a target for antibiotics. Nature reviews Drug discovery *5*, 321-332.

Briers, Y., Schmelcher, M., Loessner, M.J., Hendrix, J., Engelborghs, Y., Volckaert, G., and Lavigne, R. (2009). The high-affinity peptidoglycan binding domain of *Pseudomonas* phage endolysin KZ144. Biochem Biophys Res Commun *383*, 187-191.

Briers, Y., Volckaert, G., Cornelissen, A., Lagaert, S., Michiels, C.W., Hertveldt, K., and Lavigne, R. (2007). Muralytic activity and modular structure of the endolysins of *Pseudomonas aeruginosa* bacteriophages phiKZ and EL. Mol Microbiol *65*, 1334-1344.

Brouillette, E., and Malouin, F. (2005). The pathogenesis and control of *Staphylococcus aureus*-induced mastitis: study models in the mouse. Microbes and infection / Institut Pasteur *7*, 560-568.

Brucato, F.H., and Pizzo, S.V. (1990). Catabolism of streptokinase and polyethylene glycol-streptokinase: evidence for transport of intact forms through the biliary system in the mouse. Blood *76*, 73-79.

Buchanan-Wollaston, V., Passiatore, J.E., and Cannon, F. (1987). The *mob* and *oriT* mobilization functions of a bacterial plasmid promote its transfer to plants. Nature *328*, 172-175.

Buchwald, U.K., and Pirofski, L. (2003). Immune therapy for infectious diseases at the dawn of the 21st century: the past, present and future role of antibody therapy, therapeutic vaccination and biological response modifiers. Current pharmaceutical design *9*, 945-968.

Burley, S.K., and Petsko, G.A. (1985). Aromatic-aromatic interaction: a mechanism of protein structure stabilization. Science *229*, 23-28.

Bustamante, N., Rico-Lastres, P., Garcia, E., Garcia, P., and Menendez, M. (2012). Thermal stability of Cpl-7 endolysin from the *Streptococcus pneumoniae* bacteriophage Cp-7; cell wall-targeting of its CW_7 motifs. PLoS One *7*, e46654.

Cadwell, R.C., and Joyce, G.F. (1992). Randomization of genes by PCR mutagenesis. PCR methods and applications *2*, 28-33.

Callanan, M.J., Russell, W.M., and Klaenhammer, T.R. (2007). Modification of *Lactobacillus* beta-glucuronidase activity by random mutagenesis. Gene *389*, 122-127.

Campbell, I.D. (2002). Timeline: the march of structural biology. Nature reviews Molecular cell biology *3*, 377-381.

Capriotti, E., Fariselli, P., and Casadio, R. (2005). I-Mutant2.0: predicting stability changes upon mutation from the protein sequence or structure. Nucleic Acids Res *33*, W306-310.

Capriotti, E., Fariselli, P., Rossi, I., and Casadio, R. (2008). A three-state prediction of single point mutations on protein stability changes. BMC Bioinformatics *9 Suppl 2*, S6.

Carpenter, J.F., Crowe, J.H., and Arakawa, T. (1990). Comparison of solute-induced protein stabilization in aqueous solution and in the frozen and dried states. Journal of dairy science *73*, 3627-3636.

Carpenter, J.F., Hand, S.C., Crowe, L.M., and Crowe, J.H. (1986). Cryoprotection of phosphofructokinase with organic solutes: characterization of enhanced protection in the presence of divalent cations. Arch Biochem Biophys *250*, 505-512.

Casadevall, A. (1996). Antibody-based therapies for emerging infectious diseases. Emerging infectious diseases *2*, 200-208.

Celia, L.K., Nelson, D., and Kerr, D.E. (2008). Characterization of a bacteriophage lysin (Ply700) from *Streptococcus uberis*. Vet Microbiol *130*, 107-117.

Centers for Disease Control and Prevention (1985). Polysaccharide vaccine for prevention of *Haemophilus influenzae* type b disease. MMWR Morbidity and mortality weekly report *34*, 201-205.

Centers for Disease Control and Prevention (2013). Antibiotic resistance threats in the United States.

Chain, E., Florey, H.W., Gardner, A.D., Heatley, N.G., Jennings, M.A., Orr-Ewing, J., and Sanders, A.G. (2005). THE CLASSIC: penicillin as a chemotherapeutic agent. 1940. Clinical orthopaedics and related research *439*, 23-26.

Chang, B.S., Beauvais, R.M., Dong, A., and Carpenter, J.F. (1996). Physical factors affecting the storage stability of freeze-dried interleukin-1 receptor antagonist: glass transition and protein conformation. Arch Biochem Biophys *331*, 249-258.

Cheng, J., Randall, A., and Baldi, P. (2006). Prediction of protein stability changes for single-site mutations using support vector machines. Proteins *62*, 1125-1132.

Cheng, Q., and Fischetti, V.A. (2007). Mutagenesis of a bacteriophage lytic enzyme PlyGBS significantly increases its antibacterial activity against group B streptococci. Appl Microbiol Biotechnol *74*, 1284-1291.

Cheng, Q., Nelson, D., Zhu, S., and Fischetti, V.A. (2005). Removal of group B streptococci colonizing the vagina and oropharynx of mice with a bacteriophage lytic enzyme. Antimicrob Agents Chemother *49*, 111-117.

Cherry, J.R., and Fidantsef, A.L. (2003). Directed evolution of industrial enzymes: an update. Curr Opin Biotechnol *14*, 438-443.

Chevalier, B.S., and Stoddard, B.L. (2001). Homing endonucleases: structural and functional insight into the catalysts of intron/intein mobility. Nucleic Acids Res *29*, 3757-3774.

Choudhury, D., Biswas, S., Roy, S., and Dattagupta, J.K. (2010). Improving thermostability of papain through structure-based protein engineering. Protein Eng Des Sel *23*, 457-467.

Cislo, M., Dabrowski, M., Weber-Dabrowska, B., and Woyton, A. (1987). Bacteriophage treatment of suppurative skin infections. Archivum immunologiae et therapiae experimentalis *35*, 175-183.

Clantin, B., Tricot, C., Lonhienne, T., Stalon, V., and Villeret, V. (2001). Probing the role of oligomerization in the high thermal stability of *Pyrococcus furiosus* ornithine carbamoyltransferase by site-specific mutants. Eur J Biochem *268*, 3937-3942.

Clarke, J., and Fersht, A.R. (1993). Engineered disulfide bonds as probes of the folding pathway of barnase: increasing the stability of proteins against the rate of denaturation. Biochemistry *32*, 4322-4329.

Coates, A., Hu, Y., Bax, R., and Page, C. (2002). The future challenges facing the development of new antimicrobial drugs. Nature reviews Drug discovery *1*, 895-910.

Colebrook, L. (1954). Almroth Wright: Provocative Doctor and Thinker (London: Heinemann).

Cook, M., Molto, E., and Anderson, C. (1989). Fluorochrome labelling in Roman period skeletons from Dakhleh Oasis, Egypt. American journal of physical anthropology *80*, 137-143.

Cooper, A., Eyles, S.J., Radford, S.E., and Dobson, C.M. (1992). Thermodynamic consequences of the removal of a disulphide bridge from hen lysozyme. J Mol Biol *225*, 939-943.

Croux, C., Ronda, C., Lopez, R., and Garcia, J.L. (1993a). Interchange of functional domains switches enzyme specificity: construction of a chimeric pneumococcal-clostridial cell wall lytic enzyme. Mol Microbiol *9*, 1019-1025.

Croux, C., Ronda, C., Lopez, R., and Garcia, J.L. (1993b). Role of the C-terminal domain of the lysozyme of *Clostridium acetobutylicum* ATCC 824 in a chimeric pneumococcal-clostridial cell wall lytic enzyme. FEBS Lett *336*, 111-114.

Crowe, J.H., Crowe, L.M., and Carpenter, J.F. (1993a). Preserving dry biomaterials: the water replacement hypothesis, part 1. BioPharm *6*, 28-29, 32-33.

Crowe, J.H., Crowe, L.M., and Carpenter, J.F. (1993b). Preserving dry biomaterials: the water replacement hypothesis, part 2. BioPharm *6*, 40-43.

Cui, L., and Su, X.Z. (2009). Discovery, mechanisms of action and combination therapy of artemisinin. Expert review of anti-infective therapy *7*, 999-1013.

Dalbadie-McFarland, G., Cohen, L.W., Riggs, A.D., Morin, C., Itakura, K., and Richards, J.H. (1982). Oligonucleotide-directed mutagenesis as a general and powerful method for studies of protein function. Proc Natl Acad Sci U S A *79*, 6409-6413.

Dalhus, B., Saarinen, M., Sauer, U.H., Eklund, P., Johansson, K., Karlsson, A., Ramaswamy, S., Bjork, A., Synstad, B., Naterstad, K., *et al.* (2002). Structural basis for thermophilic protein stability: structures of thermophilic and mesophilic malate dehydrogenases. J Mol Biol *318*, 707-721.

Daniel, A., Euler, C., Collin, M., Chahales, P., Gorelick, K.J., and Fischetti, V.A. (2010). Synergism between a novel chimeric lysin and oxacillin protects against infection by methicillin-resistant *Staphylococcus aureus*. Antimicrob Agents Chemother *54*, 1603-1612.

Dantas, G., Corrent, C., Reichow, S.L., Havranek, J.J., Eletr, Z.M., Isern, N.G., Kuhlman, B., Varani, G., Merritt, E.A., and Baker, D. (2007). High-resolution structural and thermodynamic analysis of extreme stabilization of human procarboxypeptidase by computational protein design. J Mol Biol *366*, 1209-1221.

Daude, D., Topham, C.M., Remaud-Simeon, M., and Andre, I. (2013). Probing impact of active site residue mutations on stability and activity of *Neisseria polysaccharea* amylosucrase. Protein Sci *22*, 1754-1765.

Davies, J., and Davies, D. (2010). Origins and evolution of antibiotic resistance. Microbiol Mol Biol Rev *74*, 417-433.

de vries, J., Harms, K., Broer, I., Kriete, G., Mahn, A., Düring, K., and Wackernagel, W. (1999). The bacteriolytic activity in transgenic potatoes expressing the chimeric T4 lysozyme gene and the effect of T4 lysozyme on soil- and phytopathogenic bacteria. Systematic and applied microbiology *22*, 280-286.

DeHart, H.P., Heath, H.E., Heath, L.S., LeBlanc, P.A., and Sloan, G.L. (1995). The lysostaphin endopeptidase resistance gene (epr) specifies modification of peptidoglycan cross bridges in *Staphylococcus simulans* and *Staphylococcus aureus*. Appl Environ Microbiol *61*, 1475-1479.

Dehouck, Y., Kwasigroch, J.M., Gilis, D., and Rooman, M. (2011). PoPMuSiC 2.1: a web server for the estimation of protein stability changes upon mutation and sequence optimality. BMC Bioinformatics *12*, 151.

Deluca, M. (1976). Firefly luciferase. Advances in enzymology and related areas of molecular biology *44*, 37-68.

Diaz, E., Lopez, R., and Garcia, J.L. (1990). Chimeric phage-bacterial enzymes: a clue to the modular evolution of genes. Proc Natl Acad Sci U S A *87*, 8125-8129.

Diaz, E., Lopez, R., and Garcia, J.L. (1991). Chimeric pneumococcal cell wall lytic enzymes reveal important physiological and evolutionary traits. J Biol Chem *266*, 5464-5471.

Dietz, G.P. (2010). Cell-penetrating peptide technology to deliver chaperones and associated factors in diseases and basic research. Current pharmaceutical biotechnology *11*, 167-174.

Dietz, G.P., and Bahr, M. (2004). Delivery of bioactive molecules into the cell: the Trojan horse approach. Molecular and cellular neurosciences *27*, 85-131.

Diez-Martinez, R., de Paz, H., Bustamante, N., Garcia, E., Menendez, M., and Garcia, P. (2013). Improving the lethal effect of cpl-7, a pneumococcal phage lysozyme with broad bactericidal activity, by inverting the net charge of its cell wall-binding module. Antimicrob Agents Chemother *57*, 5355-5365.

DiMasi, J.A., Hansen, R.W., and Grabowski, H.G. (2003). The price of innovation: new estimates of drug development costs. Journal of health economics *22*, 151-185.

Djurkovic, S., Loeffler, J.M., and Fischetti, V.A. (2005). Synergistic killing of *Streptococcus pneumoniae* with the bacteriophage lytic enzyme Cpl-1 and penicillin or gentamicin depends on the level of penicillin resistance. Antimicrob Agents Chemother *49*, 1225-1228.

Domagk, G. (1935). Ein Beitrag zur Chemotherapie der bakteriellen Infektionen. . Deutsche medizinische Wochenschrift *61*.

Donovan, D.M., Dong, S., Garrett, W., Rousseau, G.M., Moineau, S., and Pritchard, D.G. (2006a). Peptidoglycan hydrolase fusions maintain their parental specificities. Appl Environ Microbiol *72*, 2988-2996.

Donovan, D.M., Lardeo, M., and Foster-Frey, J. (2006b). Lysis of staphylococcal mastitis pathogens by bacteriophage phi11 endolysin. FEMS Microbiol Lett *265*, 133-139.

Dorman, S.E., and Chaisson, R.E. (2007). From magic bullets back to the magic mountain: the rise of extensively drug-resistant tuberculosis. Nat Med *13*, 295-298.

Doyle, R.J., and Marquis, R.E. (1994). Elastic, flexible peptidoglycan and bacterial cell wall properties. Trends Microbiol *2*, 57-60.

Dubnau, D. (1999). DNA uptake in bacteria. Annu Rev Microbiol *53*, 217-244.

Düring, K., Porsch, P., Fladung, M., and Lorz, H. (1993). Transgenic potato plants resistant to the phytopathogenic bacterium *Erwinia carotovora*. The Plant journal : for cell and molecular biology *3*, 587-598.

Ehrlich, P., and Hata, S. (1910). Die Experimentelle Chemotherapie der Spirilosen, Vol 8, First edn (Berlin: Julius Springer).

Eijsink, V.G., Bjork, A., Gaseidnes, S., Sirevag, R., Synstad, B., van den Burg, B., and Vriend, G. (2004). Rational engineering of enzyme stability. J Biotechnol *113*, 105-120.

Eijsink, V.G., Gaseidnes, S., Borchert, T.V., and van den Burg, B. (2005). Directed evolution of enzyme stability. Biomolecular engineering *22*, 21-30.

Eijsink, V.G., Veltman, O.R., Aukema, W., Vriend, G., and Venema, G. (1995). Structural determinants of the stability of thermolysin-like proteinases. Nat Struct Biol *2*, 374-379.

Emmerich, R., and Löw, O. (1899). Bakteriolytische enzyme als Ursache der erworbenen Immunität und die Heilung von Infectionskrankheiten durch dieselben. Z Hyg *31*, 1-65.

Entenza, J.M., Loeffler, J.M., Grandgirard, D., Fischetti, V.A., and Moreillon, P. (2005). Therapeutic effects of bacteriophage Cpl-1 lysin against *Streptococcus pneumoniae* endocarditis in rats. Antimicrob Agents Chemother *49*, 4789-4792.

Facchiano, A.M., Colonna, G., and Ragone, R. (1998). Helix stabilizing factors and stabilization of thermophilic proteins: an X-ray based study. Protein Eng *11*, 753-760.

Falagas, M.E., and Karageorgopoulos, D.E. (2008). Pandrug resistance (PDR), extensive drug resistance (XDR), and multidrug resistance (MDR) among Gram-negative bacilli: need for international harmonization in terminology. Clin Infect Dis *46*, 1121-1122; author reply 1122.

Fallas, J.A., and Hartgerink, J.D. (2012). Computational design of self-assembling register-specific collagen heterotrimers. Nat Commun *3*, 1087.

Fenton, M., Casey, P.G., Hill, C., Gahan, C.G., Ross, R.P., McAuliffe, O., O'Mahony, J., Maher, F., and Coffey, A. (2010). The truncated phage lysin CHAP(k) eliminates *Staphylococcus aureus* in the nares of mice. Bioeng Bugs *1*, 404-407.

Filatova, L.Y., Becker, S.C., Donovan, D.M., Gladilin, A.K., and Klyachko, N.L. (2010). LysK, the enzyme lysing *Staphylococcus aureus* cells: specific kinetic features and approaches towards stabilization. Biochimie *92*, 507-513.

Finch, R. (2010). Antibiotic and Chemotherapy: Anti-Infective Agents and Their Use in Therapy, Ninth edn (W.B. Saunders Company).

Finch, R., Davey, P., Wilcox, M., and Irving, W. (2012). Antimicrobial Chemotherapy, 6th edn (Oxford: Oxford University Press).

Fischetti, V.A. (2003). Novel method to control pathogenic bacteria on human mucous membranes. Ann N Y Acad Sci *987*, 207-214.

Fischetti, V.A. (2005). Bacteriophage lytic enzymes: novel anti-infectives. Trends Microbiol *13*, 491-496.

Fischetti, V.A. (2008). Bacteriophage lysins as effective antibacterials. Curr Opin Microbiol *11*, 393-400.

Fischetti, V.A. (2010). Bacteriophage endolysins: a novel anti-infective to control Gram-positive pathogens. Int J Med Microbiol *300*, 357-362.

Fischetti, V.A., Gotschlich, E.C., and Bernheimer, A.W. (1971). Purification and physical properties of group C streptococcal phage-associated lysin. J Exp Med *133*, 1105-1117.

Fischetti, V.A., Jones, K.F., and Scott, J.R. (1985). Size variation of the M protein in group A streptococci. J Exp Med *161*, 1384-1401.

Fischetti, V.A., Nelson, D., and Schuch, R. (2006). Reinventing phage therapy: are the parts greater than the sum? Nat Biotechnol *24*, 1508-1511.

Fischetti, V.A., Zabriskie, J.B., and Gotschlich, E.C. (1972a). Fifth International Symposium on *Streptococcus pyogenes* (Amsterdam: Excerpta Medica).

Fischetti, V.A., Zabriskie, J.B., and Gotschlich, E.C., eds. (1972b). Physical, chemical and biological properties of Type 6 M-protein extracted with purified streptococcal phage-associated lysin (Amsterdam: Excerpta Medica).

Fujinami, Y., Hirai, Y., Sakai, I., Yoshino, M., and Yasuda, J. (2007). Sensitive detection of *Bacillus anthracis* using a binding protein originating from gamma-phage. Microbiology and immunology *51*, 163-169.

Gaeng, S., Scherer, S., Neve, H., and Loessner, M.J. (2000). Gene cloning and expression and secretion of *Listeria monocytogenes* bacteriophage-lytic enzymes in *Lactococcus lactis*. Appl Environ Microbiol *66*, 2951-2958.

Garcia, P., Lopez, R., Ronda, C., Garcia, E., and Tomasz, A. (1983). Mechanism of phage-induced lysis in pneumococci. Journal of general microbiology *129*, 479-487.

Gilis, D., and Rooman, M. (2000). PoPMuSiC, an algorithm for predicting protein mutant stability changes: application to prion proteins. Protein Eng *13*, 849-856.

Gilmer, D.B., Schmitz, J.E., Euler, C.W., and Fischetti, V.A. (2013). Novel bacteriophage lysin with broad lytic activity protects against mixed infection by *Streptococcus pyogenes* and methicillin-resistant *Staphylococcus aureus*. Antimicrob Agents Chemother *57*, 2743-2750.

Giver, L., Gershenson, A., Freskgard, P.O., and Arnold, F.H. (1998). Directed evolution of a thermostable esterase. Proc Natl Acad Sci U S A *95*, 12809-12813.

Glenny, A.T., and Hopkins, B.E. (1923). Diphtheria toxoid as an immunising agent. Br J Exp Pathol *4*, 283-288.

Gotschlich, E.C., Goldschneider, I., and Artenstein, M.S. (1969a). Human immunity to the meningococcus. IV. Immunogenicity of group A and group C meningococcal polysaccharides in human volunteers. J Exp Med *129*, 1367-1384.

Gotschlich, E.C., Liu, T.Y., and Artenstein, M.S. (1969b). Human immunity to the meningococcus. III. Preparation and immunochemical properties of the group A, group B, and group C meningococcal polysaccharides. J Exp Med *129*, 1349-1365.

Gould, S.J., and Subramani, S. (1988). Firefly luciferase as a tool in molecular and cell biology. Anal Biochem *175*, 5-13.

Grandgirard, D., Loeffler, J.M., Fischetti, V.A., and Leib, S.L. (2008). Phage lytic enzyme Cpl-1 for antibacterial therapy in experimental pneumococcal meningitis. J Infect Dis *197*, 1519-1522.

Greener, A., Callahan, M., and Jerpseth, B. (1996). An efficient random mutagenesis technique using an *E. coli* mutator strain. Methods Mol Biol *57*, 375-385.

Greenfield, N., and Fasman, G.D. (1969). Computed circular dichroism spectra for the evaluation of protein conformation. Biochemistry *8*, 4108-4116.

Grundbacher, F.J. (1992). Behring's discovery of diphtheria and tetanus antitoxins. Immunology today *13*, 188-190.

Grundling, A., Missiakas, D.M., and Schneewind, O. (2006). *Staphylococcus aureus* mutants with increased lysostaphin resistance. J Bacteriol *188*, 6286-6297.

Gu, J., Xu, W., Lei, L., Huang, J., Feng, X., Sun, C., Du, C., Zuo, J., Li, Y., Du, T., *et al.* (2011a). LysGH15, a novel bacteriophage lysin, protects a murine bacteremia model efficiently against lethal methicillin-resistant *Staphylococcus aureus* infection. J Clin Microbiol *49*, 111-117.

Gu, J., Zuo, J., Lei, L., Zhao, H., Sun, C., Feng, X., Du, C., Li, X., Yang, Y., and Han, W. (2011b). LysGH15 reduces the inflammation caused by lethal methicillin-resistant *Staphylococcus aureus* infection in mice. Bioeng Bugs *2*, 96-99.

Guariglia-Oropeza, V., and Helmann, J.D. (2011). *Bacillus subtilis* sigma(V) confers lysozyme resistance by activation of two cell wall modification pathways, peptidoglycan O-acetylation and D-alanylation of teichoic acids. J Bacteriol *193*, 6223-6232.

Guay, D.R. (2008). Contemporary management of uncomplicated urinary tract infections. Drugs *68*, 1169-1205.

Guerois, R., Nielsen, J.E., and Serrano, L. (2002). Predicting changes in the stability of proteins and protein complexes: a study of more than 1000 mutations. J Mol Biol *320*, 369-387.

Gupta, R., and Prasad, Y. (2011). P-27/HP endolysin as antibacterial agent for antibiotic resistant *Staphylococcus aureus* of human infections. Curr Microbiol *63*, 39-45.

Haffkine, W.M. (1897). Remarks on the plague prophylactic fluid. British medical journal, 1461.

Hakulinen, N., Turunen, O., Janis, J., Leisola, M., and Rouvinen, J. (2003). Three-dimensional structures of thermophilic beta-1,4-xylanases from *Chaetomium thermophilum* and *Nonomuraea flexuosa*. Comparison of twelve xylanases in relation to their thermal stability. Eur J Biochem *270*, 1399-1412.

Hancock, R.E., and Sahl, H.G. (2006). Antimicrobial and host-defense peptides as new anti-infective therapeutic strategies. Nat Biotechnol *24*, 1551-1557.

Hasper, H.E., Kramer, N.E., Smith, J.L., Hillman, J.D., Zachariah, C., Kuipers, O.P., de Kruijff, B., and Breukink, E. (2006). An alternative bactericidal mechanism of action for lantibiotic peptides that target lipid II. Science *313*, 1636-1637.

Heinemann, J.A., and Sprague, G.F., Jr. (1989). Bacterial conjugative plasmids mobilize DNA transfer between bacteria and yeast. Nature *340*, 205-209.

Hendrix, R.W. (2002). Bacteriophages: evolution of the majority. Theoretical population biology *61*, 471-480.

Henke, E., and Bornscheuer, U.T. (1999). Directed evolution of an esterase from *Pseudomonas fluorescens*. Random mutagenesis by error-prone PCR or a mutator strain and identification of mutants showing enhanced enantioselectivity by a resorufin-based fluorescence assay. Biological chemistry *380*, 1029-1033.

Hermoso, J.A., Monterroso, B., Albert, A., Galan, B., Ahrazem, O., Garcia, P., Martinez-Ripoll, M., Garcia, J.L., and Menendez, M. (2003). Structural basis for selective recognition of pneumococcal cell wall by modular endolysin from phage Cp-1. Structure *11*, 1239-1249.

Heselpoth, R.D., and Nelson, D.C. (2012). A new screening method for the directed evolution of thermostable bacteriolytic enzymes. J Vis Exp.

Holtje, J.V., Mirelman, D., Sharon, N., and Schwarz, U. (1975). Novel type of murein transglycosylase in *Escherichia coli*. J Bacteriol *124*, 1067-1076.

Hoopes, J.T., Stark, C.J., Kim, H.A., Sussman, D.J., Donovan, D.M., and Nelson, D.C. (2009). Use of a bacteriophage lysin, PlyC, as an enzyme disinfectant against *Streptococcus equi*. Appl Environ Microbiol *75*, 1388-1394.

Hoseki, J., Yano, T., Koyama, Y., Kuramitsu, S., and Kagamiyama, H. (1999). Directed evolution of thermostable kanamycin-resistance gene: a convenient selection marker for *Thermus thermophilus*. J Biochem *126*, 951-956.

Hutchings, R.L., S, M.S., Cabello-Villegas, J., and Mallela, K.M. (2013). Effect of antimicrobial preservatives on partial protein unfolding and aggregation. Journal of pharmaceutical sciences *102*, 365-376.

Infectious Disease Society of America (2011). Facts about antibiotic resistance.

Ioseliani, G.D., Meladze, G.D., Chkhetiia, N., Mebuke, M.G., and Kiknadze, N. (1980). [Use of bacteriophage and antibiotics for prevention of acute postoperative empyema in chronic suppurative lung diseases]. Grudnaia khirurgiia, 63-67.

Jackel, C., Kast, P., and Hilvert, D. (2008). Protein design by directed evolution. Annu Rev Biophys *37*, 153-173.

Jado, I., Lopez, R., Garcia, E., Fenoll, A., Casal, J., Garcia, P., and Spanish Pneumococcal Infection Study, N. (2003). Phage lytic enzymes as therapy for antibiotic-resistant *Streptococcus pneumoniae* infection in a murine sepsis model. J Antimicrob Chemother *52*, 967-973.

Jaenicke, R., and Bohm, G. (1998). The stability of proteins in extreme environments. Curr Opin Struct Biol *8*, 738-748.

Jensen, W.A., Armstrong, J.M., De Giorgio, J., and Hearn, M.T. (1996). Stability studies on pig heart mitochondrial malate dehydrogenase: the effect of salts and amino acids. Biochim Biophys Acta *1296*, 23-34.

Jiang, L., Althoff, E.A., Clemente, F.R., Doyle, L., Rothlisberger, D., Zanghellini, A., Gallaher, J.L., Betker, J.L., Tanaka, F., Barbas, C.F., 3rd, *et al.* (2008). De novo computational design of retro-aldol enzymes. Science *319*, 1387-1391.

Jiang, S.C., and Paul, J.H. (1998). Gene transfer by transduction in the marine environment. Appl Environ Microbiol *64*, 2780-2787.

Jobe, B.A., Grasley, A., Deveney, K.E., Deveney, C.W., and Sheppard, B.C. (1995). *Clostridium difficile* colitis: an increasing hospital-acquired illness. American journal of surgery *169*, 480-483.

Joerger, R.D. (2003). Alternatives to antibiotics: bacteriocins, antimicrobial peptides and bacteriophages. Poultry science *82*, 640-647.

Johnston, M.A., Sondergaard, C.R., and Nielsen, J.E. (2011). Integrated prediction of the effect of mutations on multiple protein characteristics. Proteins *79*, 165-178.

Kanaya, S., Oobatake, M., and Liu, Y. (1996). Thermal stability of *Escherichia coli* ribonuclease HI and its active site mutants in the presence and absence of the Mg2+ ion. Proposal of a novel catalytic role for Glu48. J Biol Chem *271*, 32729-32736.

Kanazawa, H., Fujimoto, S., and Ohara, A. (1994). Effect of radical scavengers on the inactivation of papain by ascorbic acid in the presence of cupric ions. Biological & pharmaceutical bulletin *17*, 476-481.

Karshikoff, A., and Ladenstein, R. (1998). Proteins from thermophilic and mesophilic organisms essentially do not differ in packing. Protein Eng *11*, 867-872.

Kaur, J., and Sharma, R. (2006). Directed evolution: an approach to engineer enzymes. Crit Rev Biotechnol *26*, 165-199.

Kawamura, S., Kakuta, Y., Tanaka, I., Hikichi, K., Kuhara, S., Yamasaki, N., and Kimura, M. (1996). Glycine-15 in the bend between two alpha-helices can explain the thermostability of DNA binding protein HU from *Bacillus stearothermophilus*. Biochemistry *35*, 1195-1200.

Kellogg, E.H., Leaver-Fay, A., and Baker, D. (2011). Role of conformational sampling in computing mutation-induced changes in protein structure and stability. Proteins *79*, 830-838.

Kelly, C.P., Pothoulakis, C., and LaMont, J.T. (1994). *Clostridium difficile* colitis. The New England journal of medicine *330*, 257-262.

Kelly, S.M., Jess, T.J., and Price, N.C. (2005). How to study proteins by circular dichroism. Biochim Biophys Acta *1751*, 119-139.

Kendrick, B.S., Chang, B.S., Arakawa, T., Peterson, B., Randolph, T.W., Manning, M.C., and Carpenter, J.F. (1997). Preferential exclusion of sucrose from recombinant interleukin-1 receptor antagonist: role in restricted conformational mobility and compaction of native state. Proc Natl Acad Sci U S A *94*, 11917-11922.

Kerr, D.E., Plaut, K., Bramley, A.J., Williamson, C.M., Lax, A.J., Moore, K., Wells, K.D., and Wall, R.J. (2001). Lysostaphin expression in mammary glands confers protection against staphylococcal infection in transgenic mice. Nat Biotechnol *19*, 66-70.

Khan, S., and Vihinen, M. (2010). Performance of protein stability predictors. Hum Mutat *31*, 675-684.

Kim, G.J., Cheon, Y.H., and Kim, H.S. (2000). Directed evolution of a novel N-carbamylase/D-hydantoinase fusion enzyme for functional expression with enhanced stability. Biotechnol Bioeng *68*, 211-217.

Kim, K.P., Cha, J.D., Jang, E.H., Klumpp, J., Hagens, S., Hardt, W.D., Lee, K.Y., and Loessner, M.J. (2008). PEGylation of bacteriophages increases blood circulation time and reduces T-helper type 1 immune response. Microb Biotechnol *1*, 247-257.

Kim, W.S., Salm, H., and Geider, K. (2004). Expression of bacteriophage phiEa1h lysozyme in *Escherichia coli* and its activity in growth inhibition of Erwinia amylovora. Microbiology *150*, 2707-2714.

Kimura, S., Kanaya, S., and Nakamura, H. (1992). Thermostabilization of *Escherichia coli* ribonuclease HI by replacing left-handed helical Lys95 with Gly or Asn. J Biol Chem *267*, 22014-22017.

Kite, P., Eastwood, K., Sugden, S., and Percival, S.L. (2004). Use of in vivo-generated biofilms from hemodialysis catheters to test the efficacy of a novel antimicrobial catheter lock for biofilm eradication in vitro. J Clin Microbiol *42*, 3073-3076.

Klevens, R.M., Edwards, J.R., Richards, C.L., Jr., Horan, T.C., Gaynes, R.P., Pollock, D.A., and Cardo, D.M. (2007). Estimating health care-associated infections and deaths in U.S. hospitals, 2002. Public health reports *122*, 160-166.

Knepp, V.M., Whatley, J.L., Muchnik, A., and Calderwood, T.S. (1996). Identification of antioxidants for prevention of peroxide-mediated oxidation of recombinant human ciliary neurotrophic factor and recombinant human nerve growth factor. PDA journal of pharmaceutical science and technology / PDA *50*, 163-171.

Knowles, J.R., and Albery, W.J. (1977). Perfection in enzyme catalysis: the energetics of triose phosphate isomerase. Acc Chem Res *10*, 105-111.

Koch, C., and Hoiby, N. (2000). Diagnosis and treatment of cystic fibrosis. Respiration; international review of thoracic diseases *67*, 239-247.

Kochetkova, V.A., Mamontov, A.S., Moskovtseva, R.L., Erastova, E.I., Trofimov, E.I., Popov, M.I., and Dzhubalieva, S.K. (1989). [Phagotherapy of postoperative suppurative-inflammatory complications in patients with neoplasms]. Sovetskaia meditsina, 23-26.

Kohn, W.D., Kay, C.M., and Hodges, R.S. (1997). Salt effects on protein stability: two-stranded alpha-helical coiled-coils containing inter- or intrahelical ion pairs. J Mol Biol *267*, 1039-1052.

Kolle, W., and Hetsch, H. (1929). Experimental Bacteriology, Seventh edn (London: Allen and Unwin).

Komor, R.S., Romero, P.A., Xie, C.B., and Arnold, F.H. (2012). Highly thermostable fungal cellobiohydrolase I (Cel7A) engineered using predictive methods. Protein Eng Des Sel *25*, 827-833.

Koutsioulis, D., Wang, E., Tzanodaskalaki, M., Nikiforaki, D., Deli, A., Feller, G., Heikinheimo, P., and Bouriotis, V. (2008). Directed evolution on the cold adapted properties of TAB5 alkaline phosphatase. Protein Eng Des Sel *21*, 319-327.

Krause, R.M. (1957). Studies on bacteriophages of hemolytic streptococci. I. Factors influencing the interaction of phage and susceptible host cell. J Exp Med *106*, 365-384.

Kretzer, J.W., Lehmann, R., Schmelcher, M., Banz, M., Kim, K.P., Korn, C., and Loessner, M.J. (2007). Use of high-affinity cell wall-binding domains of bacteriophage endolysins for immobilization and separation of bacterial cells. Appl Environ Microbiol *73*, 1992-2000.

Kucharewicz-Krukowska, A., and Slopek, S. (1987). Immunogenic effect of bacteriophage in patients subjected to phage therapy. Archivum immunologiae et therapiae experimentalis *35*, 553-561.

Kuhlman, B., Dantas, G., Ireton, G.C., Varani, G., Stoddard, B.L., and Baker, D. (2003). Design of a novel globular protein fold with atomic-level accuracy. Science *302*, 1364-1368.

Kumar, S., and Nussinov, R. (2001). How do thermophilic proteins deal with heat? Cell Mol Life Sci *58*, 1216-1233.

Kumar, S., Tsai, C.J., Ma, B., and Nussinov, R. (2000a). Contribution of salt bridges toward protein thermostability. J Biomol Struct Dyn *17 Suppl 1*, 79-85.

Kumar, S., Tsai, C.J., and Nussinov, R. (2000b). Factors enhancing protein thermostability. Protein Eng *13*, 179-191.

Kwarcinski, W., Lazarkiewicz, B., Weber-Dabrowska, B., Rudnicki, J., Kaminski, K., and Sciebura, M. (1994). [Bacteriophage therapy in the treatment of recurrent subphrenic and subhepatic abscess with jejunal fistula after stomach resection]. Polski tygodnik lekarski *49*, 535.

Laemmli, U.K. (1970). Cleavage of structural proteins during the assembly of the head of bacteriophage T4. Nature *227*, 680-685.

Lai, M.J., Lin, N.T., Hu, A., Soo, P.C., Chen, L.K., Chen, L.H., and Chang, K.C. (2011). Antibacterial activity of *Acinetobacter baumannii* phage varphiAB2 endolysin (LysAB2) against both gram-positive and gram-negative bacteria. Appl Microbiol Biotechnol *90*, 529-539.

Lai, Y.P., Huang, J., Wang, L.F., Li, J., and Wu, Z.R. (2004). A new approach to random mutagenesis in vitro. Biotechnol Bioeng *86*, 622-627.

Lam, X.M., Yang, J.Y., and Cleland, J.L. (1997). Antioxidants for prevention of methionine oxidation in recombinant monoclonal antibody HER2. Journal of pharmaceutical sciences *86*, 1250-1255.

Lawrence, J.G. (2005). Horizontal and vertical gene transfer: the life history of pathogens. Contributions to microbiology *12*, 255-271.

Leaver-Fay, A., Tyka, M., Lewis, S.M., Lange, O.F., Thompson, J., Jacak, R., Kaufman, K., Renfrew, P.D., Smith, C.A., Sheffler, W., *et al.* (2011). ROSETTA3: an object-oriented software suite for the simulation and design of macromolecules. Methods Enzymol *487*, 545-574.

Levine, M.M., and Pierce, N.F. (1992). Immunity and Vaccine Development (New York: Plenum Medical Book Co.).

Lew, W., Pai, M., Oxlade, O., Martin, D., and Menzies, D. (2008). Initial drug resistance and tuberculosis treatment outcomes: systematic review and meta-analysis. Ann Intern Med *149*, 123-134.

Lewis, K. (2007). Persister cells, dormancy and infectious disease. Nature reviews Microbiology *5*, 48-56.

Li, Y., Zhang, J., Tai, D., Middaugh, C.R., Zhang, Y., and Fang, J. (2012). PROTS: a fragment based protein thermo-stability potential. Proteins *80*, 81-92.

Litvinova, A.M., Chtetsova, V.M., and Kavtreva, I.G. (1978). [Evaluation of efficacy of the use of coli-Proteus bacteriophage in intestinal dysbacteriosis in premature infants]. Voprosy okhrany materinstva i detstva *23*, 42-44.

Liu, B., and Pop, M. (2009). ARDB--Antibiotic Resistance Genes Database. Nucleic Acids Res *37*, D443-447.

Liu, L., Li, Y., Liotta, D., and Lutz, S. (2009). Directed evolution of an orthogonal nucleoside analog kinase via fluorescence-activated cell sorting. Nucleic Acids Res *37*, 4472-4481.

Loeffler, J.M., Djurkovic, S., and Fischetti, V.A. (2003). Phage lytic enzyme Cpl-1 as a novel antimicrobial for pneumococcal bacteremia. Infect Immun *71*, 6199-6204.

Loeffler, J.M., and Fischetti, V.A. (2003). Synergistic lethal effect of a combination of phage lytic enzymes with different activities on penicillin-sensitive and -resistant *Streptococcus pneumoniae* strains. Antimicrob Agents Chemother *47*, 375-377.

Loeffler, J.M., Nelson, D., and Fischetti, V.A. (2001). Rapid killing of *Streptococcus pneumoniae* with a bacteriophage cell wall hydrolase. Science *294*, 2170-2172.

Loessner, M.J. (2005). Bacteriophage endolysins--current state of research and applications. Curr Opin Microbiol *8*, 480-487.

Loessner, M.J., Kramer, K., Ebel, F., and Scherer, S. (2002). C-terminal domains of *Listeria monocytogenes* bacteriophage murein hydrolases determine specific recognition and high-affinity binding to bacterial cell wall carbohydrates. Mol Microbiol *44*, 335-349.

Loessner, M.J., Wendlinger, G., and Scherer, S. (1995). Heterogeneous endolysins in *Listeria monocytogenes* bacteriophages: a new class of enzymes and evidence for conserved holin genes within the siphoviral lysis cassettes. Mol Microbiol *16*, 1231-1241.

Lohner, K., and Blondelle, S.E. (2005). Molecular mechanisms of membrane perturbation by antimicrobial peptides and the use of biophysical studies in the design of novel peptide antibiotics. Combinatorial chemistry & high throughput screening *8*, 241-256.

Lopez, R., and Garcia, E. (2004). Recent trends on the molecular biology of pneumococcal capsules, lytic enzymes, and bacteriophage. FEMS Microbiol Rev *28*, 553-580.

Lopez, R., Garcia, E., Garcia, P., and Garcia, J.L. (1997). The pneumococcal cell wall degrading enzymes: a modular design to create new lysins? Microb Drug Resist *3*, 199-211.

Love, K. (2008). Directed Evolution: Engineering Biocatalysts (Massachusetts Institute of Technology).

Low, L.Y., Yang, C., Perego, M., Osterman, A., and Liddington, R. (2011). Role of net charge on catalytic domain and influence of cell wall binding domain on bactericidal activity, specificity, and host range of phage lysins. J Biol Chem *286*, 34391-34403.

Lowy, I. (1996). Producing a trustworthy knowledge: early field trials of anti-cholera vaccines in India. (Paris: Elsevier).

Lu, X., Hirata, H., Yamaji, Y., Ugaki, M., and Namba, S. (2001). Random mutagenesis in a plant viral genome using a DNA repair-deficient mutator *Escherichia coli* strain. J Virol Methods *94*, 37-43.

Lu, X.M., Jin, X.B., Zhu, J.Y., Mei, H.F., Ma, Y., Chu, F.J., Wang, Y., and Li, X.B. (2010). Expression of the antimicrobial peptide cecropin fused with human lysozyme in *Escherichia coli*. Appl Microbiol Biotechnol *87*, 2169-2176.

Luttinger, P. (1915). Whooping cough: its treatment and prophylaxis, based on the Bordet-Gengou etiology. NY Med J *101*.

Lutz, S., and Patrick, W.M. (2004). Novel methods for directed evolution of enzymes: quality, not quantity. Curr Opin Biotechnol *15*, 291-297.

Machius, M., Declerck, N., Huber, R., and Wiegand, G. (2003). Kinetic stabilization of *Bacillus licheniformis* alpha-amylase through introduction of hydrophobic residues at the surface. J Biol Chem *278*, 11546-11553.

Maeda, N., Kanai, T., Atomi, H., and Imanaka, T. (2002). The unique pentagonal structure of an archaeal Rubisco is essential for its high thermostability. J Biol Chem *277*, 31656-31662.

Mahoney, J.F., Arnold, R.C., and Harris, A. (1943). Penicillin treatment of early syphilis-a preliminary report. American journal of public health and the nation's health *33*, 1387-1391.

Makhatadze, G.I., Loladze, V.V., Ermolenko, D.N., Chen, X., and Thomas, S.T. (2003). Contribution of surface salt bridges to protein stability: guidelines for protein engineering. J Mol Biol *327*, 1135-1148.

Mansfeld, J., Vriend, G., Dijkstra, B.W., Veltman, O.R., Van den Burg, B., Venema, G., Ulbrich-Hofmann, R., and Eijsink, V.G. (1997). Extreme stabilization of a thermolysin-like protease by an engineered disulfide bond. J Biol Chem *272*, 11152-11156.

Marshall, S.A., Morgan, C.S., and Mayo, S.L. (2002). Electrostatics significantly affect the stability of designed homeodomain variants. J Mol Biol *316*, 189-199.

Martin, A., Kather, I., and Schmid, F.X. (2002). Origins of the high stability of an in vitro-selected cold-shock protein. J Mol Biol *318*, 1341-1349.

Martin, A., Sieber, V., and Schmid, F.X. (2001). In-vitro selection of highly stabilized protein variants with optimized surface. J Mol Biol *309*, 717-726.

Masso, M., and Vaisman, II (2010). AUTO-MUTE: web-based tools for predicting stability changes in proteins due to single amino acid replacements. Protein Eng Des Sel *23*, 683-687.

Matsumura, M., Signor, G., and Matthews, B.W. (1989). Substantial increase of protein stability by multiple disulphide bonds. Nature *342*, 291-293.

Matthews, B.W. (1995). Studies on protein stability with T4 lysozyme. Adv Protein Chem *46*, 249-278.

Matthews, B.W., Nicholson, H., and Becktel, W.J. (1987). Enhanced protein thermostability from site-directed mutations that decrease the entropy of unfolding. Proc Natl Acad Sci U S A *84*, 6663-6667.

Mayer, M.J., Payne, J., Gasson, M.J., and Narbad, A. (2010). Genomic sequence and characterization of the virulent bacteriophage phiCTP1 from *Clostridium tyrobutyricum* and heterologous expression of its endolysin. Appl Environ Microbiol *76*, 5415-5422.

McCarthy, J.K., Uzelac, A., Davis, D.F., and Eveleigh, D.E. (2004). Improved catalytic efficiency and active site modification of 1,4-beta-D-glucan glucohydrolase A from Thermotoga neapolitana by directed evolution. J Biol Chem *279*, 11495-11502.

McCullers, J.A., Karlstrom, A., Iverson, A.R., Loeffler, J.M., and Fischetti, V.A. (2007). Novel strategy to prevent otitis media caused by colonizing *Streptococcus pneumoniae*. PLoS Pathog *3*, e28.

McGowan, S., Buckle, A.M., Mitchell, M.S., Hoopes, J.T., Gallagher, D.T., Heselpoth, R.D., Shen, Y., Reboul, C.F., Law, R.H., Fischetti, V.A., *et al.* (2012). X-ray crystal structure of the streptococcal specific phage lysin PlyC. Proc Natl Acad Sci U S A *109*, 12752-12757.

Meiering, E.M., Serrano, L., and Fersht, A.R. (1992). Effect of active site residues in barnase on activity and stability. J Mol Biol *225*, 585-589.

Meladze, G.D., Mebuke, M.G., Chkhetiia, N., Kiknadze, N., and Koguashvili, G.G. (1982). [Efficacy of staphylococcal bacteriophage in the treatment of purulent lung and pleural diseases]. Grudnaia khirurgiia, 53-56.

Miliutina, L.N., and Vorotyntseva, N.V. (1993). [Current strategy and tactics of etiotropic therapy of acute intestinal infections in children]. Antibiotiki i khimioterapiia = Antibiotics and chemoterapy [sic] / Ministerstvo meditsinskoi i mikrobiologicheskoi promyshlennosti SSSR *38*, 46-53.

Moreau-Marquis, S., O'Toole, G.A., and Stanton, B.A. (2009). Tobramycin and FDA-approved iron chelators eliminate *Pseudomonas aeruginosa* biofilms on cystic fibrosis cells. Am J Respir Cell Mol Biol *41*, 305-313.

Morita, M., Tanji, Y., Mizoguchi, K., Soejima, A., Orito, Y., and Unno, H. (2001a). Antibacterial activity of *Bacillus amyloliquefaciens* phage endolysin without holin conjugation. J Biosci Bioeng *91*, 469-473.

Morita, M., Tanji, Y., Orito, Y., Mizoguchi, K., Soejima, A., and Unno, H. (2001b). Functional analysis of antibacterial activity of *Bacillus amyloliquefaciens* phage endolysin against Gram-negative bacteria. FEBS Lett *500*, 56-59.

Mukaiyama, A., Haruki, M., Ota, M., Koga, Y., Takano, K., and Kanaya, S. (2006). A hyperthermophilic protein acquires function at the cost of stability. Biochemistry *45*, 12673-12679.

Nau, R., and Eiffert, H. (2002). Modulation of release of proinflammatory bacterial compounds by antibacterials: potential impact on course of inflammation and outcome in sepsis and meningitis. Clinical microbiology reviews *15*, 95-110.

Nelson, D., Loomis, L., and Fischetti, V.A. (2001). Prevention and elimination of upper respiratory colonization of mice by group A streptococci by using a bacteriophage lytic enzyme. Proc Natl Acad Sci U S A *98*, 4107-4112.

Nelson, D., Schuch, R., Chahales, P., Zhu, S., and Fischetti, V.A. (2006a). PlyC: a multimeric bacteriophage lysin. Proc Natl Acad Sci U S A *103*, 10765-10770.

Nelson, D., Schuch, R., Chahales, P., Zhu, S., and Fischetti, V.A. (2006b). PlyC: A multimeric bacteriophage lysin. Proc Natl Acad Sci USA *103*, 10765-10770.

Nelson, D., Schuch, R., Zhu, S., Tscherne, D.M., and Fischetti, V.A. (2003). Genomic sequence of C1, the first streptococcal phage. J Bacteriol *185*, 3325-3332.

Nelson, D.C., Schmelcher, M., Rodriguez-Rubio, L., Klumpp, J., Pritchard, D.G., Dong, S., and Donovan, D.M. (2012). Endolysins as antimicrobials. Advances in virus research *83*, 299-365.

Nelson, M.L., Dinardo, A., Hochberg, J., and Armelagos, G.J. (2010). Brief communication: Mass spectroscopic characterization of tetracycline in the skeletal remains of an ancient population from Sudanese Nubia 350-550 CE. American journal of physical anthropology *143*, 151-154.

Neylon, C. (2004). Chemical and biochemical strategies for the randomization of protein encoding DNA sequences: library construction methods for directed evolution. Nucleic Acids Res *32*, 1448-1459.

Ng, W.L., and Bassler, B.L. (2009). Bacterial quorum-sensing network architectures. Annual review of genetics *43*, 197-222.

Nicholson, H., Anderson, D.E., Dao-pin, S., and Matthews, B.W. (1991). Analysis of the interaction between charged side chains and the alpha-helix dipole using designed thermostable mutants of phage T4 lysozyme. Biochemistry *30*, 9816-9828.

Nicholson, H., Becktel, W.J., and Matthews, B.W. (1988). Enhanced protein thermostability from designed mutations that interact with alpha-helix dipoles. Nature *336*, 651-656.

Normark, B.H., and Normark, S. (2002). Evolution and spread of antibiotic resistance. Journal of internal medicine *252*, 91-106.

O'Flaherty, S., Coffey, A., Meaney, W., Fitzgerald, G.F., and Ross, R.P. (2005). The recombinant phage lysin LysK has a broad spectrum of lytic activity against clinically relevant staphylococci, including methicillin-resistant *Staphylococcus aureus*. J Bacteriol *187*, 7161-7164.

O'Loughlin, C.T., Miller, L.C., Siryaporn, A., Drescher, K., Semmelhack, M.F., and Bassler, B.L. (2013). A quorum-sensing inhibitor blocks *Pseudomonas aeruginosa* virulence and biofilm formation. Proc Natl Acad Sci U S A *110*, 17981-17986.

Obeso, J.M., Martinez, B., Rodriguez, A., and Garcia, P. (2008). Lytic activity of the recombinant staphylococcal bacteriophage PhiH5 endolysin active against *Staphylococcus aureus* in milk. International journal of food microbiology *128*, 212-218.

Ochman, H., Lawrence, J.G., and Groisman, E.A. (2000). Lateral gene transfer and the nature of bacterial innovation. Nature *405*, 299-304.

Oey, M., Lohse, M., Kreikemeyer, B., and Bock, R. (2009a). Exhaustion of the chloroplast protein synthesis capacity by massive expression of a highly stable protein antibiotic. The Plant journal : for cell and molecular biology *57*, 436-445.

Oey, M., Lohse, M., Scharff, L.B., Kreikemeyer, B., and Bock, R. (2009b). Plastid production of protein antibiotics against pneumonia via a new strategy for high-level expression of antimicrobial proteins. Proc Natl Acad Sci U S A *106*, 6579-6584.

Ohage, E., and Steipe, B. (1999). Intrabody construction and expression. I. The critical role of VL domain stability. J Mol Biol *291*, 1119-1128.

Oldham, E.R., and Daley, M.J. (1991). Lysostaphin: use of a recombinant bactericidal enzyme as a mastitis therapeutic. Journal of dairy science *74*, 4175-4182.

Olson, M.E., Ceri, H., Morck, D.W., Buret, A.G., and Read, R.R. (2002). Biofilm bacteria: formation and comparative susceptibility to antibiotics. Canadian journal of veterinary research = Revue canadienne de recherche veterinaire *66*, 86-92.

Orito, Y., Morita, M., Hori, K., Unno, H., and Tanji, Y. (2004). *Bacillus amyloliquefaciens* phage endolysin can enhance permeability of *Pseudomonas aeruginosa* outer membrane and induce cell lysis. Appl Microbiol Biotechnol *65*, 105-109.

Pace, C.N., Alston, R.W., and Shaw, K.L. (2000). Charge-charge interactions influence the denatured state ensemble and contribute to protein stability. Protein Sci *9*, 1395-1398.

Pack, S.P., and Yoo, Y.J. (2004). Protein thermostability: structure-based difference of amino acid between thermophilic and mesophilic proteins. J Biotechnol *111*, 269-277.

Pantoliano, M.W., Whitlow, M., Wood, J.F., Dodd, S.W., Hardman, K.D., Rollence, M.L., and Bryan, P.N. (1989). Large increases in general stability for subtilisin BPN' through incremental changes in the free energy of unfolding. Biochemistry *28*, 7205-7213.

Parish, H.J. (1965). A History of Immunization (London: E. & S. Livingstone).

Parthiban, V., Gromiha, M.M., Hoppe, C., and Schomburg, D. (2007). Structural analysis and prediction of protein mutant stability using distance and torsion potentials: role of secondary structure and solvent accessibility. Proteins *66*, 41-52.

Parthiban, V., Gromiha, M.M., and Schomburg, D. (2006). CUPSAT: prediction of protein stability upon point mutations. Nucleic Acids Res *34*, W239-242.

Pastagia, M., Euler, C., Chahales, P., Fuentes-Duculan, J., Krueger, J.G., and Fischetti, V.A. (2011). A novel chimeric lysin shows superiority to mupirocin for skin decolonization of methicillin-resistant and -sensitive *Staphylococcus aureus* strains. Antimicrob Agents Chemother *55*, 738-744.

Pasteur, L. (1880). The attenuation of the causal agent of fowl cholera. C R Acad Sci *91*, 673-680.

Patriquin, G.M., Banin, E., Gilmour, C., Tuchman, R., Greenberg, E.P., and Poole, K. (2008). Influence of quorum sensing and iron on twitching motility and biofilm formation in *Pseudomonas aeruginosa*. J Bacteriol *190*, 662-671.

Perepanova, T.S., Darbeeva, O.S., Kotliarova, G.A., Kondrat'eva, E.M., Maiskaia, L.M., Malysheva, V.F., Baiguzina, F.A., and Grishkova, N.V. (1995). [The efficacy of bacteriophage preparations in treating inflammatory urologic diseases]. Urologiia i nefrologiia, 14-17.

Perl, D., Mueller, U., Heinemann, U., and Schmid, F.X. (2000). Two exposed amino acid residues confer thermostability on a cold shock protein. Nat Struct Biol *7*, 380-383.

Perl, D., and Schmid, F.X. (2001). Electrostatic stabilization of a thermophilic cold shock protein. J Mol Biol *313*, 343-357.

Pfeiffer, R., and Kolle, W. (1896). Experimentelle Untersuchungen zur Frage der Schutzimpfung des Menschen gegen Typhus adbdominalis. Deutsche medizinische Wochenschrift *22*, 735-737.

Piatigorsky, J., Horwitz, J., and Simpson, R.T. (1977). Partial dissociation and renaturation of embryonic chick delta-crystallin. Characterization by ultracentrifugation and circular dichroism. Biochim Biophys Acta *490*, 279-289.

Pokala, N., and Handel, T.M. (2005). Energy functions for protein design: adjustment with protein-protein complex affinities, models for the unfolded state, and negative design of solubility and specificity. J Mol Biol *347*, 203-227.

Porter, C.J., Schuch, R., Pelzek, A.J., Buckle, A.M., McGowan, S., Wilce, M.C., Rossjohn, J., Russell, R., Nelson, D., Fischetti, V.A., *et al.* (2007). The 1.6 A crystal structure of the catalytic domain of PlyB, a bacteriophage lysin active against *Bacillus anthracis*. J Mol Biol *366*, 540-550.

Potapov, V., Cohen, M., and Schreiber, G. (2009). Assessing computational methods for predicting protein stability upon mutation: good on average but not in the details. Protein Eng Des Sel *22*, 553-560.

Pritchard, D.G., Dong, S., Baker, J.R., and Engler, J.A. (2004). The bifunctional peptidoglycan lysin of *Streptococcus agalactiae* bacteriophage B30. Microbiology *150*, 2079-2087.

Pritchard, D.G., Dong, S., Kirk, M.C., Cartee, R.T., and Baker, J.R. (2007). LambdaSa1 and LambdaSa2 prophage lysins of *Streptococcus agalactiae*. Appl Environ Microbiol *73*, 7150-7154.

Provencher, S.W., and Glockner, J. (1981). Estimation of globular protein secondary structure from circular dichroism. Biochemistry *20*, 33-37.

Puchkaev, A.V., Koo, L.S., and Ortiz de Montellano, P.R. (2003). Aromatic stacking as a determinant of the thermal stability of CYP119 from *Sulfolobus solfataricus*. Arch Biochem Biophys *409*, 52-58.

Raad, I., Chatzinikolaou, I., Chaiban, G., Hanna, H., Hachem, R., Dvorak, T., Cook, G., and Costerton, W. (2003). In vitro and ex vivo activities of minocycline and EDTA against microorganisms embedded in biofilm on catheter surfaces. Antimicrob Agents Chemother *47*, 3580-3585.

Raman, S., Vernon, R., Thompson, J., Tyka, M., Sadreyev, R., Pei, J., Kim, D., Kellogg, E., DiMaio, F., Lange, O., *et al.* (2009). Structure prediction for CASP8 with all-atom refinement using Rosetta. Proteins *77 Suppl 9*, 89-99.

Ramon, G., and Zoeller, C. (1926). De la valeur antigenique de l'anatoxine tetanique chez l'homme. C R Acad Sci Paris *182*, 245-247.

Ramon, G., and Zoeller, C. (1927). L'anatoxine tetanique et l'immunisation active de l'homme vis-a-vis du tetanes. Ann Inst Pasteur Paris *41*, 803-833.

Ramon, J., Saez, V., Baez, R., Aldana, R., and Hardy, E. (2005). PEGylated interferon-alpha2b: a branched 40K polyethylene glycol derivative. Pharmaceutical research *22*, 1374-1386.

Rashel, M., Uchiyama, J., Ujihara, T., Uehara, Y., Kuramoto, S., Sugihara, S., Yagyu, K., Muraoka, A., Sugai, M., Hiramatsu, K., *et al.* (2007). Efficient elimination of multidrug-resistant *Staphylococcus aureus* by cloned lysin derived from bacteriophage phi MR11. J Infect Dis *196*, 1237-1247.

Rasila, T.S., Pajunen, M.I., and Savilahti, H. (2009). Critical evaluation of random mutagenesis by error-prone polymerase chain reaction protocols, *Escherichia coli* mutator strain, and hydroxylamine treatment. Anal Biochem *388*, 71-80.

Ren, C., Chen, T., Zhang, J., Liang, L., and Lin, Z. (2009). An evolved xylose transporter from Zymomonas mobilis enhances sugar transport in Escherichia coli. Microbial cell factories *8*, 66.

Renugopalakrishnan, V., Garduno-Juarez, R., Narasimhan, G., Verma, C.S., Wei, X., and Li, P. (2005). Rational design of thermally stable proteins: relevance to bionanotechnology. Journal of nanoscience and nanotechnology *5*, 1759-1767.

Resch, G., Moreillon, P., and Fischetti, V.A. (2011a). PEGylating a bacteriophage endolysin inhibits its bactericidal activity. AMB Express *1*, 29.

Resch, G., Moreillon, P., and Fischetti, V.A. (2011b). A stable phage lysin (Cpl-1) dimer with increased antipneumococcal activity and decreased plasma clearance. International journal of antimicrobial agents *38*, 516-521.

Roberts, R.R., Hota, B., Ahmad, I., Scott, R.D., 2nd, Foster, S.D., Abbasi, F., Schabowski, S., Kampe, L.M., Ciavarella, G.G., Supino, M., *et al.* (2009). Hospital and societal costs of antimicrobial-resistant infections in a Chicago teaching hospital: implications for antibiotic stewardship. Clin Infect Dis *49*, 1175-1184.

Robertson, D.E., and Steer, B.A. (2004). Recent progress in biocatalyst discovery and optimization. Curr Opin Chem Biol *8*, 141-149.

Rothlisberger, D., Khersonsky, O., Wollacott, A.M., Jiang, L., DeChancie, J., Betker, J., Gallaher, J.L., Althoff, E.A., Zanghellini, A., Dym, O., *et al.* (2008). Kemp elimination catalysts by computational enzyme design. Nature *453*, 190-195.

Royet, J., and Dziarski, R. (2007). Peptidoglycan recognition proteins: pleiotropic sensors and effectors of antimicrobial defences. Nature reviews Microbiology *5*, 264-277.

Rozema, D., and Gellman, S.H. (1996). Artificial chaperone-assisted refolding of denatured-reduced lysozyme: modulation of the competition between renaturation and aggregation. Biochemistry *35*, 15760-15771.

Sainathrao, S., Mohan, K.V., and Atreya, C. (2009). Gamma-phage lysin PlyG sequence-based synthetic peptides coupled with Qdot-nanocrystals are useful for developing detection methods for *Bacillus anthracis* by using its surrogates, *B. anthracis*-Sterne and *B. cereus*-4342. BMC Biotechnol *9*, 67.

Sakandelidze, V.M. (1991). [The combined use of specific phages and antibiotics in different infectious allergoses]. Vrachebnoe delo, 60-63.

Sakandelidze, V.M., and Meipariani, A.N. (1974). [Use of combined phages in suppurative-inflammatory diseases]. Zhurnal mikrobiologii, epidemiologii, i immunobiologii *51*, 135-136.

Sali, D., Bycroft, M., and Fersht, A.R. (1988). Stabilization of protein structure by interaction of alpha-helix dipole with a charged side chain. Nature *335*, 740-743.

Sanz-Aparicio, J., Hermoso, J.A., Martinez-Ripoll, M., Gonzalez, B., Lopez-Camacho, C., and Polaina, J. (1998). Structural basis of increased resistance to thermal denaturation induced by single amino acid substitution in the sequence of beta-glucosidase A from *Bacillus polymyxa*. Proteins *33*, 567-576.

Sanz, J.M., Garcia, J.L., Laynez, J., Usobiaga, P., and Menendez, M. (1993). Thermal stability and cooperative domains of CPL1 lysozyme and its NH2- and COOH-terminal modules. Dependence on choline binding. J Biol Chem *268*, 6125-6130.

Sass, P., and Bierbaum, G. (2007). Lytic activity of recombinant bacteriophage phi11 and phi12 endolysins on whole cells and biofilms of *Staphylococcus aureus*. Appl Environ Microbiol *73*, 347-352.

Schicklmaier, P., and Schmieger, H. (1995). Frequency of generalized transducing phages in natural isolates of the *Salmonella typhimurium* complex. Appl Environ Microbiol *61*, 1637-1640.

Schiraldi, C., and De Rosa, M. (2002). The production of biocatalysts and biomolecules from extremophiles. Trends Biotechnol *20*, 515-521.

Schmelcher, M., Donovan, D.M., and Loessner, M.J. (2012a). Bacteriophage endolysins as novel antimicrobials. Future microbiology *7*, 1147-1171.

Schmelcher, M., Powell, A.M., Becker, S.C., Camp, M.J., and Donovan, D.M. (2012b). Chimeric phage lysins act synergistically with lysostaphin to kill mastitis-causing *Staphylococcus aureus* in murine mammary glands. Appl Environ Microbiol *78*, 2297-2305.

Schmelcher, M., Shabarova, T., Eugster, M.R., Eichenseher, F., Tchang, V.S., Banz, M., and Loessner, M.J. (2010). Rapid multiplex detection and differentiation of *Listeria* cells by use of fluorescent phage endolysin cell wall binding domains. Appl Environ Microbiol *76*, 5745-5756.

Schmelcher, M., Tchang, V.S., and Loessner, M.J. (2011). Domain shuffling and module engineering of *Listeria* phage endolysins for enhanced lytic activity and binding affinity. Microb Biotechnol *4*, 651-662.

Schmelcher, M., Waldherr, F., and Loessner, M.J. (2012c). *Listeria* bacteriophage peptidoglycan hydrolases feature high thermoresistance and reveal increased activity after divalent metal cation substitution. Appl Microbiol Biotechnol *93*, 633-643.

Schuch, R., Nelson, D., and Fischetti, V.A. (2002). A bacteriolytic agent that detects and kills *Bacillus anthracis*. Nature *418*, 884-889.

Schule, S., Schulz-Fademrecht, T., Garidel, P., Bechtold-Peters, K., and Frieb, W. (2008). Stabilization of IgG1 in spray-dried powders for inhalation. European journal of pharmaceutics and biopharmaceutics : official journal of Arbeitsgemeinschaft fur Pharmazeutische Verfahrenstechnik eV *69*, 793-807.

Schwehm, J.M., Fitch, C.A., Dang, B.N., Garcia-Moreno, E.B., and Stites, W.E. (2003). Changes in stability upon charge reversal and neutralization substitution in staphylococcal nuclease are dominated by favorable electrostatic effects. Biochemistry *42*, 1118-1128.

Schwentker, F.F., Gelman, S., and Long, P.H. (1984). Landmark article April 24, 1937. The treatment of meningococcic meningitis with sulfanilamide. Preliminary report. By Francis F. Schwentker, Sidney Gelman, and Perrin H. Long. JAMA *251*, 788-790.

Schymkowitz, J., Borg, J., Stricher, F., Nys, R., Rousseau, F., and Serrano, L. (2005a). The FoldX web server: an online force field. Nucleic Acids Res *33*, W382-388.

Schymkowitz, J.W., Rousseau, F., Martins, I.C., Ferkinghoff-Borg, J., Stricher, F., and Serrano, L. (2005b). Prediction of water and metal binding sites and their affinities by using the Fold-X force field. Proc Natl Acad Sci U S A *102*, 10147-10152.

Seeliger, D., and de Groot, B.L. (2010). Protein thermostability calculations using alchemical free energy simulations. Biophysical journal *98*, 2309-2316.

Serrano, L., Bycroft, M., and Fersht, A.R. (1991). Aromatic-aromatic interactions and protein stability. Investigation by double-mutant cycles. J Mol Biol *218*, 465-475.

Serrano, L., Day, A.G., and Fersht, A.R. (1993). Step-wise mutation of barnase to binase. A procedure for engineering increased stability of proteins and an experimental analysis of the evolution of protein stability. J Mol Biol *233*, 305-312.

Serrano, L., and Fersht, A.R. (1989). Capping and alpha-helix stability. Nature *342*, 296-299.

Serrano, L., Horovitz, A., Avron, B., Bycroft, M., and Fersht, A.R. (1990). Estimating the contribution of engineered surface electrostatic interactions to protein stability by using double-mutant cycles. Biochemistry *29*, 9343-9352.

Serrano, L., Neira, J.L., Sancho, J., and Fersht, A.R. (1992). Effect of alanine versus glycine in alpha-helices on protein stability. Nature *356*, 453-455.

Shafikhani, S., Siegel, R.A., Ferrari, E., and Schellenberger, V. (1997). Generation of large libraries of random mutants in *Bacillus subtilis* by PCR-based plasmid multimerization. BioTechniques *23*, 304-310.

Sheehan, M.M., Garcia, J.L., Lopez, R., and Garcia, P. (1997). The lytic enzyme of the pneumococcal phage Dp-1: a chimeric lysin of intergeneric origin. Mol Microbiol *25*, 717-725.

Shih, P., and Kirsch, J.F. (1995). Design and structural analysis of an engineered thermostable chicken lysozyme. Protein Sci *4*, 2063-2072.

Shoichet, B.K., Baase, W.A., Kuroki, R., and Matthews, B.W. (1995). A relationship between protein stability and protein function. Proc Natl Acad Sci U S A *92*, 452-456.

Sigal, I.S., Harwood, B.G., and Arentzen, R. (1982). Thiol-beta-lactamase: replacement of the active-site serine of RTEM beta-lactamase by a cysteine residue. Proc Natl Acad Sci U S A *79*, 7157-7160.

Singh, P.K. (2004). Iron sequestration by human lactoferrin stimulates *P. aeruginosa* surface motility and blocks biofilm formation. Biometals : an international journal on the role of metal ions in biology, biochemistry, and medicine *17*, 267-270.

Singh, P.K., Parsek, M.R., Greenberg, E.P., and Welsh, M.J. (2002). A component of innate immunity prevents bacterial biofilm development. Nature *417*, 552-555.

Slopek, S., Durlakowa, I., Weber-Dabrowska, B., Dabrowski, M., and Kucharewicz-Krukowska, A. (1984). Results of bacteriophage treatment of suppurative bacterial infections. III. Detailed evaluation of the results obtained in further 150 cases. Archivum immunologiae et therapiae experimentalis *32*, 317-335.

Slopek, S., Durlakowa, I., Weber-Dabrowska, B., Kucharewicz-Krukowska, A., Dabrowski, M., and Bisikiewicz, R. (1983a). Results of bacteriophage treatment of suppurative bacterial infections. I. General evaluation of the results. Archivum immunologiae et therapiae experimentalis *31*, 267-291.

Slopek, S., Durlakowa, I., Weber-Dabrowska, B., Kucharewicz-Krukowska, A., Dabrowski, M., and Bisikiewicz, R. (1983b). Results of bacteriophage treatment of suppurative bacterial infections. II. Detailed evaluation of the results. Archivum immunologiae et therapiae experimentalis *31*, 293-327.

Slopek, S., Kucharewicz-Krukowska, A., Weber-Dabrowska, B., and Dabrowski, M. (1985a). Results of bacteriophage treatment of suppurative bacterial infections. IV. Evaluation of the results obtained in 370 cases. Archivum immunologiae et therapiae experimentalis *33*, 219-240.

Slopek, S., Kucharewicz-Krukowska, A., Weber-Dabrowska, B., and Dabrowski, M. (1985b). Results of bacteriophage treatment of suppurative bacterial infections. V. Evaluation of the results obtained in children. Archivum immunologiae et therapiae experimentalis *33*, 241-259.

Slopek, S., Kucharewicz-Krukowska, A., Weber-Dabrowska, B., and Dabrowski, M. (1985c). Results of bacteriophage treatment of suppurative bacterial infections. VI. Analysis of treatment of suppurative staphylococcal infections. Archivum immunologiae et therapiae experimentalis *33*, 261-273.

Slopek, S., Weber-Dabrowska, B., Dabrowski, M., and Kucharewicz-Krukowska, A. (1987). Results of bacteriophage treatment of suppurative bacterial infections in the years 1981-1986. Archivum immunologiae et therapiae experimentalis *35*, 569-583.

Smith, M. (1985). In vitro mutagenesis. Annual review of genetics *19*, 423-462.

Snyder, S.L., and Sobocinski, P.Z. (1975). An improved 2,4,6-trinitrobenzenesulfonic acid method for the determination of amines. Anal Biochem *64*, 284-288.

Sokolova, T.G., Gonzalez, J.M., Kostrikina, N.A., Chernyh, N.A., Slepova, T.V., Bonch-Osmolovskaya, E.A., and Robb, F.T. (2004). *Thermosinus carboxydivorans* gen. nov., sp. nov., a new anaerobic, thermophilic, carbon-monoxide-oxidizing, hydrogenogenic bacterium from a hot pool of Yellowstone National Park. International journal of systematic and evolutionary microbiology *54*, 2353-2359.

Somero, G.N. (1975). Temperature as a selective factor in protein evolution: the adaptational strategy of "compromise". J Exp Zool *194*, 175-188.

Sordillo, L.M., and Streicher, K.L. (2002). Mammary gland immunity and mastitis susceptibility. Journal of mammary gland biology and neoplasia *7*, 135-146.

Spellberg, B., Guidos, R., Gilbert, D., Bradley, J., Boucher, H.W., Scheld, W.M., Bartlett, J.G., Edwards, J., Jr., and Infectious Diseases Society of, A. (2008). The epidemic of antibiotic-resistant infections: a call to action for the medical community from the Infectious Diseases Society of America. Clin Infect Dis *46*, 155-164.

Spiro, R.G. (1966). Analysis of sugars found in glycoproteins. Methods Enzymol *8*, 3-26.
Splith, K., and Neundorf, I. (2011). Antimicrobial peptides with cell-penetrating peptide properties and vice versa. Eur Biophys J *40*, 387-397.

Stark, C.J., Hoopes, J.T., Bonocora, R.P., and Nelson, D.C., eds. (2010). Bacteriophage lytic enzymes as antimicrobials (ASM Press).

Stellwagen, A.E., and Craig, N.L. (1997). Gain-of-function mutations in TnsC, an ATP-dependent transposition protein that activates the bacterial transposon Tn7. Genetics *145*, 573-585.

Stentz, R., Bongaerts, R.J., Gunning, A.P., Gasson, M., and Shearman, C. (2010). Controlled release of protein from viable *Lactococcus lactis* cells. Appl Environ Microbiol *76*, 3026-3031.

Stroj, L., Weber-Dabrowska, B., Partyka, K., Mulczyk, M., and Wojcik, M. (1999). [Successful treatment with bacteriophage in purulent cerebrospinal meningitis in a newborn]. Neurologia i neurochirurgia polska *33*, 693-698.

Strop, P., and Mayo, S.L. (2000). Contribution of surface salt bridges to protein stability. Biochemistry *39*, 1251-1255.

Sugai, M., Fujiwara, T., Ohta, K., Komatsuzawa, H., Ohara, M., and Suginaka, H. (1997). epr, which encodes glycylglycine endopeptidase resistance, is homologous to femAB and affects serine content of peptidoglycan cross bridges in *Staphylococcus capitis* and *Staphylococcus aureus*. J Bacteriol *179*, 4311-4318.

Sulakvelidze, A., Alavidze, Z., and Morris, J.G., Jr. (2001). Bacteriophage therapy. Antimicrob Agents Chemother *45*, 649-659.

Summers, W.C. (1999). Felix d'Herelle and the origins of molecular biology (New Haven, Conn.: Yale University Press).

Sun, D.P., Sauer, U., Nicholson, H., and Matthews, B.W. (1991). Contributions of engineered surface salt bridges to the stability of T4 lysozyme determined by directed mutagenesis. Biochemistry *30*, 7142-7153.

Sun, L., Petrounia, I.P., Yagasaki, M., Bandara, G., and Arnold, F.H. (2001). Expression and stabilization of galactose oxidase in *Escherichia coli* by directed evolution. Protein Eng *14*, 699-704.

Sweeney, C.R., Timoney, J.F., Newton, J.R., and Hines, M.T. (2005). *Streptococcus equi* infections in horses: guidelines for treatment, control, and prevention of strangles. Journal of veterinary internal medicine / American College of Veterinary Internal Medicine *19*, 123-134.

Sweeney, C.R., Whitlock, R.H., Meirs, D.A., Whitehead, S.C., and Barningham, S.O. (1987). Complications associated with *Streptococcus equi* infection on a horse farm. J Am Vet Med Assoc *191*, 1446-1448.

Szilagyi, A., and Zavodszky, P. (2000). Structural differences between mesophilic, moderately thermophilic and extremely thermophilic protein subunits: results of a comprehensive survey. Structure *8*, 493-504.

Takac, M., Witte, A., and Blasi, U. (2005). Functional analysis of the lysis genes of *Staphylococcus aureus* phage P68 in *Escherichia coli*. Microbiology *151*, 2331-2342.

Tekaia, F., Yeramian, E., and Dujon, B. (2002). Amino acid composition of genomes, lifestyles of organisms, and evolutionary trends: a global picture with correspondence analysis. Gene *297*, 51-60.

Thoma, R., Hennig, M., Sterner, R., and Kirschner, K. (2000). Structure and function of mutationally generated monomers of dimeric phosphoribosylanthranilate isomerase from *Thermotoga maritima*. Structure *8*, 265-276.

Thunnissen, A.M., Dijkstra, A.J., Kalk, K.H., Rozeboom, H.J., Engel, H., Keck, W., and Dijkstra, B.W. (1994). Doughnut-shaped structure of a bacterial muramidase revealed by X-ray crystallography. Nature *367*, 750-753.

Tian, J., Wu, N., Chu, X., and Fan, Y. (2010). Predicting changes in protein thermostability brought about by single- or multi-site mutations. BMC Bioinformatics *11*, 370.

Tigertt, W.D. (1980). Anthrax. William Smith Greenfield, M.D., F.R.C.P., Professor Superintendent, the Brown Animal Sanatory Institution (1878-81). Concerning the priority due to him for the production of the first vaccine against anthrax. The Journal of hygiene *85*, 415-420.

Tillotson, G.S., and Theriault, N. (2013). New and alternative approaches to tackling antibiotic resistance. F1000prime reports *5*, 51.

Timasheff, S.N. (1993). The control of protein stability and association by weak interactions with water: how do solvents affect these processes? Annual review of biophysics and biomolecular structure *22*, 67-97.

Toke, O. (2005). Antimicrobial peptides: new candidates in the fight against bacterial infections. Biopolymers *80*, 717-735.

Tolkacheva, T.V., Abakumov, E.M., Martynova, V.A., and Golosova, T.V. (1981). [Correction of intestinal dysbacteriosis with biological preparations in acute leukemia]. Problemy gematologii i perelivaniia krovi *26*, 29-33.

Tsuzuki, K., Tricoire, L., Courjean, O., Gibelin, N., Rossier, J., and Lambolez, B. (2005). Thermostable mutants of the photoprotein aequorin obtained by in vitro evolution. J Biol Chem *280*, 34324-34331.

Turner, M.S., Waldherr, F., Loessner, M.J., and Giffard, P.M. (2007). Antimicrobial activity of lysostaphin and a *Listeria monocytogenes* bacteriophage endolysin produced and secreted by lactic acid bacteria. Systematic and applied microbiology *30*, 58-67.

Turner, N.J. (2003). Directed evolution of enzymes for applied biocatalysis. Trends Biotechnol *21*, 474-478.

Unemo, M., and Shafer, W.M. (2011). Antibiotic resistance in Neisseria gonorrhoeae: origin, evolution, and lessons learned for the future. Ann N Y Acad Sci *1230*, E19-28.

van den Burg, B. (2003). Extremophiles as a source for novel enzymes. Curr Opin Microbiol *6*, 213-218.

van den Burg, B., and Eijsink, V.G. (2002). Selection of mutations for increased protein stability. Curr Opin Biotechnol *13*, 333-337.

Van den Burg, B., Vriend, G., Veltman, O.R., Venema, G., and Eijsink, V.G. (1998). Engineering an enzyme to resist boiling. Proc Natl Acad Sci U S A *95*, 2056-2060.

van der Sloot, A.M., Mullally, M.M., Fernandez-Ballester, G., Serrano, L., and Quax, W.J. (2004). Stabilization of TRAIL, an all-beta-sheet multimeric protein, using computational redesign. Protein Eng Des Sel *17*, 673-680.

Vankemmelbeke, M., Healy, B., Moore, G.R., Kleanthous, C., Penfold, C.N., and James, R. (2005). Rapid detection of colicin E9-induced DNA damage using *Escherichia coli* cells carrying SOS promoter-lux fusions. J Bacteriol *187*, 4900-4907.

Varea, J., Monterroso, B., Saiz, J.L., Lopez-Zumel, C., Garcia, J.L., Laynez, J., Garcia, P., and Menendez, M. (2004). Structural and thermodynamic characterization of Pal, a phage natural chimeric lysin active against pneumococci. J Biol Chem *279*, 43697-43707.

Vazquez-Boland, J.A., Kuhn, M., Berche, P., Chakraborty, T., Dominguez-Bernal, G., Goebel, W., Gonzalez-Zorn, B., Wehland, J., and Kreft, J. (2001). *Listeria* pathogenesis and molecular virulence determinants. Clinical microbiology reviews *14*, 584-640.

Vetriani, C., Maeder, D.L., Tolliday, N., Yip, K.S., Stillman, T.J., Britton, K.L., Rice, D.W., Klump, H.H., and Robb, F.T. (1998). Protein thermostability above 100 degreesC: a key role for ionic interactions. Proc Natl Acad Sci U S A *95*, 12300-12305.

Vieille, C., and Zeikus, G.J. (2001). Hyperthermophilic enzymes: sources, uses, and molecular mechanisms for thermostability. Microbiol Mol Biol Rev *65*, 1-43.

Vogt, G., and Argos, P. (1997). Protein thermal stability: hydrogen bonds or internal packing? Fold Des *2*, S40-46.

Vogt, G., Woell, S., and Argos, P. (1997). Protein thermal stability, hydrogen bonds, and ion pairs. J Mol Biol *269*, 631-643.

Vollmer, W. (2008). Structural variation in the glycan strands of bacterial peptidoglycan. FEMS Microbiol Rev *32*, 287-306.

von der Osten, C., Branner, S., Hastrup, S., Hedegaard, L., Rasmussen, M.D., Bisgard-Frantzen, H., Carlsen, S., and Mikkelsen, J.M. (1993). Protein engineering of subtilisins to improve stability in detergent formulations. J Biotechnol *28*, 55-68.

Wakabayashi, H., and Fay, P.J. (2013). Modification of interdomain interfaces within the A3C1C2 subunit of factor VIII affects its stability and activity. Biochemistry *52*, 3921-3929.

Walcher, G., Stessl, B., Wagner, M., Eichenseher, F., Loessner, M.J., and Hein, I. (2010). Evaluation of paramagnetic beads coated with recombinant *Listeria* phage endolysin-derived cell-wall-binding domain proteins for separation of *Listeria monocytogenes* from raw milk in combination with culture-based and real-time polymerase chain reaction-based quantification. Foodborne pathogens and disease *7*, 1019-1024.

Waldburger, C.D., Schildbach, J.F., and Sauer, R.T. (1995). Are buried salt bridges important for protein stability and conformational specificity? Nat Struct Biol *2*, 122-128.

Walden, H., Bell, G.S., Russell, R.J., Siebers, B., Hensel, R., and Taylor, G.L. (2001). Tiny TIM: a small, tetrameric, hyperthermostable triosephosphate isomerase. J Mol Biol *306*, 745-757.

Wall, R.J., Powell, A.M., Paape, M.J., Kerr, D.E., Bannerman, D.D., Pursel, V.G., Wells, K.D., Talbot, N., and Hawk, H.W. (2005). Genetically enhanced cows resist intramammary *Staphylococcus aureus* infection. Nat Biotechnol *23*, 445-451.

Walsh, S., Shah, A., and Mond, J. (2003). Improved pharmacokinetics and reduced antibody reactivity of lysostaphin conjugated to polyethylene glycol. Antimicrob Agents Chemother *47*, 554-558.

Wang, I.N., Deaton, J., and Young, R. (2003). Sizing the holin lesion with an endolysin-beta-galactosidase fusion. J Bacteriol *185*, 779-787.

Wang, I.N., Smith, D.L., and Young, R. (2000). Holins: the protein clocks of bacteriophage infections. Annu Rev Microbiol *54*, 799-825.

Wang, W. (1999). Instability, stabilization, and formulation of liquid protein pharmaceuticals. International journal of pharmaceutics *185*, 129-188.

Wang, Y., Sun, J.H., and Lu, C.P. (2009). Purified recombinant phage lysin LySMP: an extensive spectrum of lytic activity for swine streptococci. Curr Microbiol *58*, 609-615.

Weber-Dabrowska, B., Dabrowski, M., and Slopek, S. (1987). Studies on bacteriophage penetration in patients subjected to phage therapy. Archivum immunologiae et therapiae experimentalis *35*, 563-568.

Weisse, M.E. (2001). The fourth disease, 1900-2000. Lancet *357*, 299-301.

Whatmore, A.M., and Reed, R.H. (1990). Determination of turgor pressure in *Bacillus subtilis*: a possible role for K+ in turgor regulation. Journal of general microbiology *136*, 2521-2526.

Wheeler, J., Holland, J., Terry, J.M., and Blainey, J.D. (1980). Production of group C streptococcus phage-associated lysin and the preparation of *Streptococcus pyogenes* protoplast membranes. Journal of general microbiology *120*, 27-33.

White, P.J., Squirrell, D.J., Arnaud, P., Lowe, C.R., and Murray, J.A. (1996). Improved thermostability of the North American firefly luciferase: saturation mutagenesis at position 354. Biochem J *319 (Pt 2)*, 343-350.

Whitmore, L., and Wallace, B.A. (2004). DICHROWEB, an online server for protein secondary structure analyses from circular dichroism spectroscopic data. Nucleic Acids Res *32*, W668-673.

Winter, G., Fersht, A.R., Wilkinson, A.J., Zoller, M., and Smith, M. (1982). Redesigning enzyme structure by site-directed mutagenesis: tyrosyl tRNA synthetase and ATP binding. Nature *299*, 756-758.

Wintrode, P.L., Miyazaki, K., and Arnold, F.H. (2001). Patterns of adaptation in a laboratory evolved thermophilic enzyme. Biochim Biophys Acta *1549*, 1-8.

Wise, R. (2002). Antimicrobial resistance: priorities for action. J Antimicrob Chemother *49*, 585-586.

Witzenrath, M., Schmeck, B., Doehn, J.M., Tschernig, T., Zahlten, J., Loeffler, J.M., Zemlin, M., Muller, H., Gutbier, B., Schutte, H., *et al.* (2009). Systemic use of the endolysin Cpl-1 rescues mice with fatal pneumococcal pneumonia. Critical care medicine *37*, 642-649.

Wong, T.S., Roccatano, D., Zacharias, M., and Schwaneberg, U. (2006a). A statistical analysis of random mutagenesis methods used for directed protein evolution. J Mol Biol *355*, 858-871.

Wong, T.S., Zhurina, D., and Schwaneberg, U. (2006b). The diversity challenge in directed protein evolution. Combinatorial chemistry & high throughput screening *9*, 271-288.

Woodford, N., and Livermore, D.M. (2009). Infections caused by Gram-positive bacteria: a review of the global challenge. J Infect *59 Suppl 1*, S4-16.

Worth, C.L., Preissner, R., and Blundell, T.L. (2011). SDM--a server for predicting effects of mutations on protein stability and malfunction. Nucleic Acids Res *39*, W215-222.

Wozniak-Knopp, G., and Ruker, F. (2012). A C-terminal interdomain disulfide bond significantly stabilizes the Fc fragment of IgG. Arch Biochem Biophys *526*, 181-187.

Wright, A.E., and Semple, D. (1897). Remarks on vaccination against typhoid fever. British medical journal *1*, 256-259.

Xiao, L., and Honig, B. (1999). Electrostatic contributions to the stability of hyperthermophilic proteins. J Mol Biol *289*, 1435-1444.

Yakandawala, N., Gawande, P.V., Lovetri, K., and Madhyastha, S. (2007). Effect of ovotransferrin, protamine sulfate and EDTA combination on biofilm formation by catheter-associated bacteria. J Appl Microbiol *102*, 722-727.

Yamashita, Y., Shibata, Y., Nakano, Y., Tsuda, H., Kido, N., Ohta, M., and Koga, T. (1999). A novel gene required for rhamnose-glucose polysaccharide synthesis in *Streptococcus mutans*. J Bacteriol *181*, 6556-6559.

Yin, S., Ding, F., and Dokholyan, N.V. (2007). Eris: an automated estimator of protein stability. Nature methods *4*, 466-467.

Yoong, P., Schuch, R., Nelson, D., and Fischetti, V.A. (2004). Identification of a broadly active phage lytic enzyme with lethal activity against antibiotic-resistant *Enterococcus faecalis* and *Enterococcus faecium*. J Bacteriol *186*, 4808-4812.

Yoong, P., Schuch, R., Nelson, D., and Fischetti, V.A. (2006). PlyPH, a bacteriolytic enzyme with a broad pH range of activity and lytic action against *Bacillus anthracis*. J Bacteriol *188*, 2711-2714.

You, L., and Arnold, F.H. (1994). Directed evolution of subtilisin E in *Bacillus subtilis* to enhance total activity in aqueous dimethylformamide. Protein Eng *9*, 77-83.

Young, R. (1992). Bacteriophage lysis: mechanism and regulation. Microbiol Rev *56*, 430-481.

Yutani, K., Ogasahara, K., Tsujita, T., and Sugino, Y. (1987). Dependence of conformational stability on hydrophobicity of the amino acid residue in a series of variant proteins substituted at a unique position of tryptophan synthase alpha subunit. Proc Natl Acad Sci U S A *84*, 4441-4444.

Zarivach, R., Ben-Zeev, E., Wu, N., Auerbach, T., Bashan, A., Jakes, K., Dickman, K., Kosmidis, A., Schluenzen, F., Yonath, A., *et al.* (2002). On the interaction of colicin E3 with the ribosome. Biochimie *84*, 447-454.

Zhang, L., and Falla, T.J. (2006). Antimicrobial peptides: therapeutic potential. Expert opinion on pharmacotherapy *7*, 653-663.

Zhao, H., and Arnold, F.H. (1999). Directed evolution converts subtilisin E into a functional equivalent of thermitase. Protein Eng *12*, 47-53.

Zhao, H., Chockalingam, K., and Chen, Z. (2002). Directed evolution of enzymes and pathways for industrial biocatalysis. Curr Opin Biotechnol *13*, 104-110.

Zhi, W., Srere, P.A., and Evans, C.T. (1991). Conformational stability of pig citrate synthase and some active-site mutants. Biochemistry *30*, 9281-9286.

Zhou, H., and Zhou, Y. (2002). Distance-scaled, finite ideal-gas reference state improves structure-derived potentials of mean force for structure selection and stability prediction. Protein Sci *11*, 2714-2726.

Zhukov-Verezhnikov, N.N., Peremitina, L.D., Berillo, E.A., Komissarov, V.P., and Bardymov, V.M. (1978). [Therapeutic effect of bacteriophage preparations in the complex treatment of suppurative surgical diseases]. Sovetskaia meditsina, 64-66.

Zimmer, M., Sattelberger, E., Inman, R.B., Calendar, R., and Loessner, M.J. (2003). Genome and proteome of *Listeria monocytogenes* phage PSA: an unusual case for programmed + 1 translational frameshifting in structural protein synthesis. Mol Microbiol *50*, 303-317.

Zimmer, M., Vukov, N., Scherer, S., and Loessner, M.J. (2002). The murein hydrolase of the bacteriophage phi3626 dual lysis system is active against all tested *Clostridium perfringens* strains. Appl Environ Microbiol *68*, 5311-5317.